THE EFFECT OF DISPLACEMENT CONTROL LOADING HISTORIES ON GENRAL CONNECTING SURFACES USING FINITE ELEMENT ANALYSIS

by

SANJOG C. SABNIS

Presented to the Faculty of the graduate School of

The University of Texas at Arlington in Partial fulfillment

of the requirements

For the degree of

MASTER OF SCIENCE IN CIVIL ENGINEERING

THE UNIVERSITY OF TEXAS AT ARLINGTON

December 2008

Copyright© by Sabnis Sanjog 2008

All Right Reserved

ACKNOWLEDGEMENTS

I would like to express my sincere gratitude to Dr. Ali Abolmaali; the author's supervising professors, for his invaluable guidance and continual help throughout this study. The supervising committee members Dr. Guillermo Ramirez and Dr. Shih-Ho Chao are most appreciated and gratefully acknowledged for their valuable suggestion towards this study.

A special and personal acknowledgement is due to the Dr. Ali Abolmaali; for his unrestricted personal guidance throughout this study, for bring out the best out of my ability. Sincerer and personal thanks are extended to Lewis Crow for his assistance with valuable electronic expertise during the different phases of this study. I also want to thanks Frank for his assistance during the final stages of my study. Never the less, I also want to thanks all my office colleagues for their direct and indirect help during this study.

The last but not the least, I would like to acknowledge my parents, without their hard work, devotion, blessings, and endless support this would have not possible for me. I also want to thank my two younger sisters; Kavita and Bhagyashree, and my future wife Madhu, for their support and endless love.

December 10, 2008

ABSTRACT

THE EFFECT OF DISPLACEMENT CONTROL LOADING HISTORIES

ON GENRAL CONNECTING SURFACES USING

FINITE ELEMENT ANALYSIS

Sanjog Sabnis, M.S.

The University of Texas at Arlington, 2008

Supervising Professor: Ali Abolmaali

Displacement loading history provided by the AISC Seismic Provision 2005 is commonly used for experimental testing and analytical modeling of beam-to-column steel connection to stimulate the seismic effect. However, the basis for the above loading history is not documented in the literature.

Thus, this study developed 25 cyclic load cases by varying the frequency and magnitude of the AISC-2005 loading within a predefined envelops. The 25 load cases are obtained from five different load sets in which the concept of uniform and non-uniform

frequencies and amplitude are utilized. All the load cases are limited to the displacement equivalent to the AISC-2005 story drift recommendation of 0.06 rad.

The cyclic load cases were applied to the simple connecting surfaces consisting of: welded shear, single-bolted shear, double-bolted shear, and4-bolt tee-hanger. Also a typical 4-bolt extended end-plate connection was considered. The 3-D finite element model (FEM) of the above connections were developed by considering material, geometric, and contact non-linearity's for cyclic plasticity-based analysis of the selected connection.

Parametric study was conducted by varying the force and geometric related parameters of the connections which were then subjected to the developed loading cases. During the parametric study, the contact algorithm and element type were also varied in order to identify their effect on the analysis results. In addition, a load control loading history which was reported in the literature was used for comparison purpose. The areas under the outer loops of the hysteresis loops were calculated to represent the response. This area signifies the energy dissipation characteristics of each selected connection. The percentage difference of each parametric case subjected to different cyclic displacement loading history is documented and reported.

TABLE OF CONTENTS

ACKNOWLEDGEMENT iii

ABSTRACT iv

LIST OF ILLUSTRATION xii

LIST OF TABLES xvi

CHAPTER

1. INTRODUCTION 1

1.1 Introduction 1

1.2 Literature review 5

1.3 Goals and objectives 19

2. DEVELOPMENT OF DISPLACEMENT CONTROL LOADING HISTORY 21

2.1 Introduction 21

2.2 Development of loading sets 24

2.2.1 Displacement control loading Set I 24

2.2.2 Displacement control loading Set II 27

2.2.3 Displacement control loading Set III 32

2.2.4 Displacement control loading Set IV 36

2.2.5 Displacement control loading Set V 41

3. FINITE ELEMENT ANALYSIS 45

3.1 Introduction 45

3.2 Material Model 47

3.3 Bolt Pretension 52

3.4 Contact Modeling 54

3.5 Model Verification 56

3.6 Developments of finite element models 56

3.6.1 Welded shear surface model 56

3.6.1.1 Assembly 56

3.6.1.2 Contact Definition 57

3.6.1.3 Boundary Condition 58

3.6.2 Bolted Shear Surface Models 58

3.6.2.1 Assembly 58

3.6.2.2 Contact Definition 59

3.6.2.3 Boundary Condition 62

3.6.3 Tee- Hanger Model 63

3.6.3.1 Assembly 63

3.6.3.2 Contact Definition 63

3.6.3.3 Boundary Condition 67

3.6.4 Extended end-plate connection model 67

3.6.4.1 Assembly 67

3.6.4.2 Contact Definition 68

3.6.4.3 Boundary Condition 72

3.6.4.4 Symmetric Modeling 73

4. PARAMETRIC STUDY 74

4.1 Introduction 74

4.2 Test Cases Nomenclature 75

4.3 Geometric Variables 78

4.3.1 Welded shear surface models 78

4.3.2 Bolted shear surface models 79

4.3.3 Tee- hanger models 80

4.3.4 Extended end-plate connection model 82

4.4 Loading Cases 82

4.4.1 Displacement control loading cases 82

4.4.2 Load control loading case 83

4.5 Pretension 84

4.6 Contact 84

4.7 Element Type 84

4.8 Results of parametric study 86

5. CONCLUSION 107

5.1 Summary 107

5.2 Results and discussion 108

5.2.1 Welded shear surface models 108

5.2.1.1 Welded shear surface model Case 1 108

5.2.1.2 Welded shear surface model Case 2 109

5.2.2 Single bolted shear surface models 110

5.2.2.1 Single bolted shear surface model Case 1 110

5.2.2.2 Single bolted shear surface model Case 2 111

5.2.2.3 Single bolted shear surface model Case 3 112

5.2.3 Double bolted shear surface model 113

5.2.3.1 Double bolted shear surface model Case 1 113

5.2.3.2 Double bolted shear surface model Case 2 114

5.2.3.3 Double bolted shear surface model Case 3 116

5.2.4 Tee- hanger models 117

5.2.4.1 Tee-hanger model Case 1 117

5.2.4.2 Tee-hanger model Case 2 118

5.2.4.3 Tee-hanger model Case 3 119

5.2.5 Extended end-plate connection model 120

5.2.5.1 Extended end-plate connection model Case 1 120

5.2.5.2 Extended end-plate connection model Case 2 121

5.3 Conclusion 121

5.4 Recommendation 122

APPENDIX

A. TEST CASES 123

B. WELDED SHEAR SURFACE MODELS 145

C. SINGLE BOLTED SHEAR SURFACE MODELS 159

D. DOUBLE BOLTED SHEAR SURFACE MODELS 189

E. TEE-HANGER MODELS 219

F. EXTENDED END-PLATE CONNECTION MODELS 248

G. ENERGY DISSIPATION CHARTS 253

REFERENCES 276

BIOGRAPHICAL INFORMATION 279

LIST OF ILLUSTRATIONS

Figure Page

1-1 Displacement loading history, AISC Seismic Provision 2002 2

1-2 Welded shear surface model 3

1-3 Single bolted shear surface model 4

1-4 Double bolted shear surface model 4

1-5 Tee-hanger model 4

1-6 Extended end-plate connection 5

1-7 ECCS loading history used by Liew et al., 2004 10

1-8 Displacement loading history used by Mourad et al., 1995 11

1-9 Random displacement loading history used by Bursi, 2002 13

1-10 Displacement loading histories used by Verderame et al., 2008 15

1-11 Loading history used by Massingham and Irving P.E., 2006 17

1-12 Sinusoidal loading history used by Wang et al., 2006 18

2-1 Typical Envelop A 22

2-2 Typical Envelop B 23

2-3 Displacement load history, DLC I-1 25

2-4 Displacement load history, DLC I-2 25

2-5 Displacement load history, DLC I-1/2 26

2-6 Displacement load history, DLC I-1/3 26

2-7 Displacement load history, DLC I-1/4 27

2-8 Displacement load history, DLC II-2- 1- ½ -1/3- ¼ 30

2-9 Displacement load history, DLC II- ¼ -2 -1- ½ - 1/3 30

2-10 Displacement load history, DLC II- 1/3- ¼ -2- 1- ½ 31

2-11 Displacement load history, DLC II- ½ - 1/3- ¼ - 2 – 1 31

2-12 Displacement load history, DLC II- 1- ½ - 1/3 – ¼ - 2 32

2-13 Displacement load history, DLC III-2- 1- ½ -1/3- ¼ 34

2-14 Displacement load history, DLC III-¼ -2 -1- ½ - 1/3 34

2-15 Displacement load history, DLC III-1/3- ¼ -2- 1- ½ 35

2-16 Displacement load history, DLC III-½ - 1/3- ¼ - 2 – 1 35

2-17 Displacement load history, DLC III-1- ½ - 1/3 – ¼ - 2 36

2-18 Typical loading Set IV 38

2-19 Displacement load history, DLC IV-2- 1- ½ -1/3- ¼..... 38

2-20 Displacement loading history, DLC IV-¼ -2 -1- ½ - 1/3 39

2-21 Displacement load history, DLC IV-1/3- ¼ -2- 1- ½..... 39

2-22 Displacement load history, DLC IV-½ - 1/3- ¼ - 2 – 1 40

2-23 Displacement load history, DLC IV-1- ½ - 1/3 – ¼ - 2 40

2-24 Displacement load history, DLC V-2- 1- ½ -1/3- ¼..... 41

2-25 Displacement load history, DLC V-¼ -2 -1- ½ - 1/3 43

2-26 Displacement loading history, DLC V-1/3- ¼ -2- 1- ½..... 43

2-27 Displacement load history, DLC V-½ - 1/3- ¼ - 2 – 1 44

2-28 Displacement loading history, DLC V-1- ½ - 1/3 – ¼ - 2 44

3-1 Typical Stress-Strain Curve 49

3-2 Newton Raphson technique 51

3-3 Bauschinger Effect..... 52

3-4 Bolt Pretensions 53

3-5 Contact interactions between two surfaces; (a) beginning of step,

(b) middle step, (c) end step, prepared by Le, 2008 55

3-6 Welded shear surface model 57

3-7 Single bolted shear surface model 59

3-8 Double bolted shear surface model 59

3-9 Tee-hanger model 63

3-10 Extended end-plate connection 68

4-1Sequence in test designation 77

4-2 Welded shear surface model 79

4-3 Bolted shear surface model 80

4-4 Tee-hanger model 81

4-5 Typical Load control Loading History 83

LIST OF TABLES

Table Page

1-1 AISC Seismic Provision 2002, displacement control loading history 2

2-1 Parts of loading history 27

2-2 Loading cases in Set II 29

2-3 Loading cases in Set III 33

2-4 Loading case in Set IV 37

2-5 Loading cases in Set V 42

3-1 Various elements used in study 46

3-2 Material properties 48

3-3 Connection properties for welded connection 57

3-4 Contact properties for single bolted surface models 60

3-5 Contact properties for double bolted surface models 61

3-6 Properties for tee – hanger model 64

3-7 Contact properties for extended end-plate model 69

4-1 Geometrical combination for welded shear surface model..... 78

4-2 Geometrical combinations for single and double bolted shear surface model 80

4-3 Geometrical combinations for T- Hanger model 81

4-4 combinations for extended end plate model 82

4-5 Pretension load corresponding to bolt diameter..... 84

4-6 Welded shear surface model (SM-W-1/2) Case1 86

4-7 Welded shear surface model (SM-W-1) Case2 87

4-8 Single bolted shear surface model (SM-1B-1-1/2-FP) Case 1..... 88

4-9 Single bolted shear surface model (SM-1B-1/4-1) Case 2 90

4-10 Single bolted shear surface model (SM-1B-1-1) Case 3 92

4-11 Double bolted shear surface model (SM-2B-1-1/2) Case1..... 94

4-12 Double bolted shear surface model (SM-2B-1/4-1) Case 2..... 96

4-13 Double bolted shear surface model (SM-2B-1-1) Case 3..... 98

4-14 Tee-hanger model (T-1-1/2-1½) Case1 100

4-15 Tee-hanger model (T-1-1-2¾) Case 2 102

4-16 Tee – hanger model (T-1/2-1/2-1) Case 3..... 104

4-17 Extended end-plate connection model (EEP-1/2-1) Case 1..... 106

4-18 Extended end-plate connection model (EEP-1/2-1/2) Case 2..... 106

CHAPTER 1

INTRODUCTION

1.1 Introduction

For long period of time guideline provided by the AISC Seismic Provision 2005 for testing of moment connections has been followed by researcher. AISC Seismic Provisions 2005 suggested the application of displacement control loading as drift angle over a predefined number of cycles as shown in Table 1-1 and Figure 1-1. Guideline also suggests that the connection should sustain the minimum angular drift of 0.06 radians. In reality literature has very little evidence to support this assumption. Only resemblance was found in literature to the AISC Seismic Provisions 2005, which was SAC Loading protocol (1997).

Table 1-1 AISC Seismic Provision 2005, displacement control loading history

No. of cycles	Drift angle (rad)
6	0.00375
6	0.005
6	0.0075
4	0.01
2	0.015
2	0.02
2	0.03

Further, increase in drift angle of 0.01 after every 2 cycles until connection reaches inelastic mode.

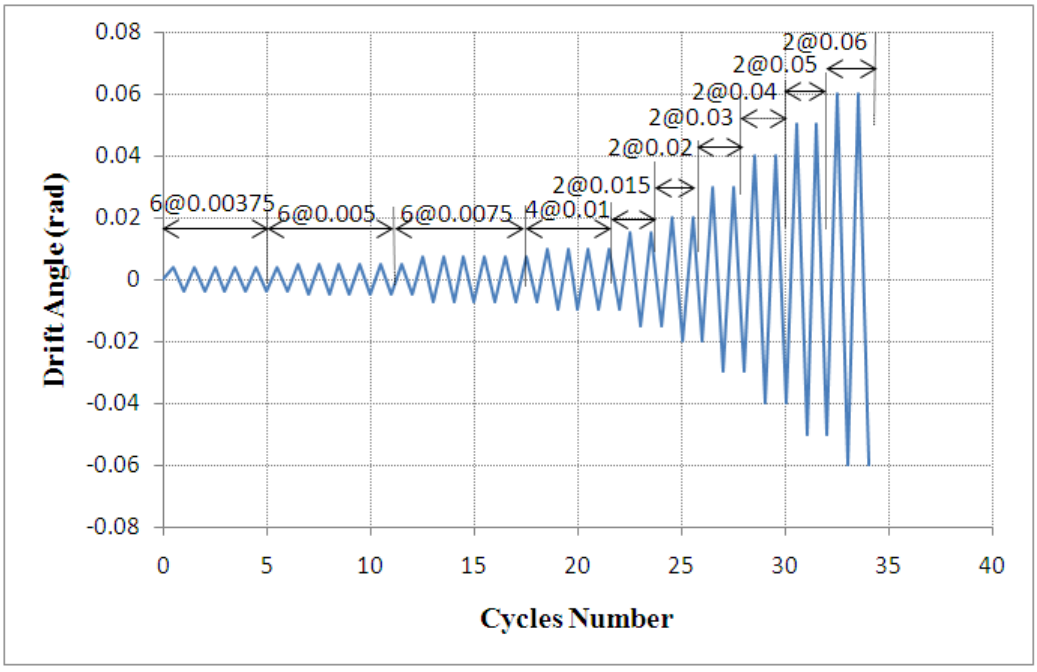

Figure 1-1 Displacement loading history, AISC Seismic Provision 2005

Insufficient evidence in literature inspires this study. Different models are developed to test under various loading conditions to evaluate the AISC guidelines provided. Models tested consist of welded shear surface, bolted shear surface, tee-hanger, and extended end-plate connections shown in Figure 1-2 to Figure 1-6. The behaviors of models are tested by 25 different loading cases which are created by varying the AISC Seismic Provisions 2005. Further, the parametric study was carried out on the connecting surface models by varying the geometry and force parameters. The impact of these parameters as individual, and in combination was studied. Energy dissipation by was obtained by calculating area under the outer loop of each hysteresis loop tested.

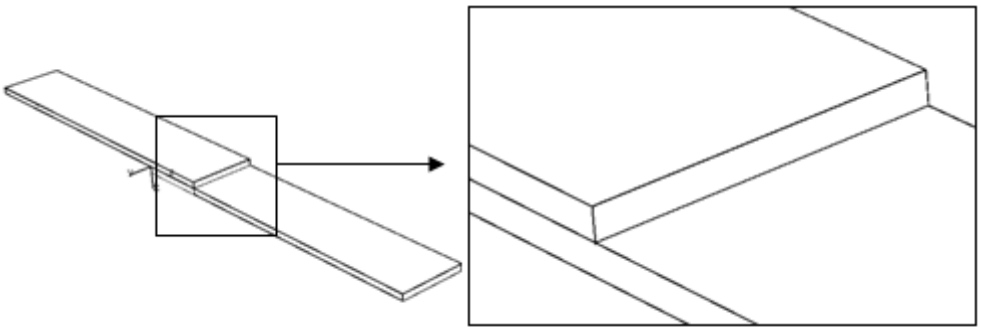

Figure 1-2 Welded shear surface model

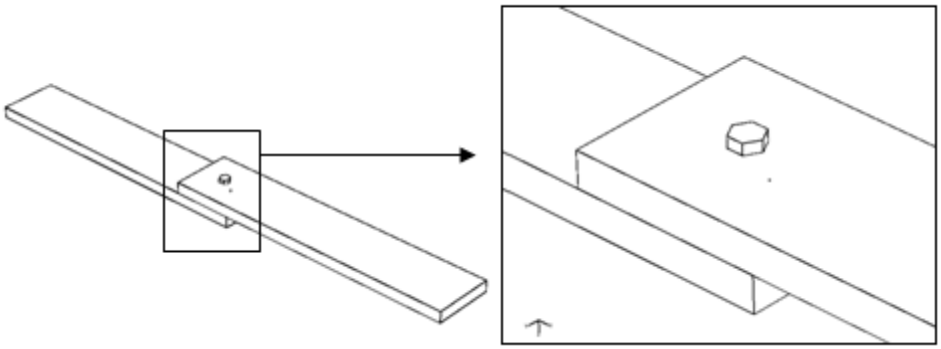

Figure 1-3 Single bolted shear surface model

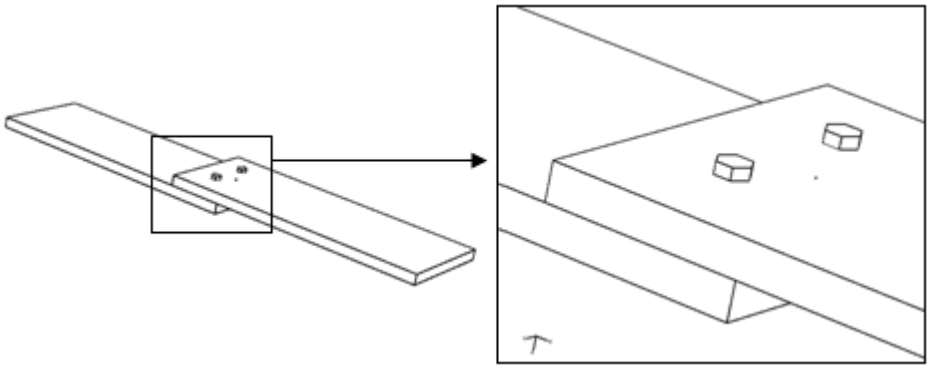

Figure 1-4 Double bolted shear surface model

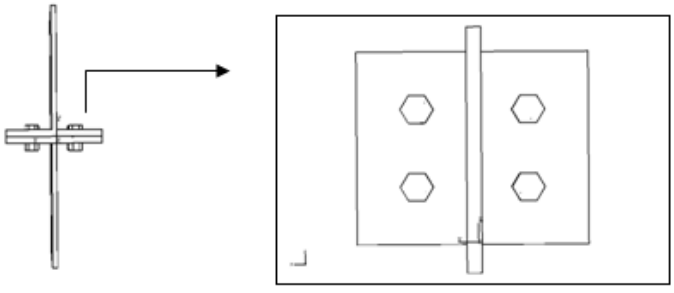

Figure 1-5 Tee-hanger model

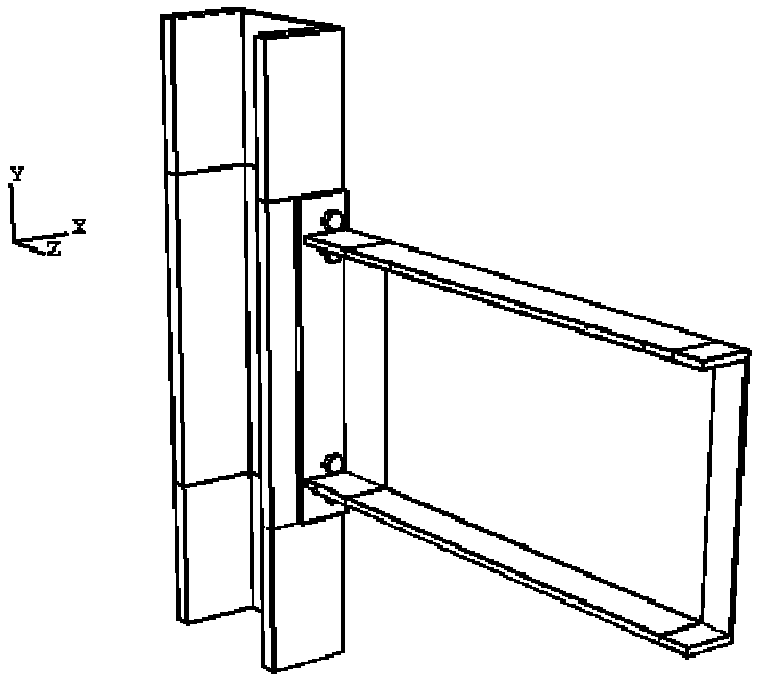

Figure 1-6 Extended end-plate connection

1.2 Literature review

Bursi and Jaspat (1998) attempted to produce the appropriate methodology for the three-dimensional non-linear finite element model of extended end plate moment resisting steel connection. While establishing the methodology for moment connection using finite element modeling, they focused on some of the important issues as constitutive relationships, step size, number of integration points, kinematic descriptions, element types and discretization. Authors also introduced a spin model for the bolt preloading. A rigid beam element was connected at bolt center to the beam. The study

carried out monotonically increasing displacement on 14 specimens to validate the finite element model with the experimental data.

Kovacs et al. (2008) investigated the response of the end-plates under cyclic loading for steel and composites (concrete fill steel I – sections) to develop favorable guideline for structural arrangement to withstand the seismic loadings. This study also proposed the semi-empirical method to approximate the cyclic hysteretic behavior of studied joints based on the knowledge of monotonic moment-rotation curve.

Yorgun and Bayramoglu (2001) attempted to compare the standard end plate connection with some of the innovative fabricated connections in order to achieve the better performance. A gap was fabricated between the end plate and the column flange to make it different from the standard moment connection. This gap between the end plate and the column flange is filled with I- shape element same as the beam section. Tests were carried out for four full-scale extended end plate connections which were subjected to monotonic and cyclic loadings. The displacement control loading protocol recommended by the ECCS was applied for testing. This study reported that connections with a gap fabricated between end plate and column flange performed better than Standard connections.

Shi et al. (2007) carried out eight full scale beams- to- column end plate moment connection tests. The specimens were tested under cyclic loadings. Aim of authors study was to investigate the influence of factors such as flush and extended type, end plate

stiffeners, column flange stiffeners, bolt size, and plate thickness. This study also proposed three failure modes in order to achieve enough of joint rotation capacity and energy dissipation capacity under earthquake loadings. Failure of end plate and column flange, the panel zone yield preceding the end plate and bolt, and the end plate fail prior to bolt are three modes of failure suggested.

The specimens were applied to a combined load and displacement loading conditions in different steps. In the first step the specimens were loaded under load control protocols until specimen yields. Under load control protocol, each step of load increment was consisted of one cycle. After yielding of specimen loading was converted to displacement control. In displacement control each displacement increment step consist of 2 number of cycle. The loading was applied at the tip of the beam.

Maggi et al. (2005) presented a parametric study result of extended end plate connections using finite element modeling tool. Authors discussed six finite element models along with their experimental specimens in order to study the overall stiffness, displacement of the end plate, and axial forces in the bolts. The parameters were varied in order to calibrate analytical model and observe changes on end plate behavior. The end plate thickness was varied from 19 to 37.5 mm and the bolt diameter was varied from 16, 19, and 22 mm. Authors observed good agreement between mode 1 and mode 3 failures, but in case of mode 2 failures more refinement in model is suggested.

In the finite element model testing, loading was applied in two parts. In first part, the temperature gradient was imposed to achieve the pre-tensioning in the bolts. Once the pre-tensioning in the bolts are achieves then loading is switch to step two. In Step 2 displacements were applied at the end of the beam which generated the bending moment in the connection.

Cabrero and Bayo (2007) presented an experiment investigation of statically loaded extended end plate connection in both major and minor axis. The proportional loading was applied for the test. The experimental test program was consisting of basic test specimens. The end plate thickness was varied in two different sets of thin plates and thick plates. The specimens were consisting for four beams connected to form an extended end plate connection. Two beams were there in major direction and other two beams was in minor directions. The loading was applied in two steps such as load control and displacement control. In first stage load control loading protocols was applied till elastic loading range, and then loading protocol was shifted to displacement control. The study reported that in case of major axis thick plates a special attention should be given to nut striping behavior which is a brittle failure.

Coelho et al. (2004) investigated the effect of end plate thickness and grade of steel on the behavior of extended end plate connection. They tested eight full scaled specimens monotonically. Tests were carried out in two sets by varying the end plate thickness and steel grade. The specimens were subjected to the monotonic tensile force in term of displacement control protocol. The displacement speed of 0.02mm/s is

maintained up to collapse of specimen. This study reported that moment resistance increases with the increases in the end plate thickness at the same time rotational capacity decreases of the section. Grade of steel is having very little influence on the any of the property of connection.

Liew et al. (1997) verified some of the test results in order to develop an analysis and design methodology for the semi rigid connections. They tested two types of connections such as top seat double web angles and extended end plate connections. Authors obtained the data in term of stiffness and moment capacity. The tests were conducted in order to study the load – displacement response, connection behavior under sequential and non sequential loading, and to compare the test results with the advance analysis to check the accuracy.

Loading history involved the loading and unloading of cycles up to collapse to evaluate the beam column connection. Initially beam column connection was loaded up to 25% of ultimate load and then unloaded. Next unloading was carried out at 80% of ultimate load. The test was control using load within the elastic limits, whereas in inelastic range test was controlled by displacement control.

Mohamadi-shooreh and Mofid (2008) presented a parametric study of bolted flush end plate connections to study working procedure to examine the initial rotational stiffness of the connection. Authors also studied the moment- rotation behavior which is significant in high rise building and industrial structures. They crated a finite element

model using SUT_DAM a nonlinear finite element program. The study compared test results with the existing literature to prove models validness. The load control loading history was adopted to obtain the results.

Liew et al. (2004) presented comparison study between steel extended end-plate connection and composite beam to column joint. Eight full- scale tests were conducted by using European Convention for Constructional Steelwork (ECCS) loading protocol as shown in Figure 1-7. The main objective of this research was to study full response of joints (rotations) when subjected to applied moment.

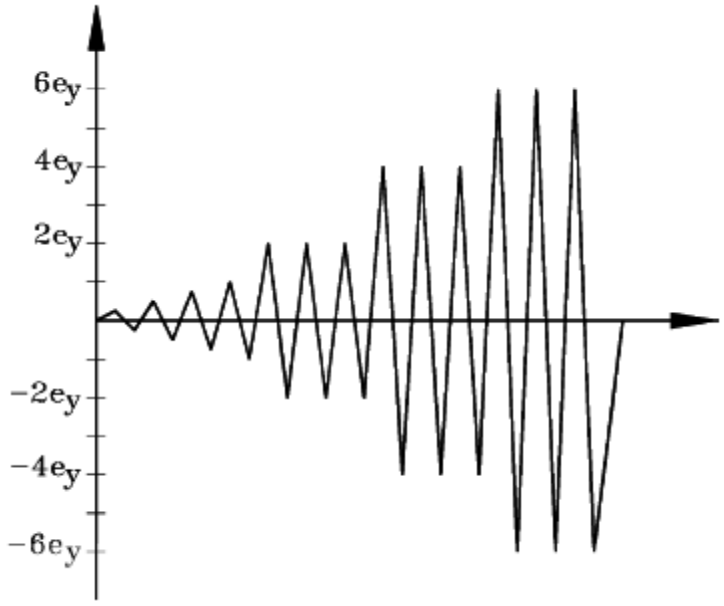

Figure 1-7 ECCS loading history used by Liew et al., 2004

Mourad et al. (1995) studied the behavior of extended end plate connection with hollow beam section using blind bolts under cyclic loading. Authors also studied the four

story frame building with bolt connection under a dynamic loading condition and compare the results with the rigid connections to see the effect of connections flexibility on the response. To create the seismic load effect authors subjected connection to quasistatic cyclic loading.

The load was applied on the beam tips in a displacement controlled manner. Initially specimens were subjected to four cycles of half expected yield load value to keep the behavior of the connection elastic in order to check the working of all components of test setup. Typical loading sequence is shown in Figure 1-8 Loading was stopped after every 5mm of displacement to proper scanning of data.

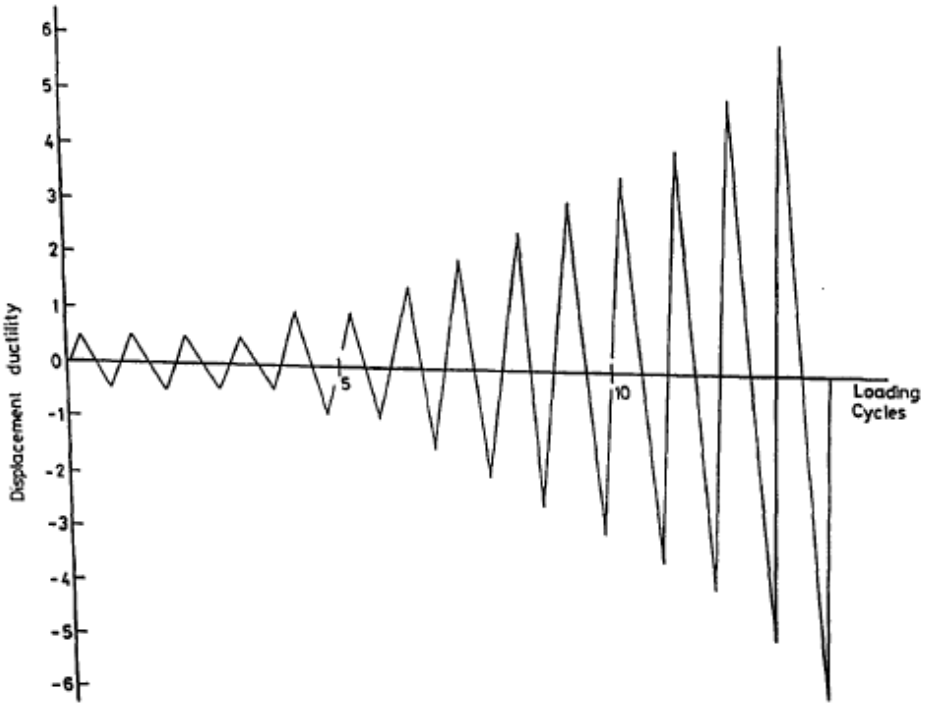

Figure 1-8 Displacement loading history used by Mourad et al., 1995

Deng et al. (2000) presented a connection element which incorporated the response stimulation and failure detection in extended end plate connection model. The stimulation of connection model hysteretic response of connection is formulated and implemented in the non-linear finite element program DRAIN-3DX. In the formulation stiffness and strength degradation and pinching are expressed as the damage index. An automatic event definition algorithm is devolved and an event to event solution scheme is followed.

Bursi et al. (2005) presented the numerical analysis of isolated T snub connection subjected to low cycle loadings. The performance of bolted partial strength beam to column joint under the seismic loading. An experimental program consists of bolted end plate joints and individual components were tested under set of constant and variable displacement amplitude. A detailed three-dimensional non-linear finite element analysis was carried out to tune the model material parameter.

This study used the random amplitude displacement loading histories in order to vary the degree of complexity. Figure 1-9 shows the different displacement loading profiles used in the analysis.

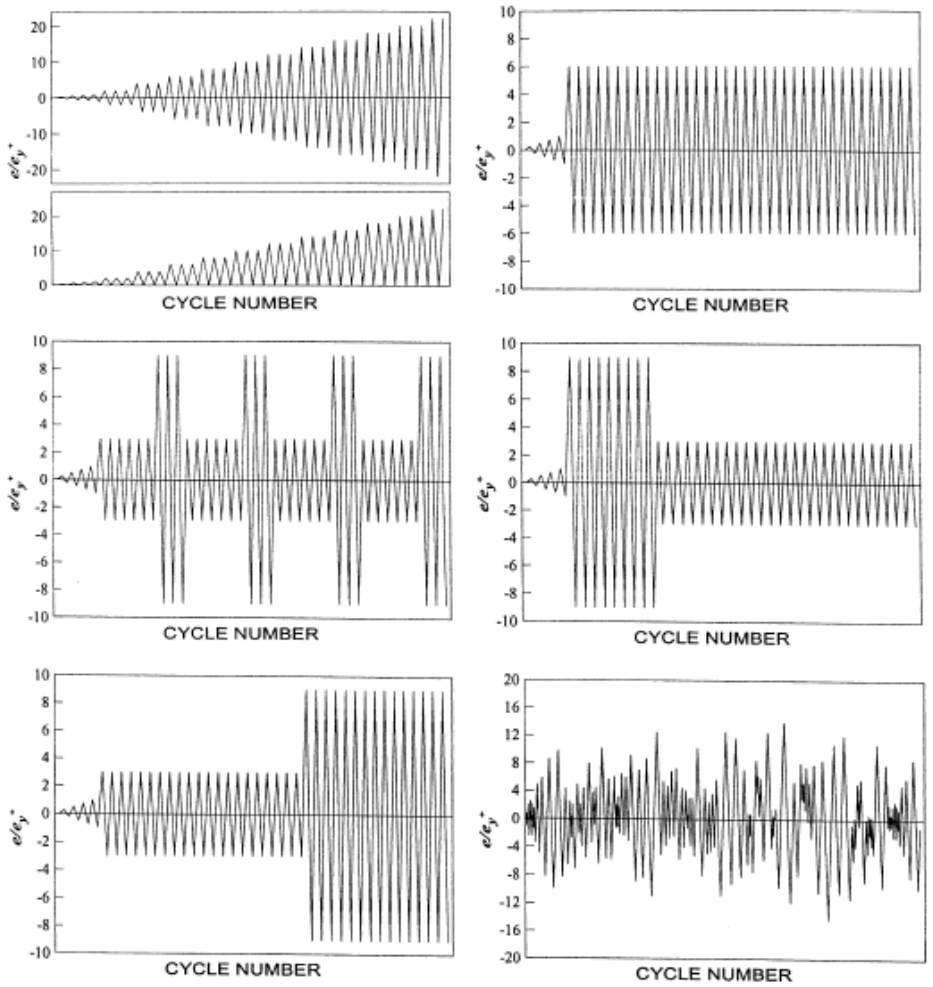

Figure 1-9 Random displacement loading history used by Bursi, 2005

Lin and Chen (2008) carried out a strained control test on magnesium alloy to evaluate the fatigue properties by push pull cyclic test at different strain amplitude at room temperature. In order to observe the effect of strain control loadings effect the material was polished with sand paper, water, and alcohol to remove the surface irregularity. Computerized Instron 8801 servo-hydraulic testing system was used to produce low cycle fatigue under total strain control. The strain control low cycle

amplitudes were applied till 10,000 cycles after which it change to load control test at a frequency of 50 Hz.

Ozgur (2008) used the load control loading protocols to study the strengthening of shear deficient RC beam by external bonding of fiber reinforced polymer (CFRC) straps under a cyclic loading. The load was applied on the cantilever portion of the beam using 10,000kN capacity hydraulic jack which was controlled by 600kN load cell. Initially author applied two cycles in the elastic region for verifying the functioning of experimental setup.

Santana et al. (2008) preformed a cyclic test under a strain control protocols in order to study the dynamic response of fatigue damage on aluminum alloy and AISI steel specimen. MTS 810 machine was used to carry out these tests under fully reversed axial total strain control mode. The smoothed specimen of diameter 3.17mm is used for testing. The loading profile was sinusoidal wave form with a frequency of 1Hz.

De-Feng et al. (2008) tested A356-T6 casting alloy under a uniaxial and multi-axial cyclic loading. Experiment was carried out on the MTS 809 machine at room temperature under displacement control condition at a frequency of 0.5Hz. The Loading was a combination of tension and torsion loading in a sinusoidal form with a phase difference of 90˚.

Verderame et al. (2008) performed cyclic tests on the RC column with the smooth reinforcing steel bars to checks its performance under seismic condition. The experiment

was carried out under the displacement control protocols. The load was applied using the two hollow actuator placed on the columns horizontally. The hydraulic actuator was capable of producing the displacement of ± 250mm. Two series of fifteen and ten predefined drift have been repeated three times until the maximum displacement of 100mm. This study used two different loading histories in order to assess the effect of magnitude on the behavior of the column. Figure 1-10 shows the two loading histories used in the experiments.

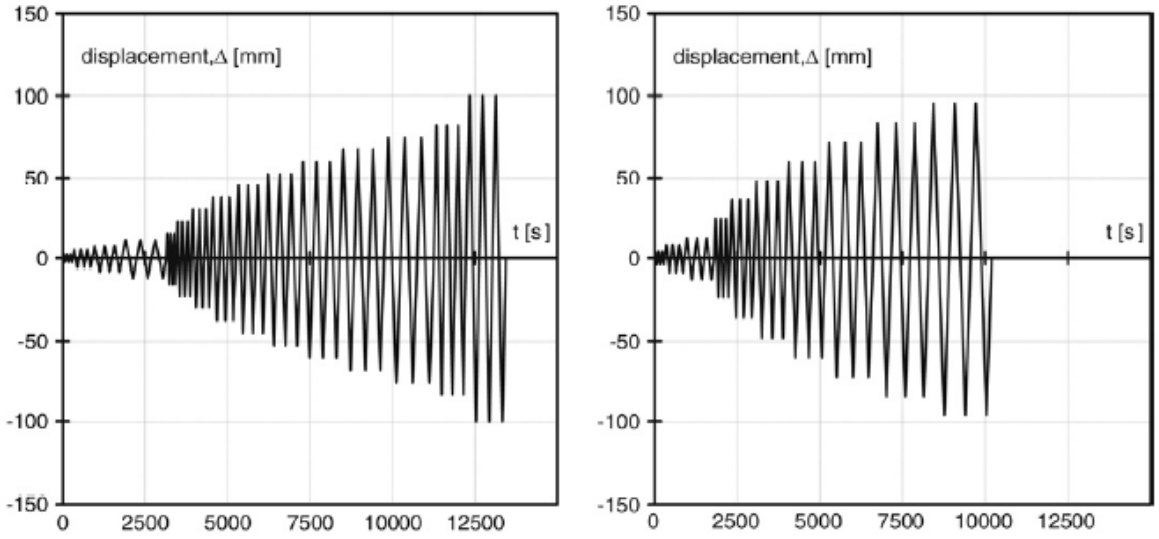

Figure 1-10 Displacement loading histories used by Verderame et al., 2008

Fan et al. (2008) created a finite element model for estimating the crack growth rate. An idea was to predict the fatigue growth rate of the stainless steel 304L based on a newly developed fatigue approach. A compact specimen was subjected to Mode I crack growth under constant amplitude loading and two step high-low sequences. The authors

also compared the results obtained from the finite element model with the experimental result available in literature.

Mace and Manconi (2008) introduce a finite element model in order to describe the method by which the dispersion relationship for a two dimensional structural components can be predicted. A typical four nodded rectangular segment is modeled applying the periodic conditions relating the nodal degree of freedom and forces. Authors crated example models of thin plate, and symmetrical laminated plate, and formed coated laminated sandwich panel. Authors found a fair resemblance in results from finite element model and experimental results.

Massingham and Irving (2006) created a finite element model to study the cylindrical Hertzain contact on a test sample subjected to alternating shear loading. Model was tested under a variable amplitude fritting fatigue in terms of shear on the cylindrical contact surface. Four nodded plain strain elements were used, and the size of elements within the contact region was kept as 25µm x 25µm. Total of 60,000 element were designed in the model.

A modeled combination of overloads containing 125% and 150% was applied First, the case of 125% overload followed by 150% in order to observe the stress distribution due to loading histories on the contact surface. Figure 1-11 presents the loading history used in this study.

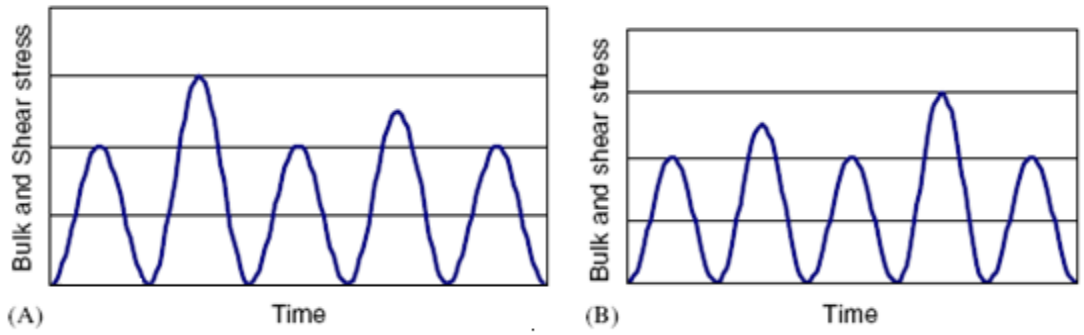

Figure 1-11 loading history used by Massingham and Irving P.E., 2006

Wang et al. (2006) carried out a four point bending test to estimate the fatigue life and deformation behavior of carbon fiber reinforced concrete. They tested twelve specimens with different mixture under a cyclic loading. Load controlled tests using a hydraulic mechanical testing system (MTS) of 10kN capacity was employed. Constant load rate of 10 N/s is applied in the form of sinusoidal wave form. The loading history was applied in two different frequencies 0.1 and 10 Hz. Figure 1-12 shows the first six cycles of loading history.

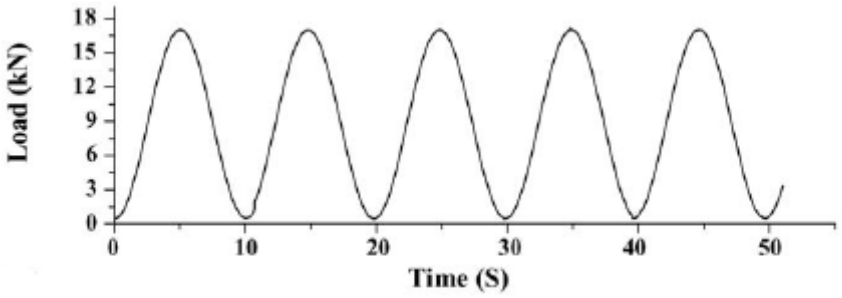

Figure 1-12 sinusoidal loading history used by Wang et al., 2006

Pirondi et al (2006) purposed a work to stimulate the ductile damage and failure involved by plain strain reversal using damage model. Cyclic loading tests were performed on various round notch bars to study the evaluation of plastic deformation and damage under multi axial stress condition. The authors crated a symmetrical finite element model using four nodded fully integrated element. The test was conducted using a servo-hydraulic testing machine under a displacement control loadings. The test was carried out with the frequency of 0.004Hz and 0.008Hz.

Lam et al. (2006) carried out experiments on the behavior of the FRP concrete under cyclic compression to check the compressive strength and ultimate strain of concrete. In this study author tested eight concrete specimens confined in the FRP. Tests were carried out under the displacement control protocols using servo-hydraulic machine. Specimen were subjected to predetermined level of loading and then unloaded, but not loaded in the reverse direction. The specimens were tested in two ways such as monotonic and cyclic loading.

Shao et al. (2006) performed cyclic tests on the 24 FRP concrete specimens. In first loading history, three cycles of 0-40% in first step and 0-100% in second step were applied. Second loading history consisted of 0-60% and 0-100% in first and second step respectively. The only difference in third loading history was 0-80% in first step when compare with second loading.

Feng et al. (2006) presented a numerical investigation on the effects of loading and unloading on the three dimensional frictional contact with the rigid foundation. Authors also investigated the sliding process during the lading and unloading process. The loading history consists of the vertical rigid motion of the cylinder controlled in terms of the displacement with a magnitude of 0.1mm the displacement is applied in one step.

1.3 Goals and objectives

The main objective of this study is to evaluate the AISC-2005 cyclic displacement loading protocol applied to connecting surface such as welded-welded and bolted welded steel connection. Thus simple connecting surfaces as well as end plate connections were considered. Specifically the following concepts were examined in order to achieve above objective.

1. To obtained different displacement loading protocols by keeping the AISC-2005 as a baseline envelop and verifying its loading magnitude and time period. This yielding to 25 loading cases that were used in this research.

2. To identify the difference in the response of connecting surface subjected to displacement and load control loading. Obviously, this study is most effective when bilinear material law with strain hardening is used during analysis.

3. The energy dissipation is considered to be the measure of response of each connection to the applied cyclic load. This is accomplished by calculating the area under the outer loop of hysteresis loop.

The scope of study was limited to the following connection types:

1. Simple welded shear model
2. Simple 1-bolted and 2-bolted shear model
3. Bolted tee-hanger model
4. Extended end-plate connection

CHAPTER 2

DEVELOPMENT OF DISPLACEMENT CONTROL LOADING HISTORY

2.1 Introduction

This chapter presents the development of 25 cyclic load cases based on the AISC-2005 Seismic Provision loading protocol. This was done by varying the frequency and amplitude of the AISC-2005 with respect two bounding envelops. The 25 loading cases are categorized based on the five load sets (Set I, II, III, IV, V) with five load cases in each set.

Envelops are referred to as Envelop A and Envelop B as shown in Figure 2-1 and Figure 2-2, respectively. Envelop A is obtained by connecting the peak amplitude points of the AISC-2005, which formed a curve-shape envelop. Envelop B is developed by connecting a 'linear' line from the first amplitude peak of the first cycle to the last amplitude peak of the last cycle.

The load sets are developed based on the following frame of thoughts:

- Load Set I: the time period of the AISC-2005 is varied uniformly.
- Load Set II: The time period of the AISC-2005 is varied non- uniformly.

- Load Set III: The same as load Set II, but in the reverse direction. This means amplitude of Set II is applied in descending order.
- Load Set IV: Amplitude of each cycles of the AISC-2005 loading protocol is stretched to touch the Envelop B. Then, the time period was varied to obtain five load cases.
- Loading Set V: Load Set IV was applied in reverse direction.

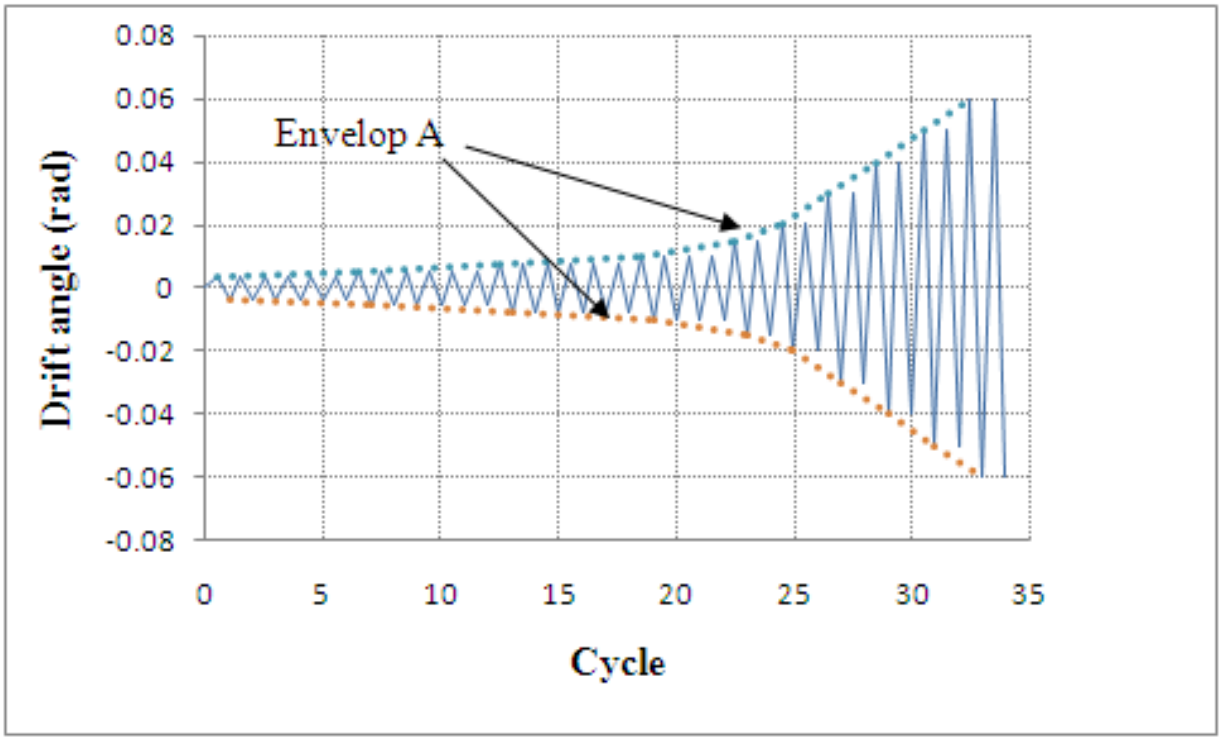

Figure 2-1 Typical Envelop A

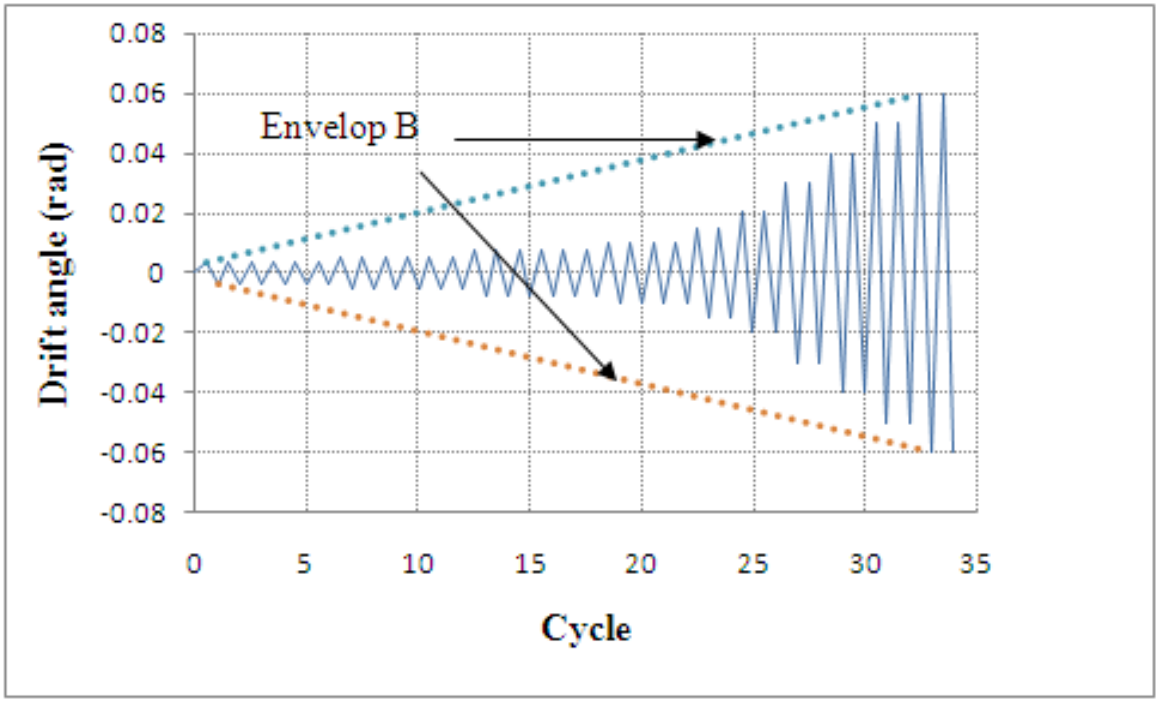

Figure 2-2 Typical Envelop B

It should be noted that AISC-2005 loading is represented in terms of drift angle rather than displacement with the maximum rotation = 0.06 rad. Thus, the value of rotation was multiplied by an arbitary beam depth of 24 in. to arrive to the displacement load history presents in this study with maximum displacement amplitude being equal to 1.44 in. (24 x 0.06).

2.2 Development of loading sets

2.2.1 Displacement control loading Set I

Load Set I is devolved by varying the time period of the AISC-2005 loading protocol uniformly with respect to Envelop A. This simply means that the time period, T, for the AISC-2005 was considered as the baseline for the period, T = 1 sec, and other load cases are obtained by T = 2 sec, T = ½ sec, T = 1/3 sec, and T = ¼ sec. This basically introduces the effect of rate of the loading on the connecting surfaces. The load case designation for load Case I is:

Displacement load case (DLC) – I – Time period (T)

where, "I" refer to the set number. For example, DLC-I-1/2 represents displacement load case in Set I with time period T = ½ sec. compared to the AISC-2005's T = 1 Sec. Figure 2-3 through Figure 2-7 represent five loading cases of the load Set I. Each figure also shows Envelop A which can be used as a tool to compare the amplitude shift with respect to the original AISC-2005 (Envelop A)

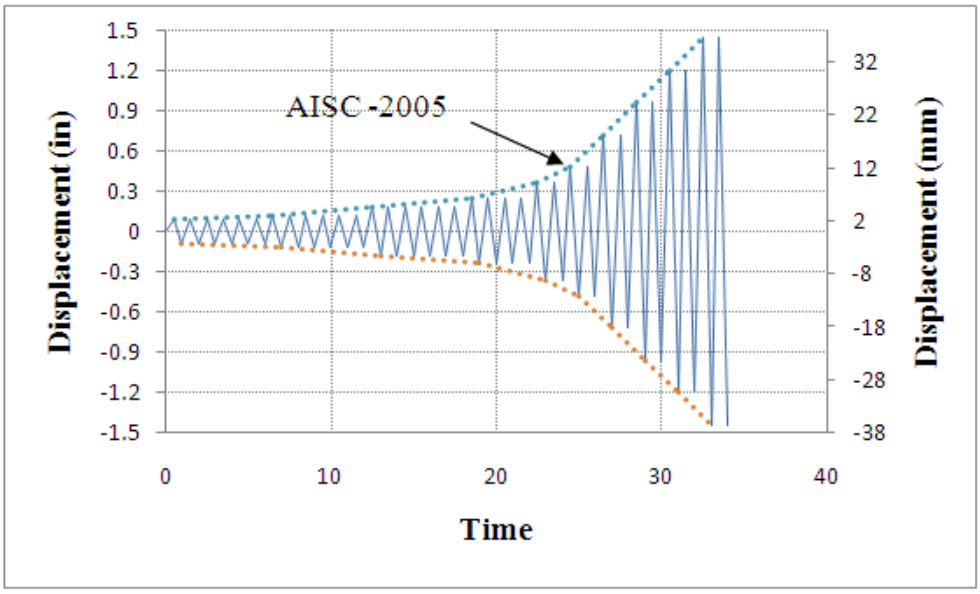

Figure 2-3 Displacement load history, DLC I-1

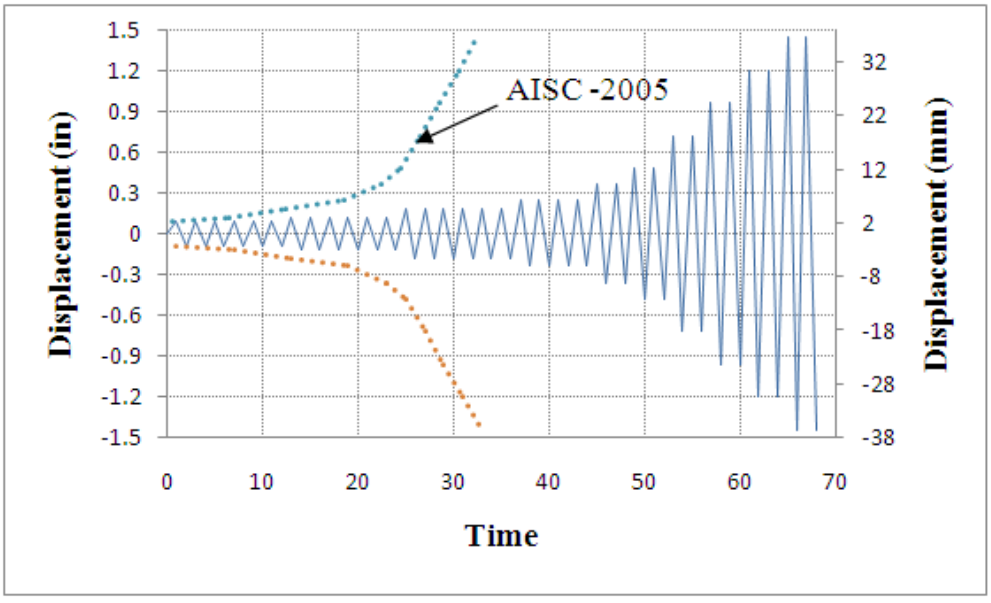

Figure 2-4 Displacement load history, DLC I-2

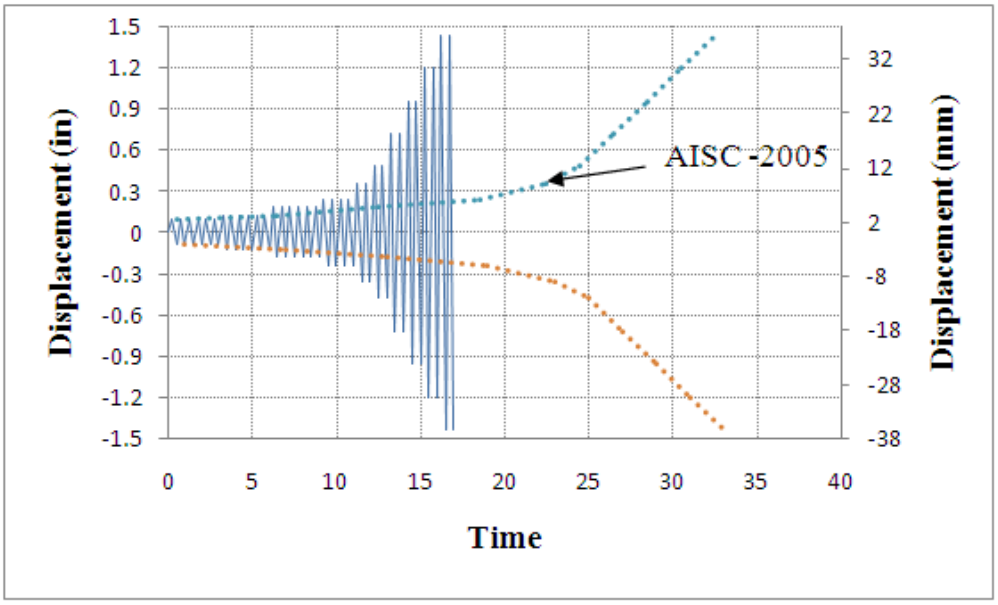

Figure 2-5 Displacement load history, DLC I-1/2

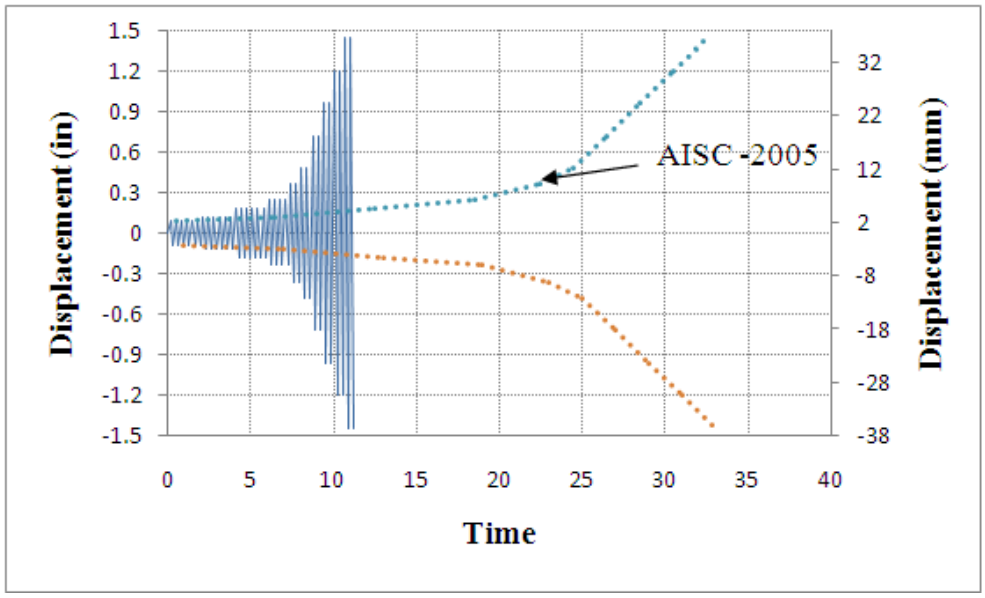

Figure 2-6 Displacement load history, DLC I-1/3

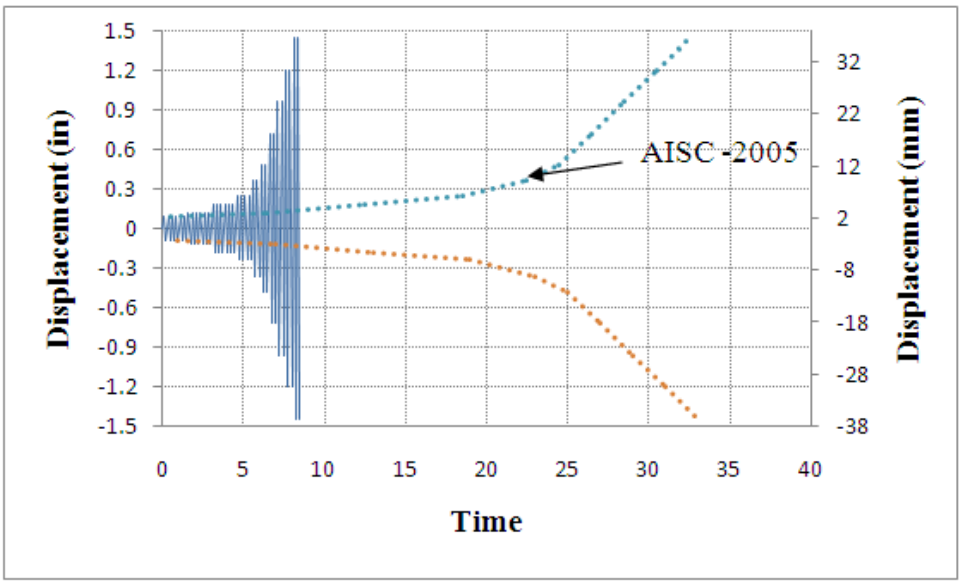

Figure 2-7 Displacement load history, DLC I-1/4

2.2.2 Displacement loading control Set II

In the Set II loading, time period of the AISC-2005 loading protocol was varied non-uniformly. The 34 loading cycles of the AISC-2005 was divided into the ten parts as shown in Table 2-1.

Table 2-1 Parts of loading history

Regions	**Part No.**	**No. of cycles**
Region I	Part 1	6 cycles
	Part 2	6 cycles
Region II	Part 3	6 cycles
	Part 4	4 cycles
	Part 5	2 cycles
	Part 6	2 cycles
	Part 7	2 cycles
Region III	Part 8	2 cycles
Region IV	Part 9	2 cycles
Region V	Part 10	2 cycles

The property of each load case devoloped for the Set II is shown in Table 2-2. For example, in Case 1, T = 2 sec was assigned for Part 1 and Part 2. Then, T = 1 sec was assign for Part 3 through Part 5. Further T = ½ sec , T = 1/3 sec, T = ¼ sec was assigned to parts respectively. This means the load Set II takes into account the time dependent frequency vibration. Figure 2-8 through Figure 2-12 presents the loading cases devoloped for Set II. The test designation for each load case of the Set II is defined as:

DLC II – $T_{\text{Region I}}$ – $T_{\text{Region II}}$ – $T_{\text{Region III}}$ – $T_{\text{Region IV}}$ – $T_{\text{Region V}}$

where, $T_{\text{Region I}}$, $T_{\text{Region II}}$, $T_{\text{Region III}}$, $T_{\text{Region IV}}$, and $T_{\text{Region V}}$ define the loading period assign to Region I through V respectively.

Table 2-2 Loading cases in Set II

Regions	**Region I**		**Region II**					**Region III**	**Region IV**	**Region V**
Parts	**Part 1**	**Part 2**	**Part 3**	**Part 4**	**Part 5**	**Part 6**	**Part 7**	**Part 8**	**Part 9**	**Part 10**
No. of cycles	6	6	6	4	2	2	2	2	2	2
Amplitude (in)	0.09	0.12	0.18	0.24	0.36	0.48	0.72	0.96	1.2	1.44
DLC II - 2- 1- 1/2- 1/3- 1/4	T = 2		T = 1					T = 1/2	T = 1/3	T = 1/4
DLC II - 1/4- 2- 1- 1/2- 1/3	T = 1/4		T = 2					T = 1	T = 1/2	T = 1/3
DLC II - 1/3- 1/4- 2- 1- 1/2	T = 1/3		T = 1/4					T = 2	T = 1	T = 1/2
DLC II - 1/2- 1/3- 1/4- 2- 1	T = 1/2		T = 1/3					T = 1/4	T = 2	T = 1
DLC II - 1- 1/2- 1/3- 1/4- 2	T = 1		T = 1/2					T = 1/3	T = 1/4	T = 2

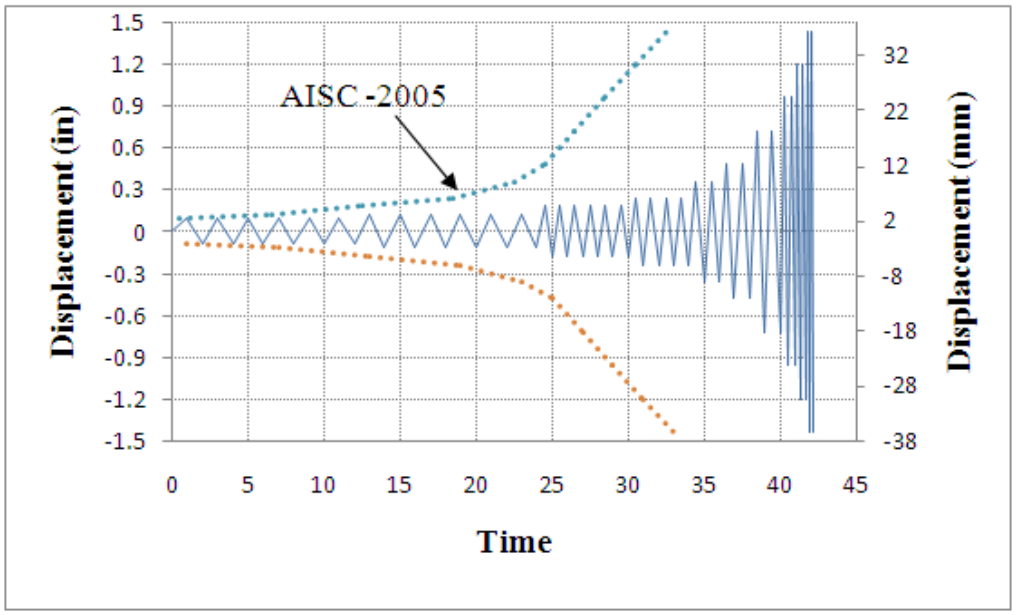

Figure 2-8 Displacement load history, DLC II-2- 1- ½ -1/3- ¼

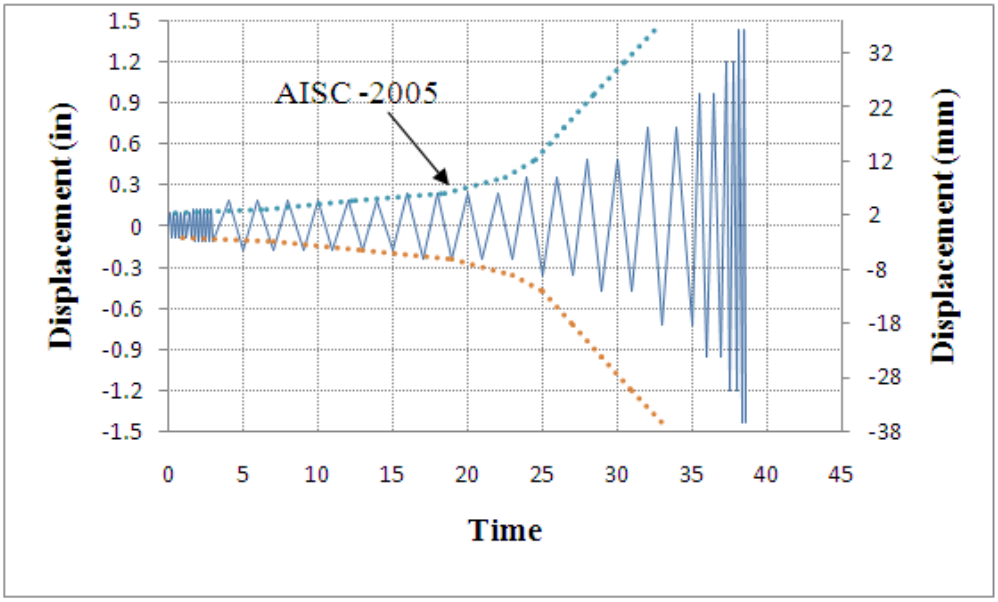

Figure 2-9 Displacement load history, DLC II- ¼ -2 -1- ½ - 1/3

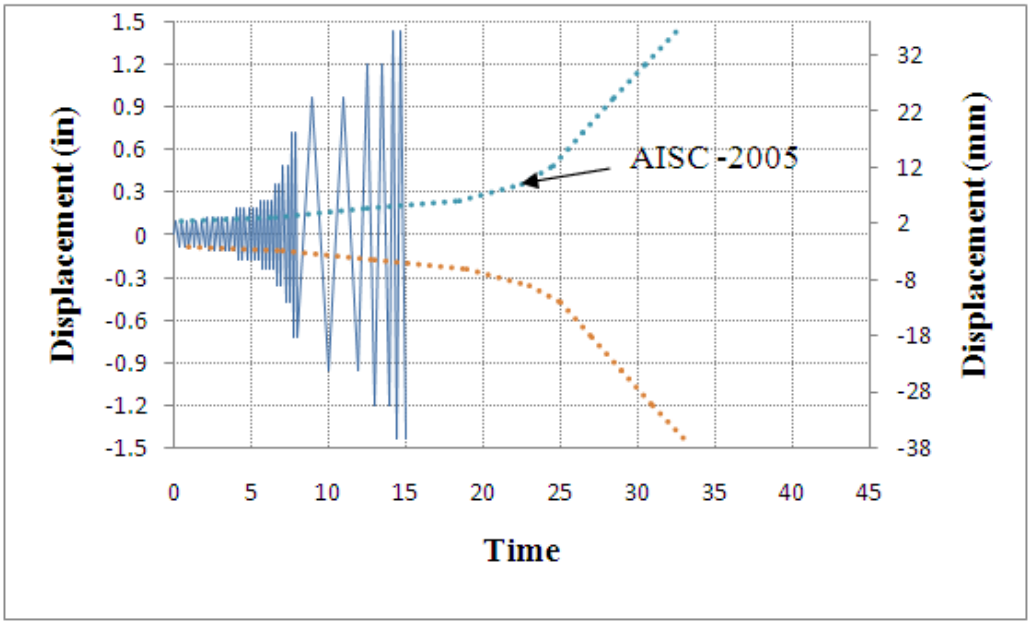

Figure 2-10 Displacement load history, DLC II- 1/3- ¼ -2- 1- ½

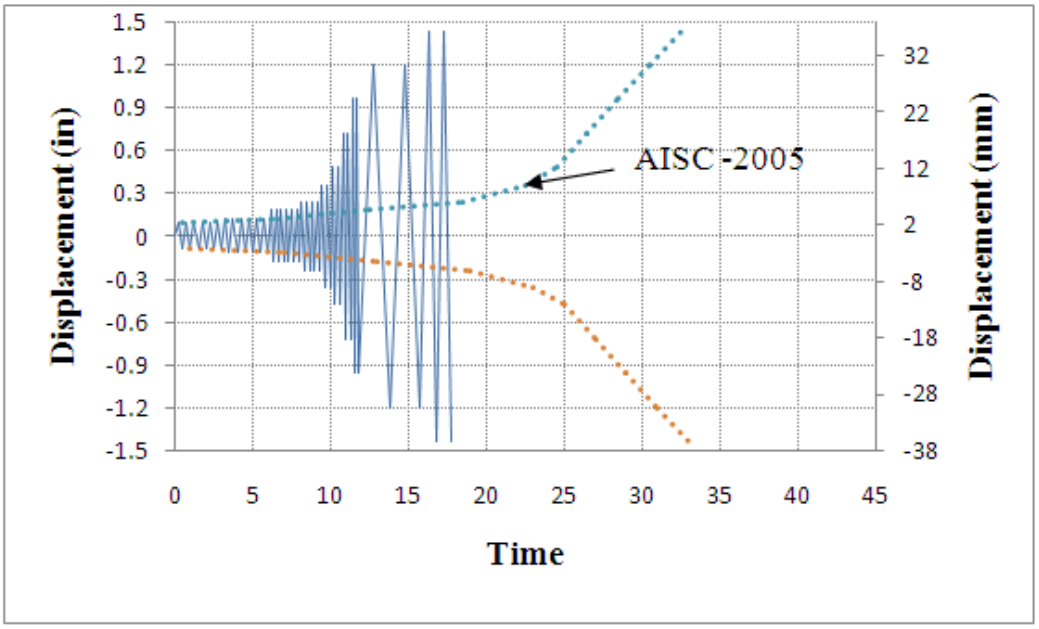

Figure 2-11 Displacement load history, DLC II- ½ - 1/3- ¼ - 2 - 1

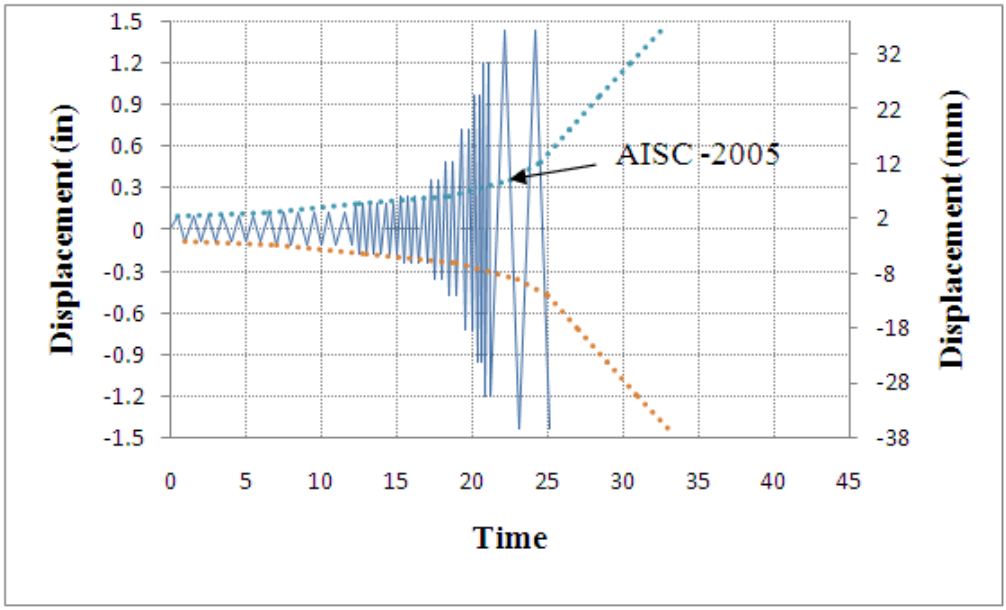

Figure 2-12 Displacement load history, DLC II- 1- ½ - 1/3 – ¼ - 2

2.2.3 Displacement control loading Set III

Five additional load cases are devoloped in Set III by appling the displacement amplitude of each load case of the Set II in reverse order. Thus, the time dependednt frequency variation of the load Set III is identical to that of load Set II. Table 2-3 tabulated the period and amplitude for each of the load cases of Set III. Figure 2-13 through Figure 2-17

Table 2-3 Loading cases in Set III

Regions	**Region I**		**Region II**					**Region III**	**Region IV**	**Region V**
Parts	**Part 10**	**Part 9**	**Part 8**	**Part 7**	**Part 6**	**Part 5**	**Part 4**	**Part 3**	**Part 2**	**Part 1**
No. of cycles	2	2	2	2	2	2	4	6	6	6
Amplitude (in)	1.44	1.2	0.96	0.72	0.48	0.36	0.24	0.18	0.12	0.09
DLC III - 2- 1- 1/2- 1/3- 1/4	T = 2		T = 1					T = 1/2	T = 1/3	T = 1/4
DLC III - 1/4- 2- 1- 1/2- 1/3	T = 1/4		T = 2					T = 1	T = 1/2	T = 1/3
DLC III - 1/3- 1/4- 2- 1- 1/2	T = 1/3		T = 1/4					T = 2	T = 1	T = 1/2
DLC III - 1/2- 1/3- 1/4- 2- 1	T = 1/2		T = 1/3					T = 1/4	T = 2	T = 1
DLC III - 1- 1/2- 1/3- 1/4- 2	T = 1		T = 1/2					T = 1/3	T = 1/4	T = 2

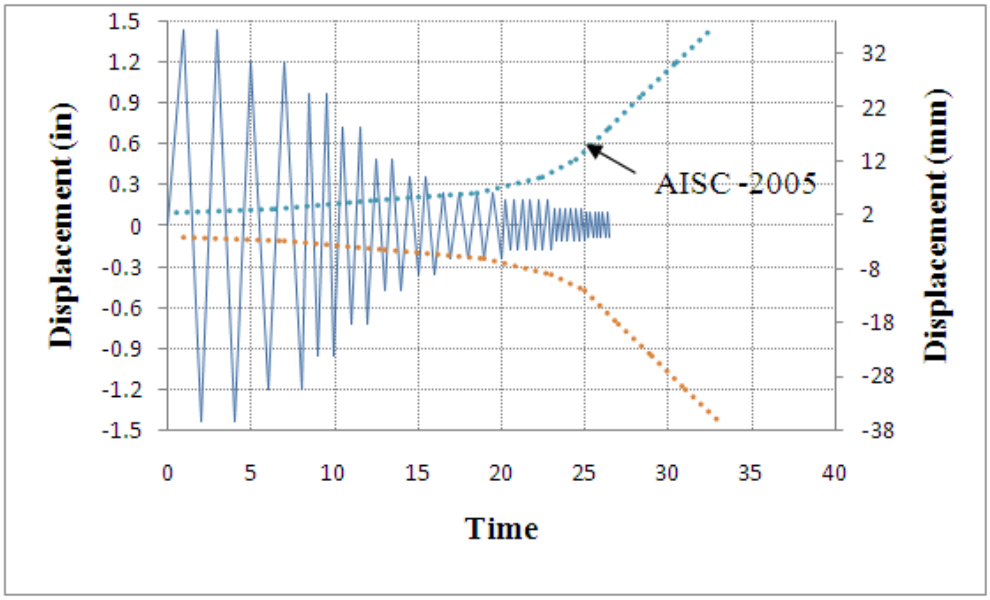

Figure 2-13 Displacement load history, DLC III-2- 1- ½ -1/3- ¼

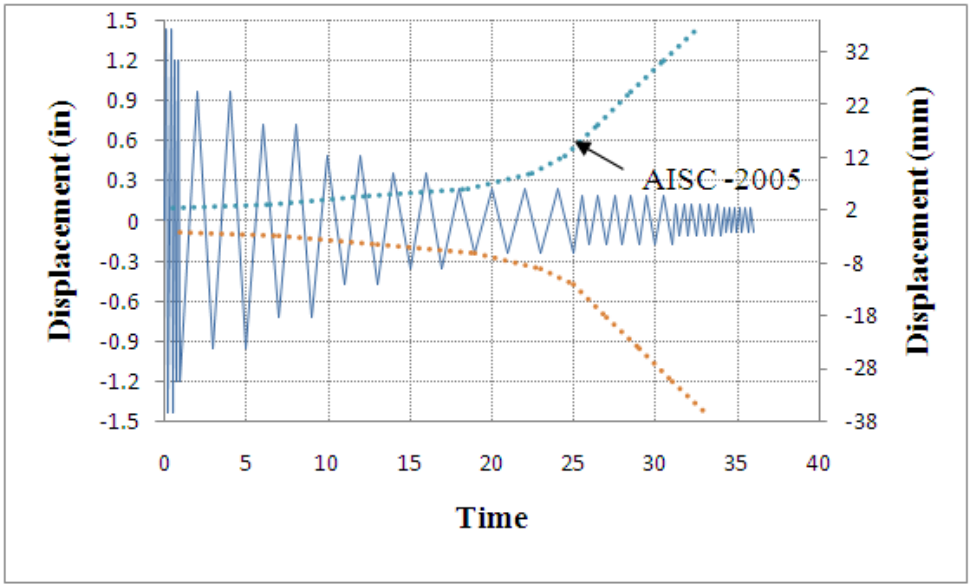

Figure 2-14 Displacement load history, DLC III-¼ -2 -1- ½ - 1/3

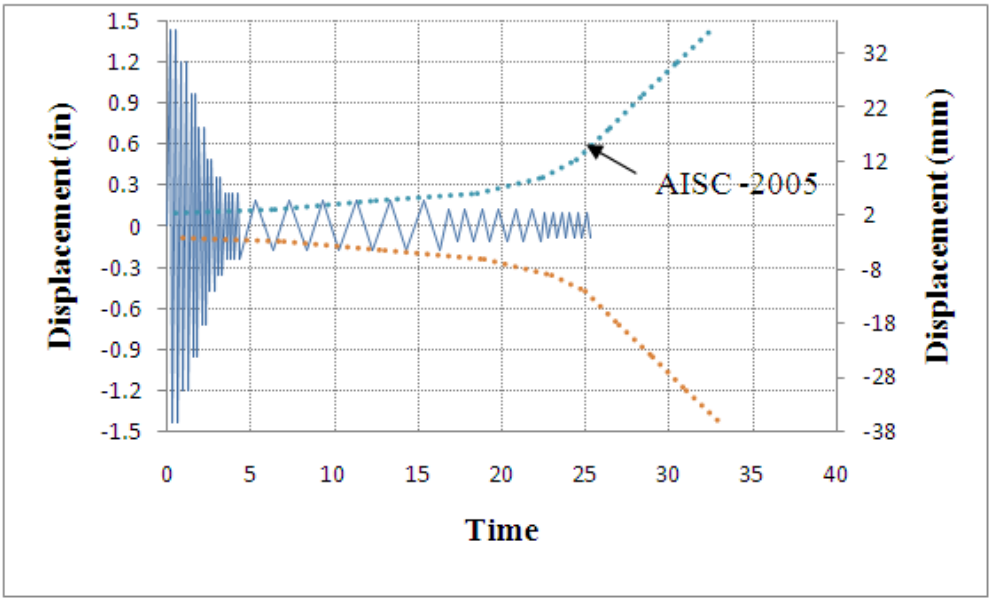

Figure 2-15 Displacement load history, DLC III-1/3- ¼ -2- 1- ½

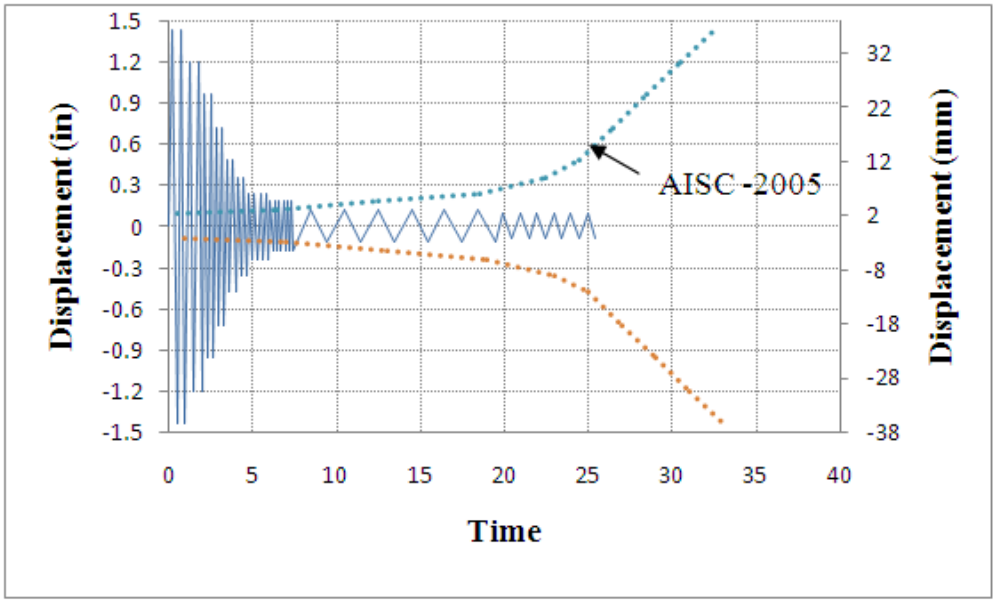

Figure 2-16 Displacement load history, DLC III-½ - 1/3- ¼ - 2 - 1

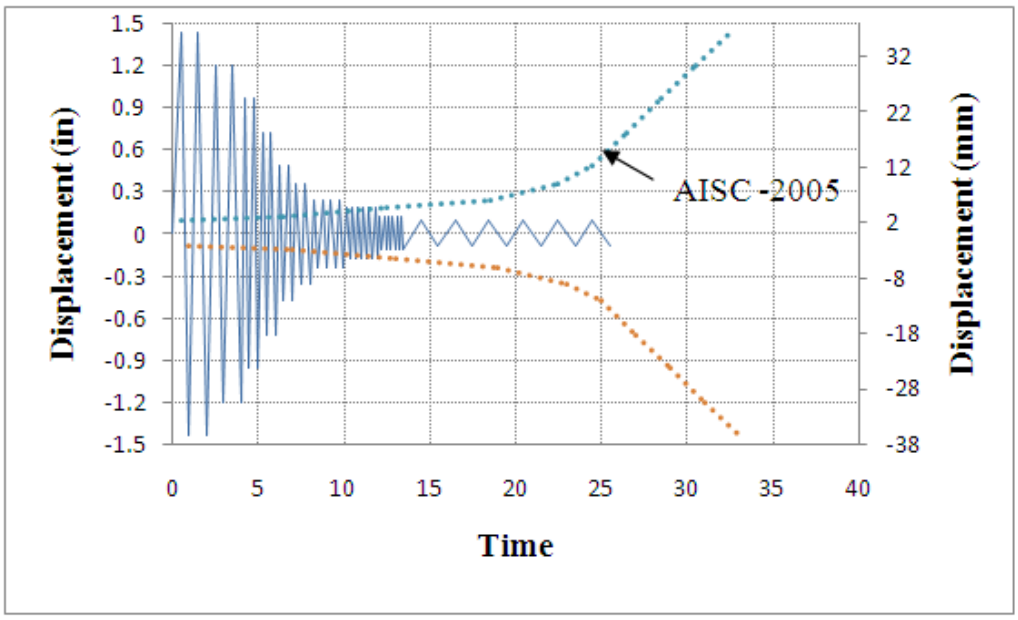

Figure 2-17 Displacement load history, DLC III-1- ½ - 1/3 – ¼ - 2

2.2.4 Displacement control loading Set IV

The Envelop B is used in this load set as a bounding envelop (Figure 2-2) the magnitude of the AISC-2005 loading protocol is streched to touched the Envelop B both on the positve and the negavtive sides of the loading history as shown Figure 2-18. Thus, the five different loading cases are devoloped by varing the baseline case (Figure 2-18) non-uniform by varing the loading period according to the algorithm used for load Set II and III. The detail of the loading time period and displacement amplitude for this load set is presented in Table 2-4. Figure 2-19 through Figure 2-23 shows the load cases of the load Set IV

Table 2-4 Loading case in Set IV

Regions	**Region I**		**Region II**					**Region III**	**Region IV**	**Region V**
Parts	**Part 1**	**Part 2**	**Part 3**	**Part 4**	**Part 5**	**Part 6**	**Part 7**	**Part 8**	**Part 9**	**Part 10**
No. of cycles	6	6	6	4	2	2	2	2	2	2
Amplitude (in)	0.09	0.336	0.6	0.84	1.008	1.104	1.152	1.248	1.334	1.44
DLC IV - 2- 1- 1/2- 1/3- 1/4	T = 2		T = 1					T = 1/2	T = 1/3	T = 1/4
DLC IV - 1/4- 2- 1- 1/2- 1/3	T = 1/4		T = 2					T = 1	T = 1/2	T = 1/3
DLC IV - 1/3- 1/4- 2- 1- 1/2	T = 1/3		T = 1/4					T = 2	T = 1	T = 1/2
DLC IV - 1/2- 1/3- 1/4- 2- 1	T = 1/2		T = 1/3					T = 1/4	T = 2	T = 1
DLC IV - 1- 1/2- 1/3- 1/4- 2	T = 1		T = 1/2					T = 1/3	T = 1/4	T = 2

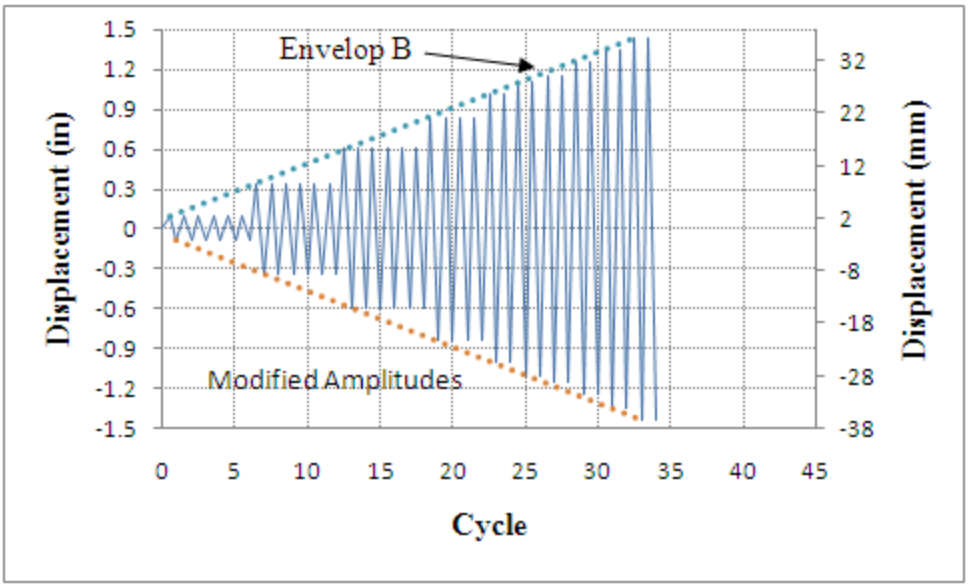

Figure 2-18 Typical loading Set IV

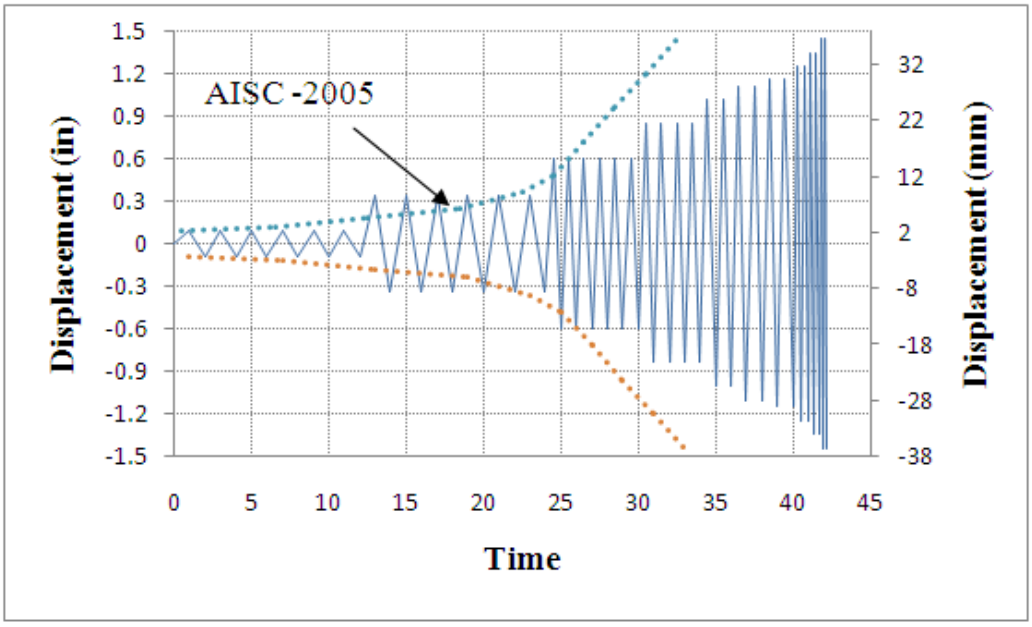

Figure 2-19 Displacement load history, DLC IV-2- 1- ½ -1/3- ¼

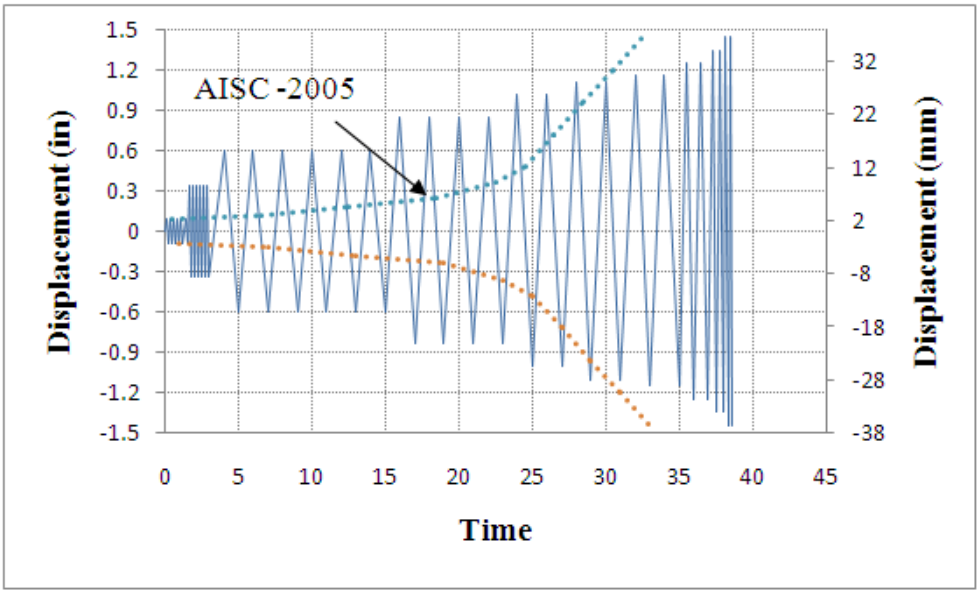

Figure 2-20 Displacement loading history, DLC IV-¼ -2 -1- ½ - 1/3

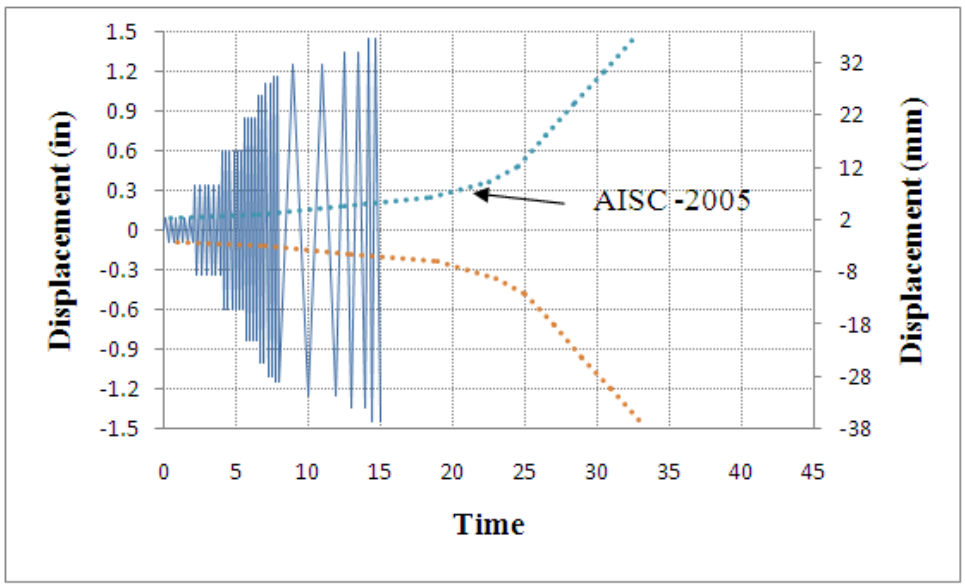

Figure 2-21 Displacement load history, DLC IV-1/3- ¼ -2- 1- ½

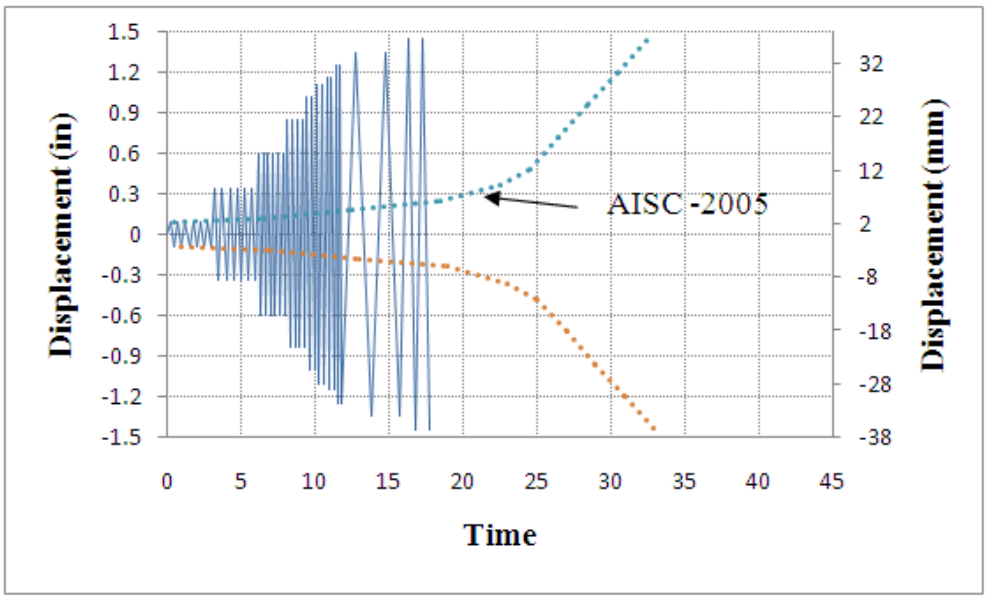

Figure 2-22 Displacement load history, DLC IV-½ - 1/3- ¼ - 2 - 1

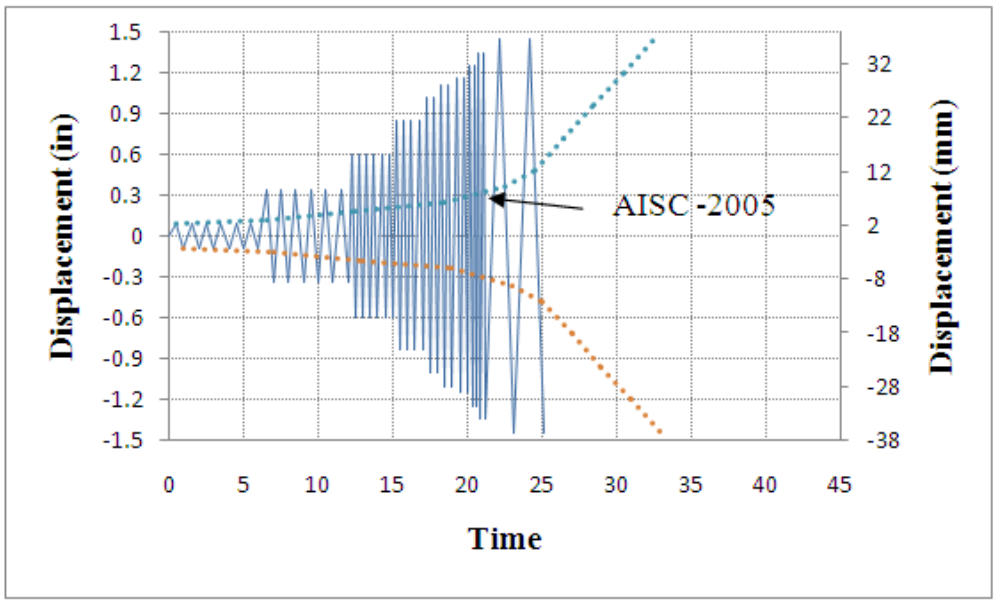

Figure 2-23 Displacement load history, DLC IV-1- ½ - 1/3 – ¼ - 2

2.2.5 Displacement control loading Set V

The loading cases for this set was obtained by appling the displacement amplitude of Set IV in reverse order as shown in Table 2-5. Figure 2-24 thorough Figure 2-28 shows the loading displacement histories devoloped in Set V.

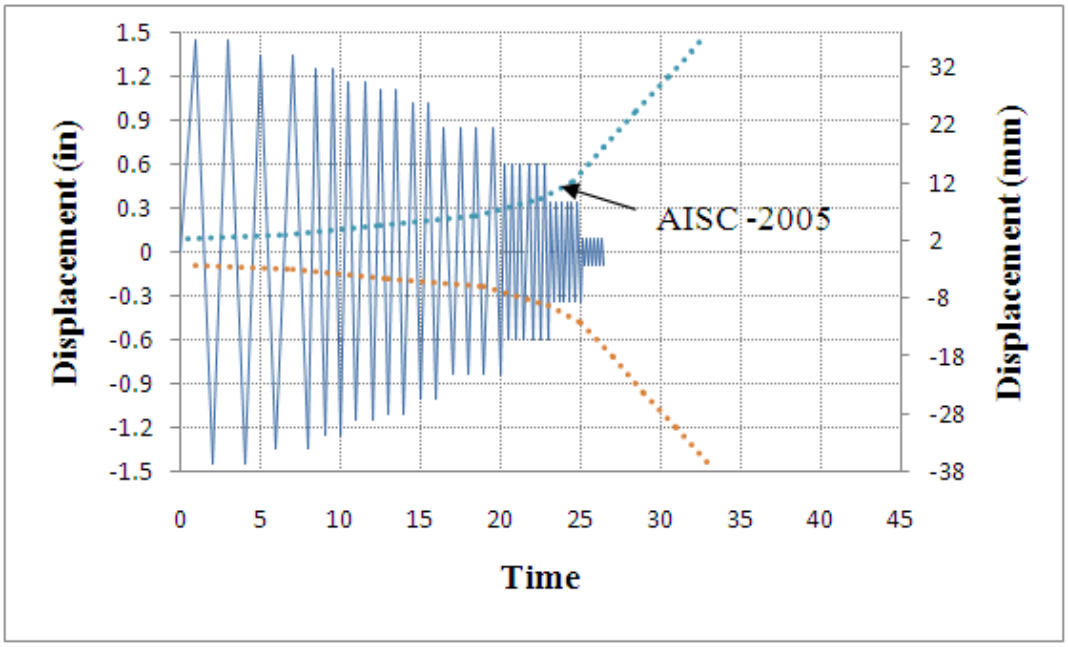

Figure 2-24 Displacement load history, DLC V-2- 1- ½ -1/3- ¼

Table 2-5 Loading cases in Set V

Regions	**Region I**		**Region II**					**Region III**	**Region IV**	**Region V**
Parts	**Part 10**	**Part 9**	**Part 8**	**Part 7**	**Part 6**	**Part 5**	**Part 4**	**Part 3**	**Part 2**	**Part 1**
No. of cycles	2	2	2	2	2	2	4	6	6	6
Amplitude (in)	1.44	1.334	1.248	1.152	1.104	1.008	0.84	0.6	0.336	0.09
DLC V - 2- 1- 1/2- 1/3- 1/4	T = 2		T = 1					T = 1/2	T = 1/3	T = 1/4
DLC V - 1/4- 2- 1- 1/2- 1/3	T = 1/4		T = 2					T = 1	T = 1/2	T = 1/3
DLC V - 1/3- 1/4- 2- 1- 1/2	T = 1/3		T = 1/4					T = 2	T = 1	T = 1/2
DLC V - 1/2- 1/3- 1/4- 2- 1	T = 1/2		T = 1/3					T = 1/4	T = 2	T = 1
DLC V - 1- 1/2- 1/3- 1/4- 2	T = 1		T = 1/2					T = 1/3	T = 1/4	T = 2

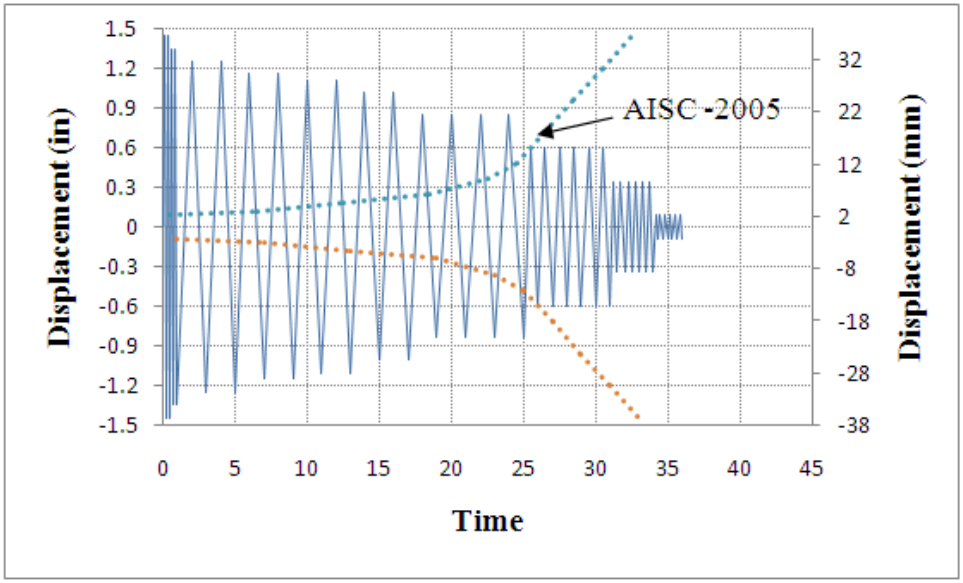

Figure 2-25 Displacement load history, DLC V-¼ -2 -1- ½ - 1/3

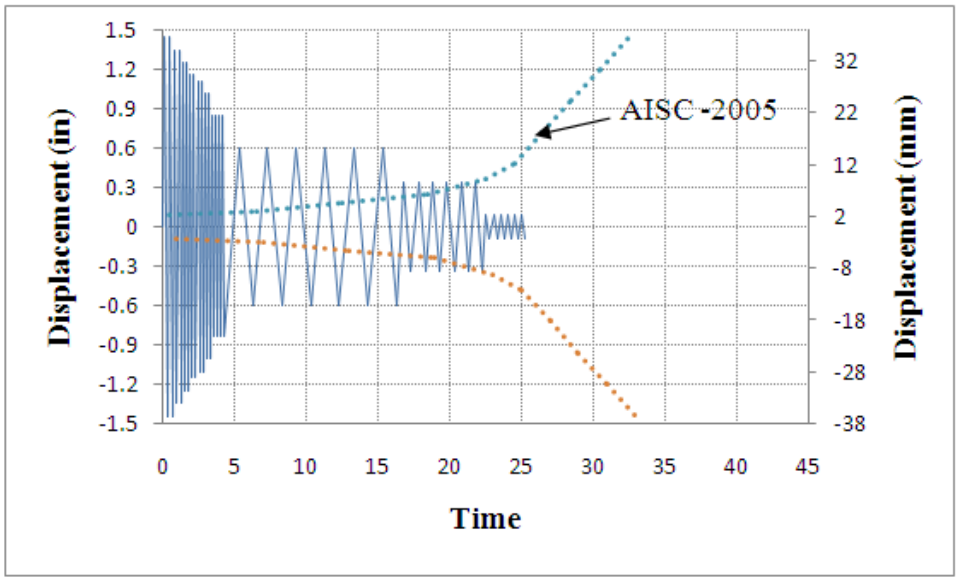

Figure 2-26 Displacement loading history, DLC V-1/3- ¼ -2- 1- ½

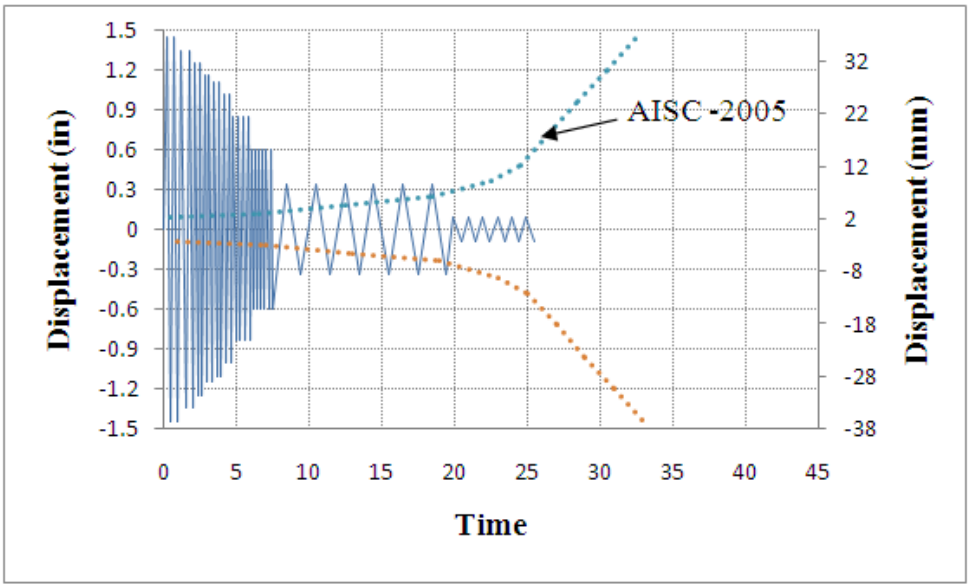

Figure 2-27 Displacement load history, DLC V-½ - 1/3- ¼ - 2 - 1

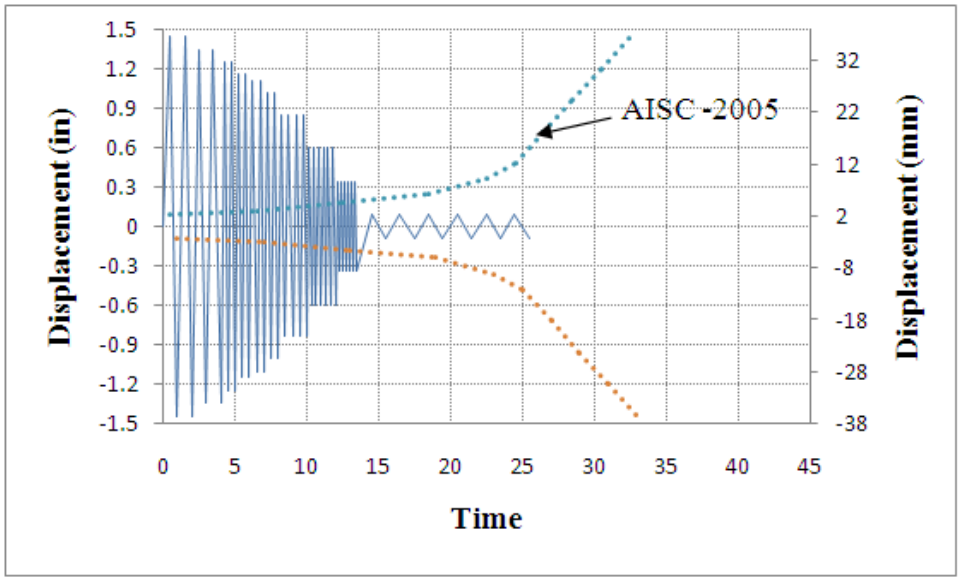

Figure 2-28 Displacement loading history, DLC V-1- ½ - 1/3 – ¼ - 2

CHAPTER 3

FINITE ELEMENT ANALYSIS

3.1 Introduction

Comprehensive non-linear three dimensional (3-D) finite element models (FEM) of connecting surfaces are developed to evaluate the significance of the AISC-2005 displacement load history on their response. Four simple connection models and one commonly used end plate connection were considered. A simple connection model includes the welded shear surface model, single and double bolted surface model, and tee- hanger model. End-plate connection assembly consisted of end plates, bolts, beams, and columns. Special attention was given to the contact surfaces in the modeling. For an example, contact between two plates and bolt was given a more importance in bolted shear and tee- hanger model. In case of the extended end plate connection, contact between end plate, column, and bolts was attended.

Classical cyclic plasticity based analysis algorithm consisted of material, geometrical, and contact nonlinearities which was used in model making process. Nonlinearity introduced in connecting surfaces by yielding was considered in model. Lagrangian algorithm was employed to account the geometrical nonlinearity.

To converge the solution, a P- convergence criterion was used in the models. In P convergence the higher order polynomial are used to define the displacement function. Energy based convergences are adopted over monotonic convergence as the models are mainly nonlinear. Figures used in following Table 3-1 are referred from ABAQUS User's Manual.

Table 3-1 Various elements used in study

Element	Description	D.O.F.	Element shape
C3D8R	Hexagonal Element	24	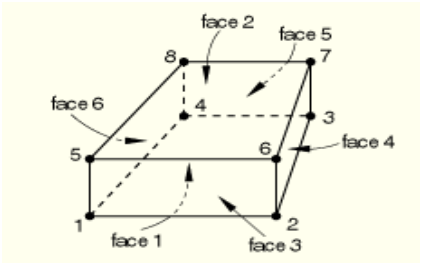
C3D20R	Hexagonal Element	60	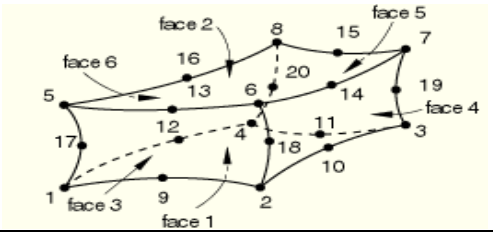
C3D4	Tetrahedral Element	12	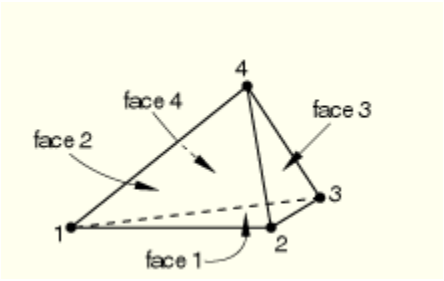

Table 3-1 - continued

C3D10M	Tetrahedral Element	30	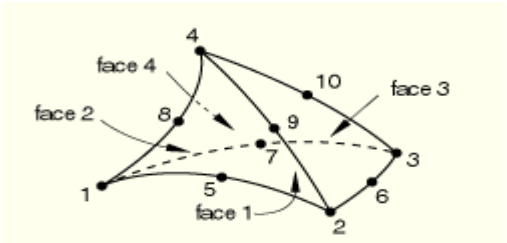

3.2 Material Model

Typically engineering materials initially responds elastically, which means deformation is fully recoverable after removal of the applied load, and specimen returns to its original shape. Once the load exceeds the yielding point, specimens do not return to its original shape. Some part of deformation remains unrecovered

Material behaviors for five different materials are defined in terms of bilinear stress-strain curve such as plates, end plate, bolts, beam, and column. These properties are defined in Table 3-2. End plate, plates, beam, and columns are made up of A36 steel, and bolts made of A325 steel. For end plate, plate, beam, column modulus of elasticity is 29000 ksi (201GPa), and first yield occurs at 36 ksi. Then material hardens to 58 ksi at 20% strain and poisons ratio of 0.29. The plastic strain at 20% strain point is $\varepsilon_p = 0.175$ (ASTM A36). Similarly, modulus of elasticity is 29000 ksi for bolts, and first yield occurs at 81 ksi to 92 ksi depending upon the bolt diameter. Then, material hardens to 105 ksi to 120 ksi at 20% strain and a poison ratio was 0.29. The plastic strain at 20%

strain point is ε_p= 0.144 (ASTM A325). Figure 3-1 is describing the material properties which were mentioned above. The initial slope of the curve is assigned as modulus of elasticity E. Post yielding stiffness identified in this case is 1% of initial stiffness. Post yield stiffness is referred as tangential stiffness (E_t = 0.01), which ensure the bilinear stress-strain relationship for the used material. Material is considered as isotropic material.

Table 3-2 Material properties

Material Properties	End plate, plate, Beam, Column (A36)	Bolt (A325)
Yield Stress (F_y)	36 ksi	92 ksi
Modulus of Elasticity (E)	29000 ksi (201 GPa)	29000 ksi (201 GPa)
Poisson's Ratio (υ)	0.29	0.29
Tangential Modulus (E_t)	290 ksi	290 ksi

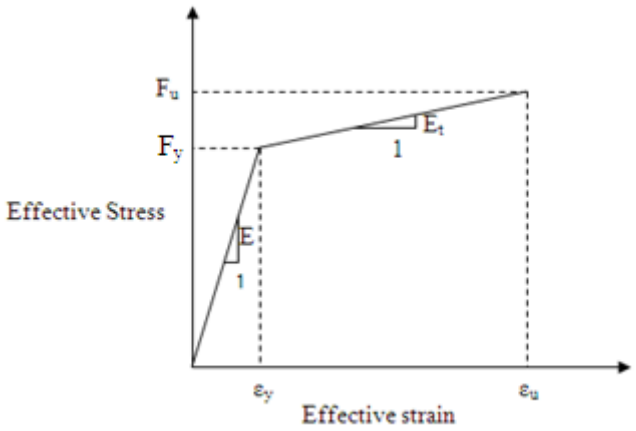

Figure 3-1 Typical Stress-Strain Curve

Linear elastic behavior was described within a material definition while defining the elasticity in ABAQUS. It is assumed that plastic strain governs the deformation in the elastic plastic analysis because the elastic strains are small. ABAQUS accounts this limitation during its analysis. The justification for dominance of plastic strain is given as; most of the engineering materials exhibit a well defined yield point, which is a very small percentage of their young's modulus. Generally, value of the yield stress is close to or less than 1% of the young's modulus of the material. Hence, the elastic strain will also be less than 1%.

Non recoverable deformation response is modeled by using the plasticity theory. In ABAQUS, non recoverable deformation is modeled using the incremental theories. The mechanical strain rate is identified in two different parts, elastic part and plastic part, in incremental theories. Nonlinear incremental solution technique was adopted due to changing contact status of bolted surfaces. Also, large deformation was one of the

reasons for the selection of nonlinear incremental technique. Loading histories were applied in small incremental load steps. Geometric nonlinearity was introduced to account for the large expected deformation by employing the large strain analysis. The advantage of applying the large strain analysis is that it negates any theoretical limitation on deformation or strain experience by element.

Newton-Raphson technique for nonlinear analysis was adopted in analysis. In Newton-Raphson, technique load is divided into a sequence of small load increments. The tangent modulus is updated in the beginning of each load step. The unbalance force was calculated at the end of single iteration, which was used to solve the incremental system equilibrium equation. Figure 3-2 shows the conceptual representation of nonlinear iteration procedure.

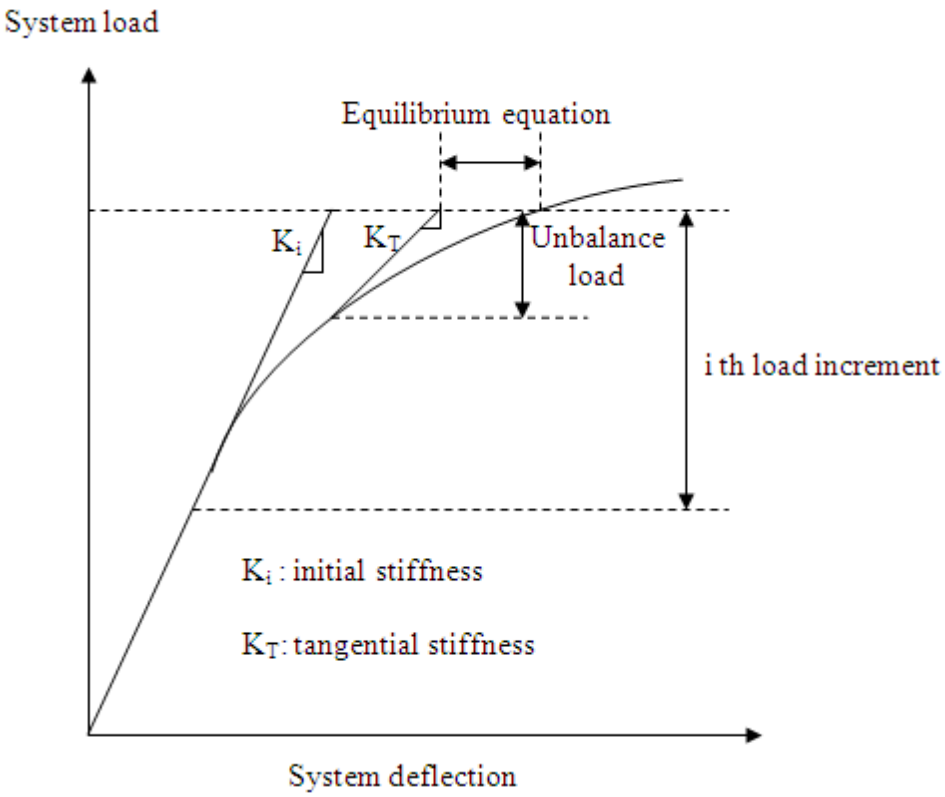

Figure 3-2 Newton Raphson technique

To stimulate the behavior of the connection under cyclic loading, a linear kinematic hardening model is employed from ABAQUS software. ABAQUS also implemented the Bauschinger effect in the model as shown in Figure 3-3

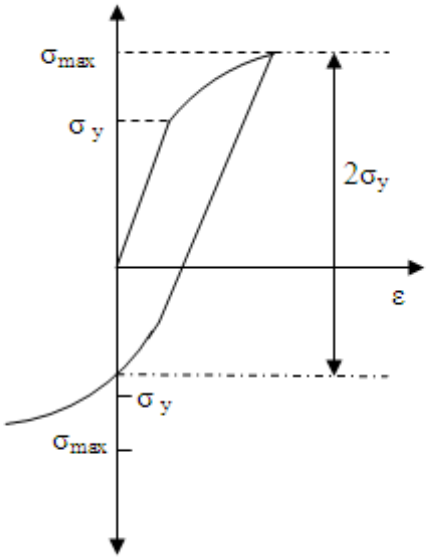

Figure 3-3 Bauschinger Effect

3.3 Bolt Pretension

Bolt pretension is the first step of load application in the entire loading process of the model. In this model, the bolts and its various components: bolt head, nut, and bolt shanks, are modeled with three dimensional solid elements. The Surface interactions between bolt shank, nut, and end plates are also defined in the model. To stimulate the effect of bolt tightening, pretension section of ABAQUS is applied. Pretension force was applied on bolts according to specification of AISC 2005. AISC 2005 defines the pretension force in terms of proof load. 70% of the bolt's ultimate tensile strength is applied as pretension load in AISC 2005. Pretension load was applied by passing an arbitrary plane through the bolt shank in ABAQUS. Then a load was applied on the

created surface due to the passing arbitrary plane in the direction perpendicular to the longitudinal axis. In previous studies of bolted models, the technique of applying a compressive force equivalent of pretension load was used to achieve the pretension effect. Technique of applying compressive force experiences a great deal of difficulty in monitoring the location of the connecting surface such as bolt head, nut, and end plates.

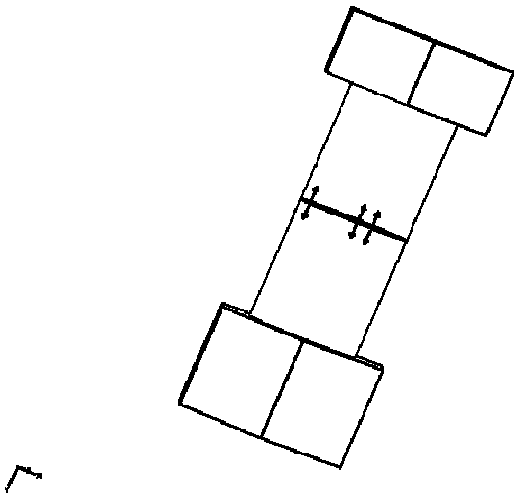

Figure 3-4 Bolt Pretensions

A wench is used to tighten a nut to the bolt for holding plates together. In the process of tightening of nut, the un-stretched grip length of the bolt shank reduces. Once the desired pretension force is applied to the bolt, the wench is removed and this reduced un-stretched grip causes the pretension in the bolt assembly. ABAQUS pretension element also follows the same procedure in an identical sequence to achieve the effect of pretension. In the analysis, the pretension load was applied in an incremental load step to achieve the desired displacement. Once the displacement is achieved it is locked and

possible material nonlinearity is introduced to the section. After the pretension procedure is completed, external load is applied on the model in an incremental manner.

3.4 Contact Modeling

Bolted connections are mainly dominated by the nonlinear algorithm due to the different status of friction between the surfaces. The contact surface between bolt shank and nut, plate to bolt, bolt head to plates, and nuts to plates are defined in the model for avoiding the numerical overlap between the connecting surfaces. All the connecting surfaces are defined in terms of the pairs. The larger part in the connecting pair is defined as the master surface and the comparatively smaller part is identified as slave surface. It was not mandatory to define larger surface as the master surface and smaller as slave. However, models devolved in this study follows above mentioned technique to maintain uniformity.

The connecting surfaces are defined with two different properties such as surface-to-surface, and node- to- surface. Both the surface- to- surface and node- to- surface algorithms are employed to two different models. No model is employed with these two algorithms at the same time. Surface- to- surface and node –to- surface algorithms are employed to connecting surfaces: bolt to plate, bolt shank to nut, nut head to plate, and plate to bolt head. In the case of the single bolted shear model the contact pairs are plate to plate, bolt head to plate, nut head to plate, bolt shank to plates, and bolt shank to nut. Similar contact pairs are identified in the case of the double bolt shear model with two bolts which connects the surface instead of one. In T model contact pairs are flange to

flange, bolt head to plate, nut to plate, and bolt shank to flange with four bolts in the model. For extended end plate connection, contact pairs are end plate to column, bolt head to end plate, nut to column flange, bolt shank to column flange, and bolt shank to end plate. In the extended end plate connection, the beam and end plate are connected to each other by tie algorithm to stimulate the effect of welding. Apart from bolted connections, one welded shear connection is modeled so two plates are connected together by defining them as a tied surface. Tie constrain stimulates the effect of welding by preventing the friction between connecting surface unlike the bolted connections.

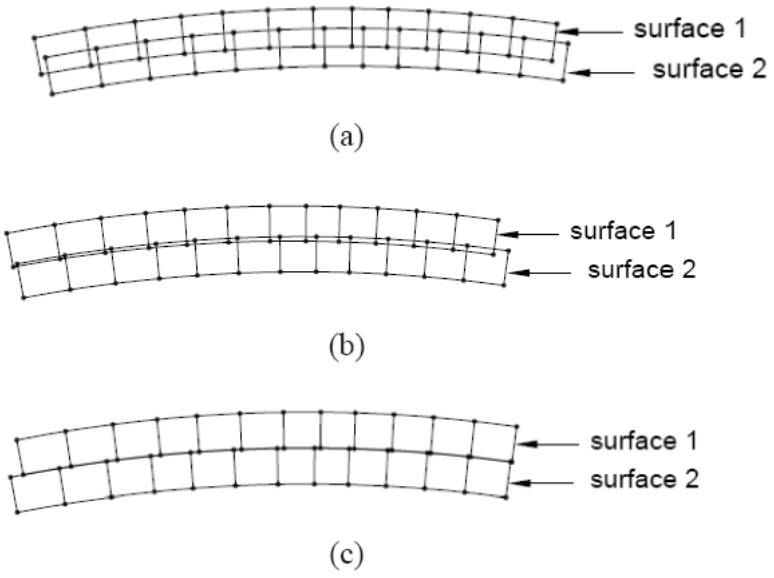

Figure 3-5 Contact interactions between two surfaces; (a) beginning of step, (b) middle step, (c) end step, prepared by Le, 2008

Distribution of contact stress is an important aspect of the contact surface modeling. To stimulate the contact surface effectively an adequate mesh density is required, because the region undergoes a plastic deformation to allow contact stress to

distribute. Both surface to surface and node to surface contact algorithms used in ABAQUS are deformable finite element. Friction plays an important role in contact algorithm. To indicate the roughness of the surface, two values for the coefficient of friction, 0.35 and 0.2, was used.

3.5 Model Verification

A convergence study was carried out on all the models developed in the project using different mesh densities. The geometrical nonlinearity algorithm was not used in the case of welded connection models. Finite element model is verified by using P-conversion technique. The numbers of elements are increased until the load- deflection curve observes no impact in P-convergence technique.

3.6 Development of finite element models

Each finite element model assembly is created by different individual parts. For example, three different parts, bolt head, bolt shank, and nut were created in the bolt model. Then the three parts were assembled to create the model. AISC 2005 guideline was followed to obtain the practically accepted dimensions.

3.6.1 Welded shear surface model

3.6.1.1 Assembly

Welded shear surface model was the simplest model among all the models. Two plates of identical thickness are welded together.

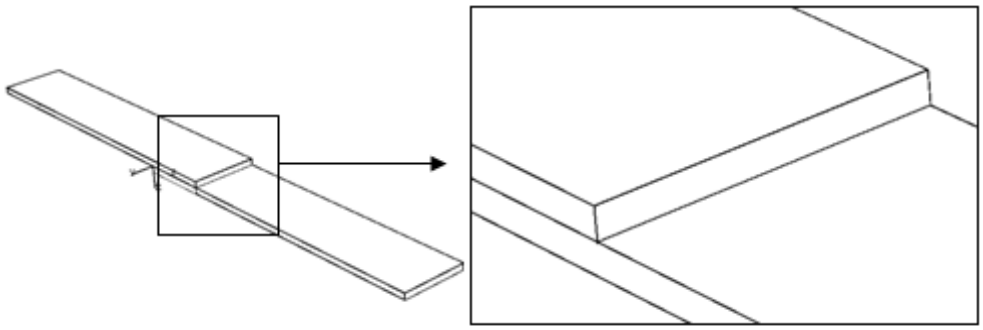

Figure 3-6 Welded shear surface model

3.6.1.2 Contact Definition

Welded connection was stimulated in the model by using tie constraints. Since there is only one connecting surface, no other contact property was defined apart from the tie constrain. Both the plates were the same dimensions; hence one surface was randomly defined as master surface and the other as slave surface.

Table 3-3 Connection properties for welded connection

Contact pair	**Master Surface**	**Slave Surface**	**Constrain**
Top- Bottom plate	Top plate	Bottom plate	Tie

3.6.1.3 Boundary Condition

Three different boundary conditions are defined in the model. Firstly one end of the connection is fixed for preventing any kind of movement. Then rollers are applied on one lateral edge of the connection in order to avoid any unwanted lateral displacement. The most important boundary condition was defined in terms of displacement control loading. To apply a deformation on a specific point on the model a roller support was attached to that point. Then the roller support was displaced in a predefined sequence.

3.6.2 Bolted Shear Surface Models

3.6.2.1 Assembly

In the case of bolted shear surface models, three main components were developed. Model consists of two plates connecting each other by bolts. Single bolted shear surface exhibit the use of one bolt, whereas double bolt connection indicates the use of two bolts for connection. As mentioned earlier, connection assemblies are developed in the parts. For example, bolts are developed in three different parts such as bolt head, bolt shank, and nut. Similarly, plates and bolts are developed individually and then assembled back to form a model.

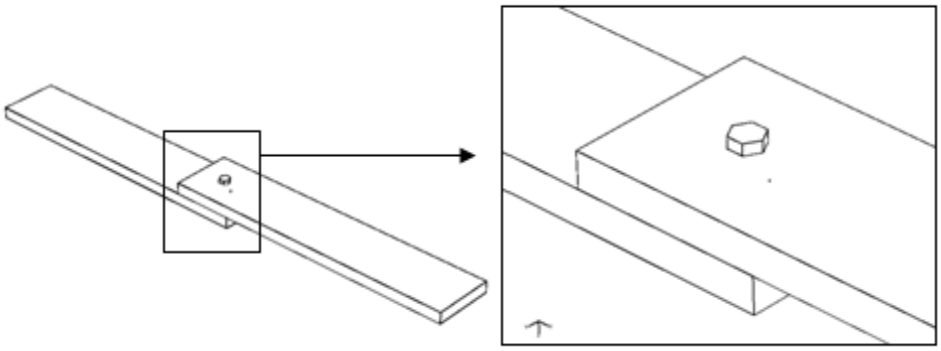

Figure 3-7 Single bolted shear surface model

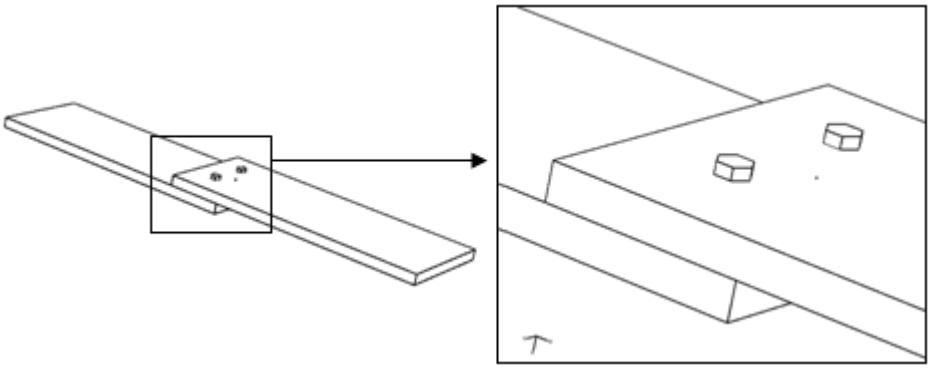

Figure 3-8 Double bolted shear surface model

3.6.2.2 Contact Definition

Single and double bolted shear models are more complex in nature than the previous model. More numbers of connecting surfaces were introduced in this type of model. In order to accurately stimulate the effects of a connecting surface various properties are defined. The most challenging connecting surface was between the bolt shank and the plates. Some other connections introduced in the model were plate to plate, bolt head to plate, and nut to plate.

Table 3-4 Contact properties for single bolted surface models

Contact pair	**Master Surface**	**Slave surface**	**Tangential behavior**		**Normal Behavior**
			Frictional Formation	**Frictional coefficient**	
Top-Bottom Plate	Top plate	Bottom plate	Penalty	0.35	Hard Contact
Bolt head-Top plate	Top plate	Bolt head	Penalty	0.2	Hard Contact
Nut-Bottom plate	Bottom plate	Nut	Penalty	0.2	Hard Contact
Bolt shank-both plates	Bolt shank	Plates	Penalty	0.2	Hard Contact
Bolt shank-Nut	Bolt shank	Nut	Penalty	0.2	Hard Contact

Table 3-5 Contact properties for double bolted surface models

Contact pair	**Master Surface**	**Slave surface**	**Tangential behavior**		**Normal Behavior**
			Frictional Formation	**Frictional coefficient**	
Top-Bottom Plate	Top plate	Bottom plate	Penalty	0.35	Hard Contact
1st Bolt head-Top plate	Top plate	Bolt head	Penalty	0.2	Hard Contact
2nd Bolt head-Top plate	Top plate	Bolt head	Penalty	0.2	Hard Contact
1st Nut-Bottom plate	Bottom plate	Nut	Penalty	0.2	Hard Contact
2nd Nut-Bottom plate	Bottom plate	Nut	Penalty	0.2	Hard Contact

Table 3-5 – continued

1st Bolt shank-both plates	Bolt shank	Plates	Penalty	0.2	Hard Contact
2nd Bolt shank-both plates	Bolt shank	Plates	Penalty	0.2	Hard Contact
1st Bolt shank-Nut	Bolt shank	Nut	Penalty	0.2	Hard Contact
2nd Bolt shank-Nut	Bolt shank	Nut	Penalty	0.2	Hard Contact

3.6.2.3 Boundary Condition

Similar to the earlier model, three boundary conditions were applied in this model. One end of the connection was fixed. Further, to prevent lateral displacement, a roller support was applied on the lateral edge of the connection. Displacement control loading was applied as a third boundary condition.

3.6.3 Tee - Hanger Model

3.6.3.1 Assembly

The tee – Hanger model consists of two T sections connected to each other by flanges using four bolts. T- Section was developed in two different parts to form an assembly, the flange, and web. Similarly bolts were also developed in three different parts as explained earlier.

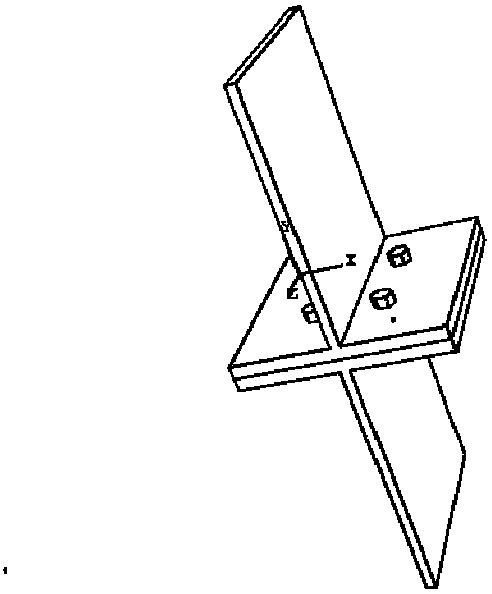

Figure 3-9 Tee-hanger model

3.6.3.2 Contact Definition

The tee – hanger model shows a contact surface between two flanges. Dimensions of both flanges are identical. Hence, one surface was selected randomly as master surface

and the other as slave surface. Contact surface between bolts and flanges was another critical surface identified in the model. In this case, flange surface is considered as master surface and bolt shank was designated as salve surface. Flange surface was identified as master surface and bolt head was considered as a slave surface in contact between flange and bolt head. Finally, the flange was considered as a master surface and nut as slave in contact between nut and flange.

Table 3-6 Properties for tee – hanger model

Contact pair	**Master Surface**	**Slave surface**	**Tangential behavior**		**Normal Behavior**
			Frictional Formation	**Frictional coefficient**	
Top-Bottom Flange	Top flange	Bottom flange	Penalty	0.35	Hard Contact
1st Bolt head-Top flange	Top flange	Bolt head	Penalty	0.2	Hard Contact
2nd Bolt head-Top flange	Top flange	Bolt head	Penalty	0.2	Hard Contact

Table 3-6 – continued

3rd Bolt head-Top flange	Top flange	Bolt head	Penalty	0.2	Hard Contact
4th Bolt head-Top flange	Top flange	Bolt head	Penalty	0.2	Hard Contact
1st Nut-Bottom flange	Bottom flange	Nut	Penalty	0.2	Hard Contact
2nd Nut-Bottom flange	Bottom flange	Nut	Penalty	0.2	Hard Contact
3rd Nut-Bottom flange	Bottom flange	Nut	Penalty	0.2	Hard Contact
4th Nut-Bottom flange	Bottom flange	Nut	Penalty	0.2	Hard Contact

Table 3-6 – continued

1st Bolt shank-both flanges	Bolt shank	Flanges	Penalty	0.2	Hard Contact
2nd Bolt shank-both flanges	Bolt shank	Flanges	Penalty	0.2	Hard Contact
3rd Bolt shank-both flanges	Bolt shank	Flanges	Penalty	0.2	Hard Contact
4th Bolt shank-both flanges	Bolt shank	Flanges	Penalty	0.2	Hard Contact
1st Bolt shank-Nut	Bolt shank	Nut	Penalty	0.2	Hard Contact
2nd Bolt shank-Nut	Bolt shank	Nut	Penalty	0.2	Hard Contact

Table 3-6 – continued

3rd Bolt shank-Nut	Bolt shank	Nut	Penalty	0.2	Hard Contact
4th Bolt shank-Nut	Bolt shank	Nut	Penalty	0.2	Hard Contact

3.6.3.3 Boundary Condition

In tee- hanger, to prevent buckling of the web section while loading, roller supports were applied on one phase of the web. Similarly, roller supports are attached on one of the lateral edges to prevent any deformation normal to loading. Displacement control loading method was used in which the roller was applied on the point to be loaded. Then the roller support was displaced at a predetermined rate.

3.6.4 Extended end-plate connection model

3.6.4.1 Assembly

Extended end-plate connection model was the most complicated assembly developed in the study. Extended end-plate assembly consisted of column, beam, end-plate, and bolts. The column was developed in two different parts; plate and L section, and assembled. The beam and end plate were developed as single parts. Bolts were again developed in three different parts and assembled.

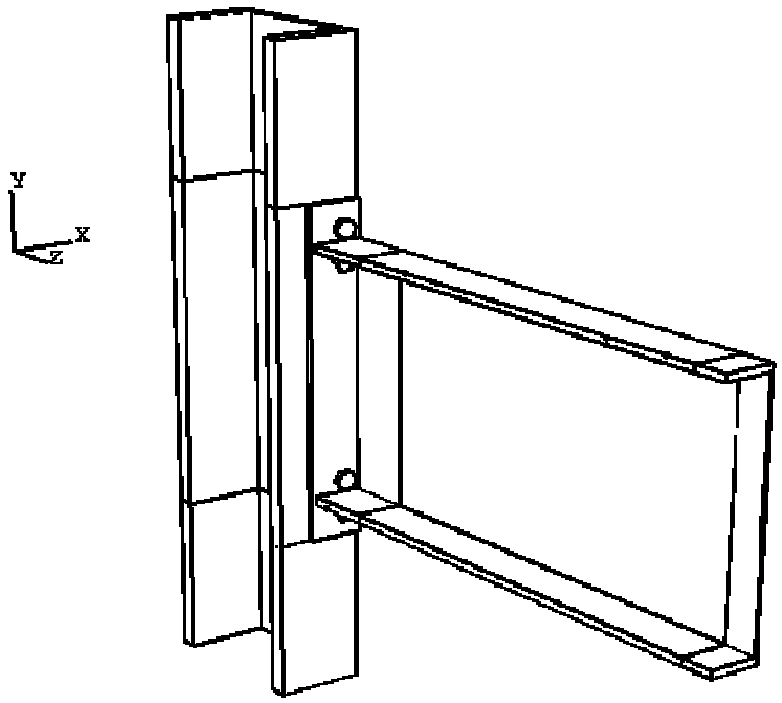

Figure 3-10 Extended end-plate connection

3.6.4.2 Contact Definition

Various contacts were identified in extended end plate connection model. Firstly, column surface and end-plate surface was identified as master surface and slave surface respectively. Beam and end-plate were merged together to stimulate the welding effect. Contact between bolt shank-end plate, and bolt shank- column was the trickiest of all. In this case, end-plate and column surfaces were identified as master surface together and bolt shank was defined as slave surface. Surface-to-surface and node-to-surface contact algorithm were applied individually to study their effect.

Table 3-7 Contact properties for extended end-plate model

Contact pair	**Master Surface**	**Slave surface**	**Tangential behavior**		**Normal Behavior**
			Frictional Formation	**Frictional coefficient**	
Column-End plate	Column	Plate	Penalty	0.35	Hard Contact
1st Bolt head-End plate	End plate	Bolt head	Penalty	0.2	Hard Contact
2nd Bolt head-End plate	End plate	Bolt head	Penalty	0.2	Hard Contact
3rd Bolt head-End plate	End plate	Bolt head	Penalty	0.2	Hard Contact
4th Bolt head-End plate	End plate	Bolt head	Penalty	0.2	Hard Contact

Table 3-7 – continued

1st Nut-column flange	Column flange	Nut	Penalty	0.2	Hard Contact
2nd Nut-column flange	Column flange	Nut	Penalty	0.2	Hard Contact
3rd Nut-column flange	Column flange	Nut	Penalty	0.2	Hard Contact
4th Nut-column flange	Column flange	Nut	Penalty	0.2	Hard Contact
1st Bolt shank-column flanges- End plate	Bolt shank	flanges	Penalty	0.2	Hard Contact

Table 3-7 – continued

2nd Bolt shank-Column flanges- End plate	Bolt shank	flanges	Penalty	0.2	Hard Contact
3rd Bolt shank-column flanges- End plate	Bolt shank	flanges	Penalty	0.2	Hard Contact
4th Bolt shank-Column flanges- End plate	Bolt shank	flanges	Penalty	0.2	Hard Contact
1st Bolt shank-Nut	Bolt shank	Nut	Penalty	0.2	Hard Contact

Table 3-7 – continued

2nd Bolt shank-Nut	Bolt shank	Nut	Penalty	0.2	Hard Contact
3rd Bolt shank-Nut	Bolt shank	Nut	Penalty	0.2	Hard Contact
4th Bolt shank-Nut	Bolt shank	Nut	Penalty	0.2	Hard Contact

3.6.4.3 Boundary Condition

Column was fixed from the top, bottom and vertical side to prevent any sort of deformation after application of load. A symmetrical fixed condition was applied on one face of the connection model because only half of the model was created due to symmetry. Roller supports were applied on the beam flange to avoid buckling of the flange. Displacement control loading was adopted to load the model by attaching a roller support. The roller support was displaced to a predefined magnitude to introduce the force in the model.

3.6.4.4 Symmetric Modeling

Symmetric modeling is a technique to reduce the complicated nature of the model by just considering half of the model. A model is called symmetric when both load and geometry are symmetrical. All the nodes on the plane of symmetry are restrained from translation in three dimensional spaces. The extended end plate connection was the only model in this study considered as symmetrical due to its load and geometrical setups. Only half of the model is considered for achieving the simplicity and reducing the time require for analysis.

CHAPTER 4

PARAMETRIC STUDY

4.1 Introduction

This chapter focuses on the parametric study carried out on the finite element models developed for connecting surfaces. Different combinations of geometric parameters, such as the level of pretension, contact properties, element type, and loading histories, were considered in the parametric study. To study the effect of each parameter on the connecting surfaces test combinations were created by varying geometric and force related variables.

Geometric variables depend on different types of connection surfaces. For example in the case of welded shear surface the only geometrical variable is plate thickness, whereas in bolted shear surfaces along with plate thickness, bolt diameter is also considered as a geometric variable. Pretension was another parameter which was varied in the study. Pretension was varied in three different stages: full pretension, half pretension, and quarter pretension. Contact property was defined in two ways, first was surface-to-surface and second was node-to-surface. In terms of element type, hexagonal element and combined element with regular and higher order were used individually and

in combination to study their effect. Loading history was given prime importance in the study. In all 25 different loading histories are developed in the process to study the effect of loading history on the connecting surfaces. A detail discussion of each parameter is carried out in the subsequent section.

4.2 Test Cases Nomenclature

443 tests were carried out on different finite element models of connecting surfaces: welded shear surface, one and two bolt shear model, tee- hanger, and extended end plate model. To identify different parameters in the test, individual variables used are defined as follows.

- t_p = plate thickness
- t_f = flange thickness
- b_d = bolt diameter
- SM = shear model
- 1B = single bolt model
- 2B= double bolt model
- W = welded model
- T = T hanger model

- PT = pretension load
- FP = full pretension
- HP = half pretension
- QP = quarter pretension
- ET = element type
- HX = hexagonal element
- C = combined element
- t_e = end plate thickness
- g = gauge distance
- C_t = contact type
- E = elastic modulus
- F_y = yield stress
- DLC = displacement load case
- EEP = extended end plate connection model
- SS = surface- to- surface

- NS = node-to- surface

In the case of defined variable, some numbers are attached to further differentiate the variable. For example DLC I-2 indicates displacement loading case two of Set-I. Further, the entire test case was termed in a specific way to make it simple to identify. For example, a test was identified as SM-W- t_p -DLC. In the nomenclature, first the type of model is defined. Then a type of connection is defined, which was welded in the above case. Then, plate thickness was defined and loading case followed next. Figure 4-1 shows the sequence of various parameters in a test designation.

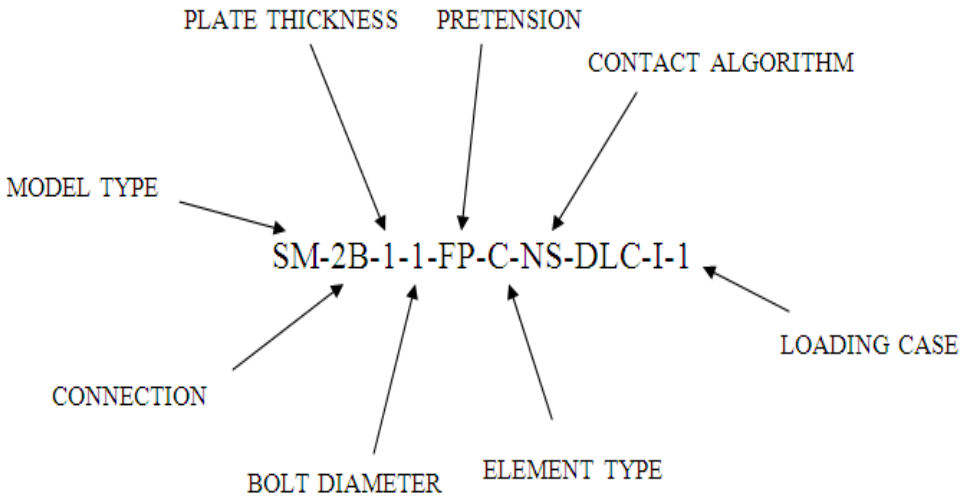

Figure 4-1 Sequence in test designation

4.3 Geometric Variables

Geometric parameter is considered to be one of the most important factors while studying the impact of various parameters on the connecting surface. In this study, commonly used simple connecting surfaces are developed along with the extended end plate connection, hence bolt diameter and plate thickness are the major variables for parametric study.

4.3.1 Welded shear surface models

In welded shear surface finite element model, the only geometrical change was plate thickness. Plate thickness was varied in two different sizes: ½ in and 1 in. Plate dimensions were kept constant apart from plate thickness. Table 4-1explains the combinations used in the model.

Table 4-1 Geometrical combination for welded shear surface model

Geometrical variable	Case 1	Case 2	Models
t_p	½ in	1 in	1. t_p = ½ in 2. t_p = 1 in

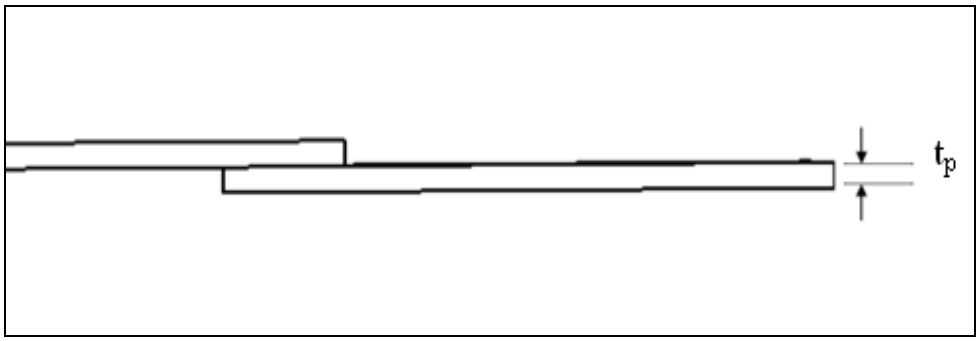

Figure 4-2 Welded shear surface model

4.3.2 Bolted shear surface models

In the case of one and two bolted shear surface finite element models, the geometrical variables are plate thickness and bolt diameter. Both plate thickness, and bolt diameter are varied two times. Then three more cases are developed by combining these two variables.

Table 4-2 Geometrical combinations for single and double bolted shear surface model

Variable parameter	Case 1	Case 2	Models
b_d	½ in	1 in	1. b_d = ½ in, t_p = 1 in
t_p	¼ in	1 in	2. b_d =1 in, t_p = ¼ in 3. b_d =1 in, t_p = 1 in

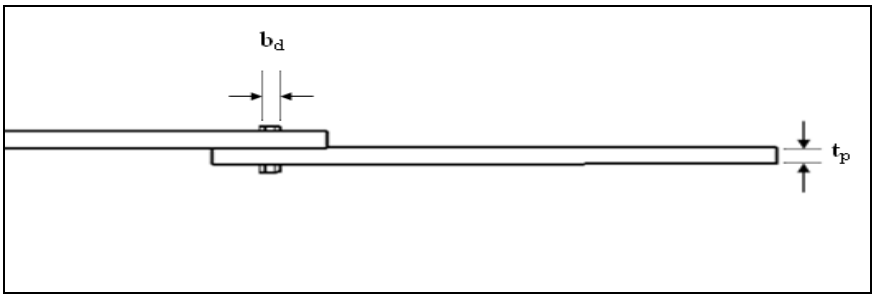

Figure 4-3 Bolted shear surface model

4.3.3 Tee- hanger models

Similarly for the tee- hanger model, two geometric variables are considered and three cases are made from the combination of two variables. Bolt diameter and flange thickness are varied for the parametric study. Apart from bolt diameter and flange thickness, gauge length is also varied within the combination. Unlike flange thickness

and bolt diameter, gauge length is not varied as an individual case. The effect of gauge length is incorporated within the model combinations.

Table 4-3 Geometrical combinations for T- Hanger model

Variable parameter	Case 1	Case 2	Models
b_d	½ in	1 in	1. b_d = ½ in, t_f = 1 in, g = 1½ in
t_f	¼ in	1 in	2. b_d =1 in, t_f = 1 in, g = 2¾ in 3. b_d = ½ in, t_f = ½ in, g = 1 in

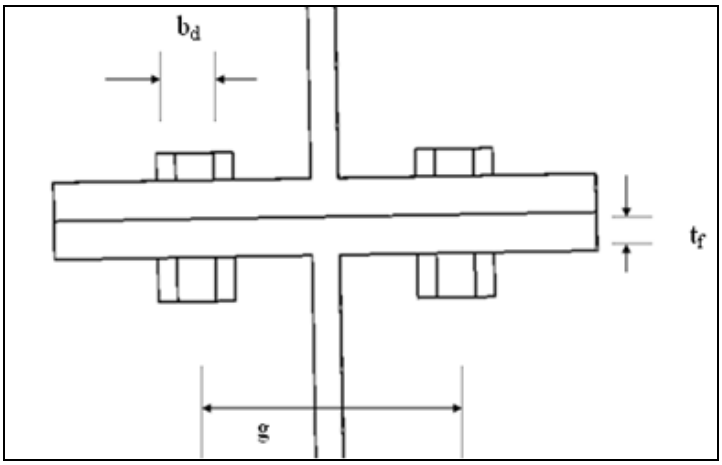

Figure 4-4 Tee-hanger model

4.3.4 Extended end-plate connection model

In the case of extended end plate connection models, the parameter was end-plate thickness and bolt diameter. Unlike other connections, all the variables are varied at a time instead of individual change. Two different combinations of extended end plate connections were formed to test.

Table 4-4 combinations for extended end plate model

Variable parameter	Case 1	Case 2	Models
t_e	½ in	1 in	1. t_e = ½ in, b_d = 1 in
b_d	½ in	1 in	2. t_e = ½ in, b_d = ½ in

4.4 Loading Cases

4.4.1 Displacement control loading cases

In the study, two approaches to load the connecting surface were adopted: displacement control and load control. Displacement loading cases are the most important aspect, which was studied to observe its impact on the connecting surface. To study the impact of loading history on the connecting surface, 25 different loading cases were developed for displacement control. These multiple cases are mainly based on two profiles. First profile is a curve and second is linear. The nature of the profile was change

to introduce the variation in magnitude of displacements. The nature of the loading profiles was inspired from the AISC Seismic Provision 2005.

4.4.2 Load control loading case

Apart from displacement control, load control technique was also used in the study. Unlike the displacement control loading case, no variation was attempted. Only one case of load control loading history was used. To start with loading one kip of load was applied in three consquative cycles. After initial three cycles the load was again increased to two kip. This pattern was followed until the load reached five kip. Once the load reached five kip, it was applied in a single cycle and the load was incresed by one kip after every cycle. Figure 4-2 shows the loading history.

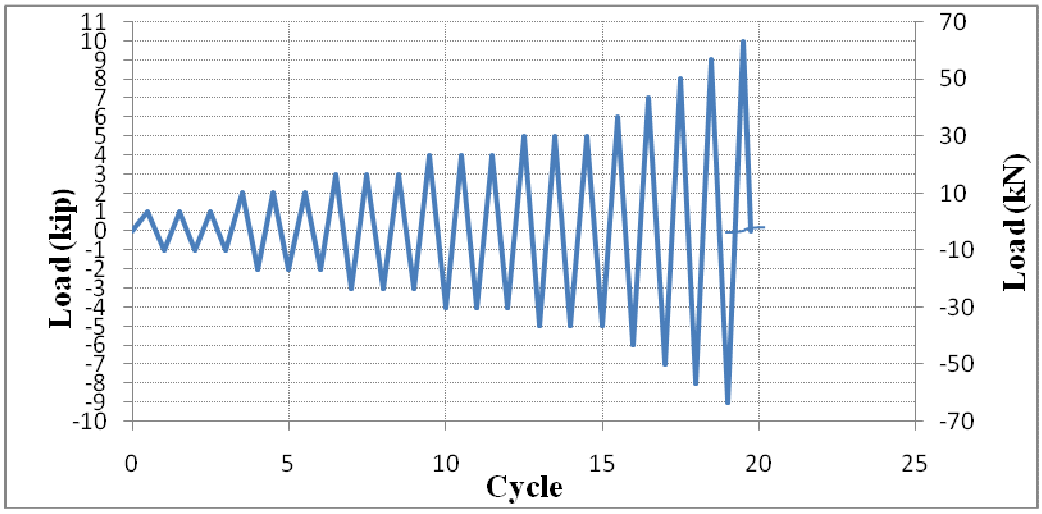

Figure 4-5 Typical Load control Loading History

4.5 Pretension

Pretension was another issue given great importance in the study. Pretension applied on the bolts depends on the bolt diameter. In the paramteric study, pretension was varied in three stages. First the full pretension was applied under the displacement control loading. Then pretension was redused to half and quarter in second and third stages respectivly. No pretension load was applied in welded connection.

Table 4-5 Pretension load corresponding to bolt diameter

Bolt diameter (in)	0.5	0.75	1	1.25	1.5	1.75	2
Pretension load (kip)	12	28	51	71	103	152	198

4.6 Contact

Contact was defined in two different ways: surface-to-surface and node-to-surface. Each case was defined individually to observe the effect. Node-to-surface contact definition was applied under the load deformation DLC I - 1.

4.7 Element Type

Three different higher order element types were used in the study: hexagonal element, tetrahydral element, and combination of the first two. All the element types were

used under the displacement control loading. Genrally combination was used in case of all type of bolted models. Bolts was assingned as tetrahydra elements and plates as hexagonal elements. In the case of welded shear surface only first two higher element types were used. Combined element type was not studied.

4.8 Results of parametric study

Table 4-6 Welded shear surface model (SM-W-1/2) Case1

Load cases	Energy Dissipation (Kip-in)	Percentage Difference (%)
DLC I-1	120.96	0.00
DLC I-2	125.52	3.63
DLC I-1/2	122.88	1.56
DLC I-1/3	119.76	-1.00
DLC I-1/4	120.48	-0.40
DLC II-2- 1- ½ -1/3- ¼	128.88	0.00
DLC II- ¼ -2 -1- ½ - 1/3	128.4	-0.37
DLC II- 1/3- ¼ -2- 1- ½	125.52	-2.68
DLC II- ½ - 1/3- ¼ - 2 - 1	126	-2.29
DLC II- 1- ½ - 1/3 - ¼ - 2	127.68	-0.94
DLC III- 2- 1- ½ -1/3- ¼	122.88	0.00
DLC III- ¼ -2 -1- ½ - 1/3	123.36	0.39
DLC III- 1/3- ¼ -2- 1- ½	124.08	0.97
DLC III- ½ - 1/3- ¼ - 2 - 1	123.36	0.39
DLC III- 1- ½ - 1/3 - ¼ - 2	123.12	0.19
DLC IV- 2- 1- ½ -1/3- ¼	128.4	0.00
DLC IV- ¼ -2 -1- ½ - 1/3	129.36	0.74
DLC IV- 1/3- ¼ -2- 1- ½	127.44	-0.75
DLC IV- ½ - 1/3- ¼ - 2 - 1	117.36	-9.41
DLC IV- 1- ½ - 1/3 - ¼ - 2	124.8	-2.88
DLC V- 2- 1- ½ -1/3- ¼	128.64	0.00
DLC V- ¼ -2 -1- ½ - 1/3	128.4	-0.19
DLC V- 1/3- ¼ -2- 1- ½	126.24	-1.90
DLC V- ½ - 1/3- ¼ - 2 - 1	125.76	-2.29
DLC V- 1- ½ - 1/3 - ¼ - 2	127.68	-0.75
LLC	121.68	-3.06

Table 4-7 Welded shear surface model (SM-W-1) Case2

Load cases	Energy dissipation (kip-in)	Percentage Difference (%)
DLC I-1	58.8	0.00
DLC I-2	58.32	-0.82
DLC I-1/2	60.48	2.78
DLC I-1/3	57.12	-2.94
DLC I-1/4	58.8	0.00
DLC II-2- 1- ½ -1/3- ¼	57.12	0.00
DLC II- ¼ -2 -1- ½ - 1/3	60.72	5.93
DLC II- 1/3- ¼ -2- 1- ½	58.56	2.46
DLC II- ½ - 1/3- ¼ - 2 - 1	59.52	4.03
DLC II- 1- ½ - 1/3 - ¼ - 2	56.64	-0.85
DLC III- 2- 1- ½ -1/3- ¼	61.44	0.00
DLC III- ¼ -2 -1- ½ - 1/3	54.48	-12.78
DLC III- 1/3- ¼ -2- 1- ½	55.68	-10.34
DLC III- ½ - 1/3- ¼ - 2 - 1	56.64	-8.47
DLC III- 1- ½ - 1/3 - ¼ - 2	57.36	-7.11
DLC IV- 2- 1- ½ -1/3- ¼	59.76	0.00
DLC IV- ¼ -2 -1- ½ - 1/3	54	-10.67
DLC IV- 1/3- ¼ -2- 1- ½	56.88	-5.06
DLC IV- ½ - 1/3- ¼ - 2 - 1	60.24	0.80
DLC IV- 1- ½ - 1/3 - ¼ - 2	59.04	-1.22
DLC V- 2- 1- ½ -1/3- ¼	58.32	0.00
DLC V- ¼ -2 -1- ½ - 1/3	62.88	7.25
DLC V- 1/3- ¼ -2- 1- ½	62.4	6.54
DLC V- ½ - 1/3- ¼ - 2 - 1	57.36	-1.67
DLC V- 1- ½ - 1/3 - ¼ - 2	59.28	1.62
LLC	54.78	-7.34

Table 4-8 Single bolted shear surface model (SM-1B-1-1/2-FP) Case 1

Load cases	Energy Dissipation (kip-in)	Percentage difference (%)
DLC I-1	47.52	0.00
DLC I-2	47.28	-0.51
DLC I-1/2	46.08	-3.13
DLC I-1/3	46.8	-1.54
DLC I-1/4	47.28	-0.51
DLC II-2- 1- ½ -1/3- ¼	46.56	0.00
DLC II- ¼ -2 -1- ½ - 1/3	47.04	1.02
DLC II- 1/3- ¼ -2- 1- ½	46.8	0.51
DLC II- ½ - 1/3- ¼ - 2 - 1	47.28	1.52
DLC II- 1- ½ - 1/3 - ¼ - 2	47.52	2.02
DLC III- 2- 1- ½ -1/3- ¼	44.4	0.00
DLC III- ¼ -2 -1- ½ - 1/3	42.96	-3.35
DLC III- 1/3- ¼ -2- 1- ½	43.68	-1.65
DLC III- ½ - 1/3- ¼ - 2 - 1	44.4	0.00
DLC III- 1- ½ - 1/3 - ¼ - 2	44.16	-0.54
DLC IV- 2- 1- ½ -1/3- ¼	48.24	0.00
DLC IV- ¼ -2 -1- ½ - 1/3	48.48	0.50
DLC IV- 1/3- ¼ -2- 1- ½	48.72	0.99
DLC IV- ½ - 1/3- ¼ - 2 - 1	45.6	-5.79
DLC IV- 1- ½ - 1/3 - ¼ - 2	46.32	-4.15
DLC V- 2- 1- ½ -1/3- ¼	48.72	0.00
DLC V- ¼ -2 -1- ½ - 1/3	49.68	1.93
DLC V- 1/3- ¼ -2- 1- ½	48.24	-1.00
DLC V- ½ - 1/3- ¼ - 2 - 1	49.2	0.98
DLC V- 1- ½ - 1/3 - ¼ - 2	47.04	-3.57
HX-DLC-I-1	38.64	-22.98
NS-DLC-I-1	25.68	-85.05
LLC	41.04	-15.79

Table 4-8 - continued

HP-DLC-I-1	43.2	0.00
HP-DLC-I-2	43.68	1.10
HP-DLC-I-1/2	43.92	1.64
HP-DLC-I-1/3	42.96	-0.56
HP-DLC-I-1/4	42.96	-0.56
QP-DLC-I-1	41.52	0.00
QP-DLC-I-2	41.04	-1.17
QP-DLC-I-1/2	42.02	1.19
QP-DLC-I-1/3	41.28	-0.58
QP-DLC-I-1/4	41.28	-0.58

Note:

- * Refer Figure 4-1 for test designation.
- ** FLNA = Full load not achieved.

Table 4-9 Single bolted shear surface model (SM-1B-1/4-1) Case 2

Load cases	Energy Dissipation (kip-in)	Percentage difference (%)
DLC I-1	47.04	0.00
DLC I-2	48.24	2.49
DLC I-1/2	47.52	1.01
DLC I-1/3	49.92	5.77
DLC I-1/4	46.56	-1.03
DLC II-2- 1- ½ -1/3- ¼	49.44	0.00
DLC II- ¼ -2 -1- ½ - 1/3	49.32	-0.24
DLC II- 1/3- ¼ -2- 1- ½	49.45	0.02
DLC II- ½ - 1/3- ¼ - 2 - 1	49.39	-0.10
DLC II- 1- ½ - 1/3 - ¼ - 2	48.25	-2.47
DLC III- 2- 1- ½ -1/3- ¼	50.4	0.00
DLC III- ¼ -2 -1- ½ - 1/3	46.56	-8.25
DLC III- 1/3- ¼ -2- 1- ½	47.76	-5.53
DLC III- ½ - 1/3- ¼ - 2 - 1	49.2	-2.44
DLC III- 1- ½ - 1/3 - ¼ - 2	48.72	-3.45
DLC IV- 2- 1- ½ -1/3- ¼	49.92	0.00
DLC IV- ¼ -2 -1- ½ - 1/3	48.48	-2.97
DLC IV- 1/3- ¼ -2- 1- ½	48.72	-2.46
DLC IV- ½ - 1/3- ¼ - 2 - 1	48.48	-2.97
DLC IV- 1- ½ - 1/3 - ¼ - 2	48.96	-1.96
DLC V- 2- 1- ½ -1/3- ¼	48.48	0.00
DLC V- ¼ -2 -1- ½ - 1/3	50.16	3.35
DLC V- 1/3- ¼ -2- 1- ½	48.96	0.98
DLC V- ½ - 1/3- ¼ - 2 - 1	50.16	3.35
DLC V- 1- ½ - 1/3 - ¼ - 2	50.16	3.35
HX-DLC-I-1	12	**FLNA
NS-DLC-I-1	16.56	**FLNA
LLC	47.52	1.01

Table 4-9 - Continued

HP-DLC-I-1	60.48	0.00
HP-DLC-I-2	59.52	-1.61
HP-DLC-I-1/2	59.76	-1.20
HP-DLC-I-1/3	59.76	-1.20
HP-DLC-I-1/4	59.76	-1.20
QP-DLC-I-1	67.68	0.00
QP-DLC-I-2	67.44	-0.36
QP-DLC-I-1/2	66	-2.55
QP-DLC-I-1/3	66.96	-1.08
QP-DLC-I-1/4	67.2	-0.71

Note:

- * Refer Figure 4-1 for test designation.
- ** FLNA = Full load not achieved.

Table 4-10 Single bolted shear surface model (SM-1B-1-1) Case 3

Load cases	Energy dissipation (kip-in)	Percentage difference (%)
DLC I-1	22.36	0.00
DLC I-2	21.36	-4.68
DLC I-1/2	22.08	-1.27
DLC I-1/3	20.64	-8.33
DLC I-1/4	21.84	-2.38
DLC II-2- 1- ½ -1/3- ¼	19.92	0.00
DLC II- ¼ -2 -1- ½ - 1/3	19.68	-1.22
DLC II- 1/3- ¼ -2- 1- ½	19.92	0.00
DLC II- ½ - 1/3- ¼ - 2 - 1	20.4	2.35
DLC II- 1- ½ - 1/3 - ¼ - 2	19.68	-1.22
DLC III- 2- 1- ½ -1/3- ¼	18.72	0.00
DLC III- ¼ -2 -1- ½ - 1/3	18	-4.00
DLC III- 1/3- ¼ -2- 1- ½	18.96	1.27
DLC III- ½ - 1/3- ¼ - 2 - 1	18.96	1.27
DLC III- 1- ½ - 1/3 - ¼ - 2	18.72	0.00
DLC IV- 2- 1- ½ -1/3- ¼	19.92	0.00
DLC IV- ¼ -2 -1- ½ - 1/3	19.44	-2.47
DLC IV- 1/3- ¼ -2- 1- ½	19.92	0.00
DLC IV- ½ - 1/3- ¼ - 2 - 1	19.44	-2.47
DLC IV- 1- ½ - 1/3 - ¼ - 2	19.44	-2.47
DLC V- 2- 1- ½ -1/3- ¼	18.48	0.00
DLC V- ¼ -2 -1- ½ - 1/3	18.24	-1.32
DLC V- 1/3- ¼ -2- 1- ½	18.24	-1.32
DLC V- ½ - 1/3- ¼ - 2 - 1	18.48	0.00
DLC V- 1- ½ - 1/3 - ¼ - 2	18.24	-1.32
HX-DLC-I-1	17.76	**FLNA
NS-DLC-I-1	12.48	**FLNA
LLC	20.07	-11.41

Table 4-10 - continued

HP-DLC-I-1	26.64	0.00
HP-DLC-I-2	26.64	0.00
HP-DLC-I-1/2	26.64	0.00
HP-DLC-I-1/3	26.4	-0.91
HP-DLC-I-1/4	26.16	-1.83
QP-DLC-I-1	29.52	0.00
QP-DLC-I-2	29.04	-1.65
QP-DLC-I-1/2	28.35	-4.13
QP-DLC-I-1/3	28.12	-4.98
QP-DLC-I-1/4	28.56	-3.36

Note:

- * Refer Figure 4-1 for test designation.
- ** FLNA = Full load not achieved.

Table 4-11 Double bolted shear surface model (SM-2B-1-1/2) Case1

Load cases	Energy dissipation (kip-in)	Percentage difference (%)
DLC I-1	88.56	0.00
DLC I-2	88.08	-0.54
DLC I-1/2	92.88	4.65
DLC I-1/3	88.08	-0.54
DLC I-1/4	91.68	3.40
DLC II-2- 1- ½ -1/3- ¼	81.84	0.00
DLC II- ¼ -2 -1- ½ - 1/3	86.4	5.28
DLC II- 1/3- ¼ -2- 1- ½	81.84	0.00
DLC II- ½ - 1/3- ¼ - 2 - 1	78.96	-3.65
DLC II- 1- ½ - 1/3 - ¼ - 2	82.8	1.16
DLC III- 2- 1- ½ -1/3- ¼	84.48	0.00
DLC III- ¼ -2 -1- ½ - 1/3	84.24	-0.28
DLC III- 1/3- ¼ -2- 1- ½	84	-0.57
DLC III- ½ - 1/3- ¼ - 2 - 1	84.24	-0.28
DLC III- 1- ½ - 1/3 - ¼ - 2	84	-0.57
DLC IV- 2- 1- ½ -1/3- ¼	83.04	0.00
DLC IV- ¼ -2 -1- ½ - 1/3	88.08	5.72
DLC IV- 1/3- ¼ -2- 1- ½	87.6	5.21
DLC IV- ½ - 1/3- ¼ - 2 - 1	90.24	7.98
DLC IV- 1- ½ - 1/3 - ¼ - 2	93.36	11.05
DLC V- 2- 1- ½ -1/3- ¼	90.72	0.00
DLC V- ¼ -2 -1- ½ - 1/3	87.6	-3.56
DLC V- 1/3- ¼ -2- 1- ½	93.36	2.83
DLC V- ½ - 1/3- ¼ - 2 - 1	85.44	-6.18
DLC V- 1- ½ - 1/3 - ¼ - 2	85.44	-6.18
HX-DLC-I-1	23.52	**FLNA
NS-DLC-I-1	29.04	**FLNA
LLC	84.24	-5.13

Table 4-11 - continued

HP-DLC-I-1	62.4	0.00
HP-DLC-I-2	63.6	1.89
HP-DLC-I-1/2	61.44	-1.56
HP-DLC-I-1/3	62.88	0.76
HP-DLC-I-1/4	61.92	-0.78
QP-DLC-I-1	46.08	0.00
QP-DLC-I-2	44.4	-3.78
QP-DLC-I-1/2	46.8	1.54
QP-DLC-I-1/3	43.92	-4.92
QP-DLC-I-1/4	46.32	0.52

Note:

- * Refer Figure 4-1 for test designation.
- ** FLNA = Full load not achieved.

Table 4-12 Double bolted shear surface model (SM-2B-1/4-1) Case 2

Load cases	Energy Dissipation (kip-in)	Percentage difference (%)
DLC I-1	73.68	0.00
DLC I-2	74.16	0.65
DLC I-1/2	74.16	0.65
DLC I-1/3	73.68	0.00
DLC I-1/4	74.64	1.29
DLC II-2- 1- ½ -1/3- ¼	72.72	0.00
DLC II- ¼ -2 -1- ½ - 1/3	69.36	-4.84
DLC II- 1/3- ¼ -2- 1- ½	71.52	-1.68
DLC II- ½ - 1/3- ¼ - 2 - 1	72.48	-0.33
DLC II- 1- ½ - 1/3 - ¼ - 2	74.4	2.26
DLC III- 2- 1- ½ -1/3- ¼	73.68	0.00
DLC III- ¼ -2 -1- ½ - 1/3	73.92	0.32
DLC III- 1/3- ¼ -2- 1- ½	74.64	1.29
DLC III- ½ - 1/3- ¼ - 2 - 1	74.16	0.65
DLC III- 1- ½ - 1/3 - ¼ - 2	73.2	-0.66
DLC IV- 2- 1- ½ -1/3- ¼	80.16	0.00
DLC IV- ¼ -2 -1- ½ - 1/3	75.12	-6.71
DLC IV- 1/3- ¼ -2- 1- ½	74.4	-7.74
DLC IV- ½ - 1/3- ¼ - 2 - 1	80.16	0.00
DLC IV- 1- ½ - 1/3 - ¼ - 2	75.6	-6.03
DLC V- 2- 1- ½ -1/3- ¼	80.4	0.00
DLC V- ¼ -2 -1- ½ - 1/3	75.6	-6.35
DLC V- 1/3- ¼ -2- 1- ½	73.92	-8.77
DLC V- ½ - 1/3- ¼ - 2 - 1	75.84	-6.01
DLC V- 1- ½ - 1/3 - ¼ - 2	74.4	-8.06
HX-DLC-I-1	24.24	**FLNA
NS-DLC-I-1	19.2	**FLNA
LLC	68.4	-7.72

Table 4-12 - continued

HP-DLC-I-1	51.6	0.00
HP-DLC-I-2	50.16	-2.87
HP-DLC-I-1/2	48.96	-5.39
HP-DLC-I-1/3	51.36	-0.47
HP-DLC-I-1/4	52.8	2.27
QP-DLC-I-1	37.2	0.00
QP-DLC-I-2	43.44	14.36
QP-DLC-I-1/2	37.92	1.90
QP-DLC-I-1/3	38.4	3.13
QP-DLC-I-1/4	42	11.43

Note:

- * Refer Figure 4-1 for test designation.
- ** FLNA = Full load not achieved.

Table 4-13 Double bolted shear surface model (SM-2B-1-1) Case 3

Load cases	Energy Dissipation (kip-in)	Percentage difference (%)
DLC I-1	35.04	0.00
DLC I-2	33.84	-3.55
DLC I-1/2	31.68	-10.61
DLC I-1/3	32.64	-7.35
DLC I-1/4	34.56	-1.39
DLC II-2- 1- ½ -1/3- ¼	37.92	0.00
DLC II- ¼ -2 -1- ½ - 1/3	35.28	-7.48
DLC II- 1/3- ¼ -2- 1- ½	32.64	-16.18
DLC II- ½ - 1/3- ¼ - 2 - 1	37.92	0.00
DLC II- 1- ½ - 1/3 - ¼ - 2	31.68	-19.70
DLC III- 2- 1- ½ -1/3- ¼	34.32	0.00
DLC III- ¼ -2 -1- ½ - 1/3	31.68	-8.33
DLC III- 1/3- ¼ -2- 1- ½	34.32	0.00
DLC III- ½ - 1/3- ¼ - 2 - 1	33.36	-2.88
DLC III- 1- ½ - 1/3 - ¼ - 2	33.6	-2.14
DLC IV- 2- 1- ½ -1/3- ¼	33.84	0.00
DLC IV- ¼ -2 -1- ½ - 1/3	32.4	-4.44
DLC IV- 1/3- ¼ -2- 1- ½	34.32	1.40
DLC IV- ½ - 1/3- ¼ - 2 - 1	34.32	1.40
DLC IV- 1- ½ - 1/3 - ¼ - 2	33.12	-2.17
DLC V- 2- 1- ½ -1/3- ¼	34.8	0.00
DLC V- ¼ -2 -1- ½ - 1/3	34.32	-1.40
DLC V- 1/3- ¼ -2- 1- ½	34.32	-1.40
DLC V- ½ - 1/3- ¼ - 2 - 1	33.84	-2.84
DLC V- 1- ½ - 1/3 - ¼ - 2	34.32	-1.40
HX-DLC-I-1	29.28	**FLNA
NS-DLC-I-1	24.24	**FLNA
LLC	32.05	-9.33

Table 4-13 - continued

HP-DLC-I-1	40.56	0.00
HP-DLC-I-2	41.52	2.31
HP-DLC-I-1/2	40.08	-1.20
HP-DLC-I-1/3	40.56	0.00
HP-DLC-I-1/4	38.16	-6.29
QP-DLC-I-1	49.44	0.00
QP-DLC-I-2	49.68	0.48
QP-DLC-I-1/2	49.92	0.96
QP-DLC-I-1/3	48.24	-2.49
QP-DLC-I-1/4	49.92	0.96

Note:

- * Refer Figure 4-1 for test designation.
- ** FLNA = Full load not achieved.

Table 4-14 Tee-hanger model (T-1-1/2-1½) Case1

Load cases	Energy Dissipation (kip-in)	Percentage difference (%)
DLC I-1	204	0.00
DLC I-2	183.36	-11.26
DLC I-1/2	171.12	-19.21
DLC I-1/3	204.48	0.23
DLC I-1/4	183.6	-11.11
DLC II-2- 1- ½ -1/3- ¼	212.16	0.00
DLC II- ¼ -2 -1- ½ - 1/3	199.68	-6.25
DLC II- 1/3- ¼ -2- 1- ½	196.56	-7.94
DLC II- ½ - 1/3- ¼ - 2 - 1	199.44	-6.38
DLC II- 1- ½ - 1/3 - ¼ - 2	212.64	0.23
DLC III- 2- 1- ½ -1/3- ¼	194.64	0.00
DLC III- ¼ -2 -1- ½ - 1/3	198	1.70
DLC III- 1/3- ¼ -2- 1- ½	194.16	-0.25
DLC III- ½ - 1/3- ¼ - 2 - 1	198	1.70
DLC III- 1- ½ - 1/3 - ¼ - 2	198.24	1.82
DLC IV- 2- 1- ½ -1/3- ¼	201.84	0.00
DLC IV- ¼ -2 -1- ½ - 1/3	201.84	0.00
DLC IV- 1/3- ¼ -2- 1- ½	197.04	-2.44
DLC IV- ½ - 1/3- ¼ - 2 - 1	198.24	-1.82
DLC IV- 1- ½ - 1/3 - ¼ - 2	201.6	-0.12
DLC V- 2- 1- ½ -1/3- ¼	202.08	0.00
DLC V- ¼ -2 -1- ½ - 1/3	199.92	-1.08
DLC V- 1/3- ¼ -2- 1- ½	200.88	-0.60
DLC V- ½ - 1/3- ¼ - 2 - 1	202.32	0.12
DLC V- 1- ½ - 1/3 - ¼ - 2	201.84	-0.12
HX-DLC-I-1	109.44	**FLNA
NS-DLC-I-1	28.8	**FLNA
LLC	178.32	-14.40

Table 4-14 - Continued

HP-DLC-I-1	187.92	0.00
HP-DLC-I-2	183.12	-2.62
HP-DLC-I-1/2	185.52	-1.29
HP-DLC-I-1/3	187.92	0.00
HP-DLC-I-1/4	185.76	-1.16
QP-DLC-I-1	96.72	0.00
QP-DLC-I-2	87.36	-10.71
QP-DLC-I-1/2	97.44	0.74
QP-DLC-I-1/3	89.28	-8.33
QP-DLC-I-1/4	94.08	-2.81

Note:

- * Refer Figure 4-1 for test designation.
- ** FLNA = Full load not achieved.

Table 4-15 Tee-hanger model (T-1-1-2¾) Case 2

Load cases	Energy Dissipation (kip-in)	Percentage Difference (%)
DLC I-1	102.48	0.00
DLC I-2	100.56	-1.91
DLC I-1/2	90.96	-12.66
DLC I-1/3	101.76	-0.71
DLC I-1/4	93.6	-9.49
DLC II-2- 1- ½ -1/3- ¼	98.88	0.00
DLC II- ¼ -2 -1- ½ - 1/3	101.76	2.83
DLC II- 1/3- ¼ -2- 1- ½	100.32	1.44
DLC II- ½ - 1/3- ¼ - 2 - 1	101.52	2.60
DLC II- 1- ½ - 1/3 - ¼ - 2	100.56	1.67
DLC III- 2- 1- ½ -1/3- ¼	96.24	0.00
DLC III- ¼ -2 -1- ½ - 1/3	94.8	-1.52
DLC III- 1/3- ¼ -2- 1- ½	91.92	-4.70
DLC III- ½ - 1/3- ¼ - 2 - 1	97.68	1.47
DLC III- 1- ½ - 1/3 - ¼ - 2	97.68	1.47
DLC IV- 2- 1- ½ -1/3- ¼	89.28	0.00
DLC IV- ¼ -2 -1- ½ - 1/3	90.72	1.59
DLC IV- 1/3- ¼ -2- 1- ½	90.24	1.06
DLC IV- ½ - 1/3- ¼ - 2 - 1	90	0.80
DLC IV- 1- ½ - 1/3 - ¼ - 2	90.24	1.06
DLC V- 2- 1- ½ -1/3- ¼	95.04	0.00
DLC V- ¼ -2 -1- ½ - 1/3	85.44	-11.24
DLC V- 1/3- ¼ -2- 1- ½	95.04	0.00
DLC V- ½ - 1/3- ¼ - 2 - 1	93.36	-1.80
DLC V- 1- ½ - 1/3 - ¼ - 2	91.68	-3.66
HX-DLC-I-1	47.28	**FLNA
NS-DLC-I-1	51.12	**FLNA
LLC	96	-6.75

Table 4-15 - continued

HP-DLC-I-1	78.24	0.00
HP-DLC-I-2	78.96	0.91
HP-DLC-I-1/2	79.44	1.51
HP-DLC-I-1/3	76.8	-1.87
HP-DLC-I-1/4	80.16	2.40
QP-DLC-I-1	57.36	0.00
QP-DLC-I-2	60.96	5.91
QP-DLC-I-1/2	59.52	3.63
QP-DLC-I-1/3	57.12	-0.42
QP-DLC-I-1/4	56.4	-1.70

Note:

- * Refer Figure 4-1 for test designation.
- ** FLNA = Full load not achieved.

Table 4-16 Tee – hanger model (T-1/2-1/2-1) Case 3

Load cases	Energy dissipation (kip-in)	Percentage difference (%)
DLC I-1	138.96	0.00
DLC I-2	133.92	-3.76
DLC I-1/2	139.44	0.34
DLC I-1/3	134.4	-3.39
DLC I-1/4	141.84	2.03
DLC II-2- 1- ½ -1/3- ¼	137.28	0.00
DLC II- ¼ -2 -1- ½ - 1/3	141.36	2.89
DLC II- 1/3- ¼ -2- 1- ½	136.08	-0.88
DLC II- ½ - 1/3- ¼ - 2 - 1	134.88	-1.78
DLC II- 1- ½ - 1/3 - ¼ - 2	141.6	3.05
DLC III- 2- 1- ½ -1/3- ¼	133.92	0.00
DLC III- ¼ -2 -1- ½ - 1/3	134.88	0.71
DLC III- 1/3- ¼ -2- 1- ½	139.2	3.79
DLC III- ½ - 1/3- ¼ - 2 - 1	135.12	0.89
DLC III- 1- ½ - 1/3 - ¼ - 2	142.08	5.74
DLC IV- 2- 1- ½ -1/3- ¼	139.2	0.00
DLC IV- ¼ -2 -1- ½ - 1/3	140.64	1.02
DLC IV- 1/3- ¼ -2- 1- ½	142.08	2.03
DLC IV- ½ - 1/3- ¼ - 2 - 1	134.88	-3.20
DLC IV- 1- ½ - 1/3 - ¼ - 2	141.84	1.86
DLC V- 2- 1- ½ -1/3- ¼	134.4	0.00
DLC V- ¼ -2 -1- ½ - 1/3	134.88	0.36
DLC V- 1/3- ¼ -2- 1- ½	138.96	3.28
DLC V- ½ - 1/3- ¼ - 2 - 1	134.4	0.00
DLC V- 1- ½ - 1/3 - ¼ - 2	141.6	5.08
HX-DLC-I-1	55.2	**FLNA
NS-DLC-I-1	42.96	**FLNA
LLC	129.89	-6.98

Table 4-16 - continued

HP-DLC-I-1	114	0.00
HP-DLC-I-2	114	0.00
HP-DLC-I-1/2	112.8	-1.06
HP-DLC-I-1/3	113.28	-0.64
HP-DLC-I-1/4	113.52	-0.42
QP-DLC-I-1	103.68	0.00
QP-DLC-I-2	105.84	2.04
QP-DLC-I-1/2	105.6	1.82
QP-DLC-I-1/3	103.2	-0.47
QP-DLC-I-1/4	106.08	2.26

Note:

- * Refer Figure 4-1 for test designation.
- ** FLNA = Full load not achieved.

Table 4-17 Extended end-plate connection model (EEP-1/2-1) Case 1

Load cases	Energy Dissipation (kip-in-rad)	Percentage Difference (%)
DLC I- 1	71.8	0.00
DLC II- ¼ -2 -1- ½ - 1/3	67.34	-6.62
DLC IV- ¼ -2 -1- ½ - 1/3	79.35	9.51
LLC	35.7	-101.12
HP- DLC I- 1	30.04	-139.01
QP- DLC I- 1	24.99	**FLNA

Note:

- * Refer Figure 4-1 for test designation.
- ** FLNA = Full load not achieved.

Table 4-18 Extended end-plate connection model (EEP-1/2-1/2) Case 2

Load cases	Energy Dissipation (kip-in-rad)	Percentage Difference (%)
DLC I- 1	46.17	0.00
DLC II- ¼ -2 -1- ½ - 1/3	41.35	-11.66
DLC IV- ¼ -2 -1- ½ - 1/3	49.37	6.48
LLC	32.62	-41.54
HP- DLC I- 1	30.55	-51.13
QP- DLC I- 1	13.84	**FLNA

CHAPTER 5

CONCLUSION

5.1 Summary

This study developed 25 cyclic displacement control loading histories by utilizing AISC Seismic Provisions 2005 as the baseline and the guideline. The research conducted is presented in five chapters as follows:

Chapter 1 explain and maps the complete literature review on the loading histories, studies related to end-plate connections, and finite element modeling.

Chapter 2 presents the methods adopted for developing the 25 different displacement loading histories, which are based on the displacement loading history suggested by the AISC Seismic Provision 2005. All loading cases are derived from two basic curved and linear profiles from which five loading sets are derived which yield to 25 load cases.

Chapter 3 presents the finite element models of four connecting surfaces used in this study. The models consist of welded shear surface model, single and double bolted shear surface model, tee – hanger model, and extended end-plate connection model.

Various aspects of the modeling process were studied in this chapter. Finite element model development process consisted of bolt pretension, contact properties, boundary conditions, model verification, and model symmetry.

Chapter 4 presents the parametric study, in which force related and geometric variable to obtain the parametric case. The thirteen different FEM model cases were subjected to the 25 displacement control loading histories developed in Chapter 2. The energy dissipation response of each connection assembly was obtained by calculating the area under the outer loop of the hysteresis loop for each connection. In addition different element types and contact algorithm were studied during the parametric study.

5.2 Results and discussion

All the results in this study were represented in the form of energy dissipated by the connection model under different scenarios.

5.2.1. Welded shear surface models

5.2.1.1 Welded shear surface model Case 1

In welded shear surface model, (t_p = ½ in), it is observed that all the models are showing uniform energy dissipation under different loading sets. All the results were compared with the first case of each respective set. In Set I, the maximum percentage difference was observed in loading case DLC I- 2 of 3.63% when compared to the DLC I- 1. At the same time, DLC I- 1/4 case showed the minimum difference in energy dissipation with -0.4%. In Set II, the maximum percentage difference in energy

dissipation was observed in Case DLC II- 1/3- ¼ -2- 1- ½ to be -2.68%, and its minimum value was -0.37% for DLC II- ¼ -2 -1- ½ - 1/3. Similarly for Set III, the maximum difference of 0.97% for DLC III- 1/3- ¼ -2- 1- ½ and the minimum difference 0.19% for DLC III- 1- ½ - 1/3 – ¼ - 2 were observed. DLC IV- ½ - 1/3- ¼ - 2 - 1 showed the maximum percentage difference in energy dissipation of -9.41% and the minimum observed as 0.74% in the DLC IV- ¼ -2 -1- ½ - 1/3. In cases of Set V, the maximum and minimum percentage difference in energy dissipation was observed in DLC V- ½ - 1/3- ¼ - 2 - 1 of -2.29% and DLC V- ¼ -2 -1- ½ - 1/3 -0.19%, respectively. No specific pattern was observed in the above results.

5.2.1.2 Welded shear surface model Case 2

The welded shear surface model (t_p = 1in) also showed fairly uniform energy dissipation. The minimum percentage difference in energy dissipation in Set I was -0.82% under the DLC I- 2. Loading Case DLC I- 1/3 showed the maximum difference in the energy dissipation of -2.94%. DLC I- 1/4 showed a perfect agreement with DLC I- 1 case which is considered as reference. In Set II, the maximum percentage difference in energy dissipation value was observed as 5.93% and the minimum value was -0.85% in the DLC II- ¼ -2 -1- ½ - 1/3 and DLC II- 1- ½ - 1/3 – ¼ - 2, respectively. DLC III -¼ - 2 -1- ½ - 1/3 shows the maximum percentage difference in energy dissipation of -12.78% and the minimum observed value was -7.11% in DLC III- 1- ½ - 1/3 – ¼ - 2 in Set III. Similarly, for Set IV, maximum of -10.67% for DLC IV- ¼ -2 -1- ½ - 1/3 and minimum of 0.8% in DLC IV- 1- ½ - 1/3 – ¼ - 2 percentage difference in energy

dissipation was observed. In the case of Set V, the maximum and minimum percentage difference in energy dissipation was observed in DLC V- ¼ -2 -1- ½ - 1/3 and DLC V- 1- ½ - 1/3 – ¼ - 2 with calculated value of 7.25% and -1.62% respectively.

5.2.2 Single bolted shear surface models

5.2.2.1 Single bolted shear surface model Case 1

In single bolted shear surface model (b_d = ½ in, t_p = 1 in) in Set I, the maximum percentage difference of -3.13% was observed in the loading case DLC I- 1/2 when compared to the DLC I- 1. At the same time, DLC I- 1/4 case showed the minimum difference in energy dissipation with -0.51%. The average difference in energy dissipation for all the load cases of Set I was observed as -1.42%. In Set II, the maximum percentage difference in energy dissipation of -2.02% was observed in the Case DLC II- 1- ½ - 1/3 – ¼ - 2 and the minimum value of -0.51% was calculated for DLC II- 1/3- ¼ - 2- 1- ½. Set II showed the average difference in energy dissipation of 1.26%. For Set III, the maximum of -3.35% for DLC III- ¼ -2 -1- ½ - 1/3 and the minimum of -0.54% in DLC III- 1- ½ - 1/3 – ¼ - 2 percentage difference in energy dissipation was observed. DLC III- ½ - 1/3- ¼ - 2 - 1 showed a complete agreement with the DLC III- 2- 1- ½ -1/3- ¼. In Set III, the average difference in energy dissipation was -1.385%. DLC IV- ½ - 1/3- ¼ - 2 - 1 showed the maximum percentage difference in energy dissipation of -5.79% and the minimum observed as 0.5% in DLC IV- ¼ -2 -1- ½ - 1/3 in Set IV. The average difference in energy dissipation for this set was -2.11%. In case of Set V, the maximum and minimum percentage difference in energy dissipation was observed in

DLC V- 5 of -3.57% and DLC V- ¼ -2 -1- ½ - 1/3 -1.93% respectively. The Average difference in energy dissipation was -0.42% in Set V.

In half pretension, Case DLC I- 1/2 showed the maximum difference in energy dissipation of 1.64% and the minimum of -0.56% for Cases DLC I- 1/3 and DLC I- 1/4. The average difference in energy dissipation was 0.41%. In quarter pretension, Case DLC I- 1/2 showed the maximum of difference in energy dissipation of 1.19% and the minimum difference in energy dissipation was observed in Case DLC I- 1/4 of 0.48%. The average difference in energy dissipation was observed as -0.29%.

5.2.2.2 Single bolted shear surface model Case 2

In single bolted shear surface model (b_d = 1 in, t_p = ¼ in) in Set I, the maximum percentage difference was observed in loading case DLC I- 1/3 of 5.77% when compared to the DLC I- 1. At the same time, DLC I- 1/4 case showed the minimum difference in energy dissipation with the value of -1.03%. The average difference in energy dissipation was observed as 2.06%. In Set II, the maximum percentage difference in energy dissipation was observed in case DLC II- 1- ½ - 1/3 – ¼ - 2 to be 2.47% and the minimum value of -0.02% for DLC II- 1/3- ¼ -2- 1- ½ was recorded. Set II showed average difference in energy dissipation was -0.7%. In Set III, the maximum of -8.25% for DLC III- ¼ -2 -1- ½ - 1/3 and the minimum of -2.44% in DLC III- ½ - 1/3- ¼ - 2 - 1 percentage difference in energy dissipation was observed. In Set III, the average difference in energy dissipation was -4.91%. DLC IV- ¼ -2 -1- ½ - 1/3 showed the maximum percentage difference in energy dissipation of -2.97% and the minimum

observed as-1.96% in DLC IV- ¼ -2 -1- ½ - 1/3 in Set IV. The average difference in energy dissipation was 2.59%. In case of Set V, the maximum and minimum percentage difference in energy dissipation was observed in DLC V- ¼ -2 -1- ½ - 1/3 of 3.35% and DLC V- 1/3- ¼ -2- 1- ½ of 0.98% respectively. The Average difference in energy dissipation was 2.75% in Set V.

In half pretension, Case DLC I- 2 the maximum difference in energy dissipation of 1.61% and the minimum of -1.2% for Cases DLC I- ¼ was recorded. The average difference in energy dissipation was -1.31%. In quarter pretension, Case DLC I- 1/2 showed the maximum of difference in energy dissipation of -2.55% and the minimum difference in energy dissipation was observed in Case DLC I- 2 to be -0.36%. The average difference in the energy dissipation value was -1.18%.

5.2.2.3 Single bolted shear surface model Case 3

In single bolted shear surface model (b_d = 1 in, t_p = 1 in) in Set I, the maximum percentage difference was observed in loading Case DLC I- 1/3 of -8.33% when compared to the DLC I- 1. At the same time, DLC I- 1/2 case showed the minimum difference in energy dissipation with the value of -1.27%. The average difference in energy dissipation was observed as -4.17%. In Set II, the maximum percentage difference in the energy dissipation was observed in case DLC II- ½ - 1/3- ¼ - 2 - 1 of 2.35% and the minimum value of -1.22% for DLC II- ¼ -2 -1- ½ - 1/3. Set II showed average difference in the energy dissipation of -0.02%. In Set III, the maximum value of -4.00% for DLC III- ¼ -2 -1- ½ - 1/3 and the minimum value of 1.27% in DLC III- 1/3- ¼

-2- 1- ½ was observed. In Set III average difference in the energy dissipation was -0.37%. DLC IV- ¼ -2 -1- ½ - 1/3 showed the maximum percentage difference in the energy dissipation of -2.47% and the minimum value observed as-1.96% in DLC IV- ½ - 1/3- ¼ - 2 - 1 in Set IV. The average difference in energy dissipation was -2.37%. In case of Set V, the maximum and minimum percentage difference in energy dissipation was observed in DLC V- ¼ -2 -1- ½ - 1/3 and DLC V- 1/3- ¼ -2- 1- ½ of 1.32% and 0.98% respectively. The Average difference in the energy dissipation was -0.91% in Set V.

In half pretension, Case DLC I- 1/4 showed the maximum difference in energy dissipation of -1.83% and the minimum of -0.91% for Cases DLC I- 1/3. The average difference in energy dissipation was -1.37%. In quarter pretension, Case DLC I- 1/3 showed the maximum of difference in energy dissipation of -4.98% and the minimum difference in energy dissipation was observed in Case DLC I- 2 of -1.65%. The average difference in the energy dissipation was observed as -3.52%.

5.2.3 Double bolted shear surface model

5.2.3.1 Double bolted shear surface model Case1

In double bolted shear surface model (b_d = ½ in, t_p = 1) in Set I, the maximum percentage difference was observed in loading Case DLC I- 1/2 of value 4.65% when compared to the DLC I- 1. At the same time, DLC I- 1/3 showed the minimum difference in energy dissipation with value of -0.54%. The average difference in the energy dissipation was observed as -1.74%. In Set II, the maximum percentage difference in energy dissipation was observed in case DLC II- ¼ -2 -1- ½ - 1/3 of 5.28% and the

minimum of -1.16% for DLC II- 5. Set II showed average difference in the energy dissipation was 0.7%. Similarly for Set III, the maximum value of 0.57% for DLC III- 1/3- ¼ -2- 1- ½ and the minimum value of-0.28% in DLC III- ½ - 1/3- ¼ - 2 - 1 percentage difference in energy dissipation was observed. In Set III average difference in the energy dissipation was -0.43%. DLC IV- 1- ½ - 1/3 – ¼ - 2 showed the maximum percentage difference in energy dissipation of value -11.05% and the minimum observed as 5.21% in DLC IV- 1/3- ¼ -2- 1- ½ in Set IV. The average difference in the energy dissipation was 7.49%. In case of Set V, the maximum and minimum percentage difference in the energy dissipation was observed in DLC V- 1- ½ - 1/3 – ¼ - 2 of -6.18 % and DLC V- 1/3- ¼ -2- 1- ½ of 2.83% respectively. The Average difference in energy dissipation was -3.28% in Set V.

In half pretension, Case DLC I- 2 showed the maximum difference in energy dissipation of value -1.89% and the minimum of value -0.76% for cases DLC I- 1/3. The average difference in energy dissipation was -0.08%. In quarter pretension, Case DLC I- 1/3 showed the maximum of difference in energy dissipation of -4.92% and the minimum difference in energy dissipation was observed in Case DLC I- 1/4 of 0.52%. The average difference in energy dissipation was observed as -1.66%.

5.2.3.2 Double bolted shear surface model Case 2

In double bolted shear surface model (b_d = 1 in, t_p = ¼ in) in Set I, the maximum percentage difference was observed in loading case DLC I- 1/4 of value 1.29% when compared to the DLC I- 1. At the same time, DLC I- 2 case showed the minimum

difference in energy dissipation with value of 0.65%. The average difference in energy dissipation was observed as 0.65%. In Set II, the maximum percentage difference in energy dissipation was observed in case DLC II- ¼ -2 -1- ½ - 1/3 value of -4.84% and the minimum value of -0.33% for DLC II- 1/3- ¼ -2- 1- ½. Set II showed average difference in the energy dissipation was -1.15%. Similarly for Set III, the maximum value of 1.29% for DLC III- 1/3- ¼ -2- 1- ½ and the minimum value of 0.32% in DLC III- ¼ -2 -1- ½ - 1/3 percentage difference in the energy dissipation were observed. In Set III average difference in the energy dissipation was 0.4%. DLC IV- 1/3- ¼ -2- 1- ½ showed the maximum percentage difference in energy dissipation of 7.74% and the minimum observed as -6.03% in DLC IV- 1- ½ - 1/3 – ¼ - 2 in Set IV. The average difference in energy dissipation was 7.29%. In case of Set V, the maximum and minimum percentage difference in the energy dissipation was observed in DLC V- 1/3- ¼ -2- 1- ½ of value - 8.77 % and DLC V- ½ - 1/3- ¼ - 2 - 1 of -6.01% respectively. The Average difference in energy dissipation was -7.29% in Set V.

In half pretension, Case DLC I- 1/2 showed the maximum difference in energy dissipation value of -5.39% and the minimum value of -0.47% for cases DLC I- 1/3. The average difference in energy dissipation was -1.62%. In quarter pretension, Case DLC I- 2 showed the maximum of difference in energy dissipation of -14.36% and the minimum difference in energy dissipation was observed in Case DLC I- 1/2 value of 1.90%. The average difference in energy dissipation was observed as 7.70%.

5.2.3.3 Double bolted shear surface model Case 3

In double bolted shear surface model (b_d = 1 in, t_p = 1 in) in Set I, the maximum percentage difference was observed in loading Case DLC I- 1/2 of 10.61% when compared to the DLC I- 1. At the same time, DLC I- 1/4 case showed the minimum difference in the energy dissipation with value of -1.39%. The average difference in energy dissipation was observed as -5.37%. In Set II, the maximum percentage difference in energy dissipation was observed in Case DLC II- 1/3- ¼ -2- 1- ½ of -16.18% and the minimum value of -7.48% for DLC II- ¼ -2 -1- ½ - 1/3. Set II showed average difference in the energy dissipation was -10.48%. Similarly for Set III, the maximum value of -8.33% for DLC III- ¼ -2 -1- ½ - 1/3 and the minimum value of -2.14% in DLC III- 1- ½ - 1/3 – ¼ - 2 percentage difference in energy dissipation were observed. In Set III average difference in energy dissipation was -3.34%. DLC IV- ¼ -2 -1- ½ - 1/3 showed the maximum percentage difference in energy dissipation value of -4.44% and the minimum value observed as 1.40% in DLC IV- ½ - 1/3- ¼ - 2 - 1 in Set IV. The average difference in energy dissipation was of -0.95%. In case of Set V, the maximum and minimum percentage difference in energy dissipation was observed in DLC V- ½ - 1/3- ¼ - 2 - 1 of -2.84 % and DLC V- ¼ -2 -1- ½ - 1/3 of -1.4% respectively. The Average difference in energy dissipation was -0.95% in Set V.

In half pretension, Case DLC I- 1/3 showed the maximum difference in energy dissipation of -6.29% and the minimum of -1.20% for cases DLC I- 1/2. The average difference in energy dissipation was -1.3%. In quarter pretension, Case DLC I- 1/3

showed the maximum of difference in energy dissipation of -2.49% and the minimum difference in energy dissipation was observed in Case DLC I- 2 of 0.48%. The average difference in energy dissipation was observed as -0.03%.

5.2.4 Tee- hanger models

5.2.4.1 Tee-hanger model Case 1

In tee - hanger model (b_d = ½ in, t_f = 1 in, g = 1 ½ in) in Set I, the maximum percentage difference was observed in loading Case DLC I- 1/2 of value 19.21% when compared to the DLC I- 1. At the same time, DLC I- 1/3 case showed the minimum difference in energy dissipation with value of 0.23%. The average difference in the energy dissipation was observed as -10.34%. In Set II, the maximum percentage difference in energy dissipation was observed in case DLC II- 1/3- ¼ -2- 1- ½ of value -7.94% and the minimum value of -0.23% for DLC II- 1- ½ - 1/3 – ¼ - 2. Set II showed average difference in energy dissipation was -5.09%. Similarly for Set III, the maximum of 1.82% for DLC III- 1- ½ - 1/3 – ¼ - 2 and the minimum of -0.25% in DLC III- 1/3- ¼ -2- 1- ½ percentage difference in energy dissipation were observed. In Set III average difference in the energy dissipation was 1.24%. DLC IV- 1/3- ¼ -2- 1- ½ showed the maximum percentage difference in the energy dissipation of -2.44% and the minimum value observed as -0.12% in DLC IV- 1- ½ - 1/3 – ¼ - 2 in Set IV. The average difference in the energy dissipation was -1.1%. In case of Set V, the maximum and minimum percentage difference in energy dissipation was observed in DLC V- ¼ -2 -1-

½ - 1/3 and DLC V- ½ - 1/3- ¼ - 2 - 1 of -1.08 % and 0.12% respectively. The Average difference in energy dissipation was of value -0.42% in Set V.

In half pretension, Case DLC I- 2 showed the maximum difference in energy dissipation of -2.62% and the minimum value of -1.16% for cases DLC I- 1/4. The average difference in energy dissipation was of value -1.27%. In quarter pretension, Case DLC I- 2 showed the maximum of difference in energy dissipation of value -10.71% and the minimum difference in energy dissipation was observed in Case DLC I- 1/2 of value 0.74%. The average difference in energy dissipation was observed as -5.28%.

5.2.4.2 Tee-hanger model Case 2

In tee - hanger model (b_d = 1 in, t_f = 1 in, g = 2 ¾ in) in Set I, the maximum percentage difference was observed in loading case DLC I- 1/2 of value -12.66% when compared to the DLC I- 1. At the same time, DLC I- 1/3 case showed the minimum difference in energy dissipation with value of -0.71%. The average difference in energy dissipation was observed as -6.19%. In Set II, the maximum percentage difference in energy dissipation was observed in case DLC II- ¼ -2 -1- ½ - 1/3 of value 2.83% and the minimum value of 1.44% for DLC II- 1/3- ¼ -2- 1- ½. Set II showed average difference in the energy dissipation was 2.14%. Similarly for Set III, the maximum of -4.70% for DLC III- 1/3- ¼ -2- 1- ½ and the minimum of 1.47% in DLC III- 1- ½ - 1/3 – ¼ - 2 percentage difference in energy dissipation were observed. In Set III average difference in energy dissipation was of value -0.82%. DLC IV- ¼ -2 -1- ½ - 1/3 showed the maximum percentage difference in energy dissipation of 1.59% and the minimum

observed as 0.8% in DLC IV- 1- ½ - 1/3 – ¼ - 2 in Set IV. The average difference in energy dissipation was of value -1.13%. In case of Set V, the maximum and minimum percentage difference in energy dissipation was observed in DLC V- ¼ -2 -1- ½ - 1/and DLC V- ½ - 1/3- ¼ - 2 - 1 of value -11.24 % and -1.8% respectively. The Average difference in energy dissipation was 4.18% in Set V.

In half pretension, Case DLC I- 1/4 showed the maximum difference in energy dissipation of 2.4% and the minimum of 0.91% for Cases DLC I- 2. The average difference in energy dissipation was 0.74%. In quarter pretension, Case DLC I- 2 showed the maximum of difference in energy dissipation of 5.91% and the minimum difference in energy dissipation was observed in Case DLC I- 1/3 of -0.42%. The average difference in energy dissipation was observed as 1.86%.

5.2.4.3 Tee-hanger model Case 3

In tee - hanger model (b_d = ½ in, t_f = ½ in, g = 1 in) in Set I, the maximum percentage difference was observed in loading Case DLC I- 2 of -3.76% when compared to the DLC I- 1. At the same time, DLC I- 1/2 case showed the minimum difference in energy dissipation with value of 0.34%. The average difference in energy dissipation was observed as -1.18%. In Set II, the maximum percentage difference in energy dissipation was observed in case DLC II- 1- ½ - 1/3 – ¼ - 2 of value 3.05% and the minimum value of -0.88% for DLC II- 1/3- ¼ -2- 1- ½. Set II showed average difference in energy dissipation was 0.82%. Similarly for Set III, the maximum of 5.74% for DLC III- 1- ½ - 1/3 – ¼ - 2 and the minimum value of 0.71% in DLC III- ¼ -2 -1- ½ - 1/3 percentage

difference in energy dissipation were observed. In Set III average difference in the energy dissipation was 2.78%. DLC IV- ½ - 1/3- ¼ - 2 - 1 showed the maximum percentage difference in energy dissipation of -3.20% and the minimum observed as 1.02% in DLC IV- ¼ -2 -1- ½ - 1/3 in Set IV. The average difference in energy dissipation was 0.43%. In case of Set V, the maximum and minimum percentage difference in energy dissipation was observed in DLC V- 1- ½ - 1/3 – ¼ - 2 and DLC V- ¼ -2 -1- ½ - 1/3 of 5.08% and 0.36% respectively. The Average difference in the energy dissipation was 2.18% in Set V.

In half pretension, Case DLC I- 1/2 showed the maximum difference in energy dissipation of -1.06% and the minimum of -0.42% for Cases DLC I- 1/4. The average difference in energy dissipation was -0.53%. In quarter pretension, Case DLC I- 1/4 showed the maximum of difference in energy dissipation of 2.26% and the minimum difference in energy dissipation was observed in Case DLC I- 1/3 of -0.47%. The average difference in energy dissipation was observed as 1.41%.

5.2.5 Extended end-plate connection model

5.2.5.1 Extended end-plate connection model Case 1

In extended end-plate connection (b_d = 1 in, t_e = ½ in) DLC I- 1 was considered as reference for comparison. It is observed that DLC II- ¼ -2 -1- ½ - 1/3 showed the difference in the energy dissipation of -6.62%. At the same time DLC IV- ¼ -2 -1- ½ - 1/3 Showed 9.51% difference in energy Dissipation. When half pretension model with loading of DLC I- 1 was compared with full pretension DLC I- 1 showed difference of -

101.12%. Similarly for quarter pretension, the difference in energy dissipation was -139.01%.

5.2.5.2 Extended end-plate connection model Case 2

Similarly in extended end-plate connection (b_d = ½ in, t_e = ½ in), DLC I- 1 was considered as reference for comparison. It is observed that DLC II- ¼ -2 -1- ½ - 1/3 showed the difference in energy dissipation of -11.66%. At the same time DLC IV- ¼ -2 -1- ½ - 1/3 Showed 6.48% difference in energy Dissipation. When half pretension model with loading of DLC I- 1 was compared with full pretension DLC I- 1 showed difference of -41.54%. Similarly for quarter pretension the difference in energy dissipation was -51.13%.

5.3 Conclusion

The conclusion of the study advances in the following forefronts:

1. The effect of cyclic loading frequency and the time dependent loading frequency on the response of the shear models tested were not propound with the majority of the difference in the energy dissipation being below 10% when compare to their respective cases. However the isolated cases with difference in energy dissipation as high as 19.7% were observed.

2. The effect of the time depended frequency cyclic load on the response of the tee – hanger connection was also not noticeable. However there were six cases in

which difference in energy dissipation were above 10% with maximum value of 19.21%.

3. The effect of developed load cases on the energy dissipation of the two cases of the extended end-plate connections followed similar trends as those of the simple connection models. The maximum difference value of 11.66% was recorded for the above connection cases.

4. The study of the effect of the contact algorithm on the response of the connecting surfaces was not successful for all the cases due to non-convergence of the finite element model. However for the single case that the final solution was obtained, profound difference in energy dissipation was observed (85%).

5. No specific trends were observed in the results of this study.

5.4 Recommendation

The effect of the element type and contact algorithm (even though limited and not within the scope of the study) showed profound difference for the case that were analyzed successfully. Thus, it is recommended that the effect of the contact algorithm and element type to be studied for connection subjected to cyclic displacement loading history.

APPENDIX A

TEST CASES

Table A-1 Welded shear surface model Case1

Test No.	tp	Contact	DLC	LLC
1	1	SS	DLC I - 1	-
2	1	SS	DLC I - 2	-
3	1	SS	DLC I - 3	-
4	1	SS	DLC I - 4	-
5	1	SS	DLC I - 5	-
6	1	SS	DLC II - 1	-
7	1	SS	DLC II - 2	-
8	1	SS	DLC II - 3	-
9	1	SS	DLC II - 4	-
10	1	SS	DLC II - 5	-
11	1	SS	DLC III - 1	-
12	1	SS	DLC III - 2	-
13	1	SS	DLC III - 3	-
14	1	SS	DLC III - 4	-
15	1	SS	DLC III - 5	-
16	1	SS	DLC IV - 1	-
17	1	SS	DLC IV - 2	-
18	1	SS	DLC IV - 3	-
19	1	SS	DLC IV - 4	-
20	1	SS	DLC IV - 5	-
21	1	SS	DLC V - 1	-
22	1	SS	DLC V - 2	-
23	1	SS	DLC V - 3	-
24	1	SS	DLC V - 4	-
25	1	SS	DLC V - 5	-
26	1	SS	DLC I - 1	-
27	1	NS	DLC I - 1	-
28	1	SS	DLC I - 1	LLC

Table A-2 Welded shear surface model Case 2

Test No.	tp	Contact	DLC	LLC
1	½	SS	DLC I - 1	-
2	½	SS	DLC I - 2	-
3	½	SS	DLC I - 3	-
4	½	SS	DLC I - 4	-
5	½	SS	DLC I - 5	-
6	½	SS	DLC II - 1	-
7	½	SS	DLC II - 2	-
8	½	SS	DLC II - 3	-
9	½	SS	DLC II - 4	-
10	½	SS	DLC II - 5	-
11	½	SS	DLC III - 1	-
12	½	SS	DLC III - 2	-
13	½	SS	DLC III - 3	-
14	½	SS	DLC III - 4	-
15	½	SS	DLC III - 5	-
16	½	SS	DLC IV - 1	-
17	½	SS	DLC IV - 2	-
18	½	SS	DLC IV - 3	-
19	½	SS	DLC IV - 4	-
20	½	SS	DLC IV - 5	-
21	½	SS	DLC V - 1	-
22	½	SS	DLC V - 2	-
23	½	SS	DLC V - 3	-
24	½	SS	DLC V - 4	-
25	½	SS	DLC V - 5	-
26	½	SS	DLC I - 1	-
27	½	NS	DLC I - 1	-
28	½	SS	DLC I - 1	LLC

Table A-3 Single bolted shear surface model Case 1

Test No.	t_p	b_d	P_t	Contact	E_t	DLC	LLC
1	1	½	FP	SS	C	DLC I - 1	-
2	1	½	FP	SS	C	DLC I - 2	-
3	1	½	FP	SS	C	DLC I - 3	-
4	1	½	FP	SS	C	DLC I - 4	-
5	1	½	FP	SS	C	DLC I - 5	-
6	1	½	FP	SS	C	DLC II - 1	-
7	1	½	FP	SS	C	DLC II - 2	-
8	1	½	FP	SS	C	DLC II - 3	-
9	1	½	FP	SS	C	DLC II - 4	-
10	1	½	FP	SS	C	DLC II - 5	-
11	1	½	FP	SS	C	DLC III - 1	-
12	1	½	FP	SS	C	DLC III - 2	-
13	1	½	FP	SS	C	DLC III - 3	-
14	1	½	FP	SS	C	DLC III - 4	-
15	1	½	FP	SS	C	DLC III - 5	-
16	1	½	FP	SS	C	DLC IV - 1	-
17	1	½	FP	SS	C	DLC IV - 2	-
18	1	½	FP	SS	C	DLC IV - 3	-
19	1	½	FP	SS	C	DLC IV - 4	-
20	1	½	FP	SS	C	DLC IV - 5	-
21	1	½	FP	SS	C	DLC V - 1	-
22	1	½	FP	SS	C	DLC V - 2	-
23	1	½	FP	SS	C	DLC V - 3	-
24	1	½	FP	SS	C	DLC V - 4	-
25	1	½	FP	SS	C	DLC V - 5	-
26	1	½	HP	SS	C	DLC I - 2	-
27	1	½	HP	SS	C	DLC I - 3	-
28	1	½	HP	SS	C	DLC I - 4	-
29	1	½	HP	SS	C	DLC I - 5	-
30	1	½	HP	SS	C	DLC I - 1	-

Table A-3 - continued

31	1	½	QP	SS	C	DLC I - 2	-
32	1	½	QP	SS	C	DLC I - 3	-
33	1	½	QP	SS	C	DLC I - 4	-
34	1	½	QP	SS	C	DLC I - 5	-
35	1	½	QP	SS	C	DLC I - 1	-
36	1	½	FP	SS	HX	DLC I - 1	-
37	1	½	FP	NS	C	DLC I - 1	-
38	1	½	FP	SS	C	DLC I - 1	-
39	1	½	FP	SS	C	-	LLC

Table A-4 Single bolted shear surface model Case 2

Test No.	t_p	b_d	P_t	Contact	E_t	DLC	LLC
1	¼	1	FP	SS	C	DLC I - 1	-
2	¼	1	FP	SS	C	DLC I - 2	-
3	¼	1	FP	SS	C	DLC I - 3	-
4	¼	1	FP	SS	C	DLC I - 4	-
5	¼	1	FP	SS	C	DLC I - 5	-
6	¼	1	FP	SS	C	DLC II - 1	-
7	¼	1	FP	SS	C	DLC II - 2	-
8	¼	1	FP	SS	C	DLC II - 3	-
9	¼	1	FP	SS	C	DLC II - 4	-
10	¼	1	FP	SS	C	DLC II - 5	-
11	¼	1	FP	SS	C	DLC III - 1	-
12	¼	1	FP	SS	C	DLC III - 2	-
13	¼	1	FP	SS	C	DLC III - 3	-
14	¼	1	FP	SS	C	DLC III - 4	-
15	¼	1	FP	SS	C	DLC III - 5	-
16	¼	1	FP	SS	C	DLC IV - 1	-
17	¼	1	FP	SS	C	DLC IV - 2	-
18	¼	1	FP	SS	C	DLC IV - 3	-
19	¼	1	FP	SS	C	DLC IV - 4	-
20	¼	1	FP	SS	C	DLC IV - 5	-
21	¼	1	FP	SS	C	DLC V - 1	-
22	¼	1	FP	SS	C	DLC V - 2	-
23	¼	1	FP	SS	C	DLC V - 3	-
24	¼	1	FP	SS	C	DLC V - 4	-
25	¼	1	FP	SS	C	DLC V - 5	-
26	¼	1	HP	SS	C	DLC I - 1	-
27	¼	1	HP	SS	C	DLC I - 2	-
28	¼	1	HP	SS	C	DLC I - 3	-
29	¼	1	HP	SS	C	DLC I - 4	-
30	¼	1	HP	SS	C	DLC I - 5	-

Table A-4 - continued

31	¼	1	QP	SS	C	DLC I - 1	-
32	¼	1	QP	SS	C	DLC I - 2	-
33	¼	1	QP	SS	C	DLC I - 3	-
34	¼	1	QP	SS	C	DLC I - 4	-
35	¼	1	QP	SS	C	DLC I - 5	-
36	¼	1	FP	SS	HX	DLC I - 1	-
37	¼	1	FP	NS	C	DLC I - 1	-
38	¼	1	FP	SS	C	DLC I - 1	-
39	¼	1	FP	SS	C	-	LLC

Table A-5 Single bolted shear surface model Case 3

Test No.	t_p	b_d	P_t	Contact	E_t	DLC	LLC
1	1	1	FP	SS	C	DLC I - 1	-
2	1	1	FP	SS	C	DLC I - 2	-
3	1	1	FP	SS	C	DLC I - 3	-
4	1	1	FP	SS	C	DLC I - 4	-
5	1	1	FP	SS	C	DLC I - 5	-
6	1	1	FP	SS	C	DLC II - 1	-
7	1	1	FP	SS	C	DLC II - 2	-
8	1	1	FP	SS	C	DLC II - 3	-
9	1	1	FP	SS	C	DLC II - 4	-
10	1	1	FP	SS	C	DLC II - 5	-
11	1	1	FP	SS	C	DLC III - 1	-
12	1	1	FP	SS	C	DLC III - 2	-
13	1	1	FP	SS	C	DLC III - 3	-
14	1	1	FP	SS	C	DLC III - 4	-
15	1	1	FP	SS	C	DLC III - 5	-
16	1	1	FP	SS	C	DLC IV - 1	-
17	1	1	FP	SS	C	DLC IV - 2	-
18	1	1	FP	SS	C	DLC IV - 3	-
19	1	1	FP	SS	C	DLC IV - 4	-
20	1	1	FP	SS	C	DLC IV - 5	-
21	1	1	FP	SS	C	DLC V - 1	-
22	1	1	FP	SS	C	DLC V - 2	-
23	1	1	FP	SS	C	DLC V - 3	-
24	1	1	FP	SS	C	DLC V - 4	-
25	1	1	FP	SS	C	DLC V - 5	-
26	1	1	HP	SS	C	DLC I - 1	-
27	1	1	HP	SS	C	DLC I - 2	-
28	1	1	HP	SS	C	DLC I - 3	-
29	1	1	HP	SS	C	DLC I - 4	-
30	1	1	HP	SS	C	DLC I - 5	-

Table A-5 - continued

31	1	1	QP	SS	C	DLC I - 1	-
32	1	1	QP	SS	C	DLC I - 2	-
33	1	1	QP	SS	C	DLC I - 3	-
34	1	1	QP	SS	C	DLC I - 4	-
35	1	1	QP	SS	C	DLC I - 5	-
36	1	1	FP	SS	HX	DLC I - 1	-
37	1	1	FP	NS	C	DLC I - 1	-
38	1	1	FP	SS	C	DLC I - 1	-
39	1	1	FP	SS	C	-	LLC

Table A-6 Double bolted shear surface model Case 1

Test No.	t_p	b_d	P_t	Contact	E_t	DLC	LLC
1	1	½	FP	SS	C	DLC I - 1	-
2	1	½	FP	SS	C	DLC I - 2	-
3	1	½	FP	SS	C	DLC I - 3	-
4	1	½	FP	SS	C	DLC I - 4	-
5	1	½	FP	SS	C	DLC I - 5	-
6	1	½	FP	SS	C	DLC II - 1	-
7	1	½	FP	SS	C	DLC II - 2	-
8	1	½	FP	SS	C	DLC II - 3	-
9	1	½	FP	SS	C	DLC II - 4	-
10	1	½	FP	SS	C	DLC II - 5	-
11	1	½	FP	SS	C	DLC III - 1	-
12	1	½	FP	SS	C	DLC III - 2	-
13	1	½	FP	SS	C	DLC III - 3	-
14	1	½	FP	SS	C	DLC III - 4	-
15	1	½	FP	SS	C	DLC III - 5	-
16	1	½	FP	SS	C	DLC IV - 1	-
17	1	½	FP	SS	C	DLC IV - 2	-
18	1	½	FP	SS	C	DLC IV - 3	-
19	1	½	FP	SS	C	DLC IV - 4	-
20	1	½	FP	SS	C	DLC IV - 5	-
21	1	½	FP	SS	C	DLC V - 1	-
22	1	½	FP	SS	C	DLC V - 2	-
23	1	½	FP	SS	C	DLC V - 3	-
24	1	½	FP	SS	C	DLC V - 4	-
25	1	½	FP	SS	C	DLC V - 5	-
26	1	½	HP	SS	C	DLC I - 2	-
27	1	½	HP	SS	C	DLC I - 3	-
28	1	½	HP	SS	C	DLC I - 4	-
29	1	½	HP	SS	C	DLC I - 5	-
30	1	½	HP	SS	C	DLC I - 1	-

Table A-6 - continued

31	1	½	QP	SS	C	DLC I - 2	-
32	1	½	QP	SS	C	DLC I - 3	-
33	1	½	QP	SS	C	DLC I - 4	-
34	1	½	QP	SS	C	DLC I - 5	-
35	1	½	QP	SS	C	DLC I - 1	-
36	1	½	FP	SS	HX	DLC I - 1	-
37	1	½	FP	NS	C	DLC I - 1	-
38	1	½	FP	SS	C	DLC I - 1	-
39	1	½	FP	SS	C	-	LLC

Table A-7 Double bolted shear surface model Case 2

Test No.	t_p	b_d	P_t	Contact	E_t	DLC	LLC
1	¼	1	FP	SS	C	DLC I - 1	-
2	¼	1	FP	SS	C	DLC I - 2	-
3	¼	1	FP	SS	C	DLC I - 3	-
4	¼	1	FP	SS	C	DLC I - 4	-
5	¼	1	FP	SS	C	DLC I - 5	-
6	¼	1	FP	SS	C	DLC II - 1	-
7	¼	1	FP	SS	C	DLC II - 2	-
8	¼	1	FP	SS	C	DLC II - 3	-
9	¼	1	FP	SS	C	DLC II - 4	-
10	¼	1	FP	SS	C	DLC II - 5	-
11	¼	1	FP	SS	C	DLC III - 1	-
12	¼	1	FP	SS	C	DLC III - 2	-
13	¼	1	FP	SS	C	DLC III - 3	-
14	¼	1	FP	SS	C	DLC III - 4	-
15	¼	1	FP	SS	C	DLC III - 5	-
16	¼	1	FP	SS	C	DLC IV - 1	-
17	¼	1	FP	SS	C	DLC IV - 2	-
18	¼	1	FP	SS	C	DLC IV - 3	-
19	¼	1	FP	SS	C	DLC IV - 4	-
20	¼	1	FP	SS	C	DLC IV - 5	-
21	¼	1	FP	SS	C	DLC V - 1	-
22	¼	1	FP	SS	C	DLC V - 2	-
23	¼	1	FP	SS	C	DLC V - 3	-
24	¼	1	FP	SS	C	DLC V - 4	-
25	¼	1	FP	SS	C	DLC V - 5	-
26	¼	1	HP	SS	C	DLC I - 1	-
27	¼	1	HP	SS	C	DLC I - 2	-
28	¼	1	HP	SS	C	DLC I - 3	-
29	¼	1	HP	SS	C	DLC I - 4	-
30	¼	1	HP	SS	C	DLC I - 5	-

Table A-7 - continued

31	¼	1	QP	SS	C	DLC I - 1	-
32	¼	1	QP	SS	C	DLC I - 2	-
33	¼	1	QP	SS	C	DLC I - 3	-
34	¼	1	QP	SS	C	DLC I - 4	-
35	¼	1	QP	SS	C	DLC I - 5	-
36	¼	1	FP	SS	HX	DLC I - 1	-
37	¼	1	FP	NS	C	DLC I - 1	-
38	¼	1	FP	SS	C	DLC I - 1	-
39	¼	1	FP	SS	C	-	LLC

Table A-8 Double bolted shear surface model Case 3

Test No.	t_p	b_d	P_t	Contact	E_t	DLC	LLC
1	1	1	FP	SS	C	DLC I - 1	-
2	1	1	FP	SS	C	DLC I - 2	-
3	1	1	FP	SS	C	DLC I - 3	-
4	1	1	FP	SS	C	DLC I - 4	-
5	1	1	FP	SS	C	DLC I - 5	-
6	1	1	FP	SS	C	DLC II - 1	-
7	1	1	FP	SS	C	DLC II - 2	-
8	1	1	FP	SS	C	DLC II - 3	-
9	1	1	FP	SS	C	DLC II - 4	-
10	1	1	FP	SS	C	DLC II - 5	-
11	1	1	FP	SS	C	DLC III - 1	-
12	1	1	FP	SS	C	DLC III - 2	-
13	1	1	FP	SS	C	DLC III - 3	-
14	1	1	FP	SS	C	DLC III - 4	-
15	1	1	FP	SS	C	DLC III - 5	-
16	1	1	FP	SS	C	DLC IV - 1	-
17	1	1	FP	SS	C	DLC IV - 2	-
18	1	1	FP	SS	C	DLC IV - 3	-
19	1	1	FP	SS	C	DLC IV - 4	-
20	1	1	FP	SS	C	DLC IV - 5	-
21	1	1	FP	SS	C	DLC V - 1	-
22	1	1	FP	SS	C	DLC V - 2	-
23	1	1	FP	SS	C	DLC V - 3	-
24	1	1	FP	SS	C	DLC V - 4	-
25	1	1	FP	SS	C	DLC V - 5	-
26	1	1	HP	SS	C	DLC I - 1	-
27	1	1	HP	SS	C	DLC I - 2	-
28	1	1	HP	SS	C	DLC I - 3	-
29	1	1	HP	SS	C	DLC I - 4	-
30	1	1	HP	SS	C	DLC I - 5	-

Table A-8 - continued

31	1	1	QP	SS	C	DLC I - 1	-
32	1	1	QP	SS	C	DLC I - 2	-
33	1	1	QP	SS	C	DLC I - 3	-
34	1	1	QP	SS	C	DLC I - 4	-
35	1	1	QP	SS	C	DLC I - 5	-
36	1	1	FP	SS	HX	DLC I - 1	-
37	1	1	FP	NS	C	DLC I - 1	-
38	1	1	FP	SS	C	DLC I - 1	-
39	1	1	FP	SS	C	-	LLC

Table A-9 T-Hanger model Case 1

Test No.	t_f	b_d	g	P_t	Contact	E_t	DLC	LLC
1	1	1	2¾	FP	SS	C	DLC I - 1	-
2	1	1	2¾	FP	SS	C	DLC I - 2	-
3	1	1	2¾	FP	SS	C	DLC I - 3	-
4	1	1	2¾	FP	SS	C	DLC I - 4	-
5	1	1	2¾	FP	SS	C	DLC I - 5	-
6	1	1	2¾	FP	SS	C	DLC II - 1	-
7	1	1	2¾	FP	SS	C	DLC II - 2	-
8	1	1	2¾	FP	SS	C	DLC II - 3	-
9	1	1	2¾	FP	SS	C	DLC II - 4	-
10	1	1	2¾	FP	SS	C	DLC II - 5	-
11	1	1	2¾	FP	SS	C	DLC III - 1	-
12	1	1	2¾	FP	SS	C	DLC III - 2	-
13	1	1	2¾	FP	SS	C	DLC III - 3	-
14	1	1	2¾	FP	SS	C	DLC III - 4	-
15	1	1	2¾	FP	SS	C	DLC III - 5	-
16	1	1	2¾	FP	SS	C	DLC IV - 1	-
17	1	1	2¾	FP	SS	C	DLC IV - 2	-
18	1	1	2¾	FP	SS	C	DLC IV - 3	-
19	1	1	2¾	FP	SS	C	DLC IV - 4	-
20	1	1	2¾	FP	SS	C	DLC IV - 5	-
21	1	1	2¾	FP	SS	C	DLC V - 1	-
22	1	1	2¾	FP	SS	C	DLC V - 2	-
23	1	1	2¾	FP	SS	C	DLC V - 3	-
24	1	1	2¾	FP	SS	C	DLC V - 4	-
25	1	1	2¾	FP	SS	C	DLC V - 5	-
26	1	1	2¾	HP	SS	C	DLC I - 1	-
27	1	1	2¾	HP	SS	C	DLC I - 2	-
28	1	1	2¾	HP	SS	C	DLC I - 3	-
29	1	1	2¾	HP	SS	C	DLC I - 4	-
30	1	1	2¾	HP	SS	C	DLC I - 5	-

Table A-9 - continued

31	1	1	2¾	QP	SS	C	DLC I - 1	-
32	1	1	2¾	QP	SS	C	DLC I - 2	-
33	1	1	2¾	QP	SS	C	DLC I - 3	-
34	1	1	2¾	QP	SS	C	DLC I - 4	-
35	1	1	2¾	QP	SS	C	DLC I - 5	-
36	1	1	2¾	FP	SS	HX	DLC I - 1	-
37	1	1	2¾	FP	NS	C	DLC I - 1	-
38	1	1	2¾	FP	SS	C	DLC I - 1	-

Table A-10 T-Hanger model Case 2

Test No.	t_f	b_d	g	P_t	Contact	E_t	DLC	LLC
1	½	½	1	FP	SS	C	DLC I - 1	-
2	½	½	1	FP	SS	C	DLC I - 2	-
3	½	½	1	FP	SS	C	DLC I - 3	-
4	½	½	1	FP	SS	C	DLC I - 4	-
5	½	½	1	FP	SS	C	DLC I - 5	-
6	½	½	1	FP	SS	C	DLC II - 1	-
7	½	½	1	FP	SS	C	DLC II - 2	-
8	½	½	1	FP	SS	C	DLC II - 3	-
9	½	½	1	FP	SS	C	DLC II - 4	-
10	½	½	1	FP	SS	C	DLC II - 5	-
11	½	½	1	FP	SS	C	DLC III - 1	-
12	½	½	1	FP	SS	C	DLC III - 2	-
13	½	½	1	FP	SS	C	DLC III - 3	-
14	½	½	1	FP	SS	C	DLC III - 4	-
15	½	½	1	FP	SS	C	DLC III - 5	-
16	½	½	1	FP	SS	C	DLC IV - 1	-
17	½	½	1	FP	SS	C	DLC IV - 2	-
18	½	½	1	FP	SS	C	DLC IV - 3	-
19	½	½	1	FP	SS	C	DLC IV - 4	-
20	½	½	1	FP	SS	C	DLC IV - 5	-
21	½	½	1	FP	SS	C	DLC V - 1	-
22	½	½	1	FP	SS	C	DLC V - 2	-
23	½	½	1	FP	SS	C	DLC V - 3	-
24	½	½	1	FP	SS	C	DLC V - 4	-
25	½	½	1	FP	SS	C	DLC V - 5	-
26	½	½	1	HP	SS	C	DLC I - 1	-
27	½	½	1	HP	SS	C	DLC I - 2	-
28	½	½	1	HP	SS	C	DLC I - 3	-
29	½	½	1	HP	SS	C	DLC I - 4	-
30	½	½	1	HP	SS	C	DLC I - 5	-

Table A-10 - continued

31	½	½	1	QP	SS	C	DLC I - 1	-
32	½	½	1	QP	SS	C	DLC I - 2	-
33	½	½	1	QP	SS	C	DLC I - 3	-
34	½	½	1	QP	SS	C	DLC I - 4	-
35	½	½	1	QP	SS	C	DLC I - 5	-
36	½	½	1	FP	SS	HX	DLC I - 1	-
37	½	½	1	FP	NS	C	DLC I - 1	-
38	½	½	1	FP	SS	C	DLC I - 1	-
39	½	½	1	FP	SS	C	-	LLC

Table A-11 T-Hanger model Case 3

Test No.	t_f	b_d	g	P_t	Contact	E_t	DLC	LLC
1	1	1	2¾	FP	SS	C	DLC I - 1	-
2	1	1	2¾	FP	SS	C	DLC I - 2	-
3	1	1	2¾	FP	SS	C	DLC I - 3	-
4	1	1	2¾	FP	SS	C	DLC I - 4	-
5	1	1	2¾	FP	SS	C	DLC I - 5	-
6	1	1	2¾	FP	SS	C	DLC II - 1	-
7	1	1	2¾	FP	SS	C	DLC II - 2	-
8	1	1	2¾	FP	SS	C	DLC II - 3	-
9	1	1	2¾	FP	SS	C	DLC II - 4	-
10	1	1	2¾	FP	SS	C	DLC II - 5	-
11	1	1	2¾	FP	SS	C	DLC III - 1	-
12	1	1	2¾	FP	SS	C	DLC III - 2	-
13	1	1	2¾	FP	SS	C	DLC III - 3	-
14	1	1	2¾	FP	SS	C	DLC III - 4	-
15	1	1	2¾	FP	SS	C	DLC III - 5	-
16	1	1	2¾	FP	SS	C	DLC IV - 1	-
17	1	1	2¾	FP	SS	C	DLC IV - 2	-
18	1	1	2¾	FP	SS	C	DLC IV - 3	-
19	1	1	2¾	FP	SS	C	DLC IV - 4	-
20	1	1	2¾	FP	SS	C	DLC IV - 5	-
21	1	1	2¾	FP	SS	C	DLC V - 1	-
22	1	1	2¾	FP	SS	C	DLC V - 2	-
23	1	1	2¾	FP	SS	C	DLC V - 3	-
24	1	1	2¾	FP	SS	C	DLC V - 4	-
25	1	1	2¾	FP	SS	C	DLC V - 5	-
26	1	1	2¾	HP	SS	C	DLC I - 1	-
27	1	1	2¾	HP	SS	C	DLC I - 2	-
28	1	1	2¾	HP	SS	C	DLC I - 3	-
29	1	1	2¾	HP	SS	C	DLC I - 4	-
30	1	1	2¾	HP	SS	C	DLC I - 5	-

Table A-11 - continued

31	1	½	1½	HP	SS	C	DLC I - 1	-
32	1	½	1½	QP	SS	C	DLC I - 2	-
33	1	½	1½	QP	SS	C	DLC I - 3	-
34	1	½	1½	QP	SS	C	DLC I - 4	-
35	1	½	1½	QP	SS	C	DLC I - 5	-
36	1	½	1½	QP	SS	C	DLC I - 1	-
37	1	½	1½	FP	SS	HX	DLC I - 1	-
38	1	½	1½	FP	NS	C	DLC I - 1	-
39	1	½	1½	FP	SS	C	-	LLC

Table A-12 Extended end plate connection model Case 1

Test No	b_d	t_e	P_t	DCL	E_t	LLC
1	1	½	FP	DLC I - 1	C	-
2	1	½	FP	DLC IV - 1	C	-
3	1	½	HP	DLC I - 1	C	-
4	1	½	QP	DLC I - 1	C	-
5	1	½	FP	-	C	LLC

Table A-13 Extended end plate connection model Case 2

Test No	b_d	t_e	P_t	DCL	E_t	LLC
1	½	½	FP	DLC I - 1	C	-
2	½	½	FP	DLC IV - 1	C	-
3	½	½	HP	DLC I - 1	C	-
4	½	½	QP	DLC I - 1	C	-
5	½	½	FP	-	C	LLC

APPENDIX B

WELDED SHEAR SURFACE MODELS

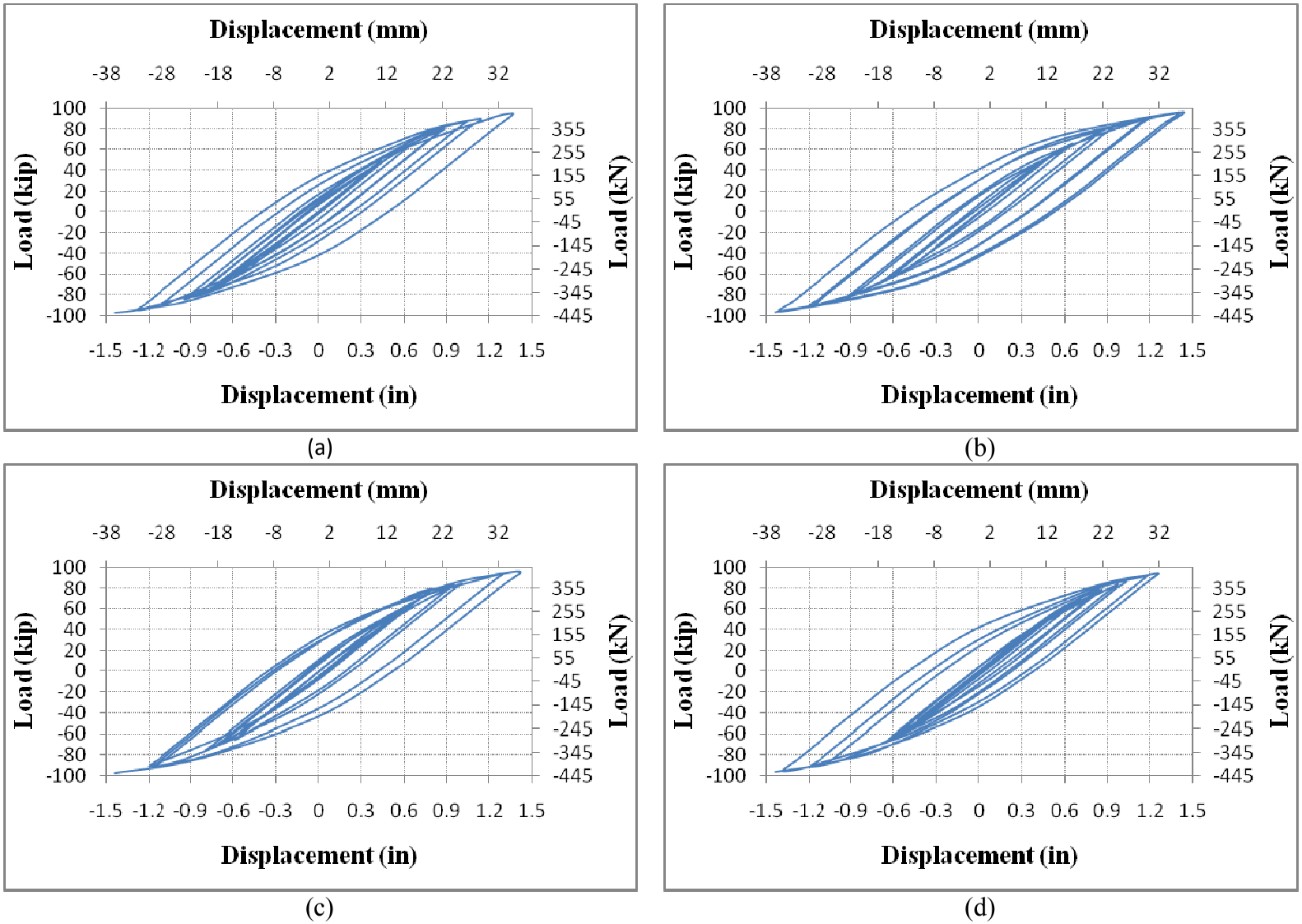

Figure B-1 Load-Displacement Cyclic Plots for: (a) SM-W-1/2-DLC-I-1; (b) SM-W-1/2-DLC-I-2; (c) SM-W-1/2-DLC-I-3; and (d) SM-W-1/2-DLC-I-4

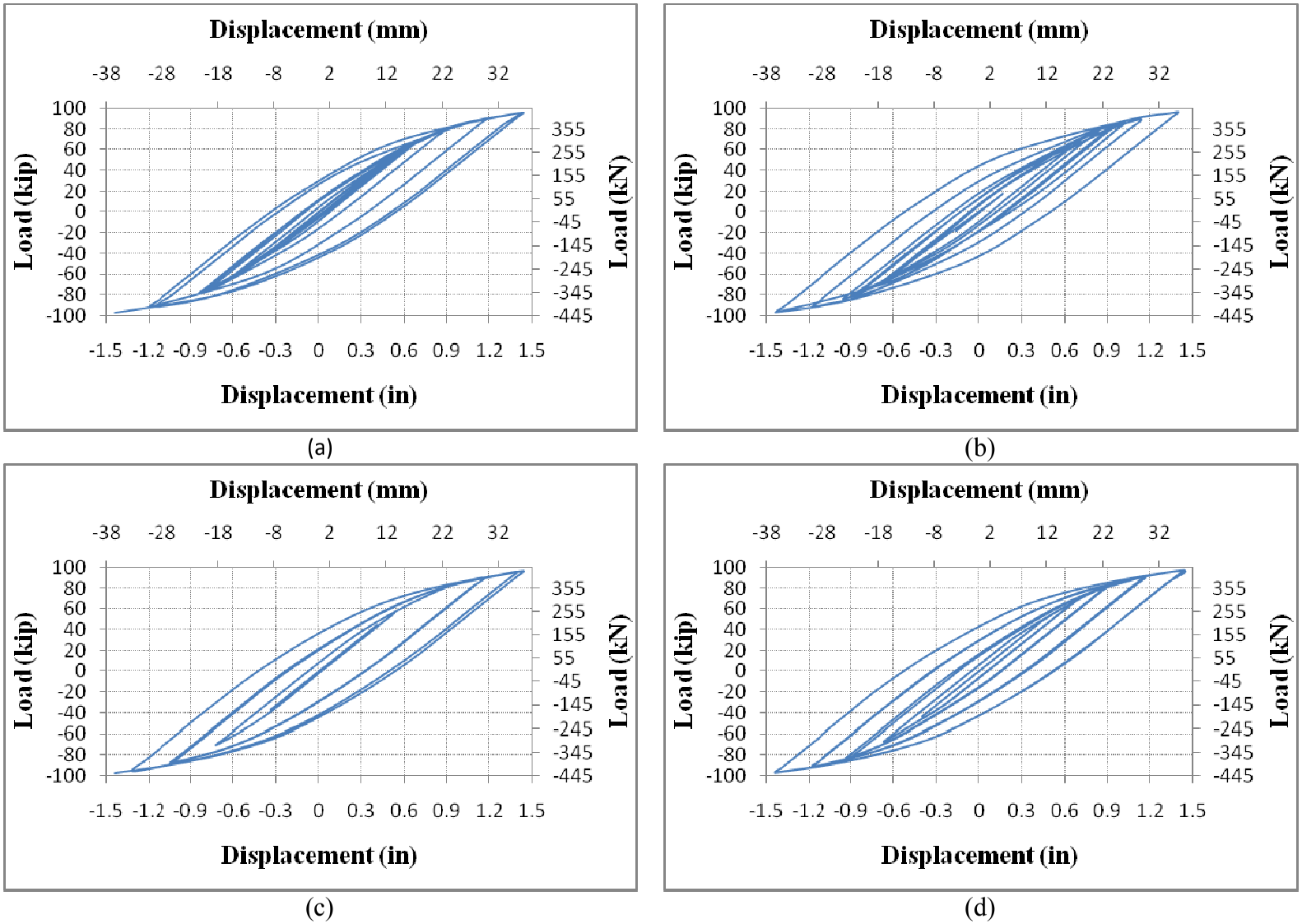

Figure B-2 Load-Displacement Cyclic Plots for: (a) SM-W-1/2-DLC-I-5; (b) SM-W-1/2-DLC-II-1; (c) SM-W-1/2-DLC-II-2; and (d) SM-W-1/2-DLC-II-3

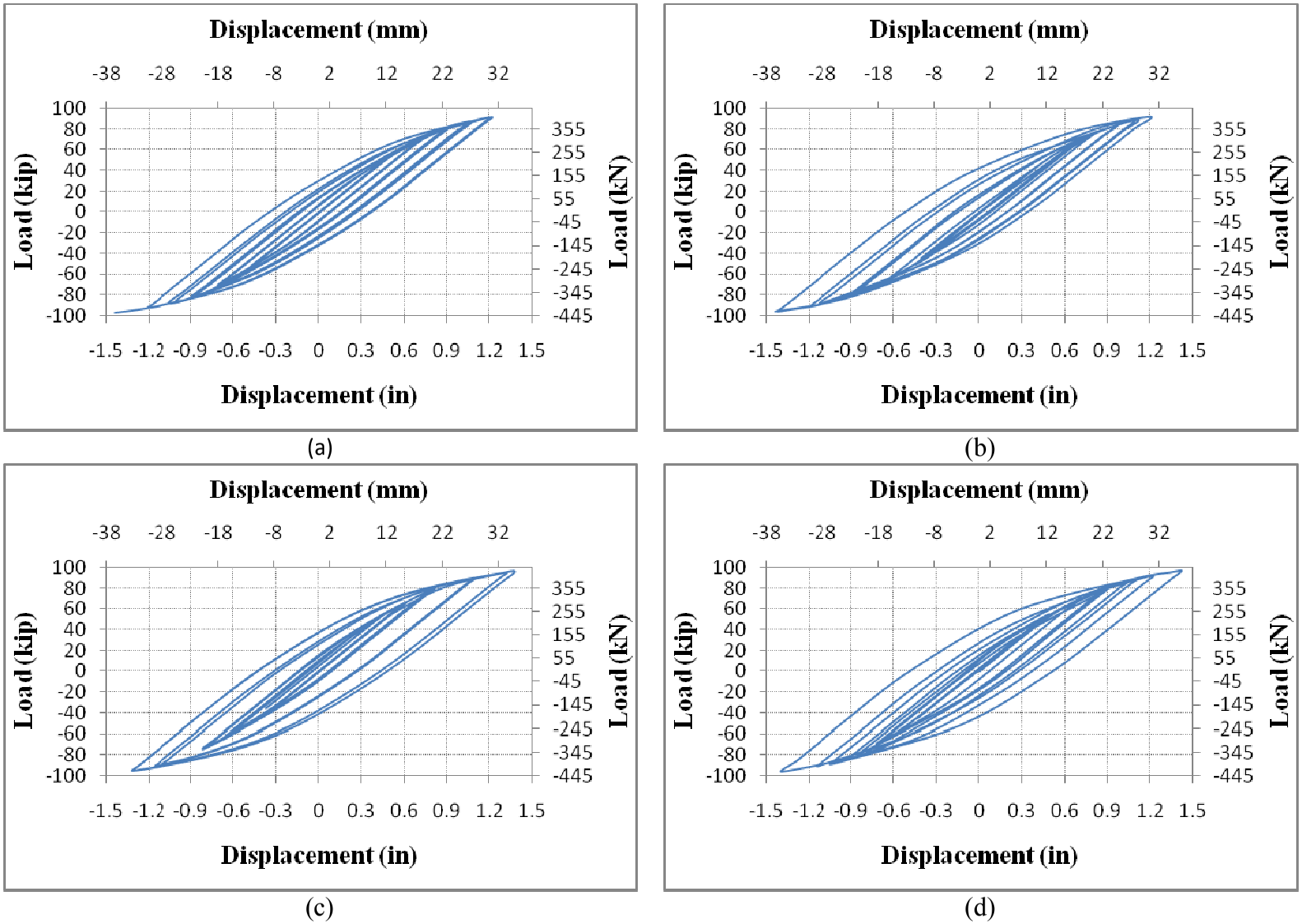

Figure B-3 Load-Displacement Cyclic Plots for: (a) SM-W-1/2-DLC-II-4; (b) SM-W-1/2-DLC-II-5; (c) SM-W-1-DLC-III-1; and (d) SM-W-1/2-DLC-III-2

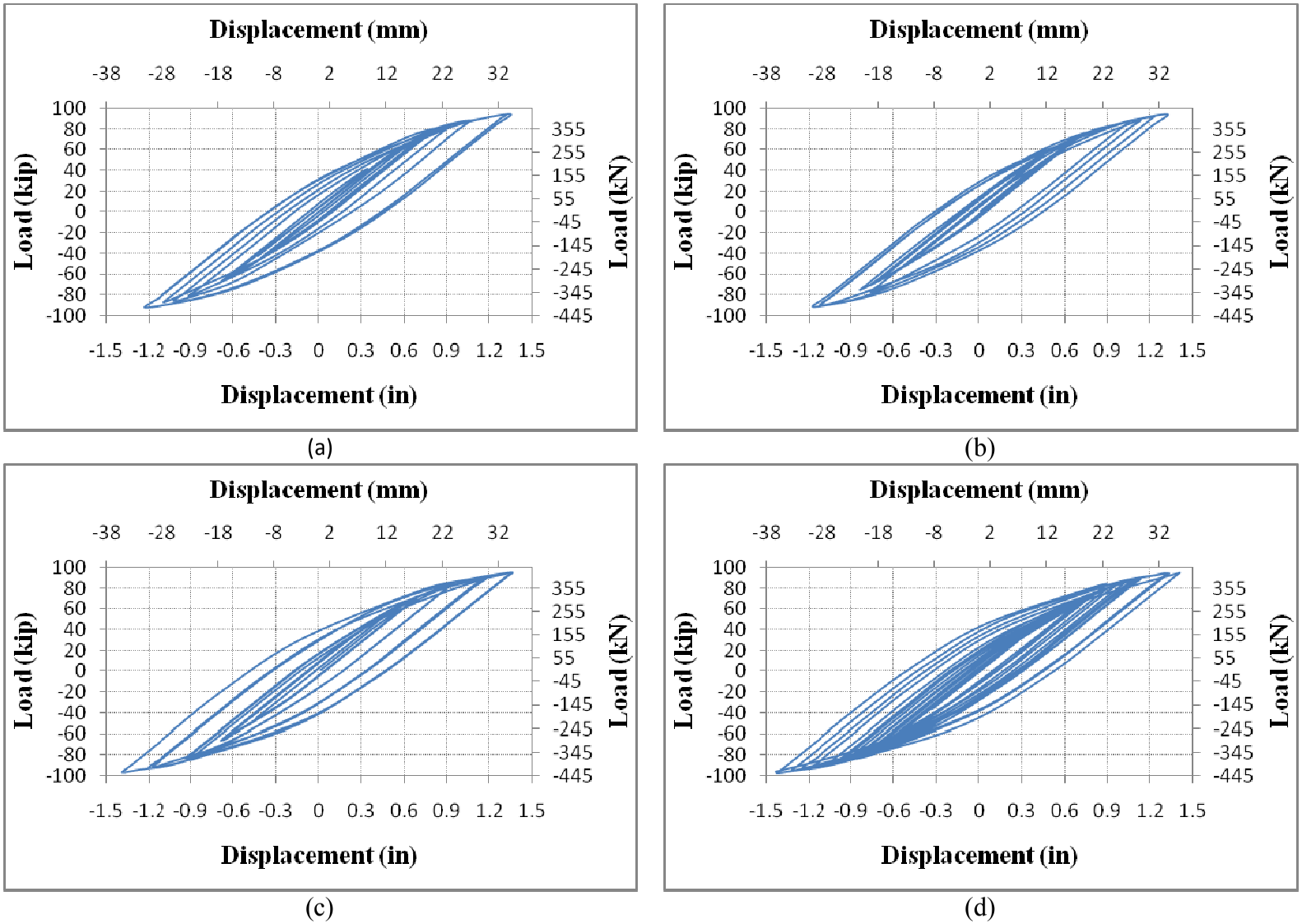

Figure B-4 Load-Displacement Cyclic Plots for: (a) SM-W-1/2-DLC-III-3; (b) SM-W-1/2-DLC-III-4; (c) SM-W-1/2-DLC-III-5; and (d) SM-W-1/2-DLC-IV-1

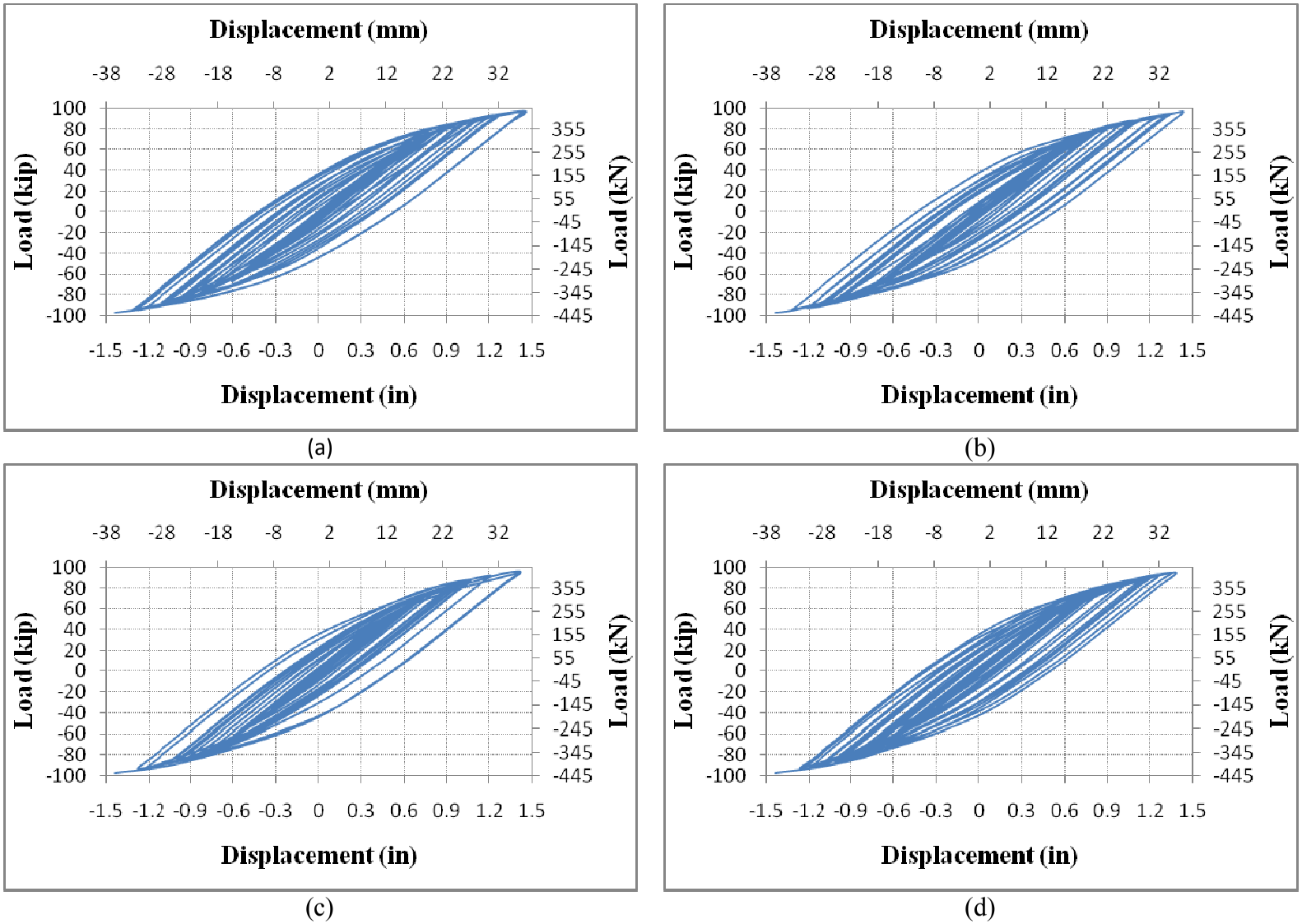

Figure B-5 Load-Displacement Cyclic Plots for: (a) SM-W-1/2-DLC-IV-2; (b) SM-W-1/2-DLC-IV-3; (c) SM-W-1/2-DLC-IV-4; and (d) SM-W-1/2-DLC-IV-5

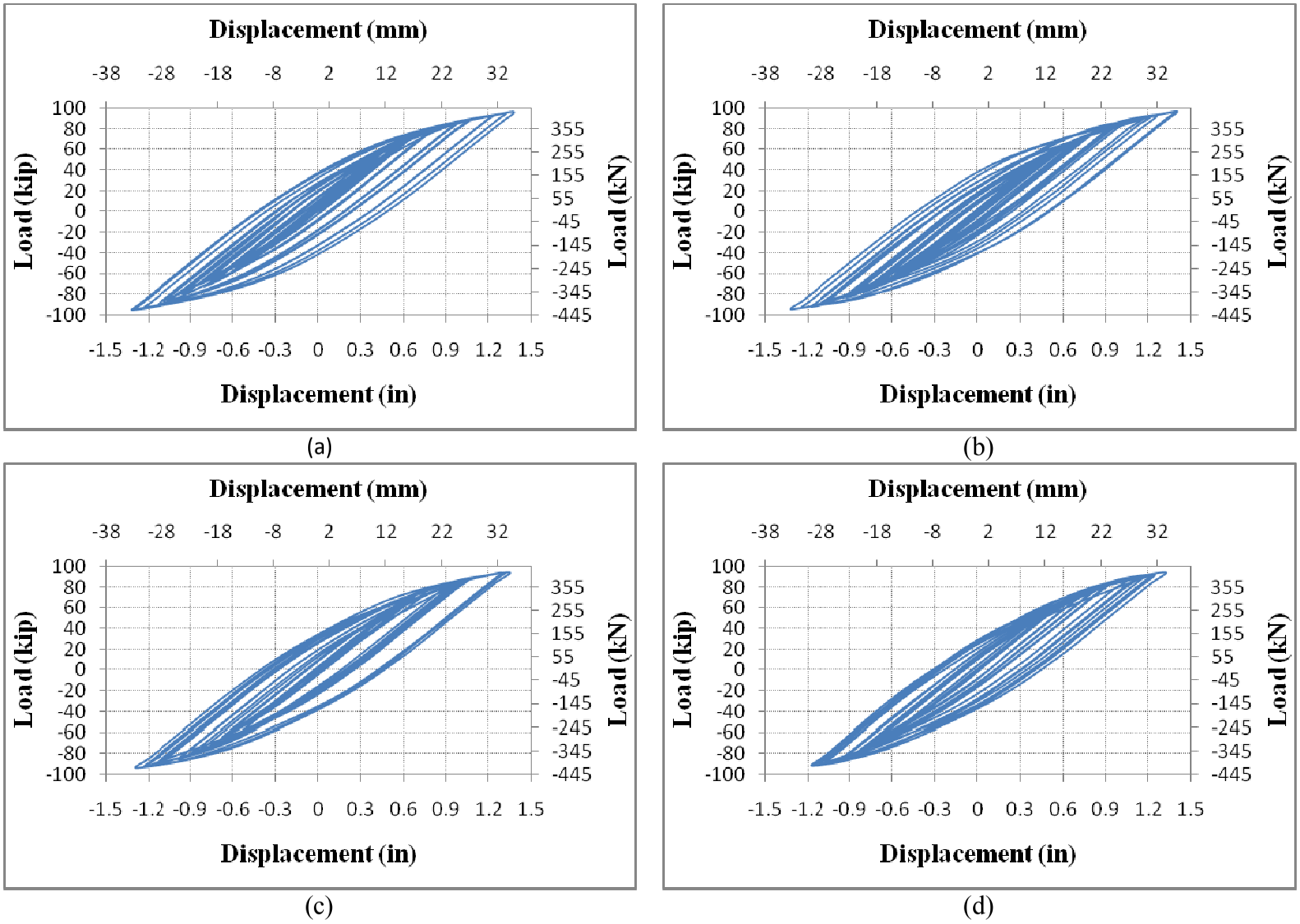

Figure B-6 Load-Displacement Cyclic Plots for: (a) SM-W-1/2-DLC-V-1; (b) SM-W-1/2-DLC-V-2; (c) SM-W-1/2-DLC-V-3; and (d) SM-W-1/2-DLC-V-4

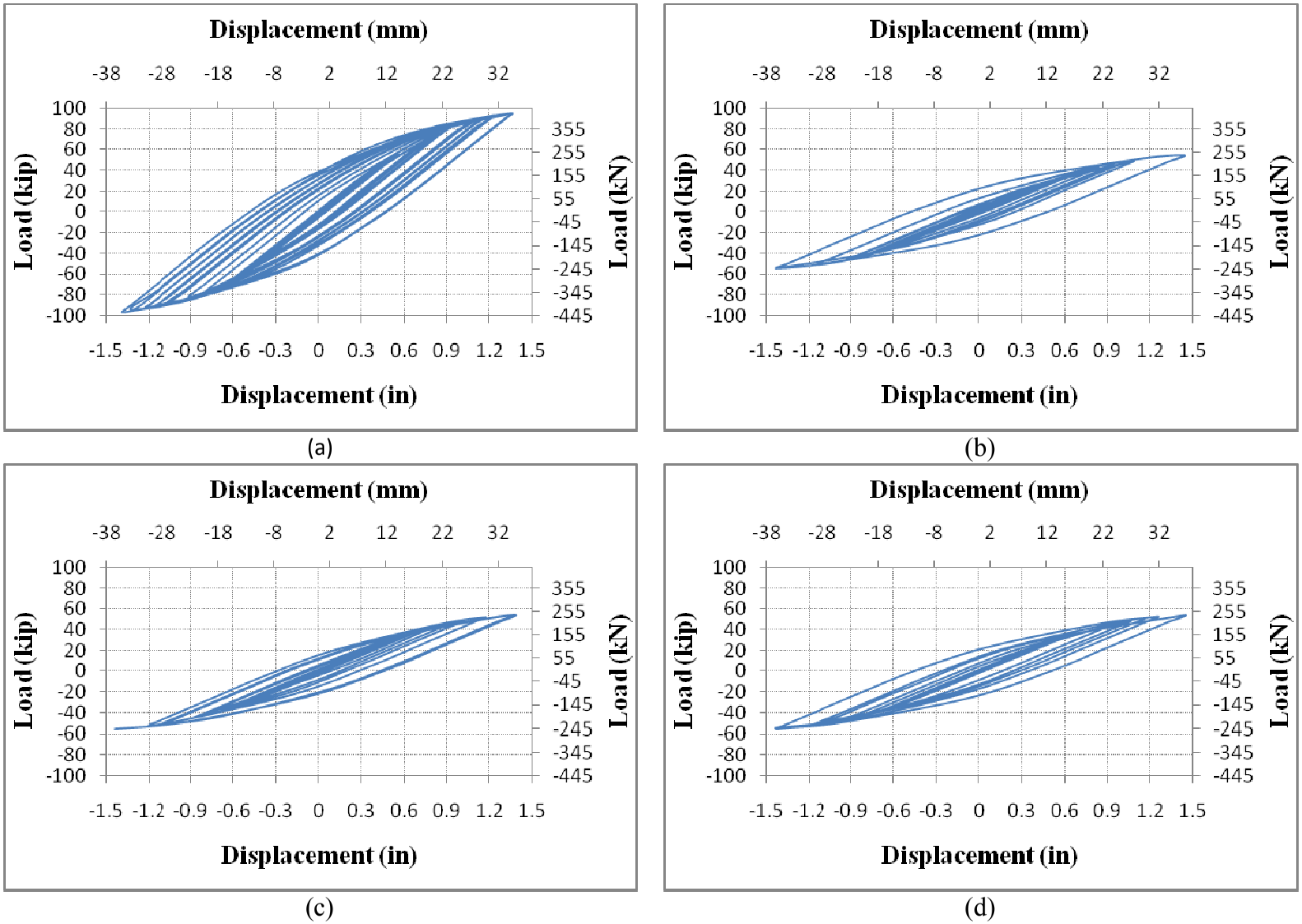

Figure B-7 Load-Displacement Cyclic Plots for: (a) SM-W-1/2-DLC-V-5; (b) SM-W-1-DLC-I-1; (c) SM-W-1-DLC-I-2; and (d) SM-W-1-DLC-I-3

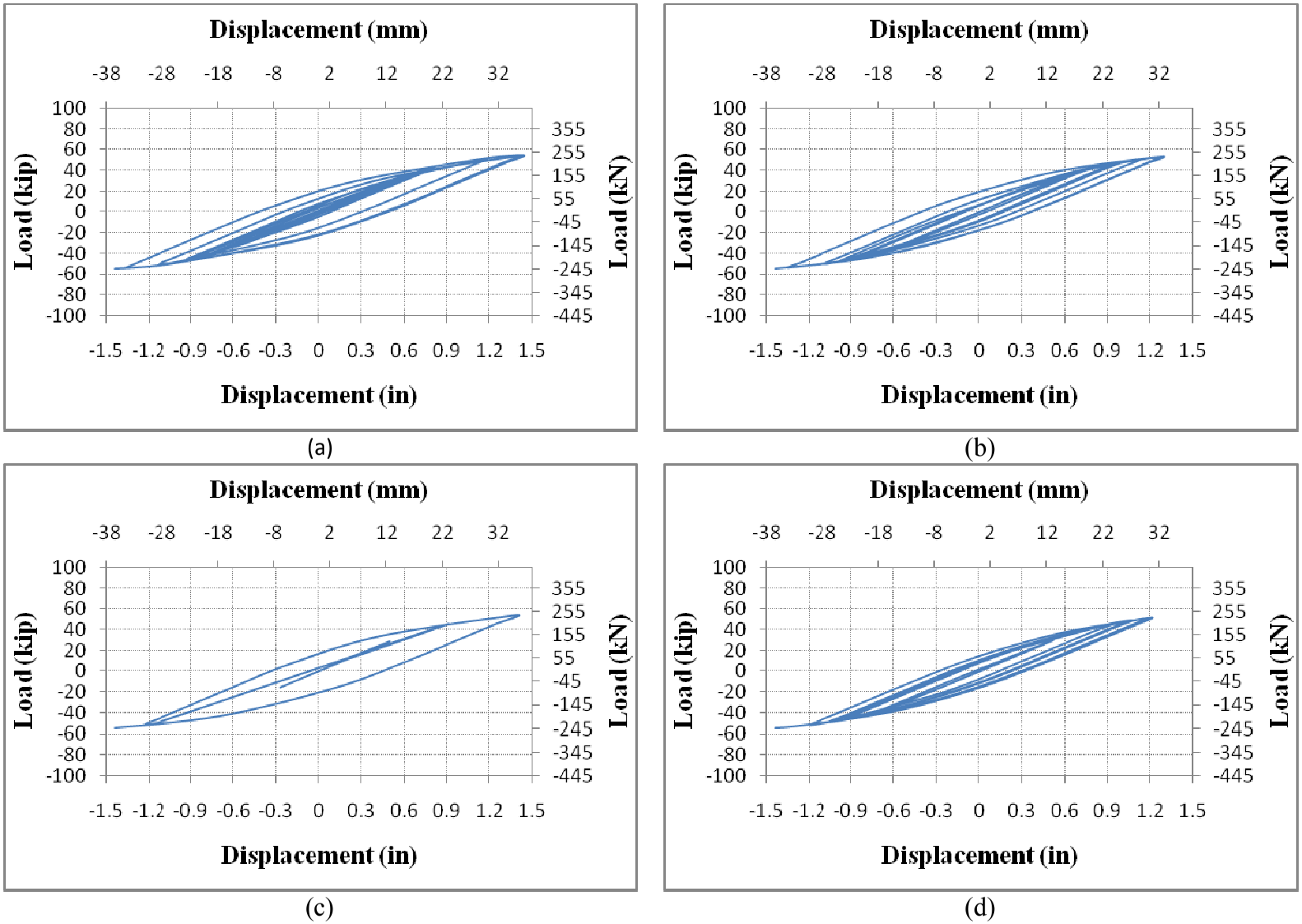

Figure B-8 Load-Displacement Cyclic Plots for: (a) SM-W-1-DLC-I-4; (b) SM-W-1-DLC-I-5; (c) SM-W-1-DLC-II-1; and (d) SM-W-1-DLC-II-2

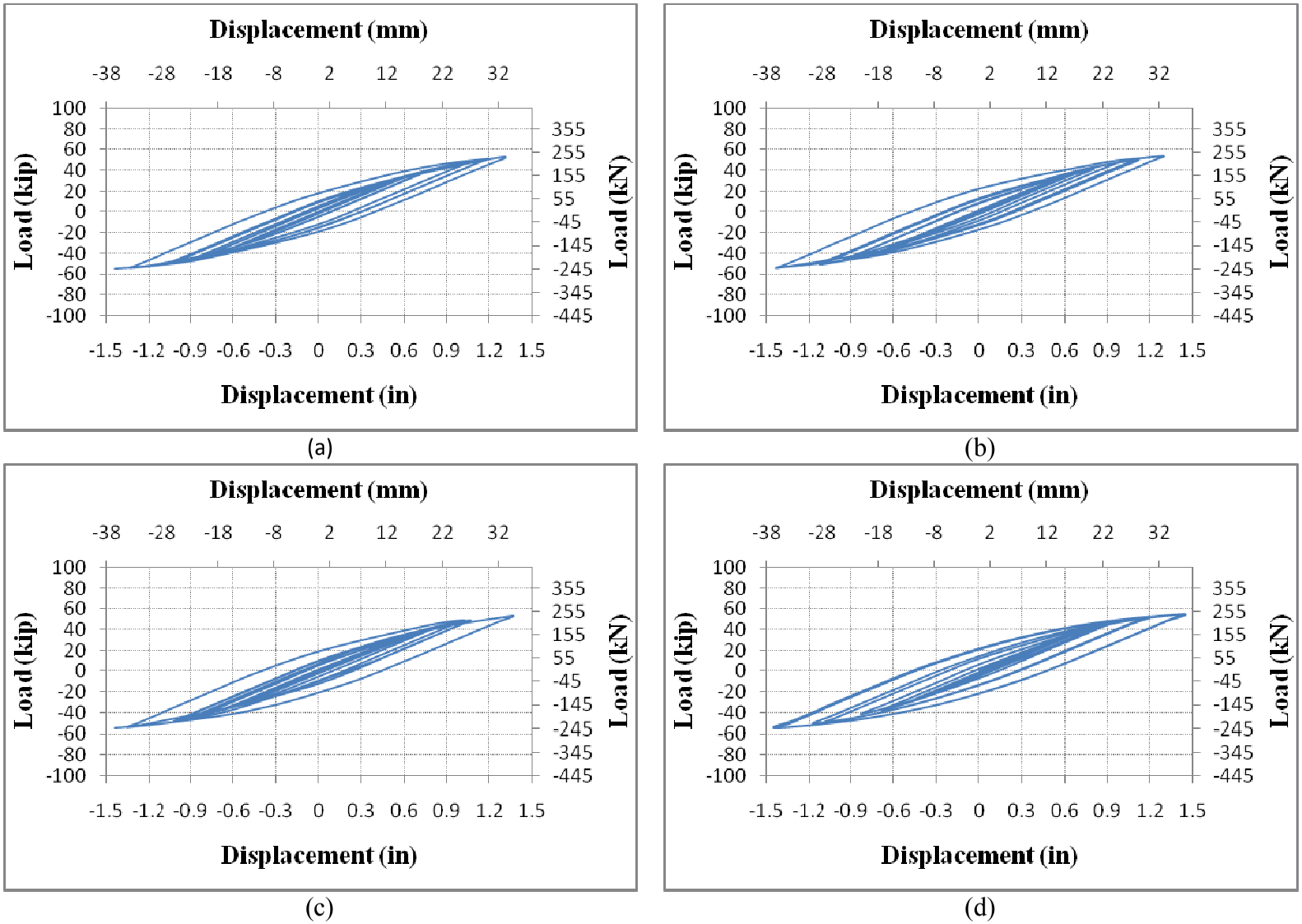

Figure B-9 Load-Displacement Cyclic Plots for: (a) SM-W-1-DLC-II-3; (b) SM-W-1-DLC-II-4; (c) SM-W-1-DLC-II-5; and (d) SM-W-1-DLC-III-1

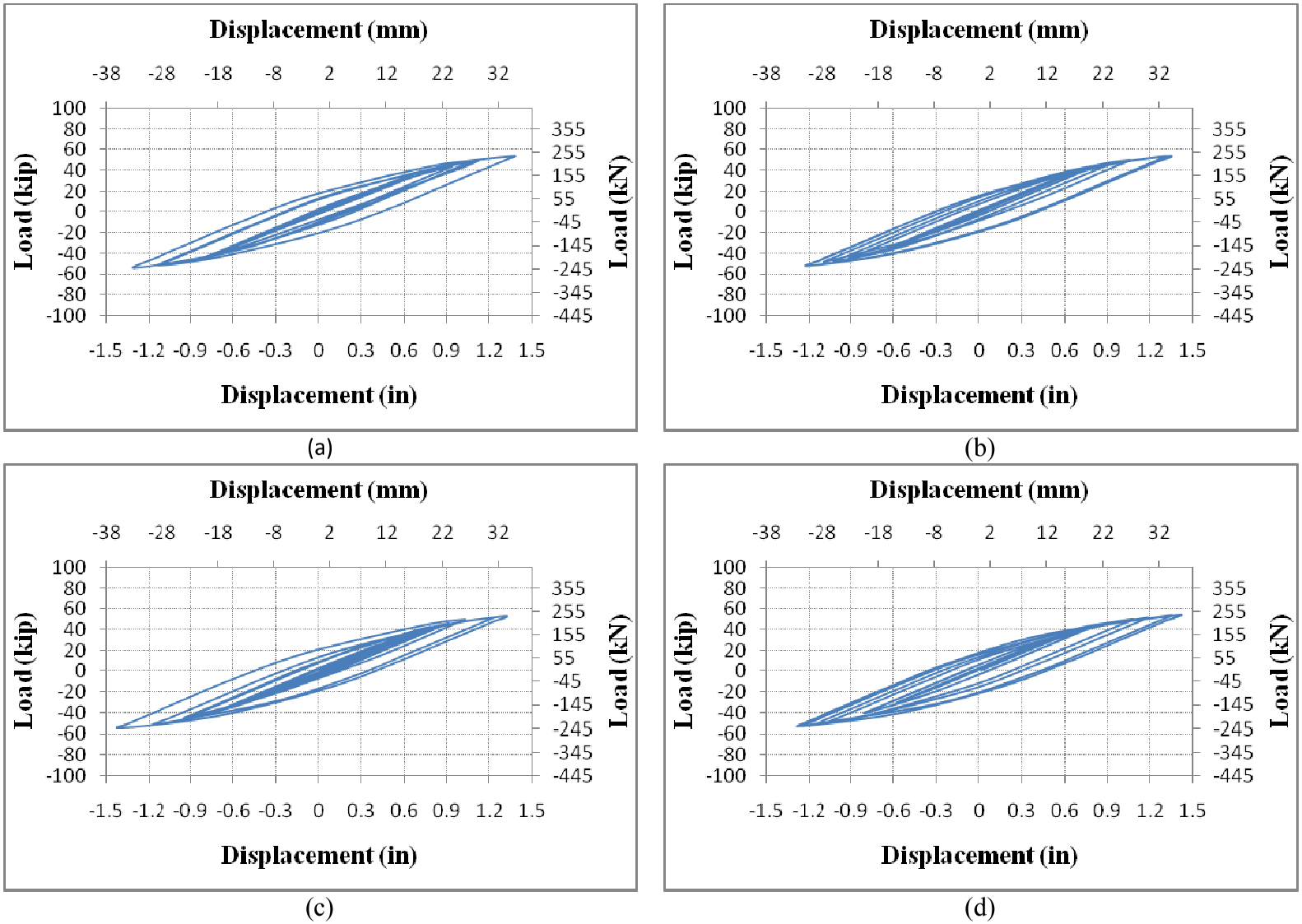

Figure B-10 Load-Displacement Cyclic Plots for: (a) SM-W-1-DLC-III-2; (b) SM-W-1-DLC-III-3; (c) SM-W-1-DLC-III-4; and (d) SM-W-1-DLC-III-5

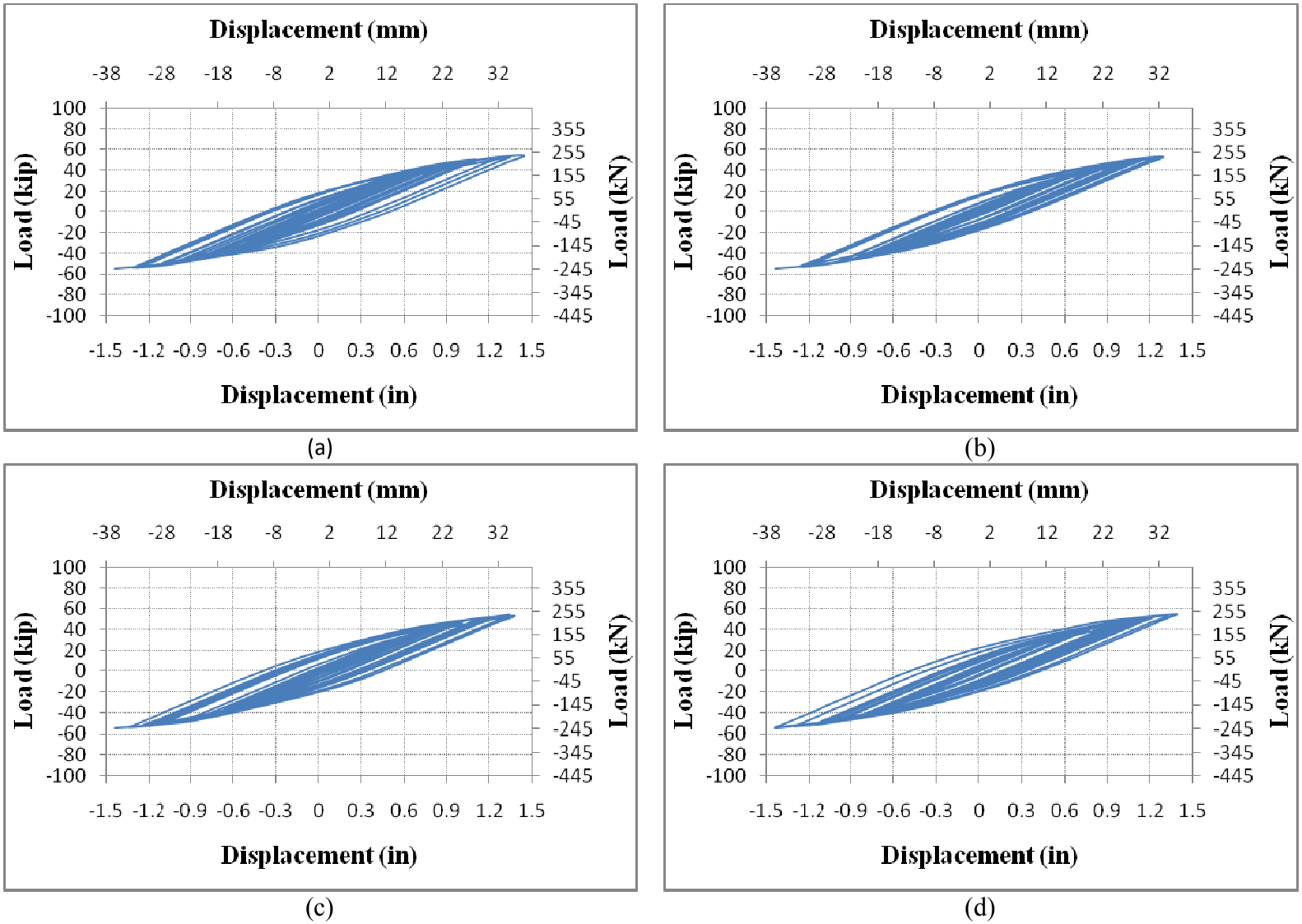

Figure B-11 Load-Displacement Cyclic Plots for: (a) SM-W-1-DLC-IV-1; (b) SM-W-1-DLC-IV-2; (c) SM-W-1-DLC-IV-3; and (d) SM-W-1-DLC-IV-4

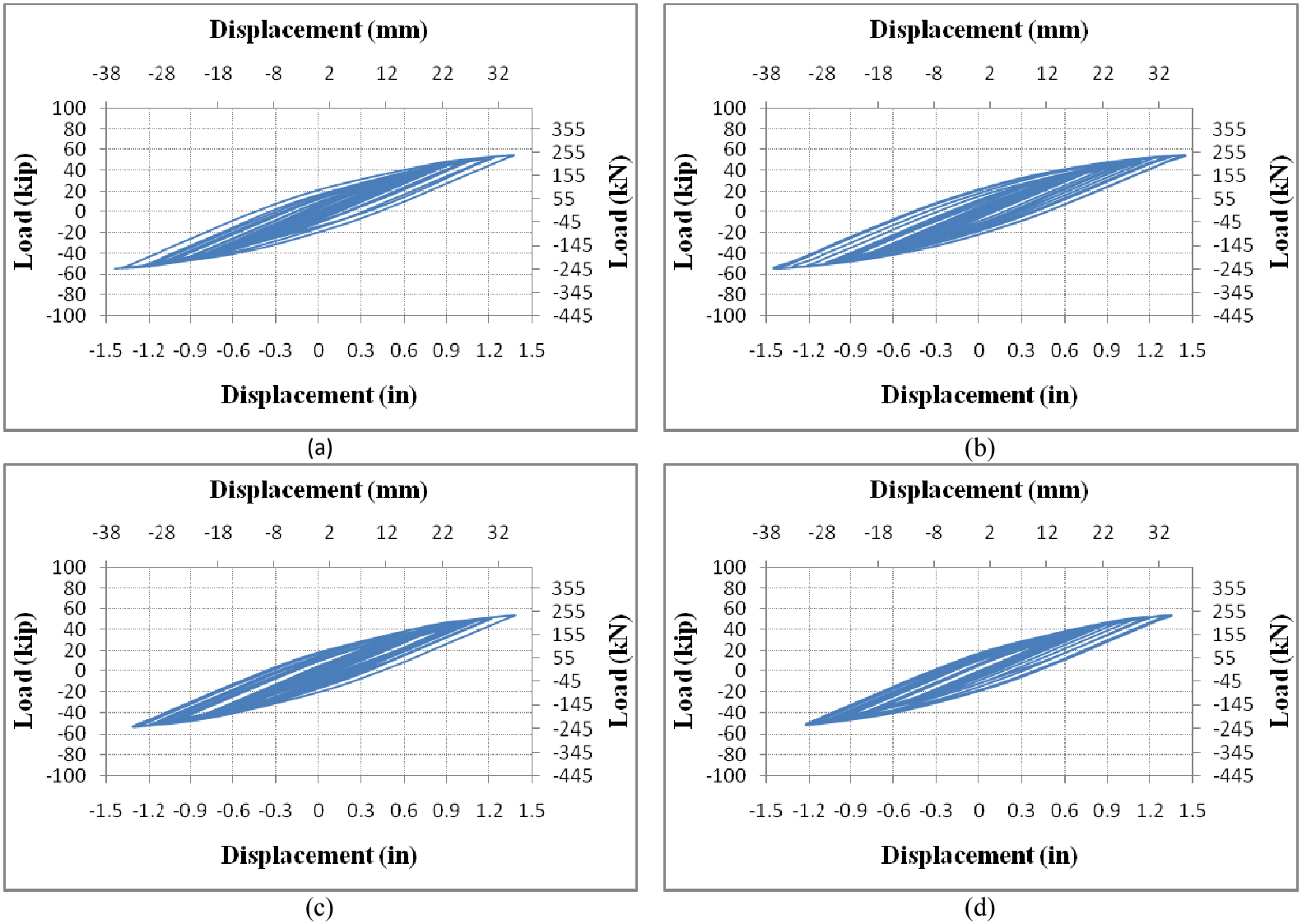

Figure B-12 Load-Displacement Cyclic Plots for: (a) SM-W-1-DLC-IV-5; (b) SM-W-1-DLC-V-1; (c) SM-W-1-DLC-V-2; and (d) SM-W-1-DLC-V-3

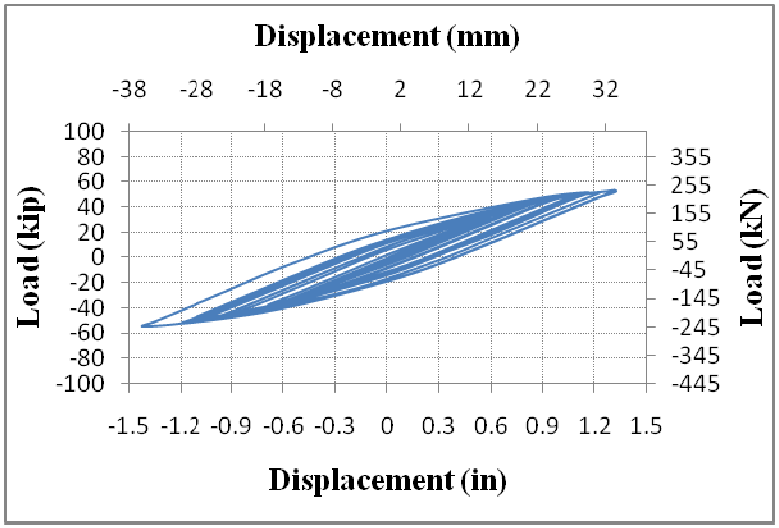

(a)

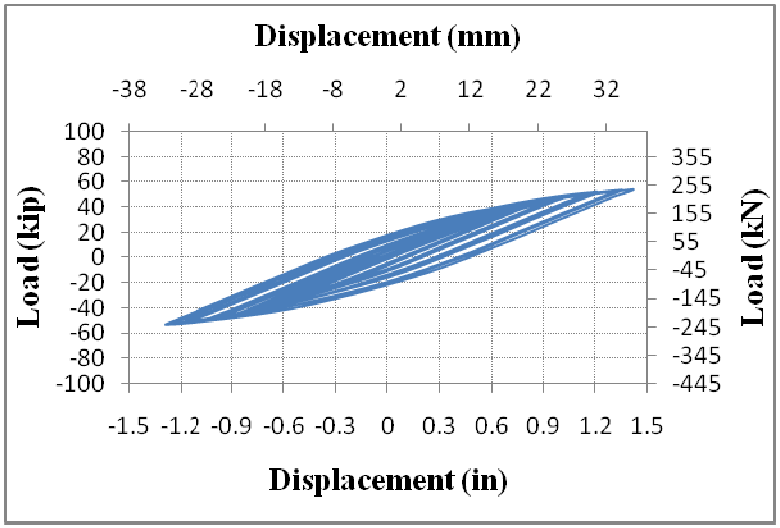

(b)

Figure B-13 Load-Displacement Cyclic Plots for: (a) SM-W-1-DLC-V-4; and (b) SM-W-1-DLC-V-5

APPENDIX C

SINGLE BOLTED SHEAR SURFACE MODELS

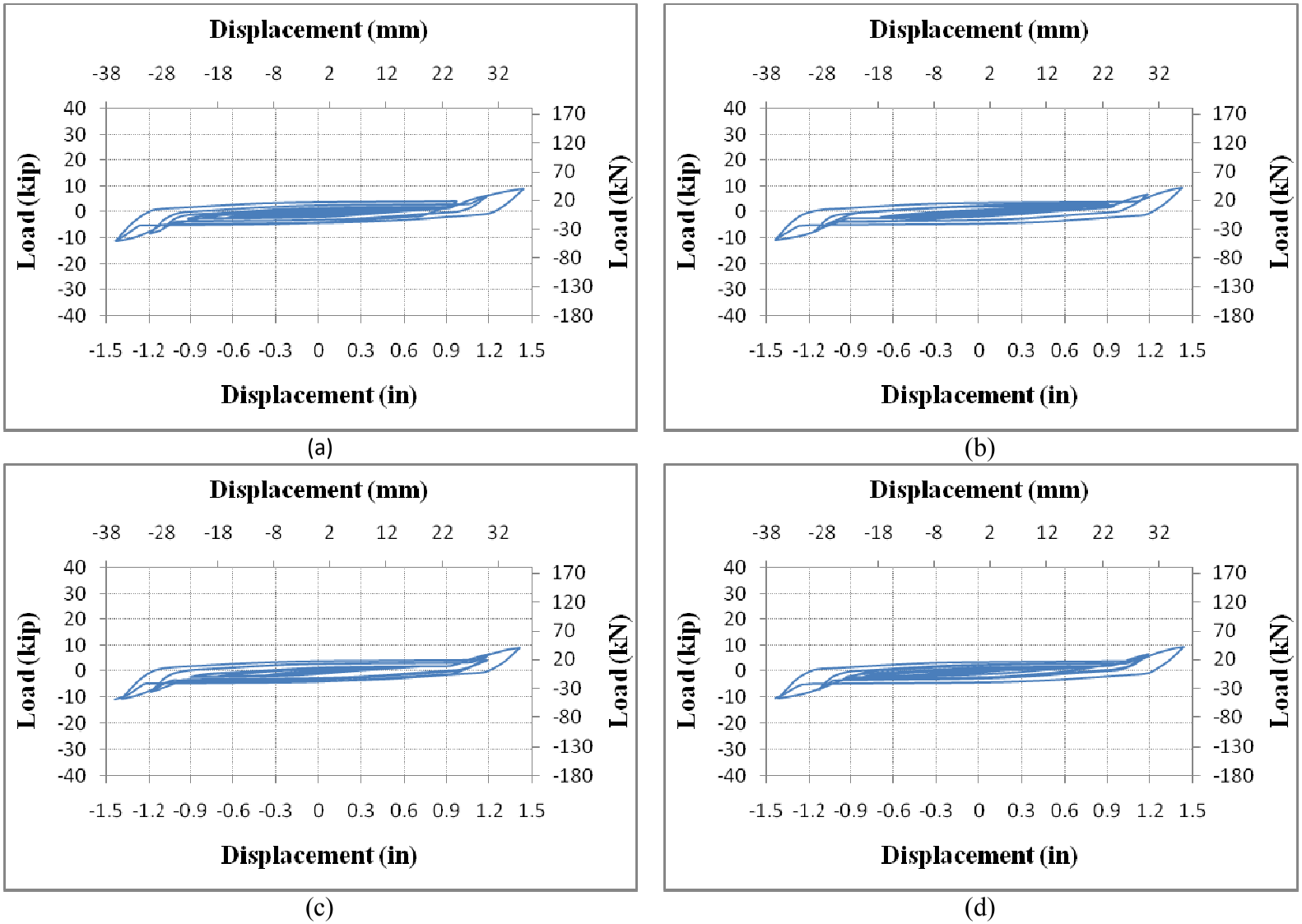

Figure C-1 Load-Displacement Cyclic Plots for: (a) SM-1B-1-1/2-FP-C-SS-DLC-I-1; (b) SM-1B-1-1/2-FP-C-SS-DLC-I-2; (c) SM-1B-1-1/2- FP-C-SS-DLC-I-3; and (d) SM-1B-1-1/2-FP-C-SS-DLC-I-4

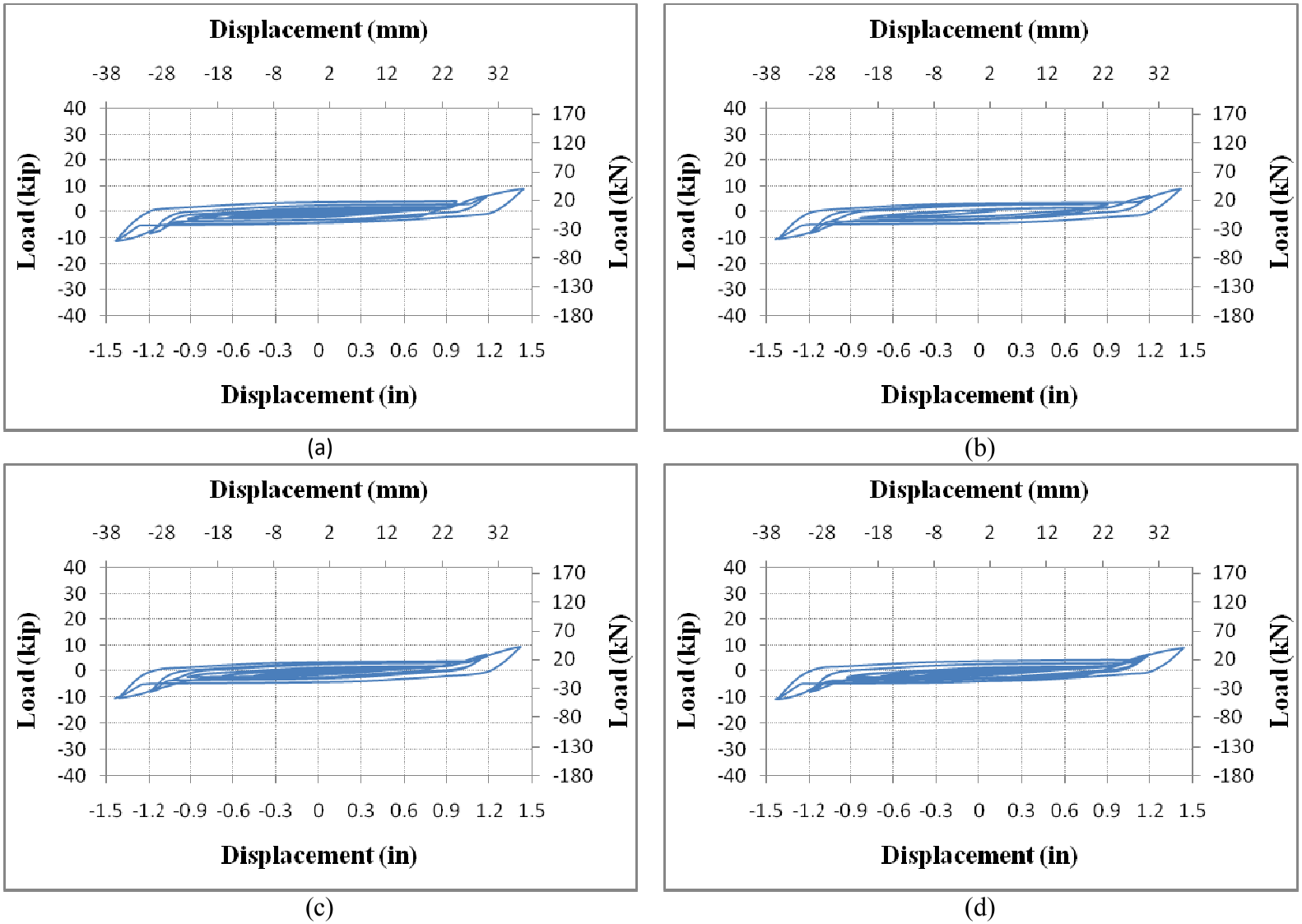

Figure C-2 Load-Displacement Cyclic Plots for: (a) SM-1B-1-1/2-FP-C-SS-DLC-I-5; (b) SM-1B-1-1/2-FP-C-SS-DLC-II-1; (c) SM-1B-1-1/2- FP-C-SS-DLC-II-2; and (d) SM-1B-1-1/2-FP-C-SS-DLC-II-3

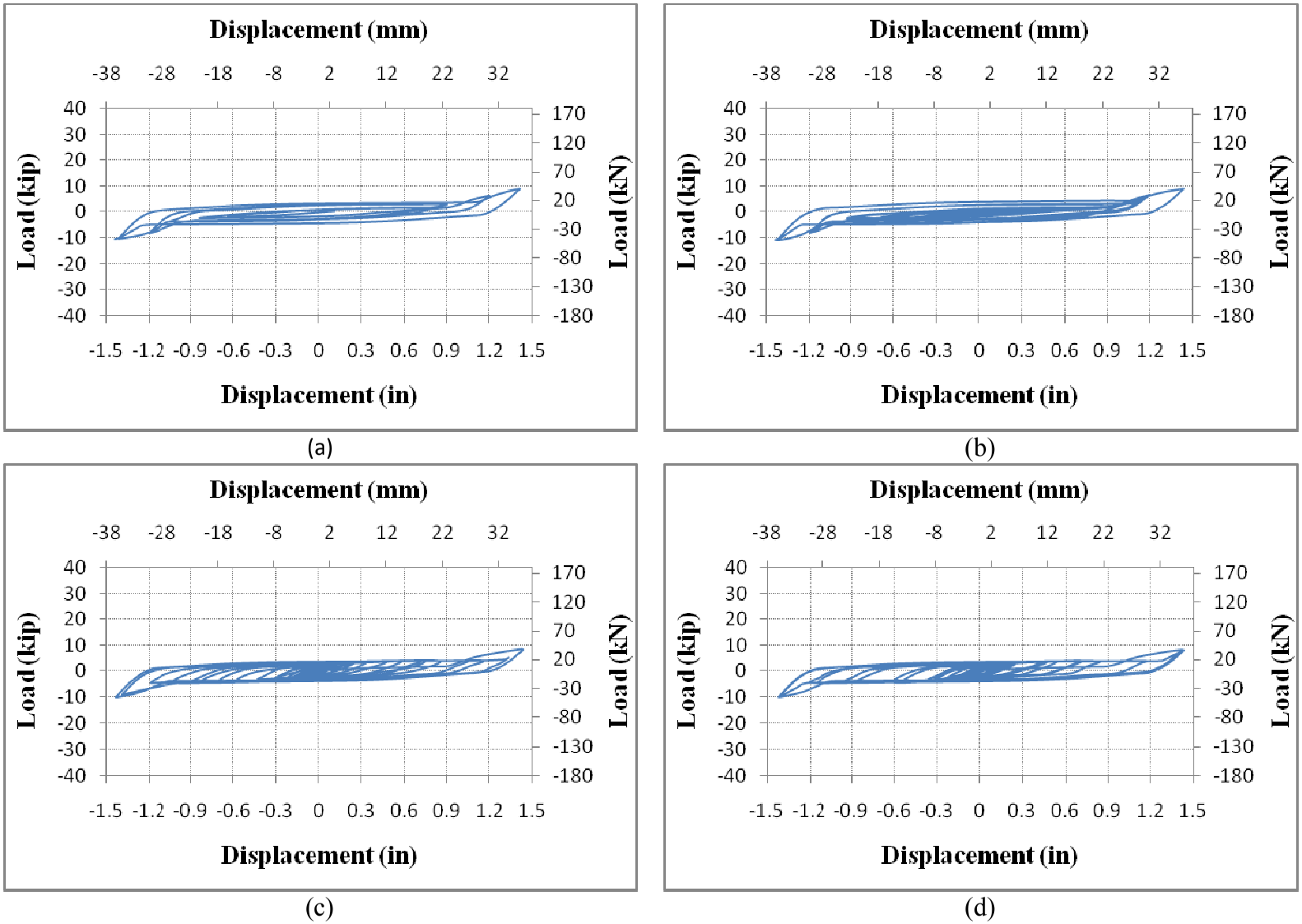

Figure C-3 Load-Displacement Cyclic Plots for: (a) SM-1B-1-1/2-FP-C-SS-DLC-II-4; (b) SM-1B-1-1/2-FP-C-SS-DLC-II-5; (c) SM-1B-1-1/2- FP-C-SS-DLC-III-1; and (d) SM-1B-1-1/2-FP-C-SS-DLC-III-2

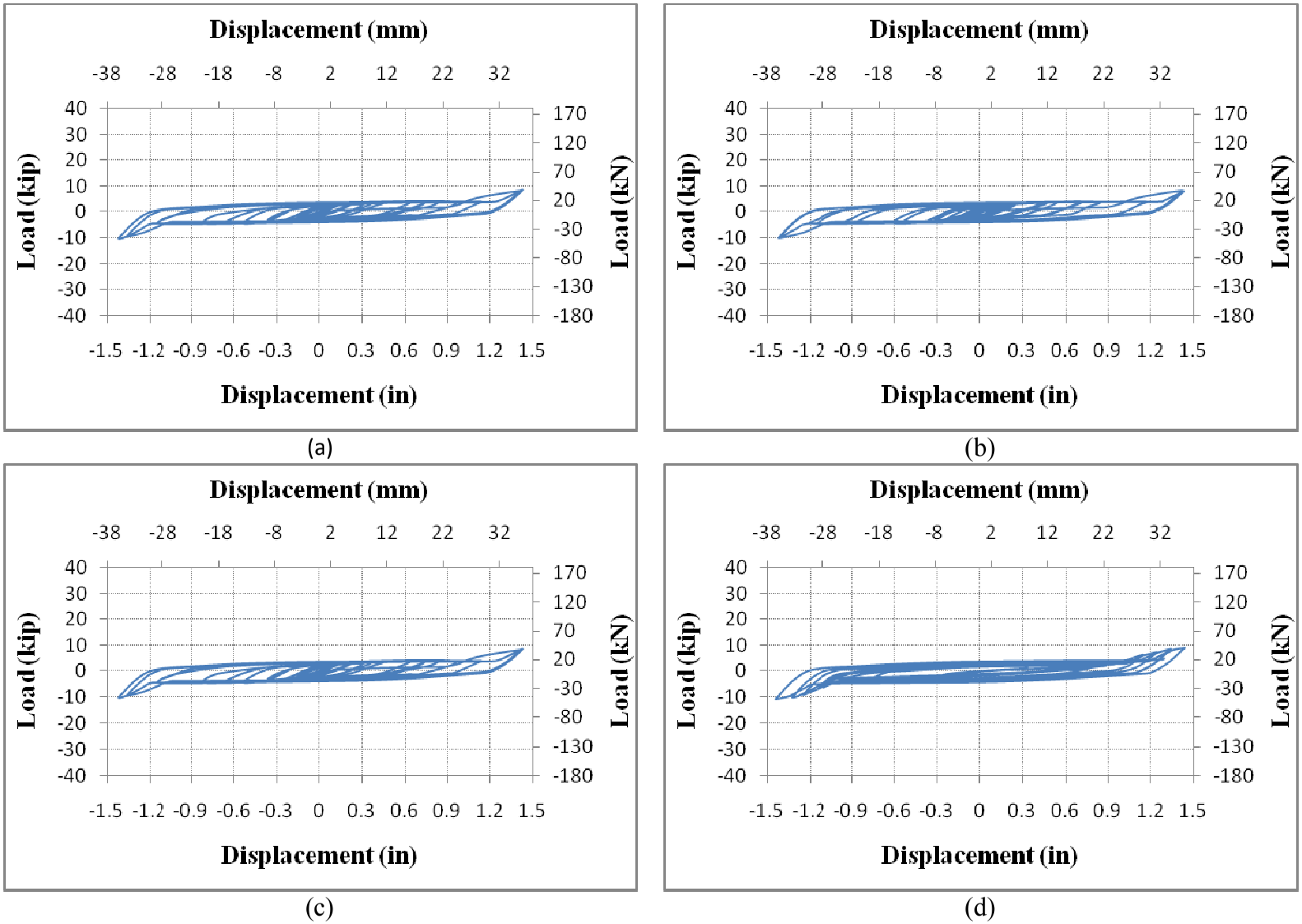

Figure C-4 Load-Displacement Cyclic Plots for: (a) SM-1B-1-1/2-FP-C-SS-DLC-III-3; (b) SM-1B-1-1/2-FP-C-SS-DLC-III-4; (c) SM-1B-1-1/2- FP-C-SS-DLC-III-5; and (d) SM-1B-1-1/2-FP-C-SS-DLC-IV-1

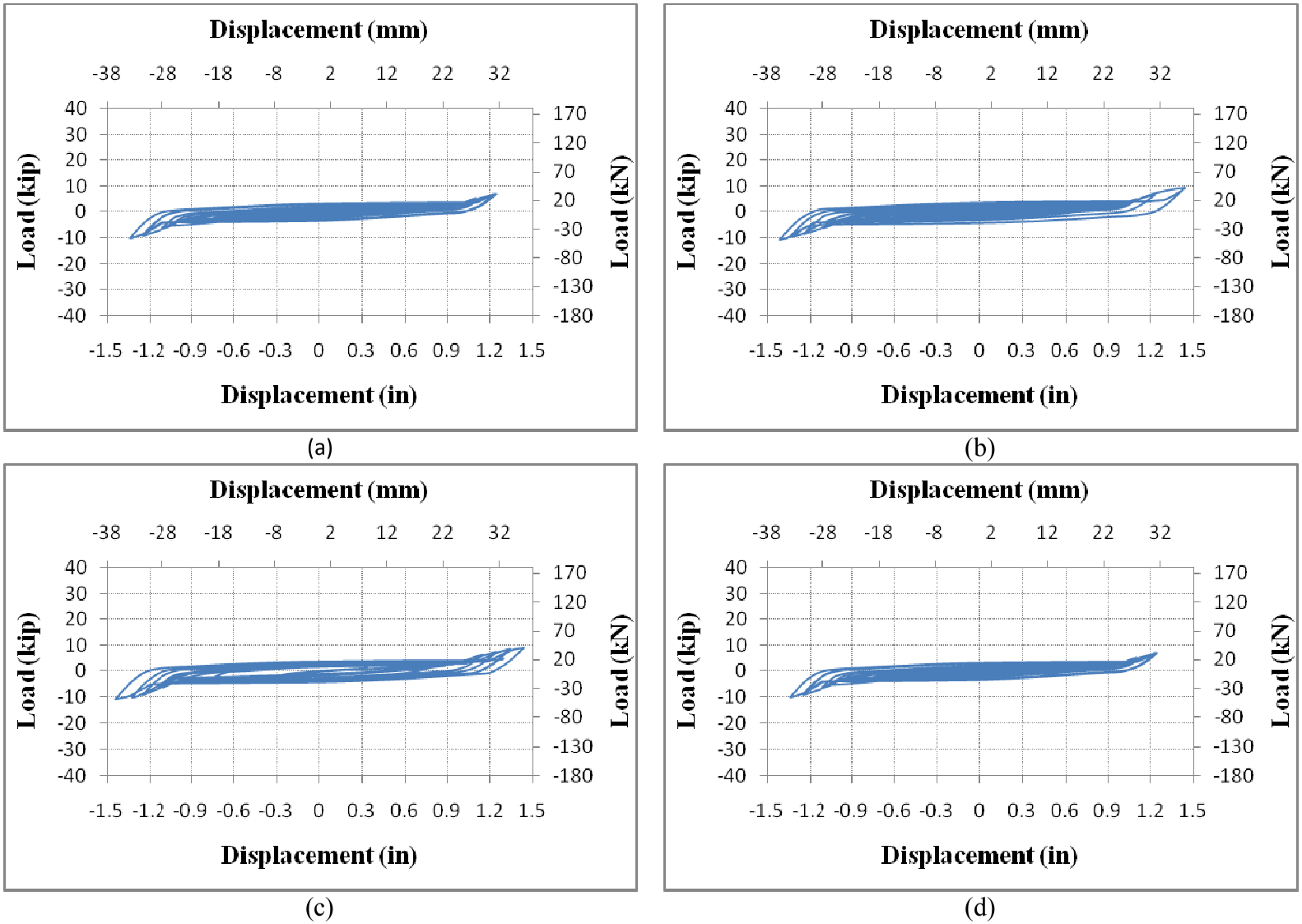

Figure C-5 Load-Displacement Cyclic Plots for: (a) SM-1B-1-1/2-FP-C-SS-DLC-IV-2; (b) SM-1B-1-1/2-FP-C-SS-DLC-IV-3; (c) SM-1B-1-1/2- FP-C-SS-DLC-IV-4; and (d) SM-1B-1-1/2-FP-C-SS-DLC-IV-5

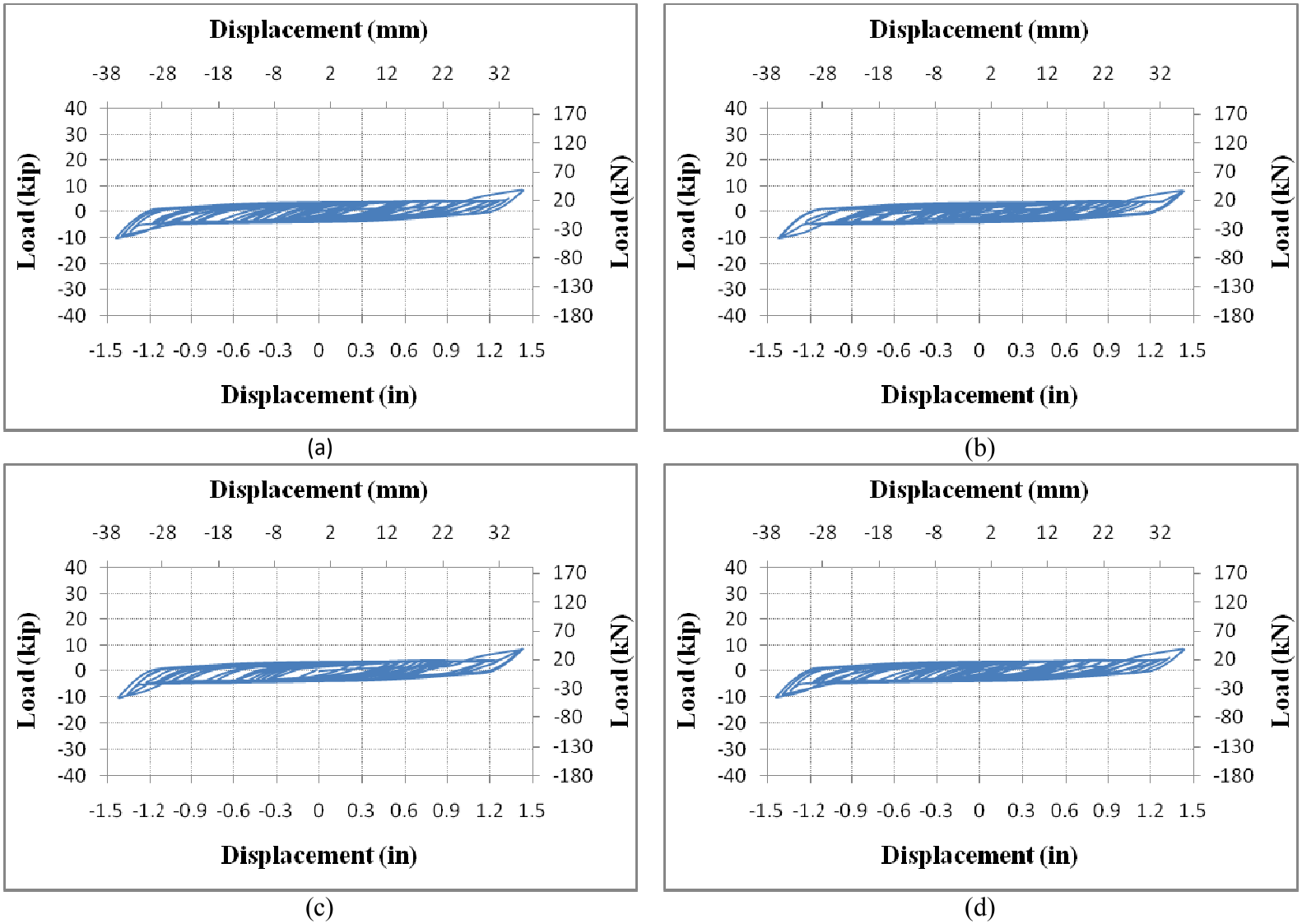

Figure C-6 Load-Displacement Cyclic Plots for: (a) SM-1B-1-1/2-FP-C-SS-DLC-V-1; (b) SM-1B-1-1/2-FP-C-SS-DLC-V-2; (c) SM-1B-1-1/2- FP-C-SS-DLC-V-3; and (d) SM-1B-1-1/2-FP-C-SS-DLC-V-4

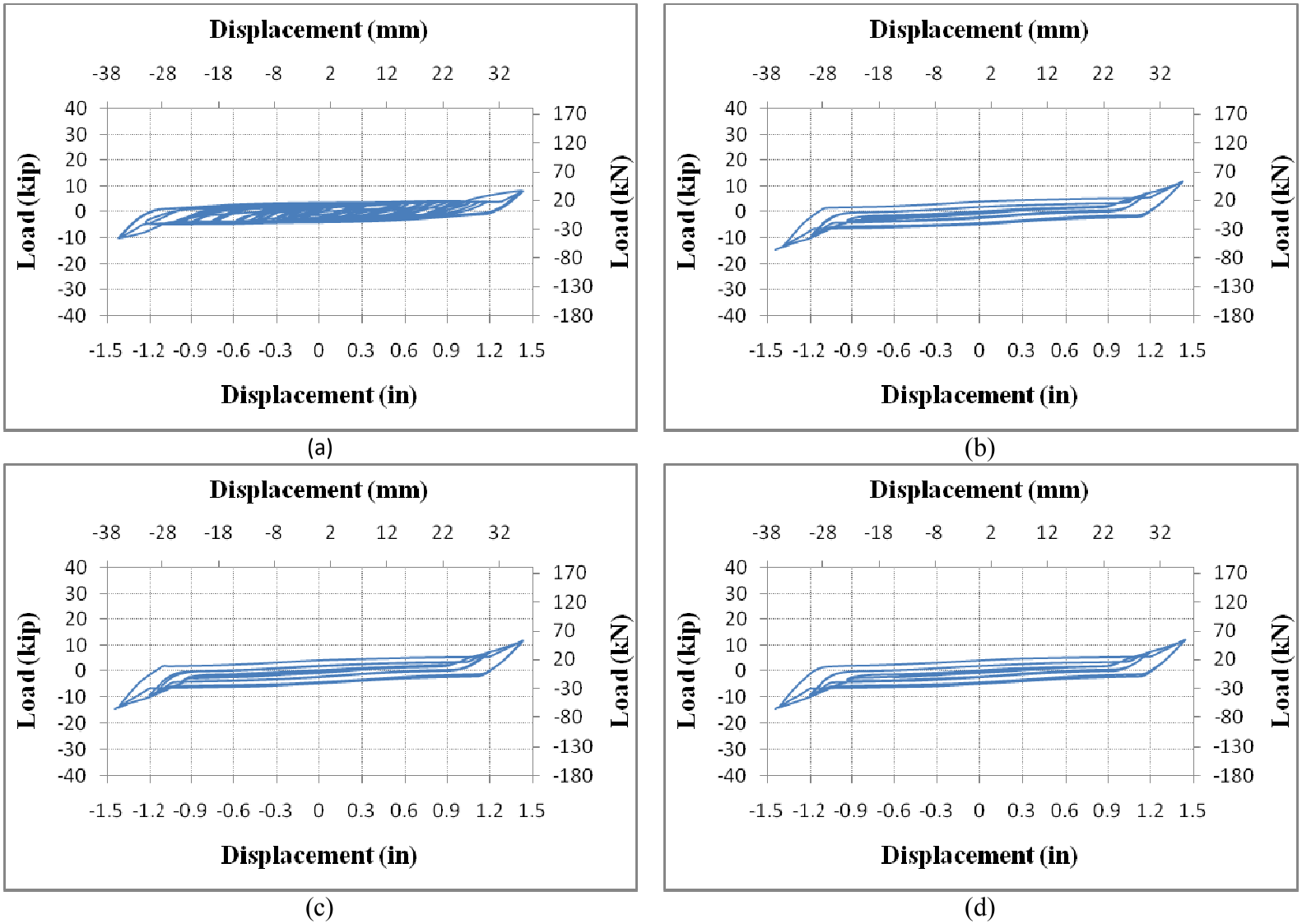

Figure C-7 Load-Displacement Cyclic Plots for: (a) SM-1B-1-1/2-FP-C-SS-DLC-V-5; (b) SM-1B-1-1/2-HP-C-SS-DLC-I-1; (c) SM-1B-1-1/2-HP-C-SS-DLC-I-2; and (d) SM-1B-1-1/2-HP-C-SS-DLC-I-3

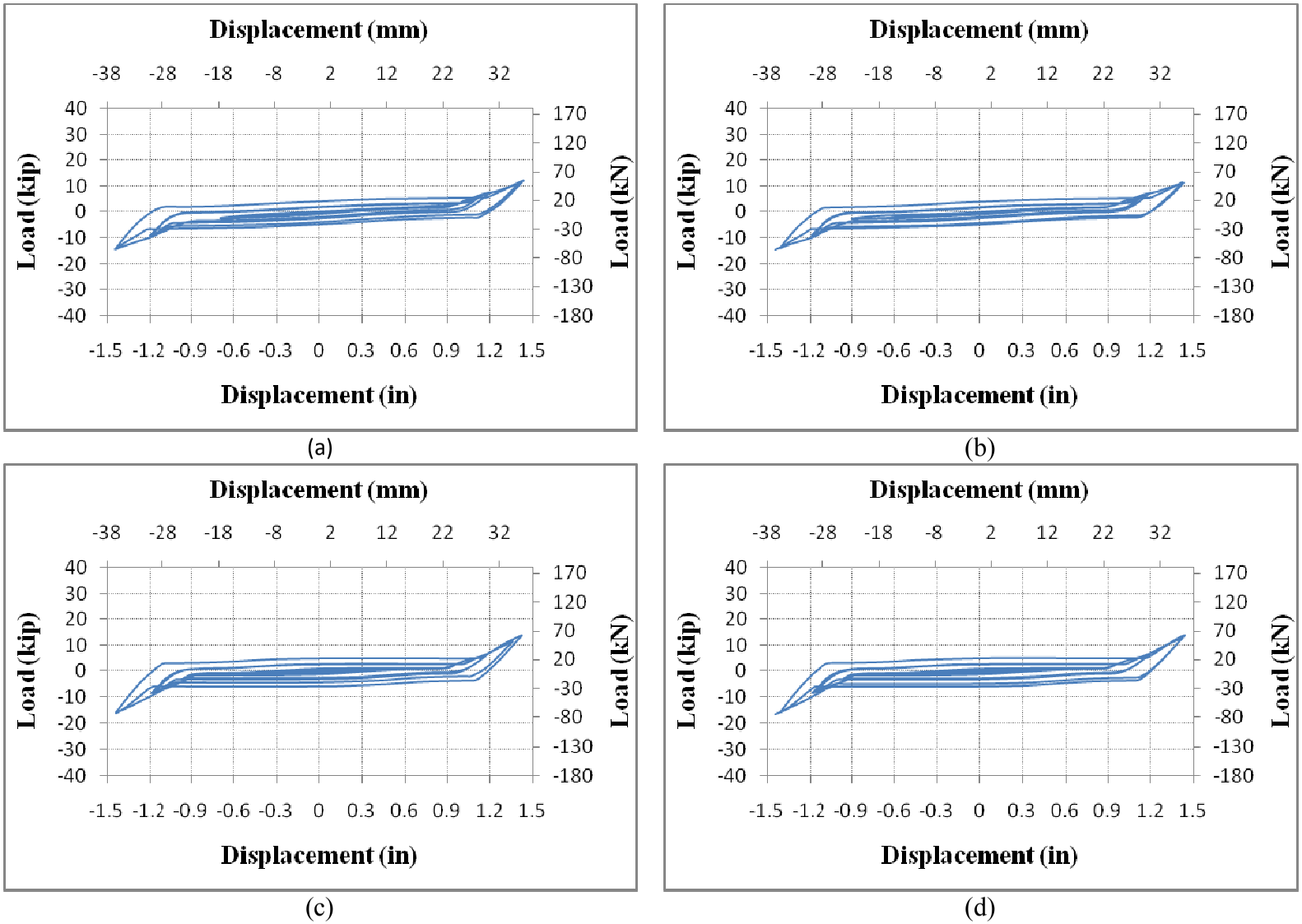

Figure C-8 Load-Displacement Cyclic Plots for: (a) SM-1B-1-1/2-HP-C-SS-DLC-I-4; (b) SM-1B-1-1/2-HP-C-SS-DLC-I-5; (c) SM-1B-1-1/2-QP-C-SS-DLC-I-1; and (d) SM-1B-1-1/2-QP-C-SS-DLC-I-2

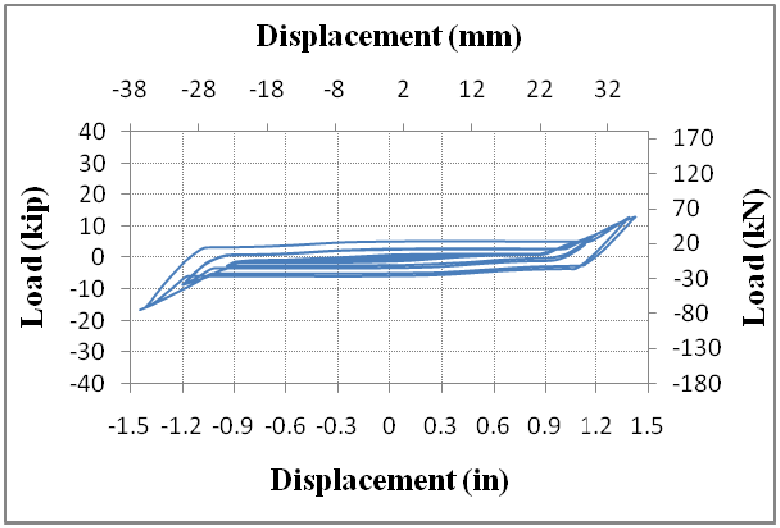

(a)

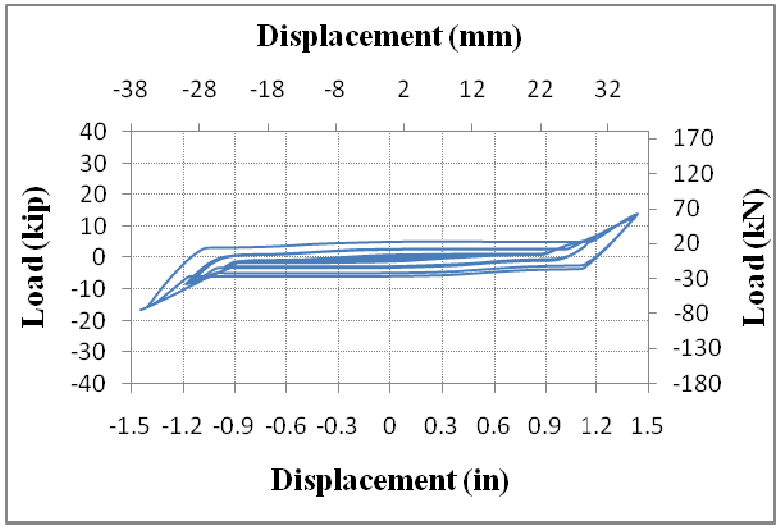

(b)

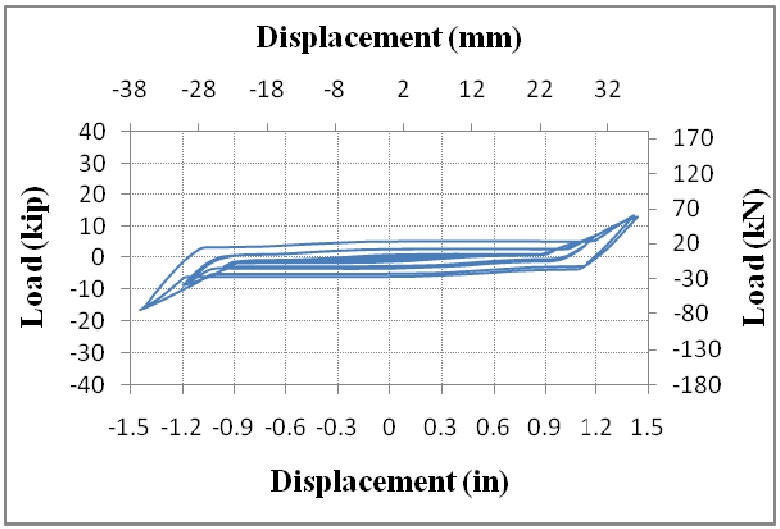

(c)

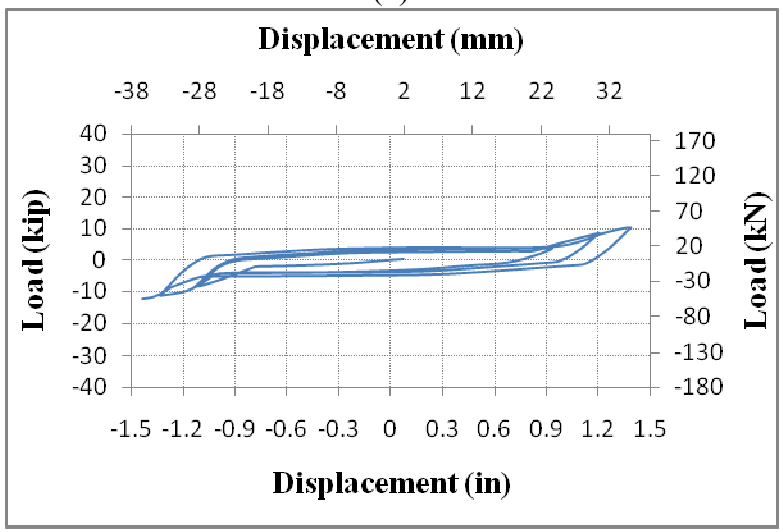

(d)

Figure C-9 Load-Displacement Cyclic Plots for: (a) SM-1B-1-1/2-QP-C-SS-DLC-I-3; (b) SM-1B-1-1/2-QP-C-SS-DLC-I-4; (c) SM-1B-1-1/2-QP-C-SS-DLC-I-5; and (d) SM-1B-1-1/2-FP-HX-SS-DLC-I-1

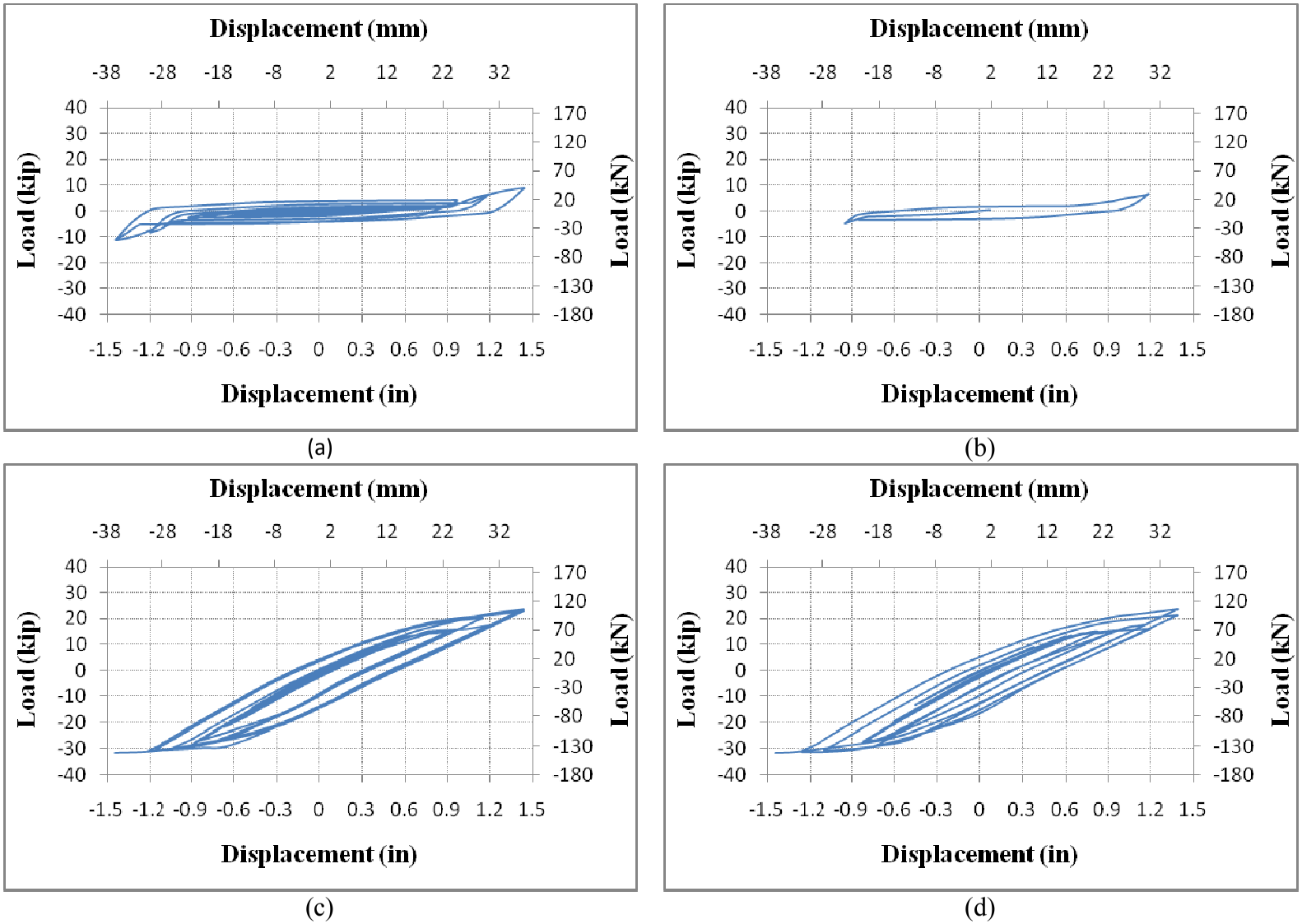

Figure C-10 Load-Displacement Cyclic Plots for: (a) SM-1B-1-1/2-FP-C-SS-DLC-I-1; (b) SM-1B-1-1/2-FP-C-NS-DLC-I-1; (c) SM-1B-1/4-1-FP-C-SS-DLC-I-1; and (d) SM-1B-1/4-1-FP-C-SS-DLC-I-2

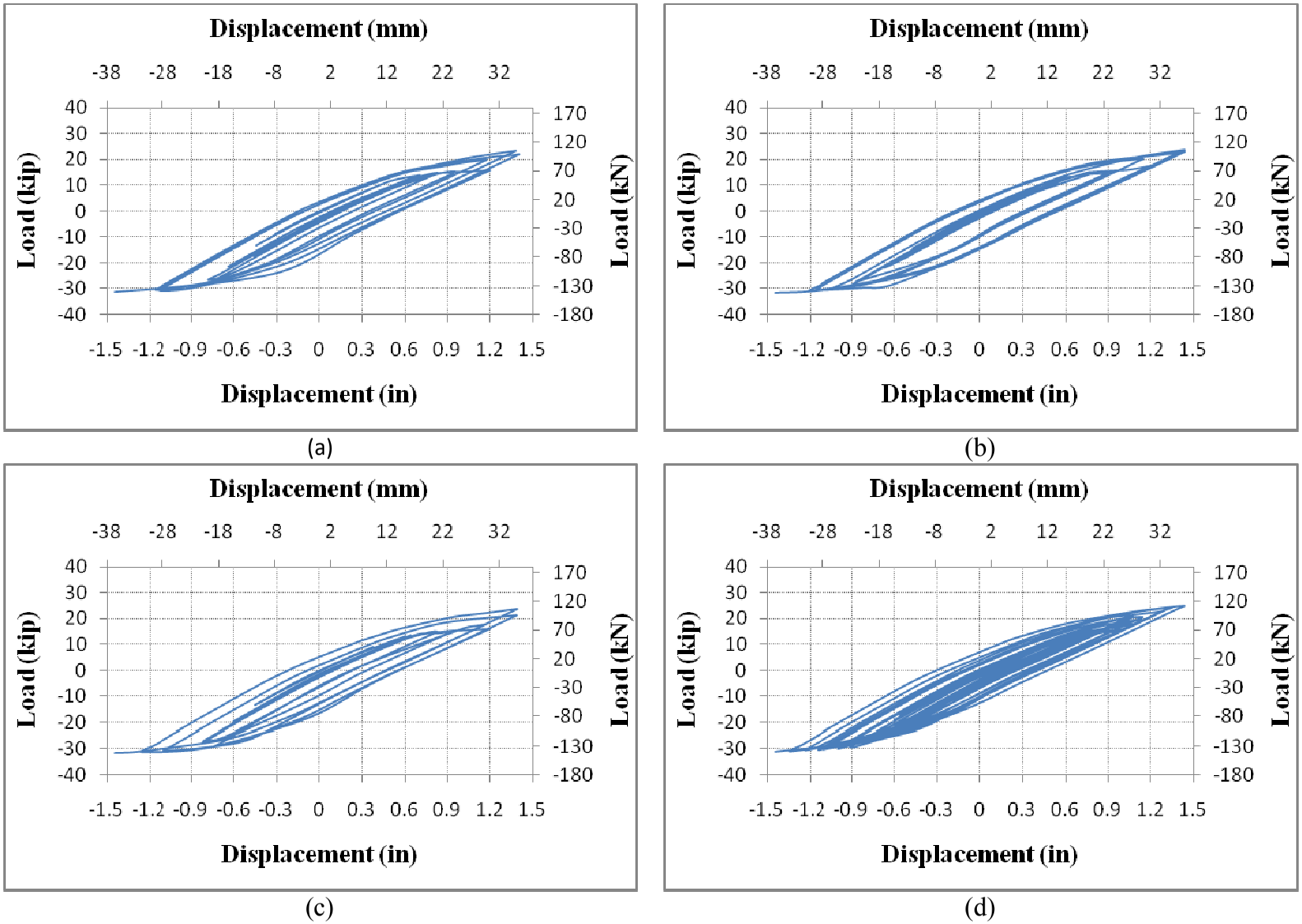

Figure C-11 Load-Displacement Cyclic Plots for: (a) SM-1B-1/4-1-FP-C-SS-DLC-I-3; (b) SM-1B-1/4-1-FP-C-SS-DLC-I-4; (c) SM-1B-1/4-1-FP-C-SS-DLC-I-5; and (d) SM-1B-1/4-1-FP-C-SS-DLC-II-1

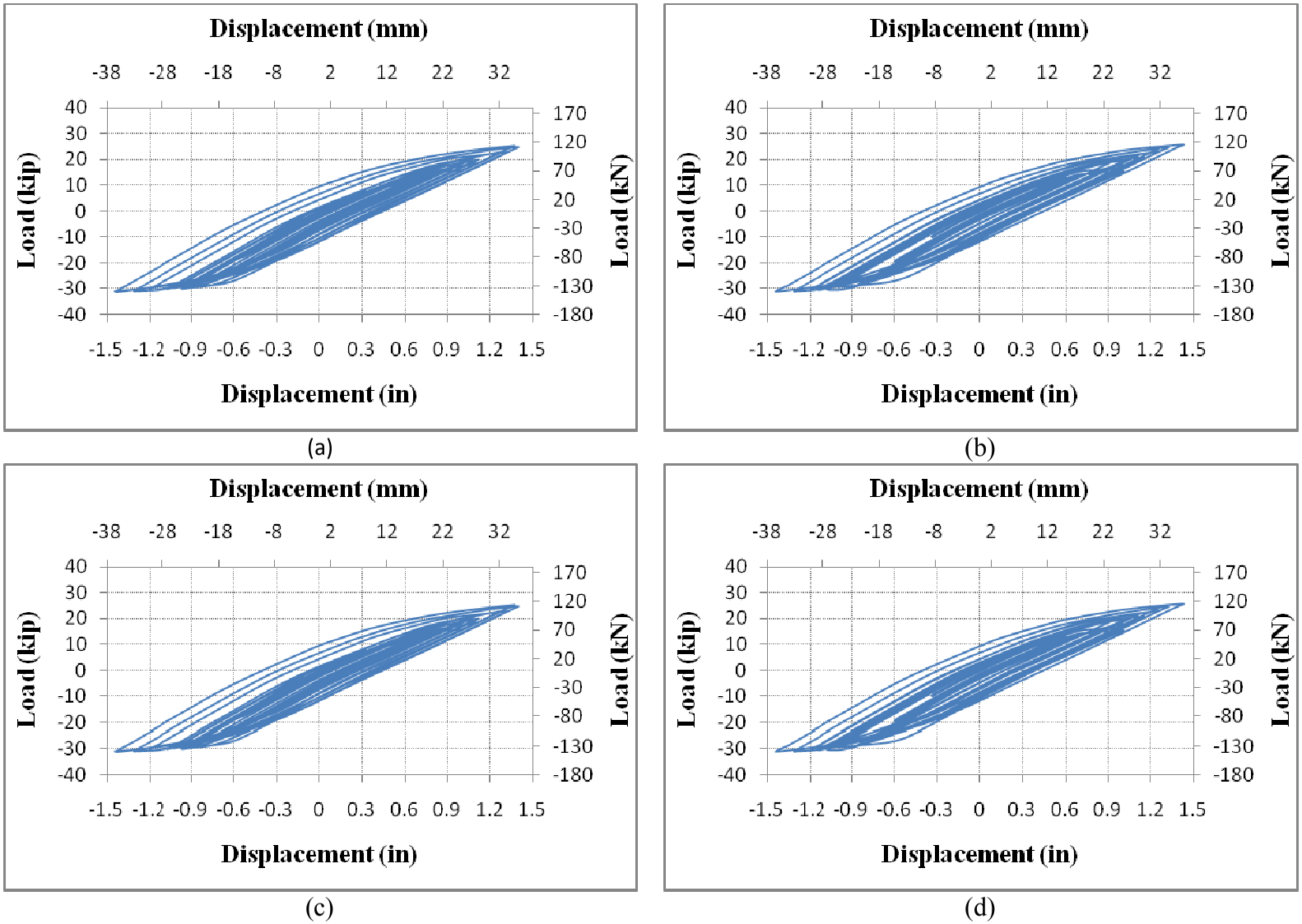

Figure C-12 Load-Displacement Cyclic Plots for: (a) SM-1B-1/4-1-FP-C-SS-DLC-II-2; (b) SM-1B-1/4-1-FP-C-SS-DLC-II-3; (c) SM-1B-1/4-1-FP-C-SS-DLC-II-4; and (d) SM-1B-1/4-1-FP-C-SS-DLC-II-5

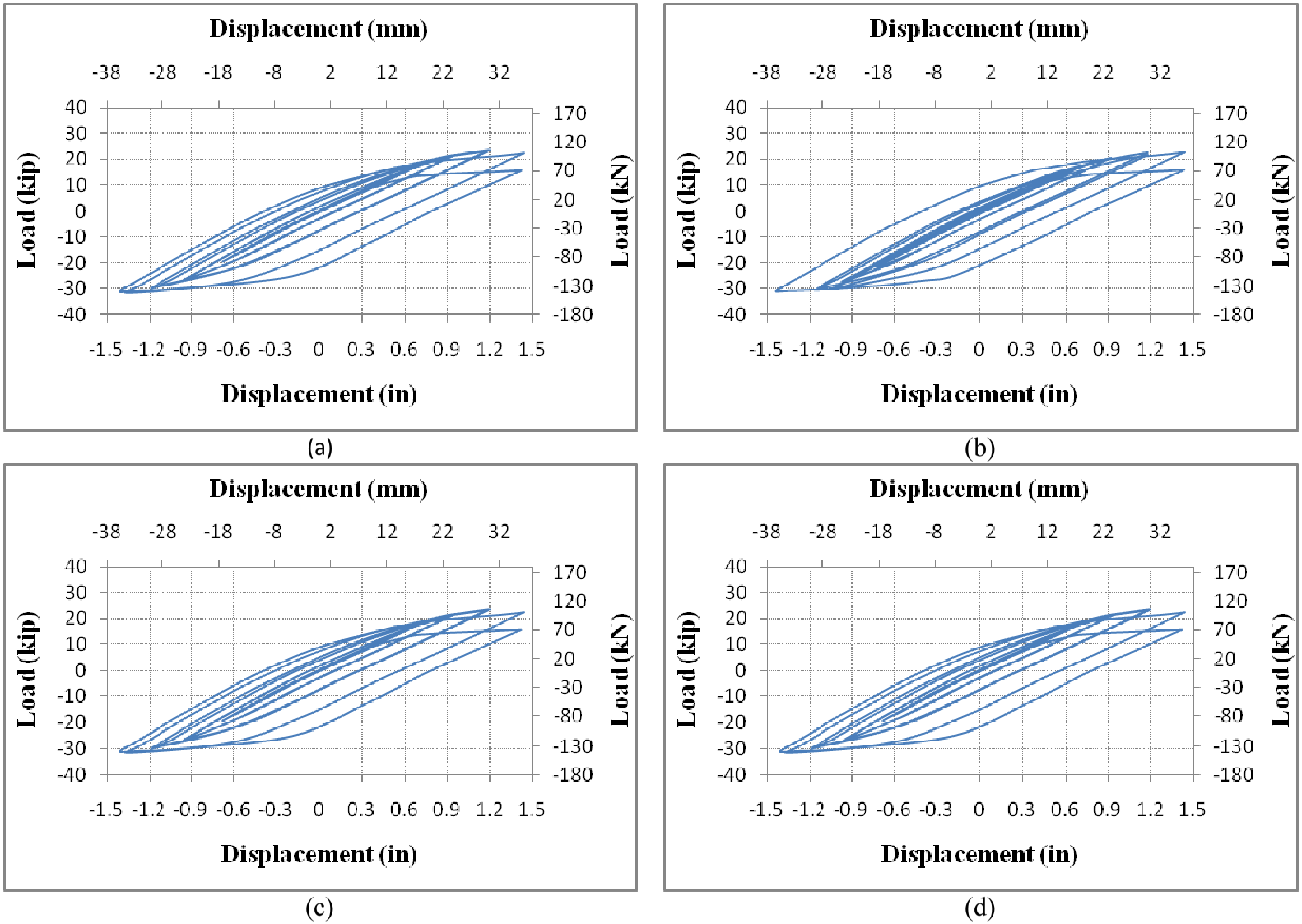

Figure C-13 Load-Displacement Cyclic Plots for: (a) SM-1B-1/4-1-FP-C-SS-DLC-III-1; (b) SM-1B-1/4-1-FP-C-SS-DLC-III-2; (c) SM-1B-1/4-1-FP-C-SS-DLC-III-3; and (d) SM-1B-1/4-1-FP-C-SS-DLC-III-4

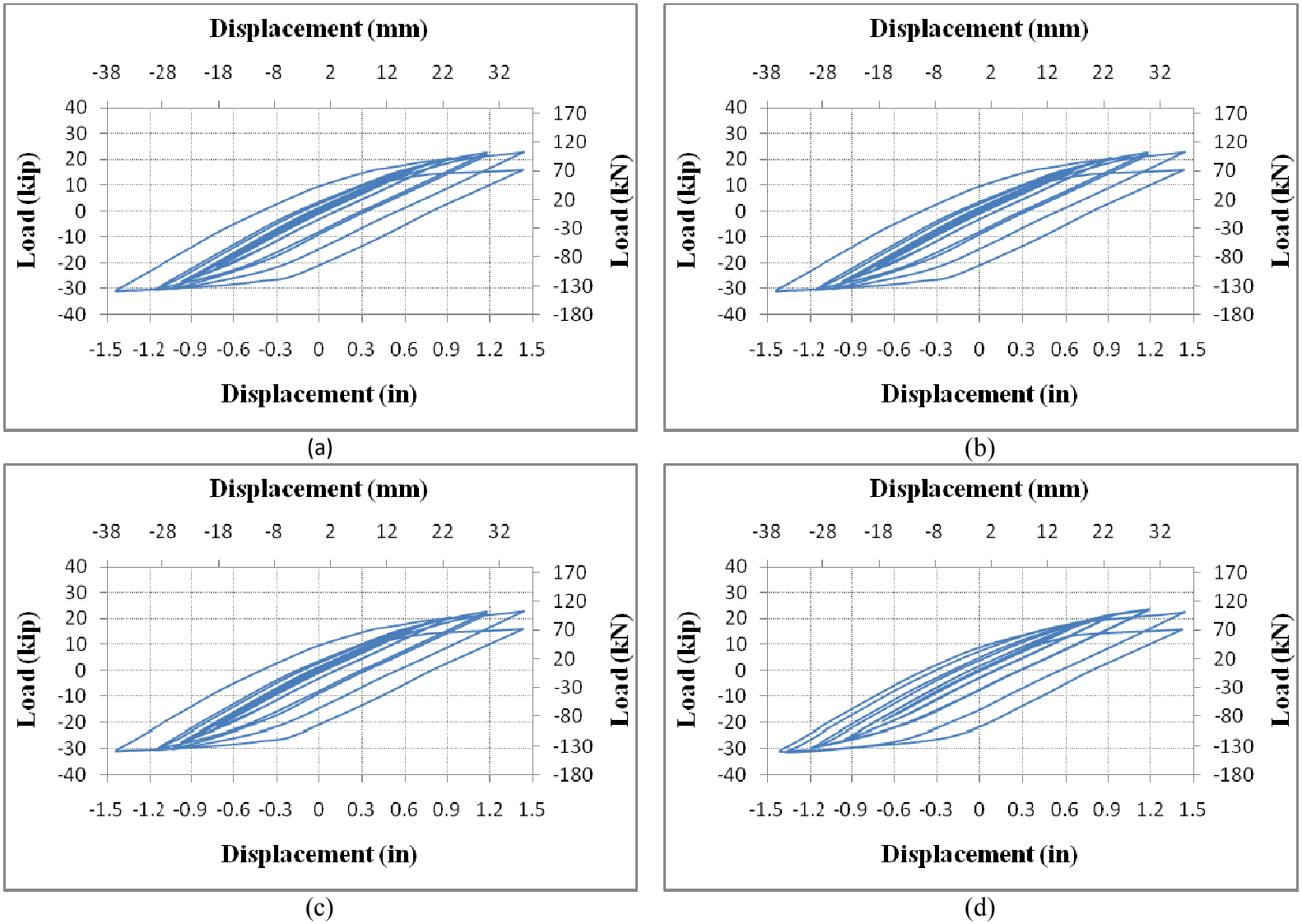

Figure C-14 Load-Displacement Cyclic Plots for: (a) SM-1B-1/4-1-FP-C-SS-DLC-III-5; (b) SM-1B-1/4-1-FP-C-SS-DLC-IV-1; (c) SM-1B-1/4-1-FP-C-SS-DLC-IV-2; and (d) SM-1B-1/4-1-FP-C-SS-DLC-IV-3

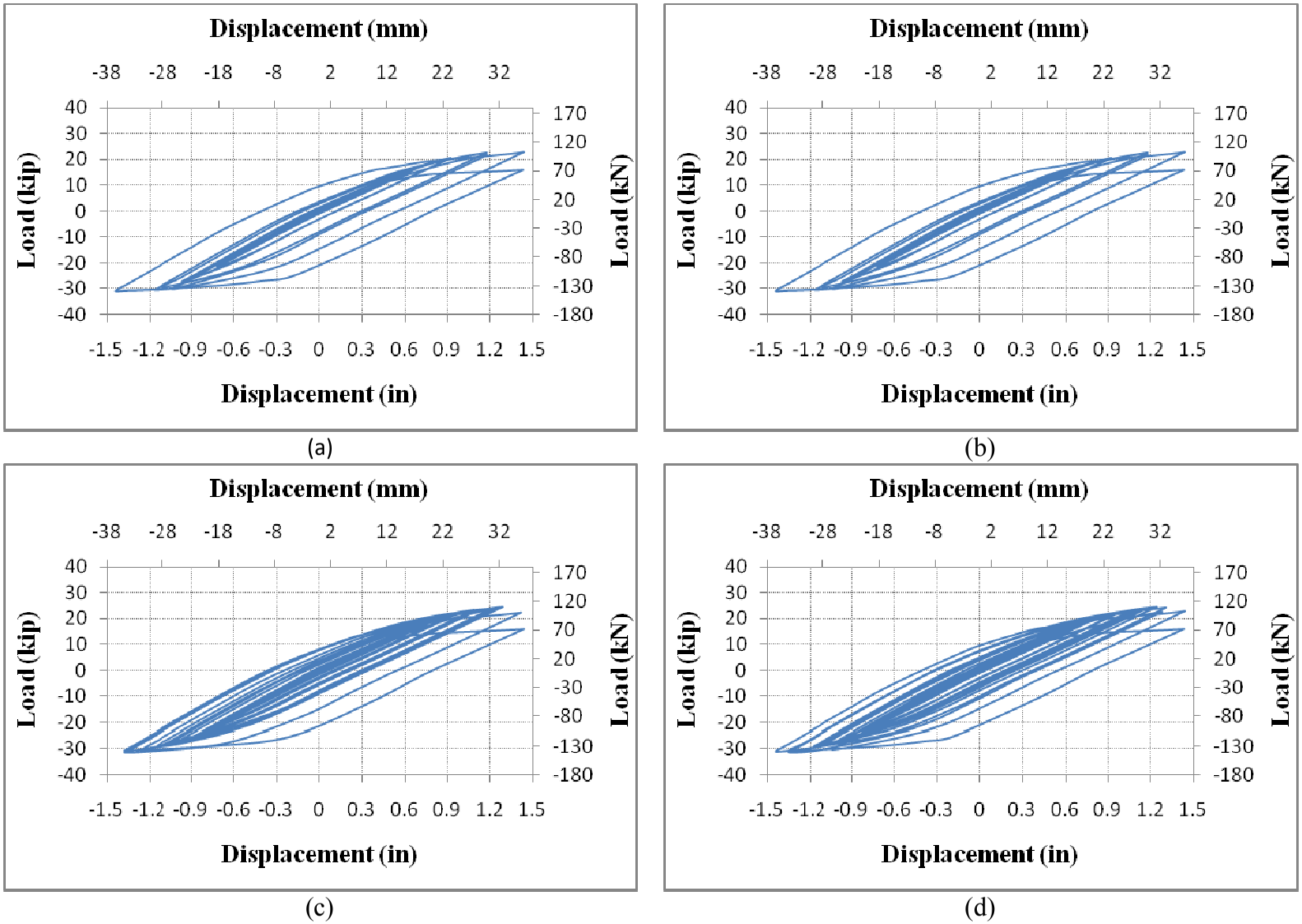

Figure C-15 Load-Displacement Cyclic Plots for: (a) SM-1B-1/4-1-FP-C-SS-DLC-IV-4; (b) SM-1B-1/4-1-FP-C-SS-DLC-IV-5; (c) SM-1B-1/4-1-FP-C-SS-DLC-V-1; and (d) SM-1B-1/4-1-FP-C-SS-DLC-V-2

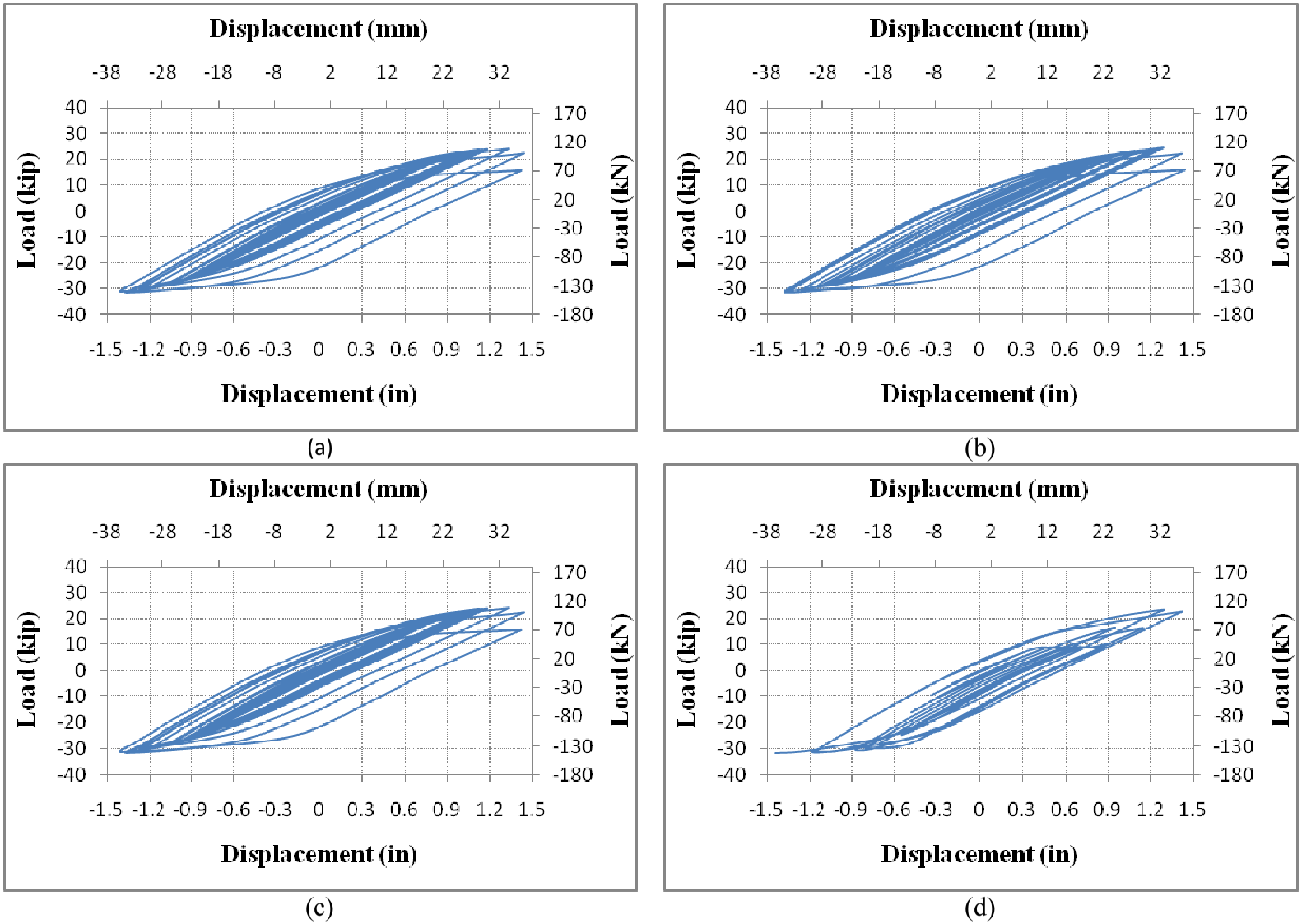

Figure C-16 Load-Displacement Cyclic Plots for: (a) SM-1B-1/4-1-FP-C-SS-DLC-V-3; (b) SM-1B-1/4-1-FP-C-SS-DLC-V-4; (c) SM-1B-1/4-1-FP-C-SS-DLC-V-5; and (d) SM-1B-1/4-1-HP-C-SS-DLC-I-1

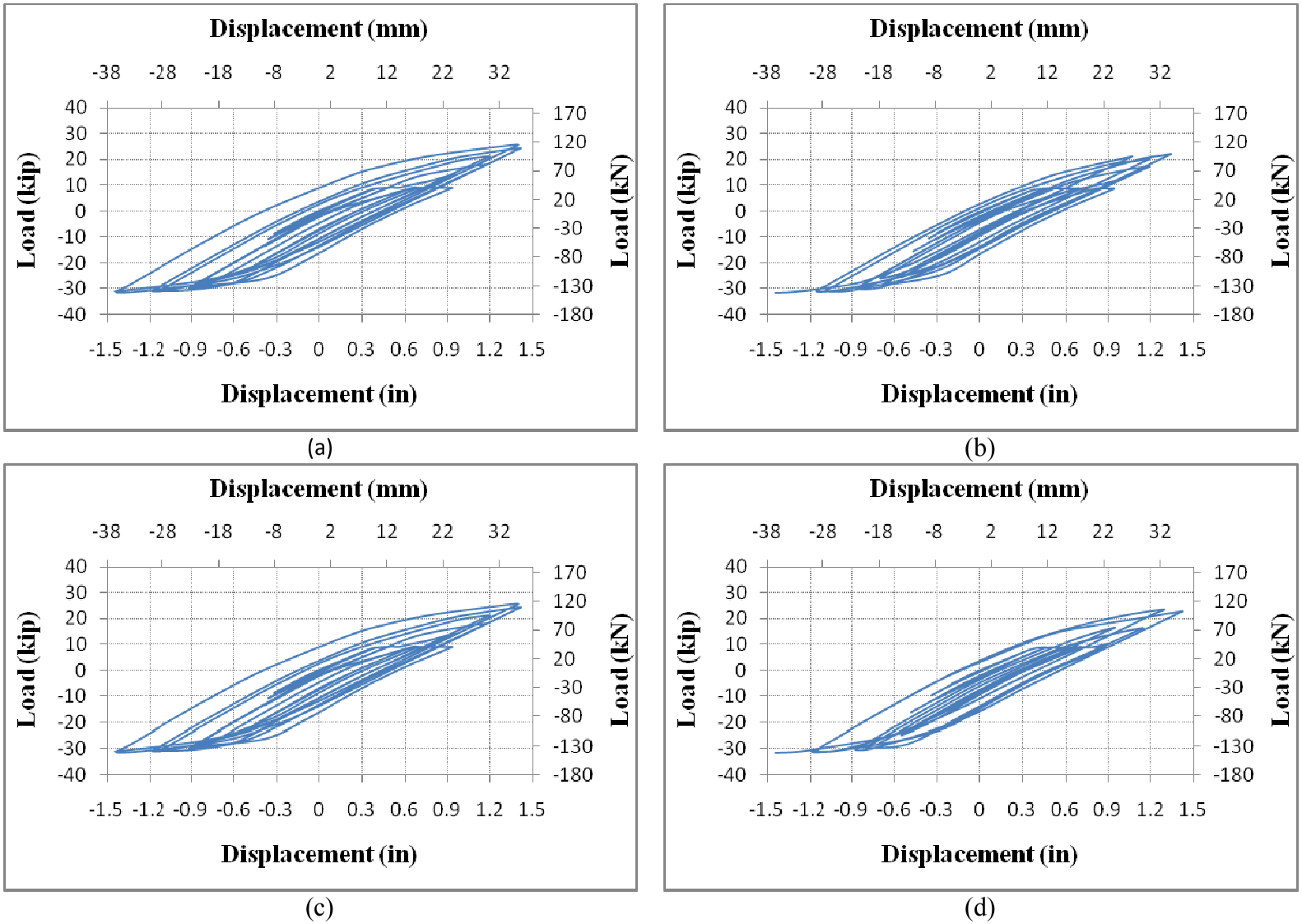

Figure C-17 Load-Displacement Cyclic Plots for: (a) SM-1B-1/4-1-HP-C-SS-DLC-I-2; (b) SM-1B-1/4-1-HP-C-SS-DLC-I-3; (c) SM-1B-1/4-1-HP-C-SS-DLC-I-4; and (d) SM-1B-1/4-1-HP-C-SS-DLC-I-5

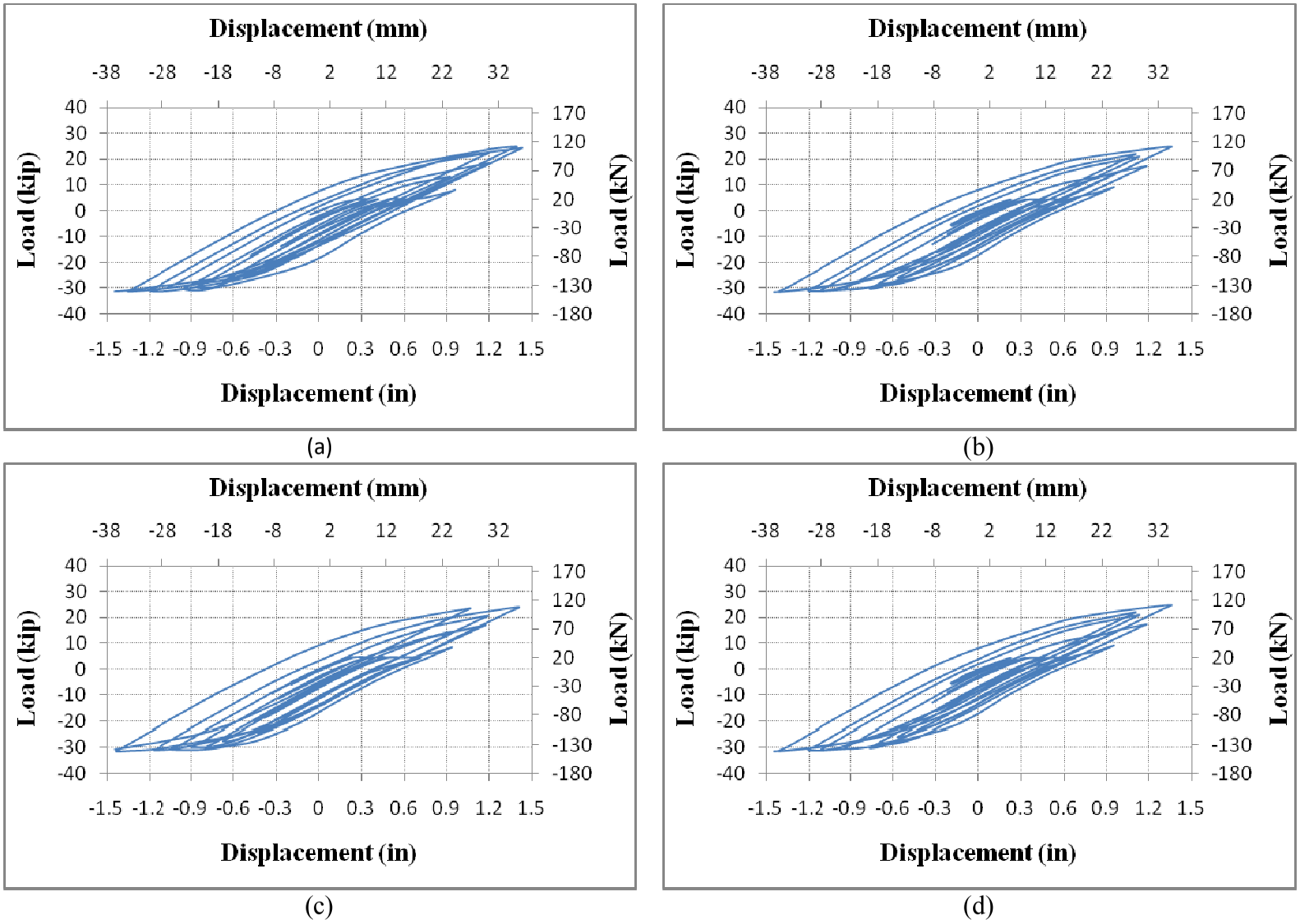

Figure C-18 Load-Displacement Cyclic Plots for: (a) SM-1B-1/4-1-QP-C-SS-DLC-I-1; (b) SM-1B-1/4-1-QP-C-SS-DLC-I-2; (c) SM-1B-1/4-1-QP-C-SS-DLC-I-3; and (d) SM-1B-1/4-1-QP-C-SS-DLC-I-4

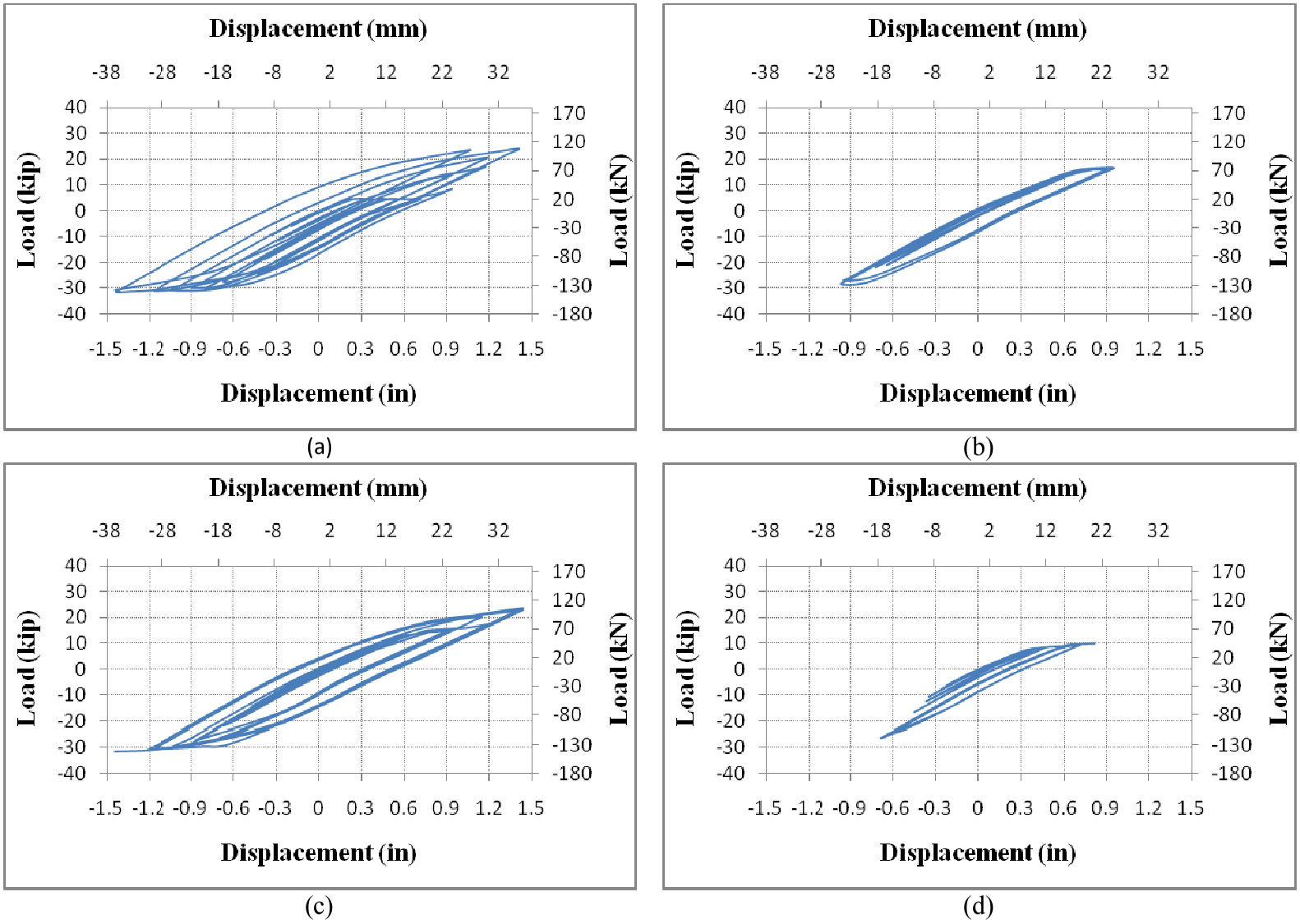

Figure C-19 Load-Displacement Cyclic Plots for: (a) SM-1B-1/4-1-QP-C-SS-DLC-I-5; (b) SM-1B-1/4-1-FP-HX-SS-DLC-I-1; (c) SM-1B-1/4-1-FP-C-SS-DLC-I-1; and (d) SM-1B-1/4-1-FP-C-NS-DLC-I-1

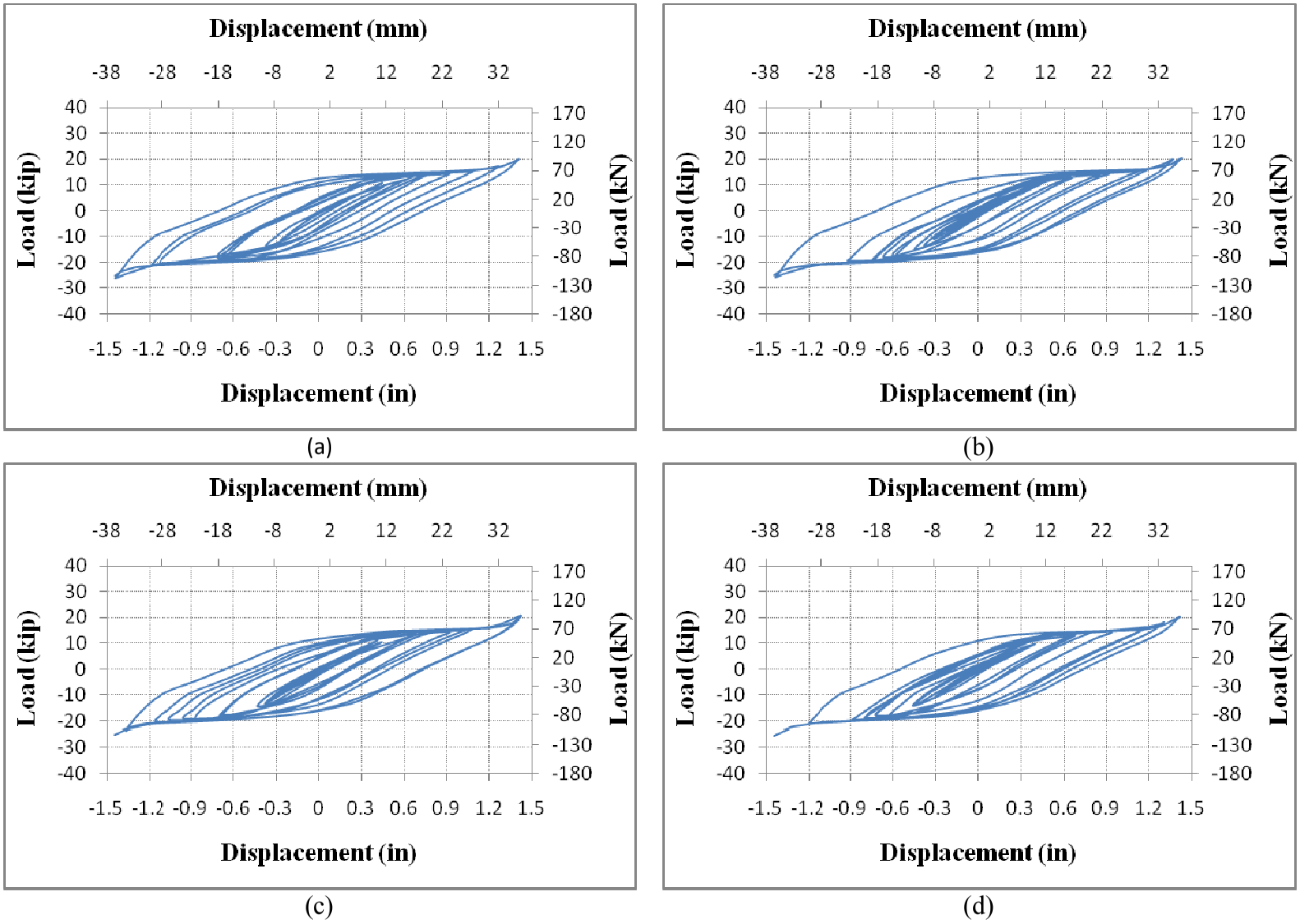

Figure C-20 Load-Displacement Cyclic Plots for: (a) SM-1B-1-1-FP-C-SS-DLC-I-1; (b) SM-1B-1-1-FP-C-SS-DLC-I-2; (c) SM-1B-1-1-FP-C-SS-DLC-I-3; and (d) SM-1B-1-1-FP-C-SS-DLC-I-4

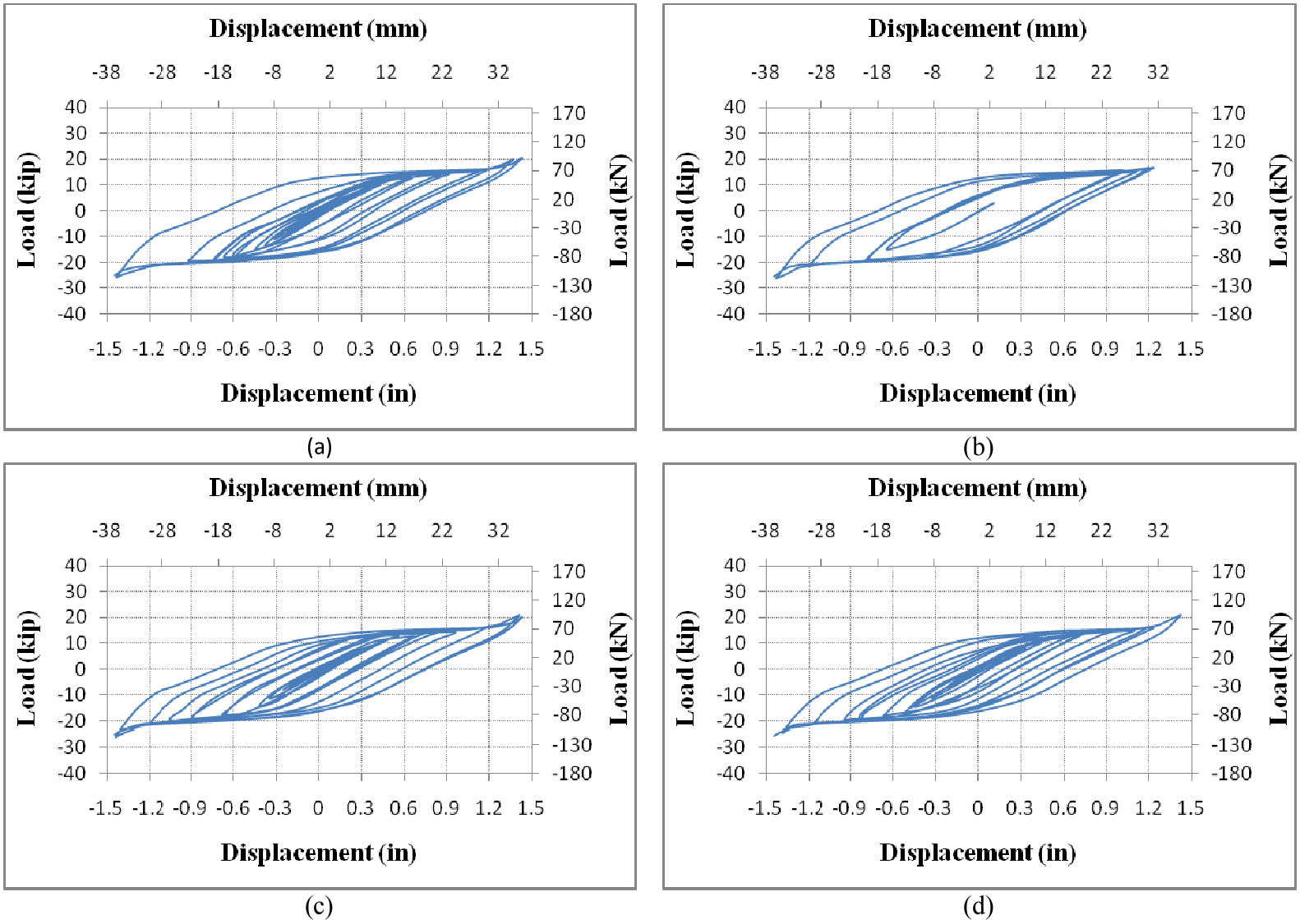

Figure C-21 Load-Displacement Cyclic Plots for: (a) SM-1B-1-1-FP-C-SS-DLC-I-5; (b) SM-1B-1-1-FP-C-SS-DLC-II-1; (c) SM-1B-1-1-FP-C-SS-DLC-II-2; and (d) SM-1B-1-1-FP-C-SS-DLC-II-3

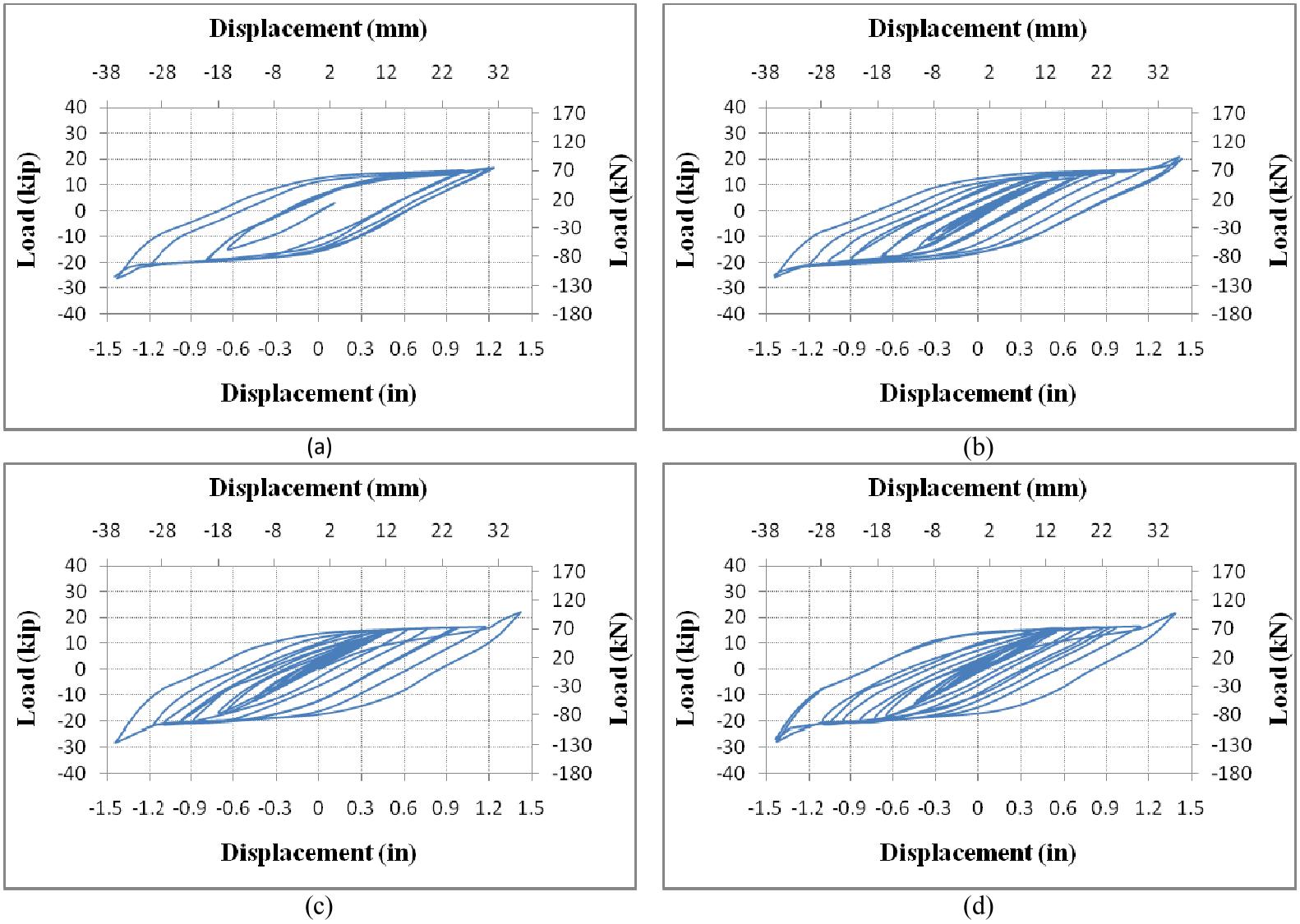

Figure C-22 Load-Displacement Cyclic Plots for: (a) SM-1B-1-1-FP-C-SS-DLC-II-4; (b) SM-1B-1-1-FP-C-SS-DLC-II-5; (c) SM-1B-1-1-FP-C-SS-DLC-III-1; and (d) SM-1B-1-1-FP-C-SS-DLC-III-2

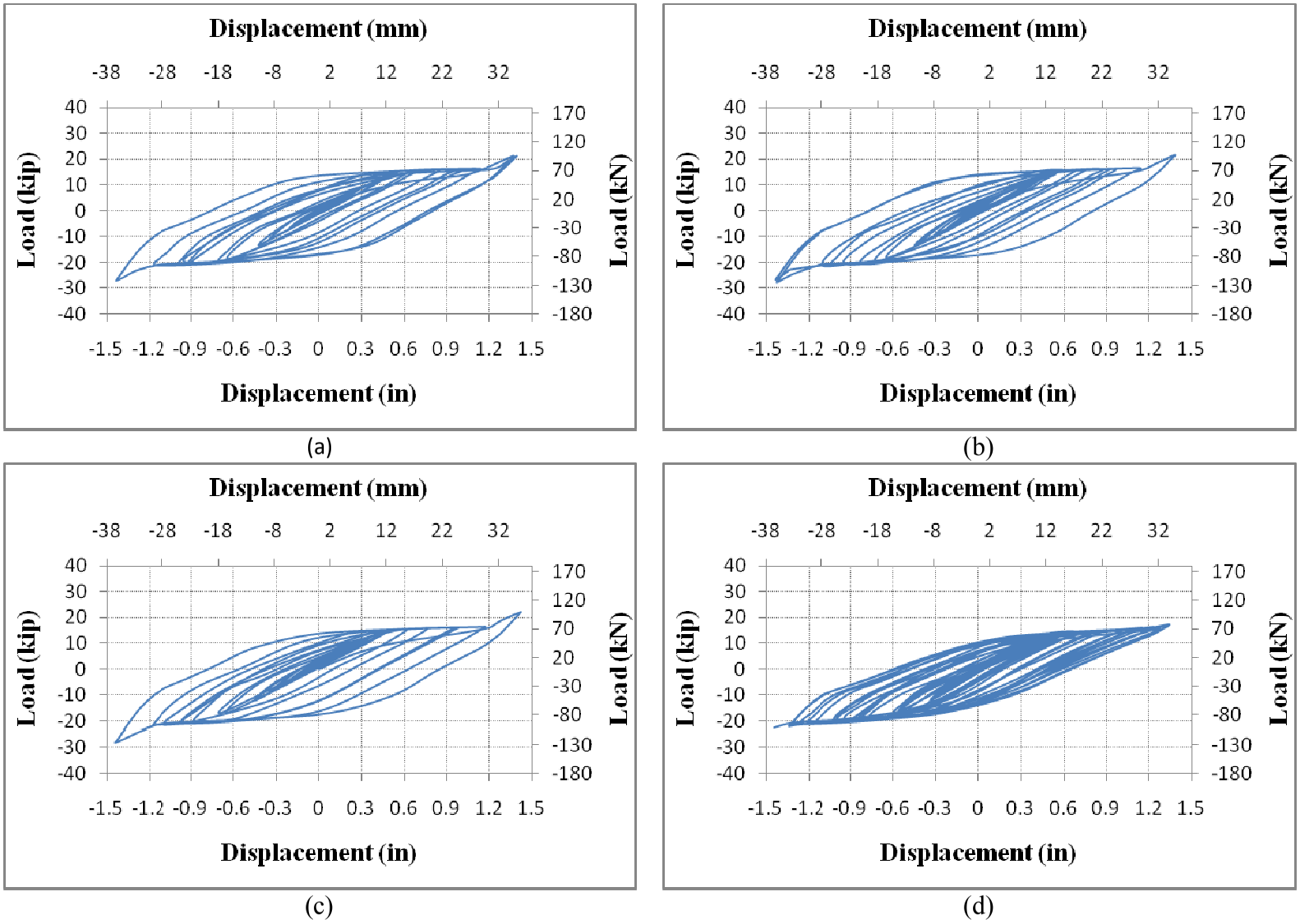

Figure C-23 Load-Displacement Cyclic Plots for: (a) SM-1B-1-1-FP-C-SS-DLC-III-3; (b) SM-1B-1-1-FP-C-SS-DLC-III-4; (c) SM-1B-1-1-FP-C-SS-DLC-III-5; and (d) SM-1B-1-1-FP-C-SS-DLC-IV-1

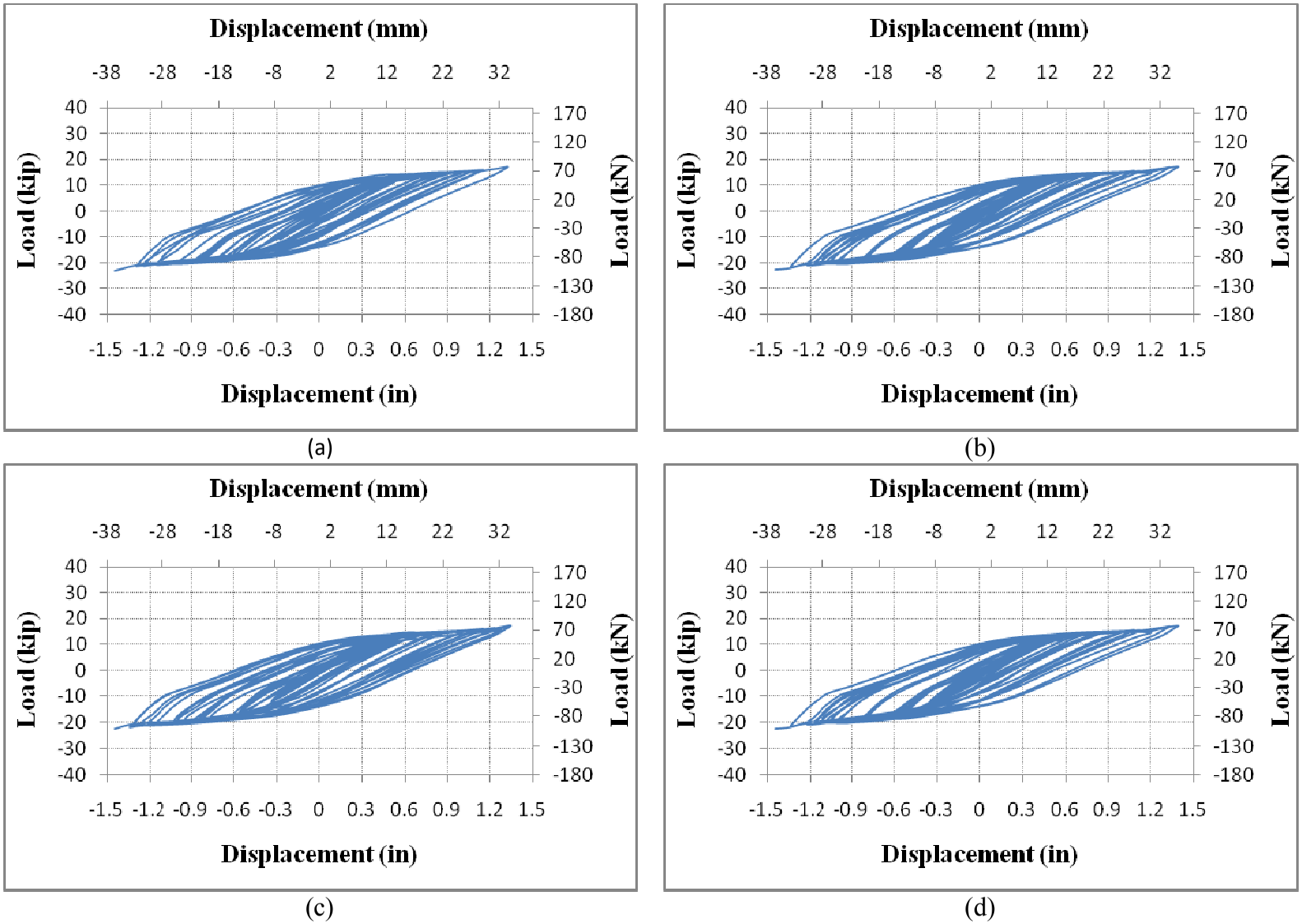

Figure C-24 Load-Displacement Cyclic Plots for: (a) SM-1B-1-1-FP-C-SS-DLC-IV-2; (b) SM-1B-1-1-FP-C-SS-DLC-IV-3; (c) SM-1B-1-1-FP-C-SS-DLC-IV-4; and (d) SM-1B-1-1-FP-C-SS-DLC-IV-5

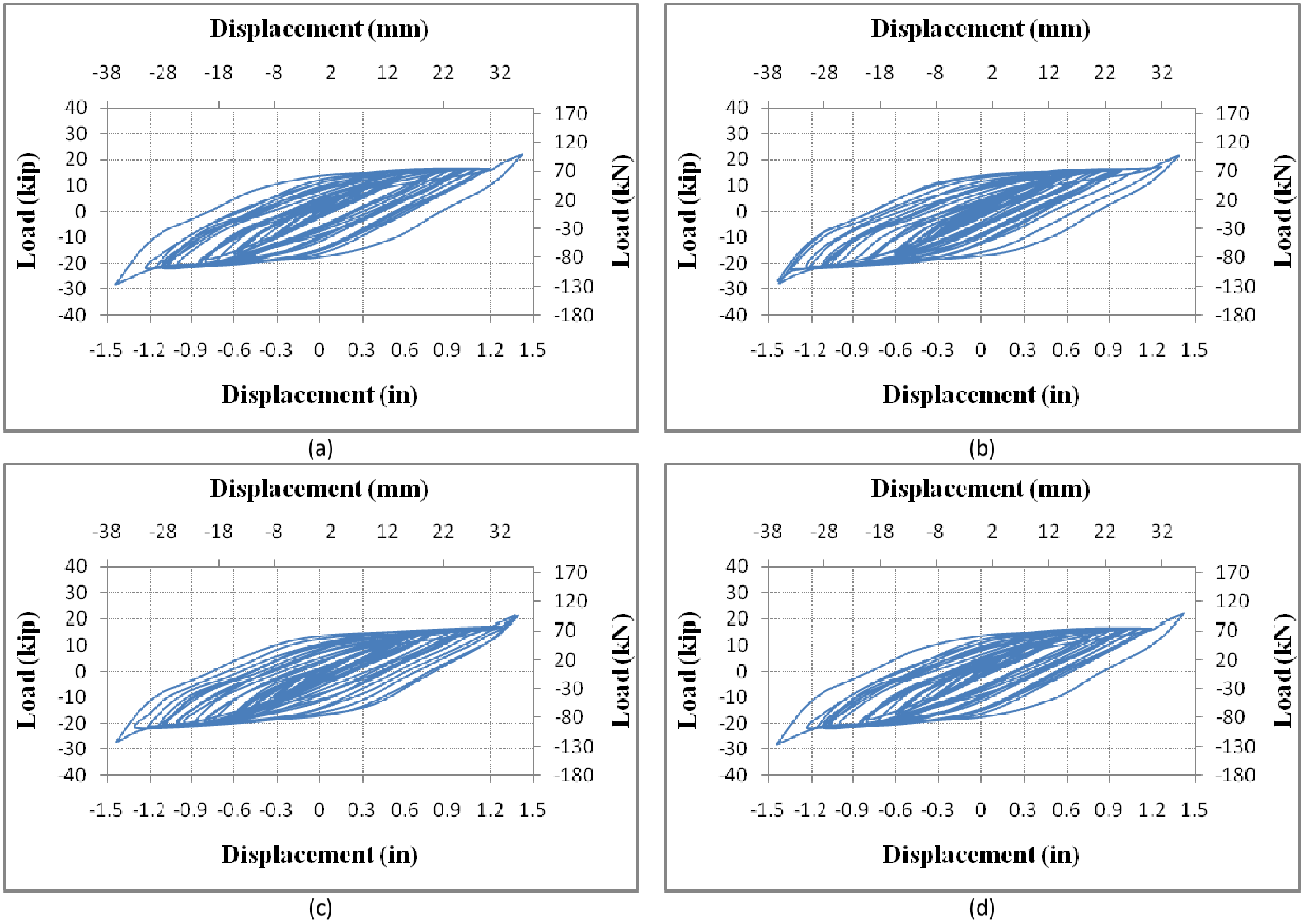

Figure C-25 Load-Displacement Cyclic Plots for: (a) SM-1B-1-1-FP-C-SS-DLC-V-1; (b) SM-1B-1-1-FP-C-SS-DLC-V-2; (c) SM-1B-1-1-FP-C-SS-DLC-V-3; and (d) SM-1B-1-1-FP-C-SS-DLC-V-4

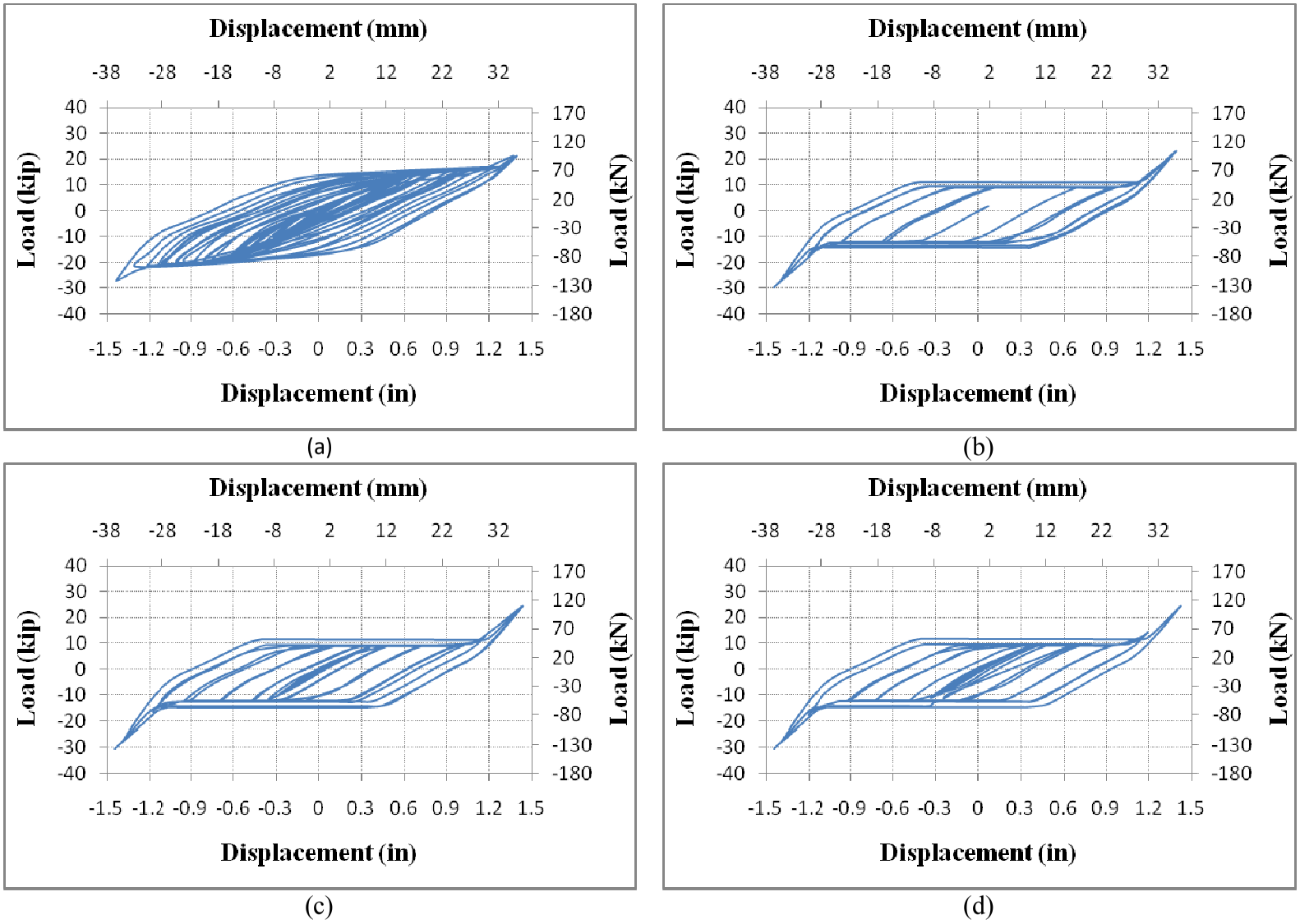

Figure C-26 Load-Displacement Cyclic Plots for: (a) SM-1B-1-1-FP-C-SS-DLC-V-5; (b) SM-1B-1-1-HP-C-SS-DLC-I-1; (c) SM-1B-1-1-HP-C-SS-DLC-I-2; and (d) SM-1B-1-1-HP-C-SS-DLC-I-3

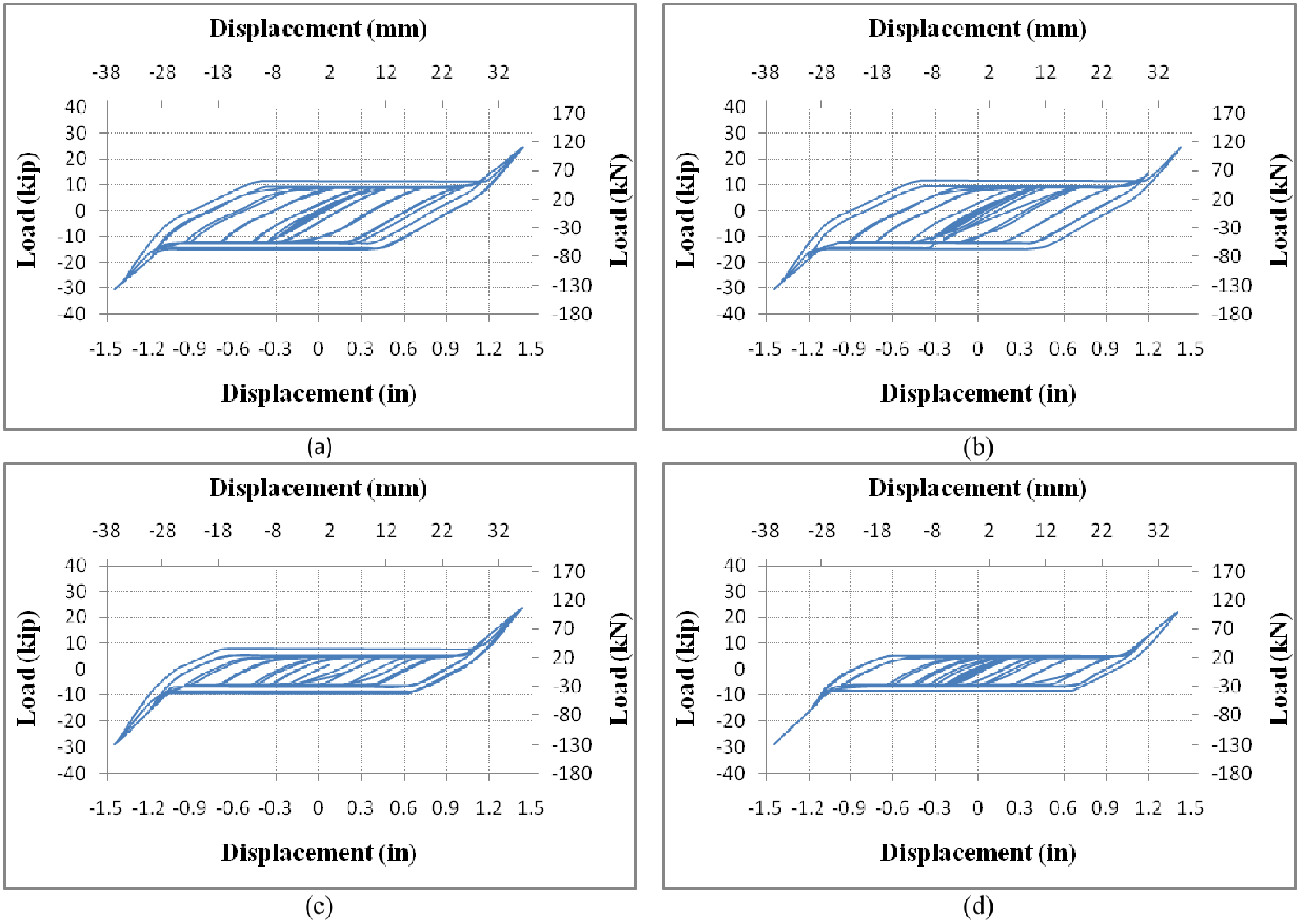

Figure C-27 Load-Displacement Cyclic Plots for: (a) SM-1B-1-1-HP-C-SS-DLC-I-4; (b) SM-1B-1-1-HP-C-SS-DLC-I-5; (c) SM-1B-1-1-QP-C-SS-DLC-I-1; and (d) SM-1B-1-1-QP-C-SS-DLC-I-2

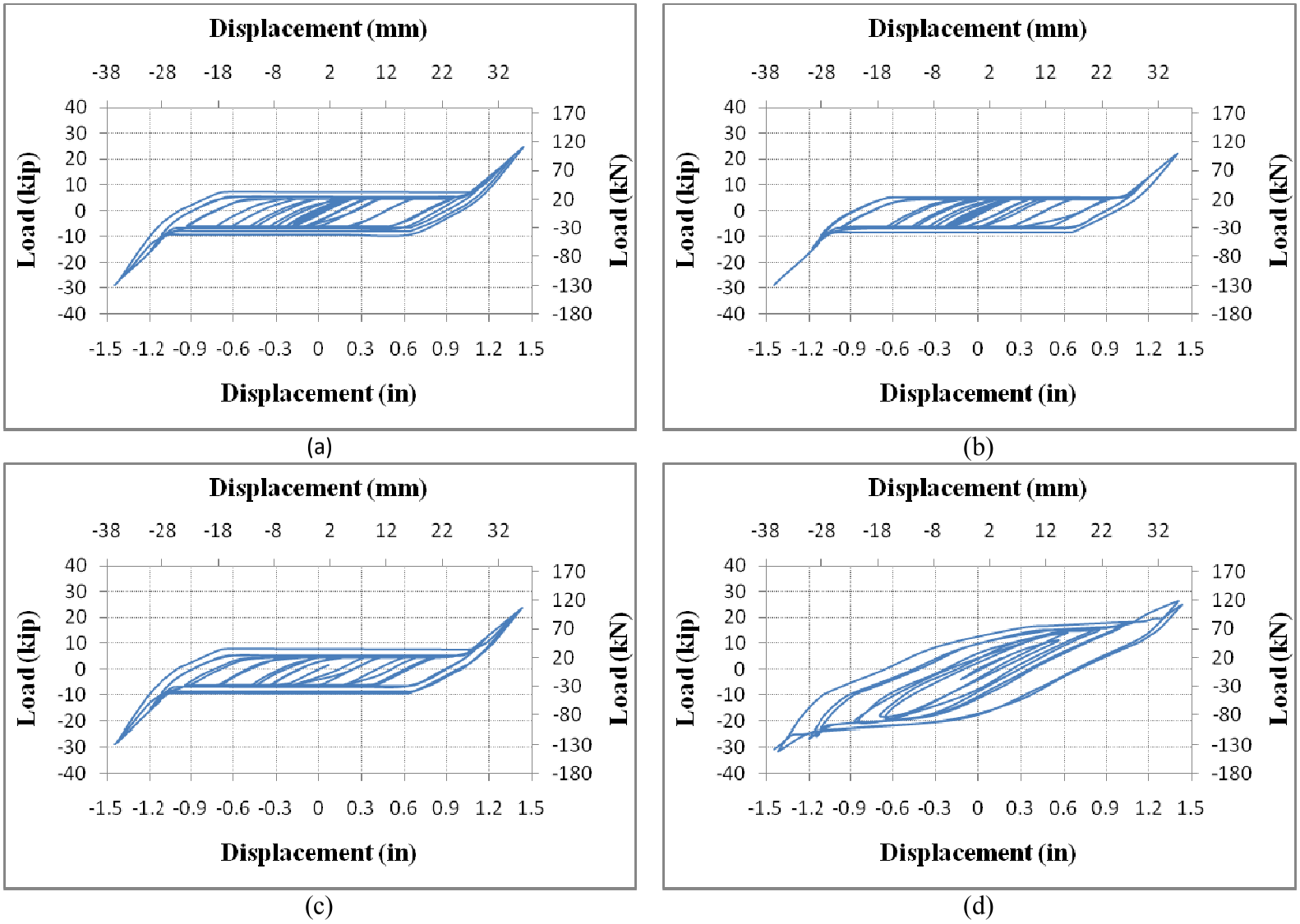

Figure C-28 Load-Displacement Cyclic Plots for: (a) SM-1B-1-1-QP-C-SS-DLC-I-3; (b) SM-1B-1-1-QP-C-SS-DLC-I-4; (c) SM-1B-1-1-QP-C-SS-DLC-I-5; and (d) SM-1B-1-1-FP-HX-SS-DLC-I-1

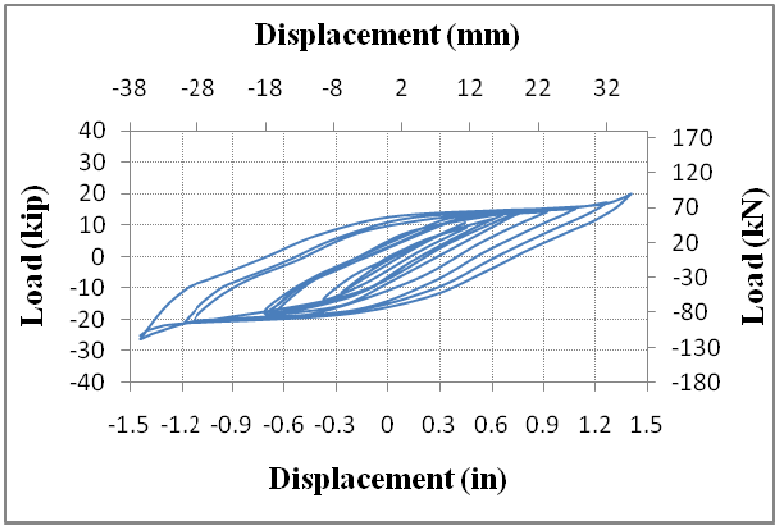

(a)

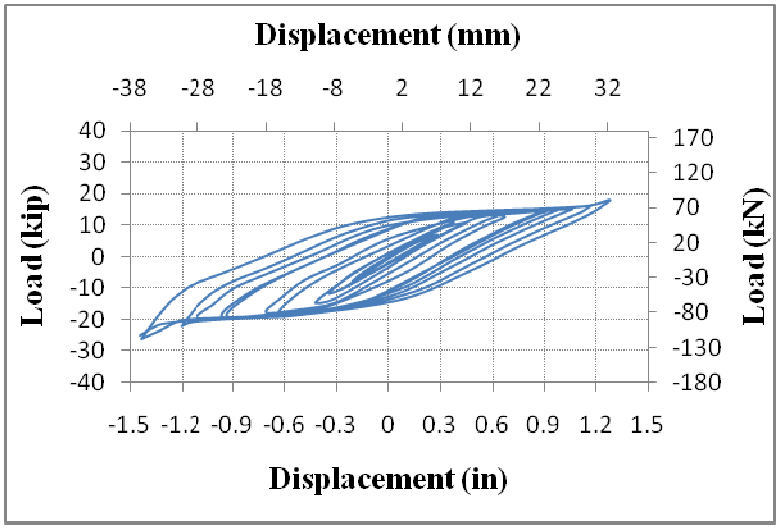

(b)

Figure C-29 Load-Displacement Cyclic Plots for: (a) SM-1B-1-1-FP-C-SS-DLC-I-1; and (b) SM-1B-1-1-FP-C-NS-DLC-I-1

APPENDIX D

DOUBLE BOLTED SHEAR SURFACE MODELS

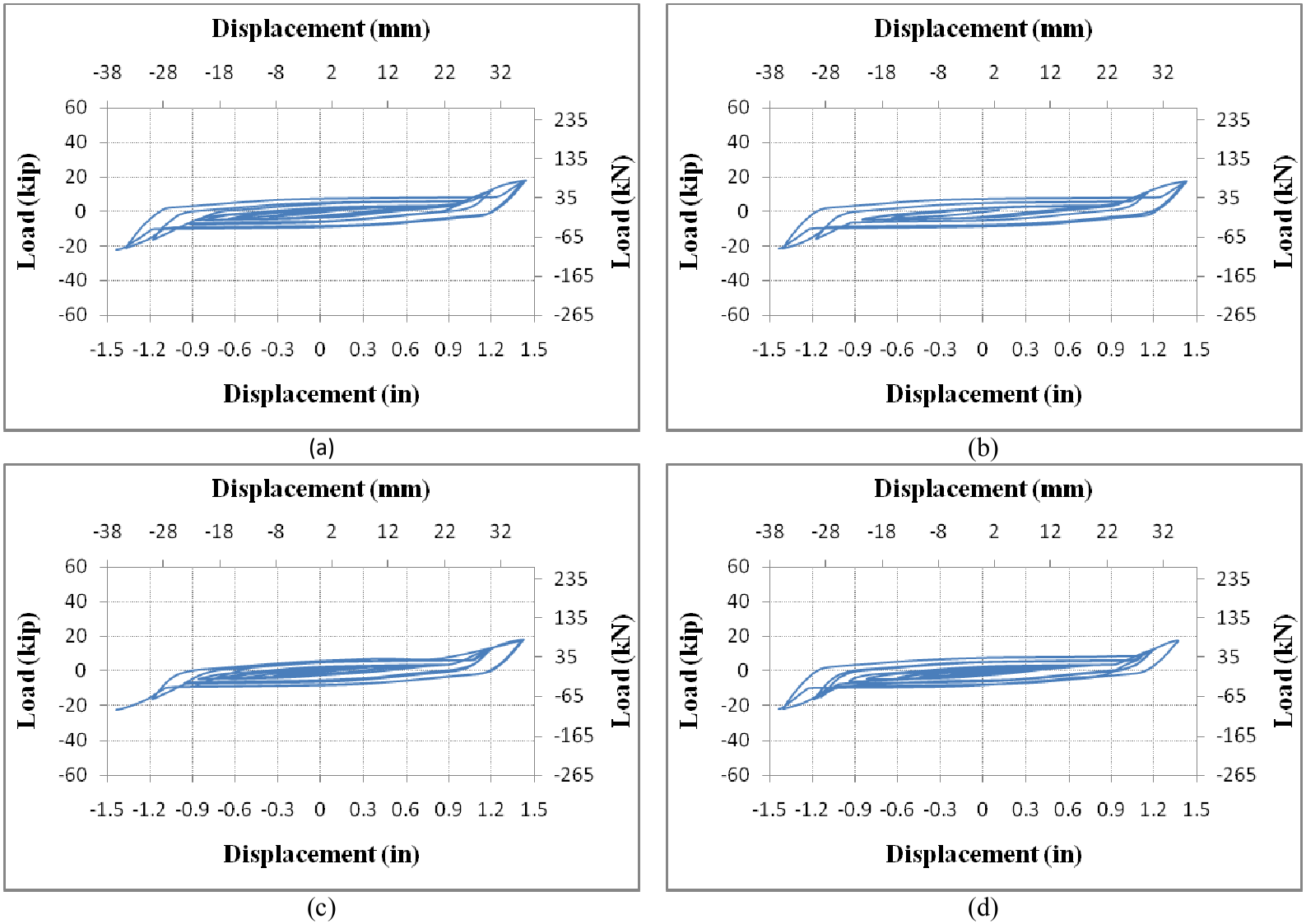

Figure D-1 Load-Displacement Cyclic Plots for: (a) SM-2B-1-1/2-FP-C-SS-DLC-I-1; (b) SM-2B-1-1/2-FP-C-SS-DLC-I-2; (c) SM-2B-1-1/2-FP-C-SS-DLC-I-3; and (d) SM-2B-1-1/2-FP-C-SS-DLC-I-4

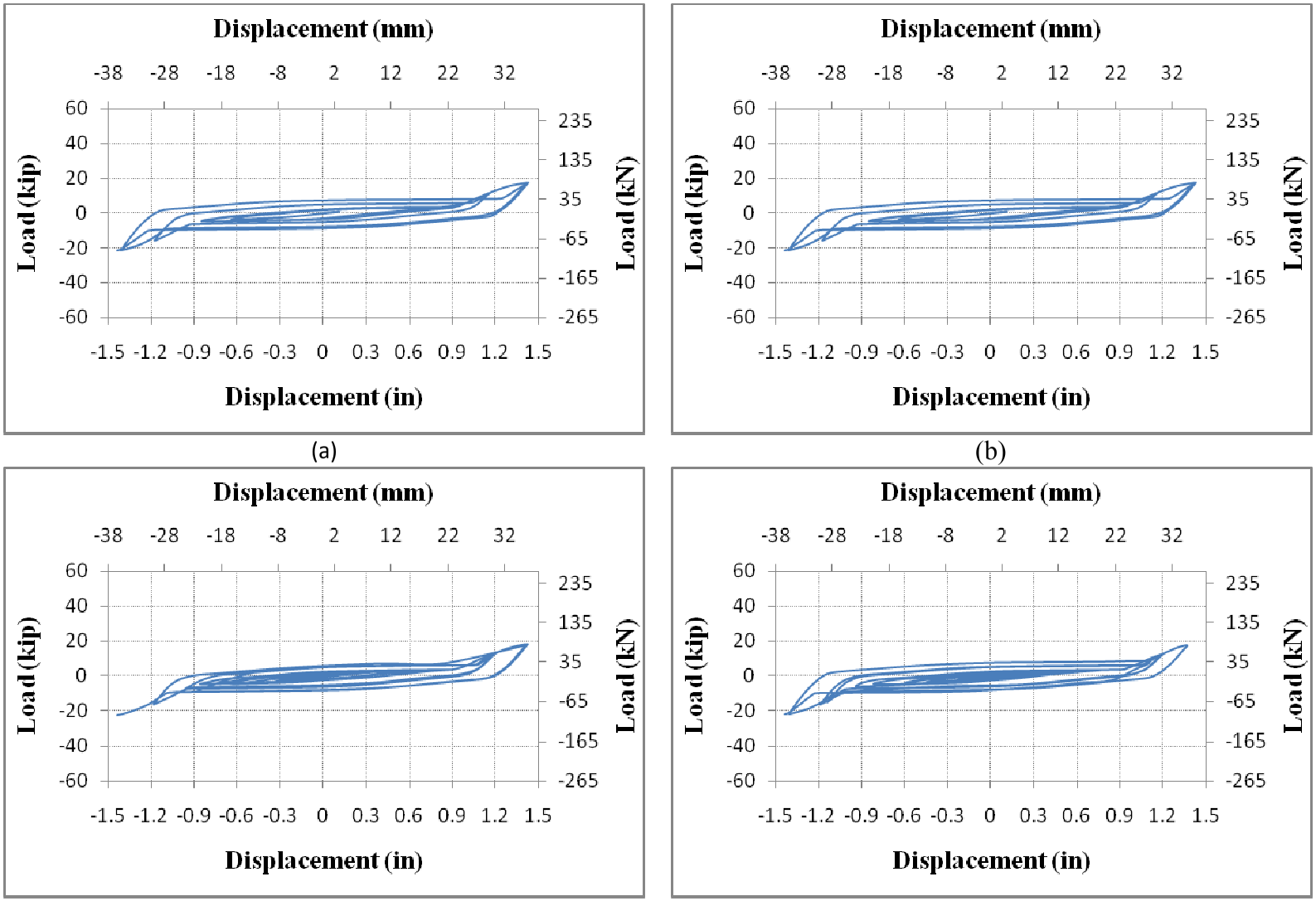

Figure D-2 Load-Displacement Cyclic Plots for: (a) SM-2B-1-1/2-FP-C-SS-DLC-I-5; (b) SM-2B-1-1/2-FP-C-SS-DLC-II-1; (c) SM-2B-1-1/2-FP-C-SS-DLC-II-2; and (d) SM-2B-1-1/2-FP-C-SS-DLC-II-3

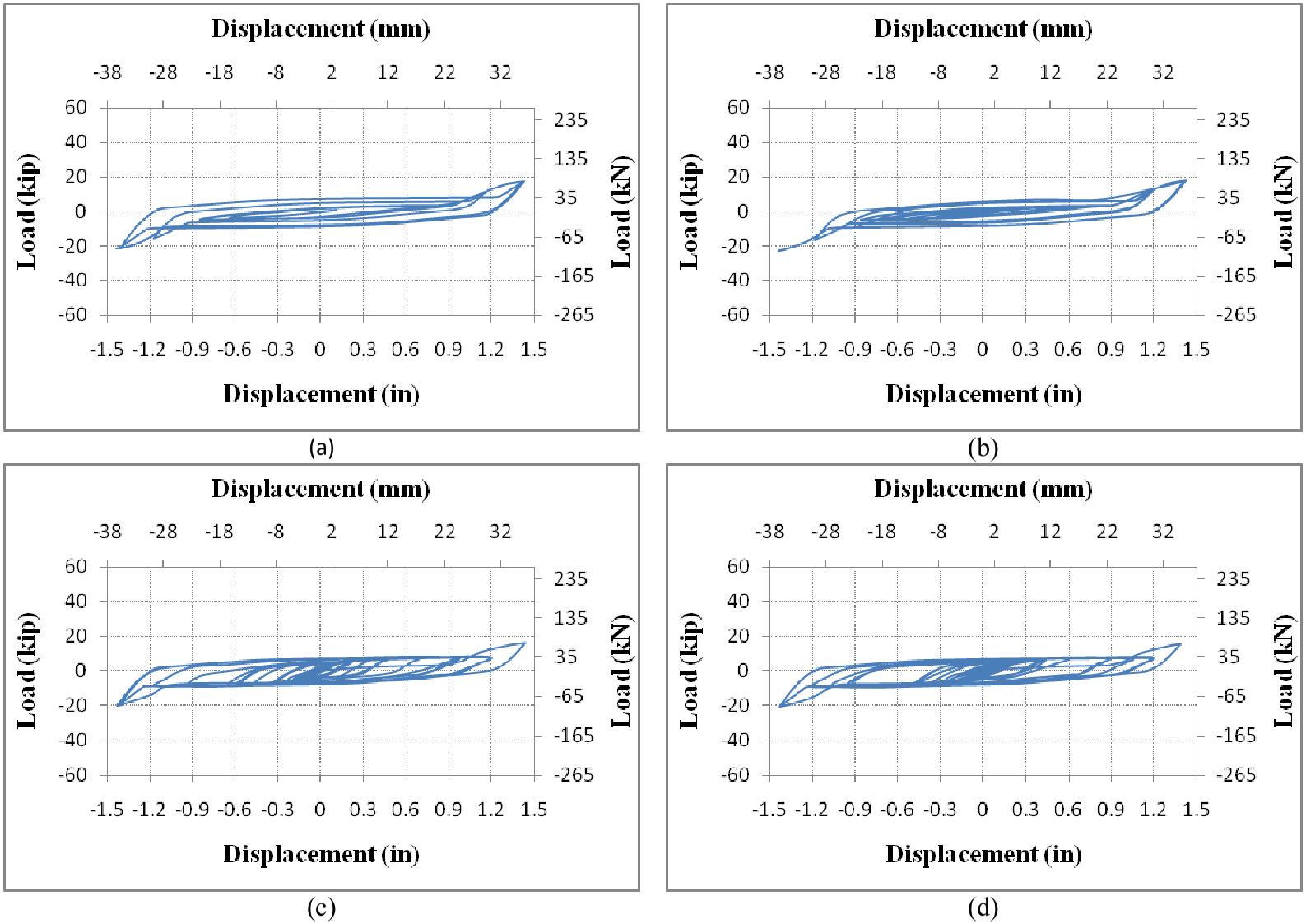

Figure D-3 Load-Displacement Cyclic Plots for: (a) SM-2B-1-1/2-FP-C-SS-DLC-II-4; (b) SM-2B-1-1/2-FP-C-SS-DLC-II-5; (c) SM-2B-1-1/2-FP-C-SS-DLC-III-1; and (d) SM-2B-1-1/2-FP-C-SS-DLC-III-2

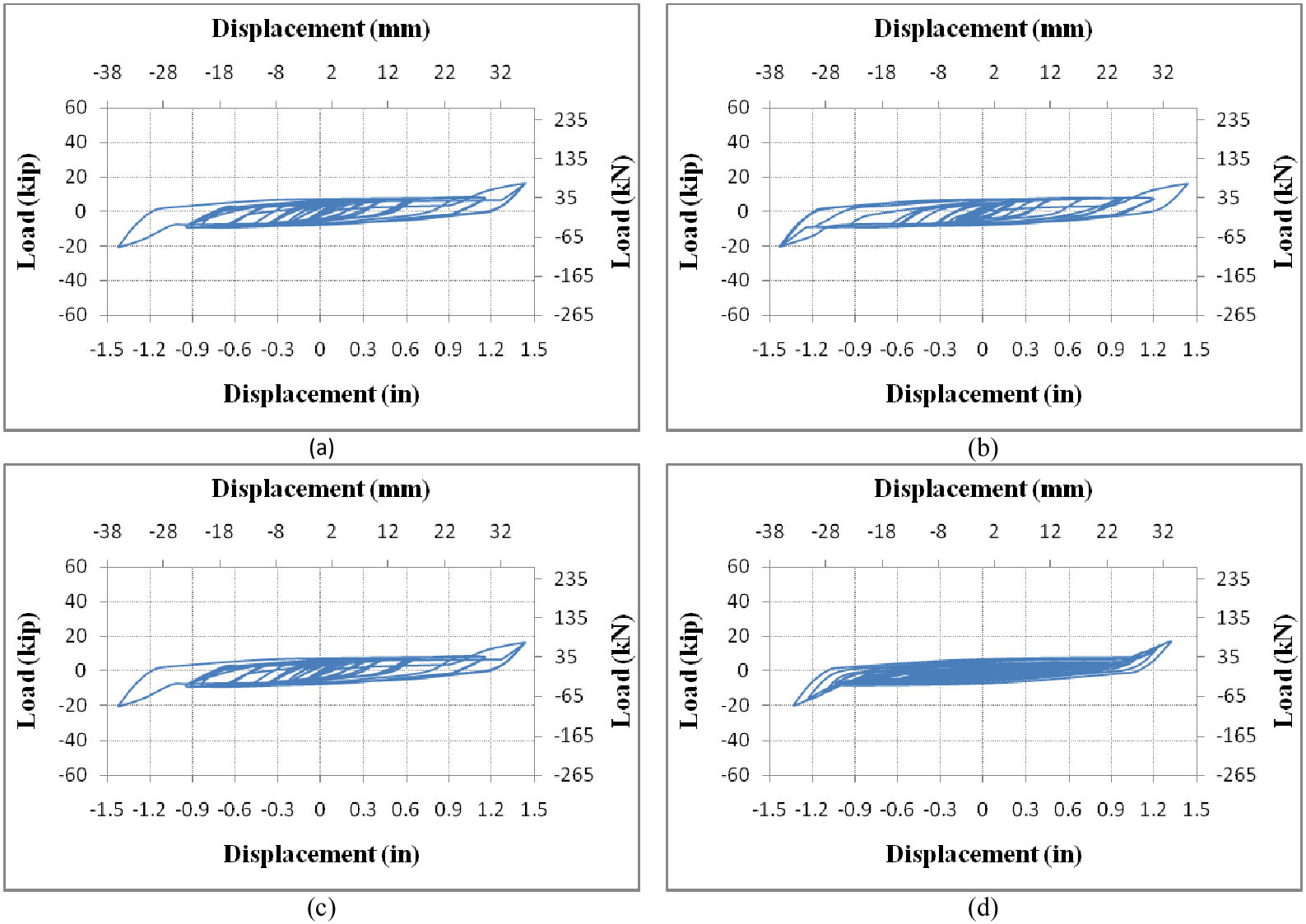

Figure D-4 Load-Displacement Cyclic Plots for: (a) SM-2B-1-1/2-FP-C-SS-DLC-III-3; (b) SM-2B-1-1/2-FP-C-SS-DLC-III-4; (c) SM-2B-1-1/2-FP-C-SS-DLC-III-5; and (d) SM-2B-1-1/2-FP-C-SS-DLC-IV-1

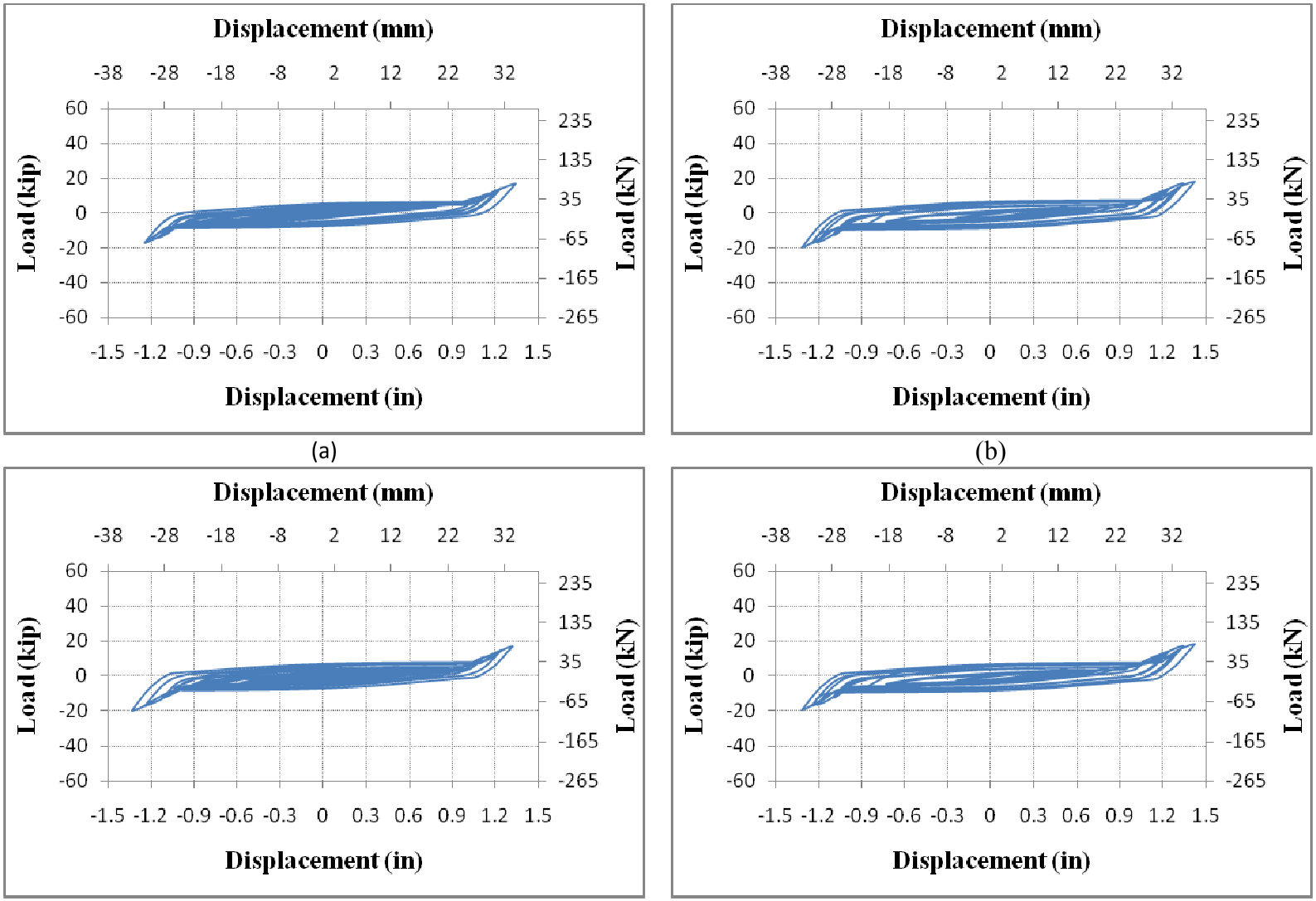

Figure D-5 Load-Displacement Cyclic Plots for: (a) SM-2B-1-1/2-FP-C-SS-DLC-IV-2; (b) SM-2B-1-1/2-FP-C-SS-DLC-IV-3; (c) SM-2B-1-1/2-FP-C-SS-DLC-IV-4; and (d) SM-2B-1-1/2-FP-C-SS-DLC-IV-5

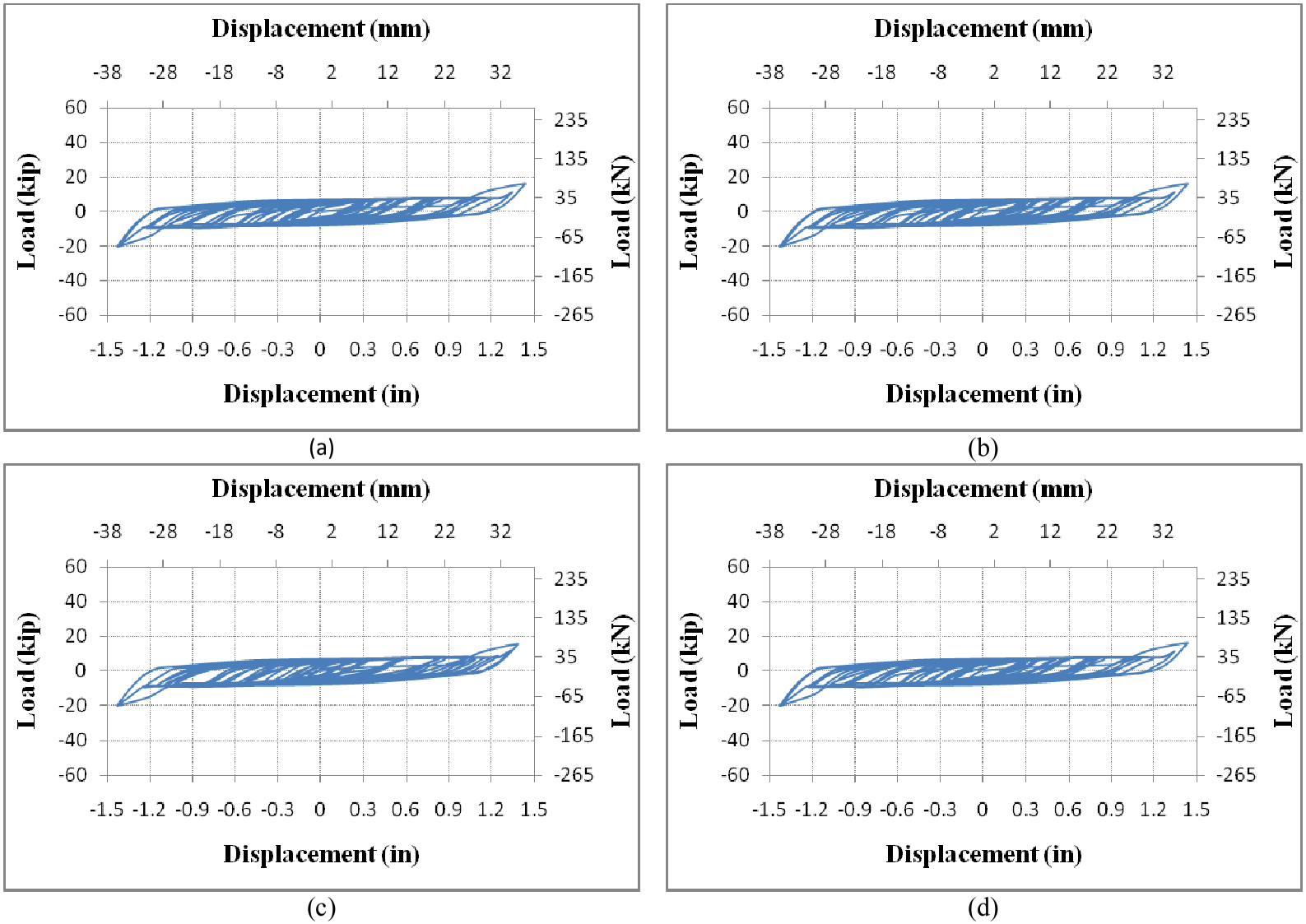

Figure D-6 Load-Displacement Cyclic Plots for: (a) SM-2B-1-1/2-FP-C-SS-DLC-V-1; (b) SM-2B-1-1/2-FP-C-SS-DLC-V-2; (c) SM-2B-1-1/2-FP-C-SS-DLC-V-3; and (d) SM-2B-1-1/2-FP-C-SS-DLC-V-4

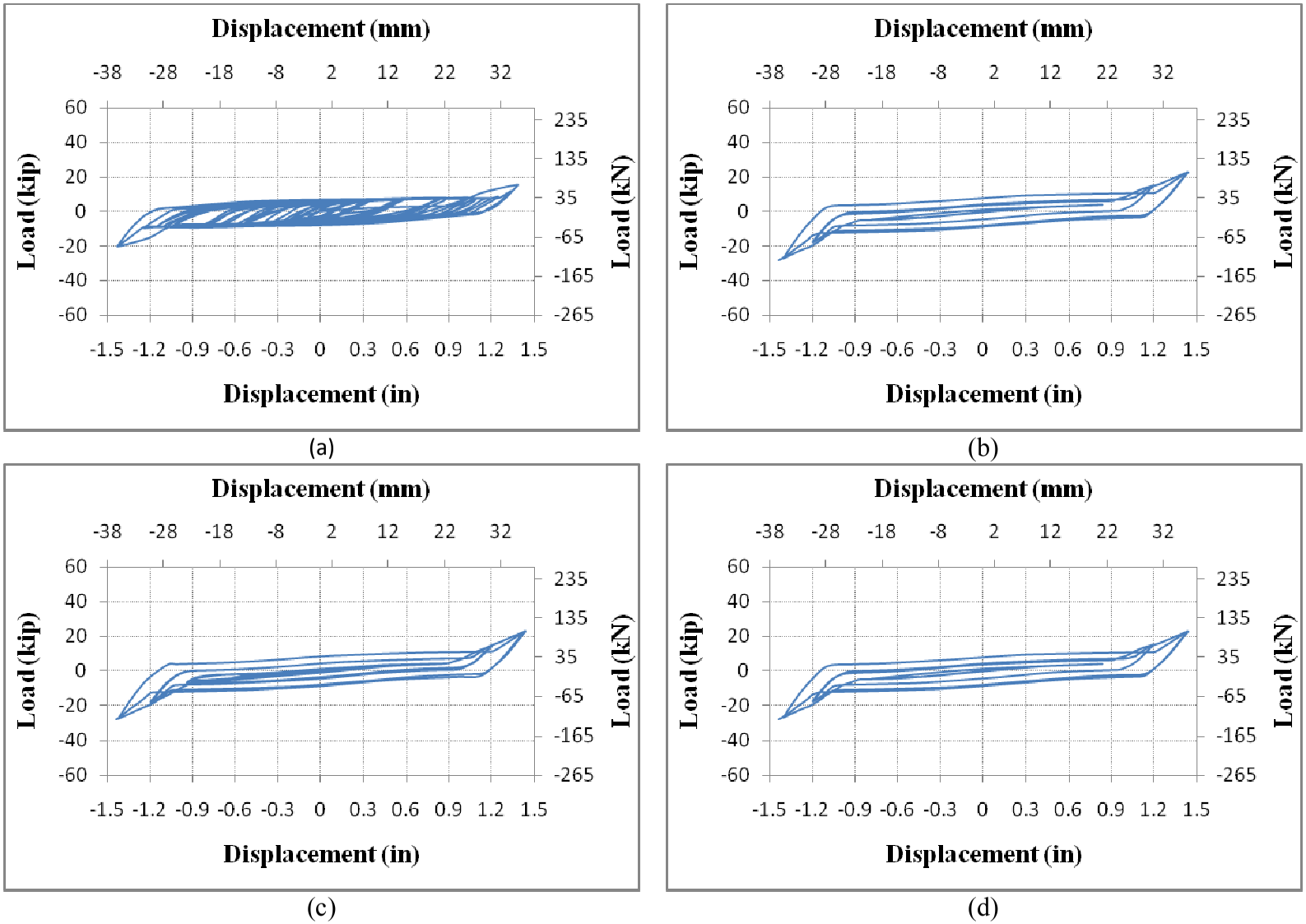

Figure D-7 Load-Displacement Cyclic Plots for: (a) SM-2B-1-1/2-FP-C-SS-DLC-V-5; (b) SM-2B-1-1/2-HP-C-SS-DLC-I-1; (c) SM-2B-1-1/2-HP-C-SS-DLC-I-2; and (d) SM-2B-1-1/2-HP-C-SS-DLC-I-3

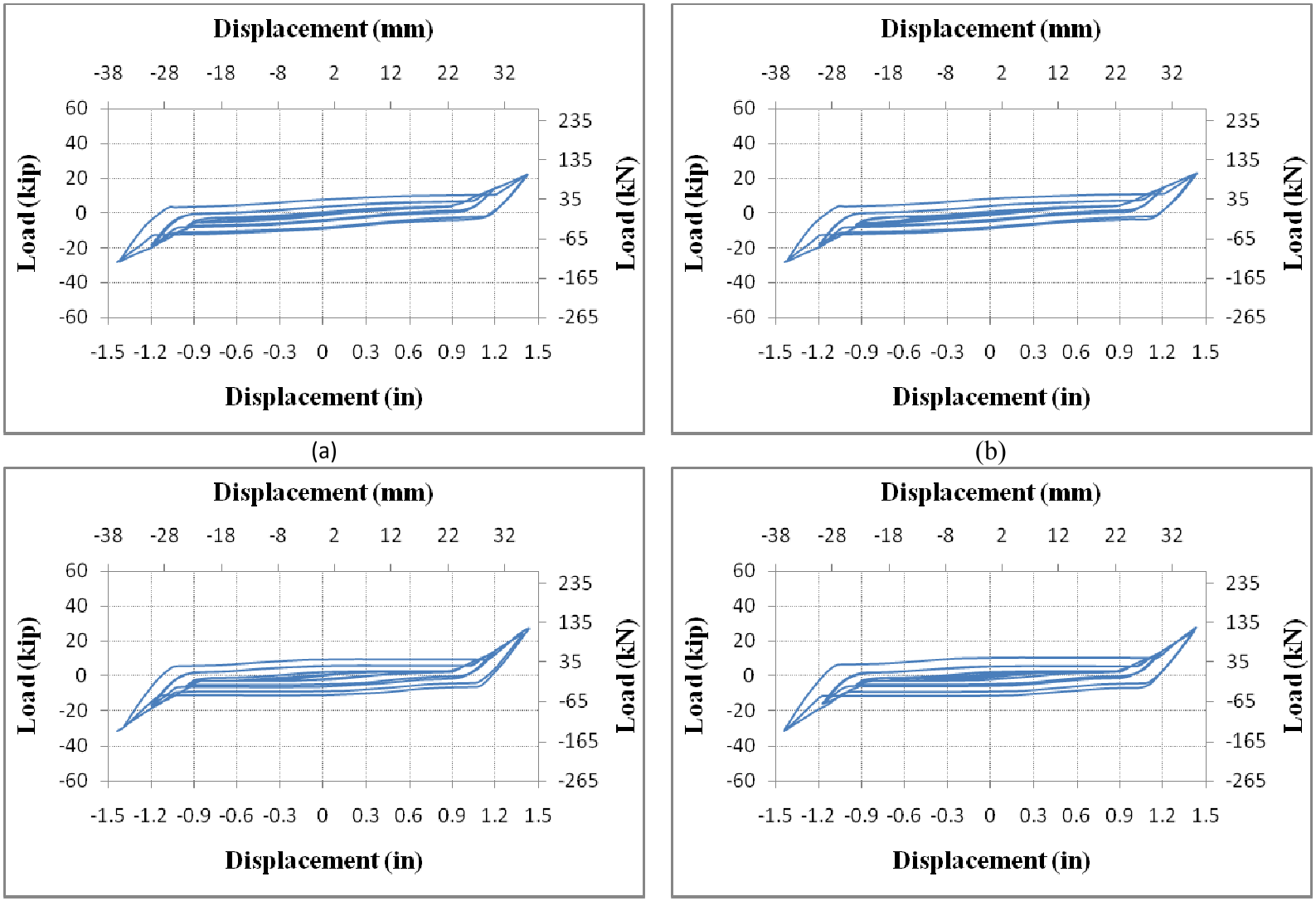

Figure D-8 Load-Displacement Cyclic Plots for: (a) SM-2B-1-1/2-HP-C-SS-DLC-I-4; (b) SM-2B-1-1/2-HP-C-SS-DLC-I-5; (c) SM-2B-1-1/2-QP-C-SS-DLC-I-1; and (d) SM-2B-1-1/2-QP-C-SS-DLC-I-2

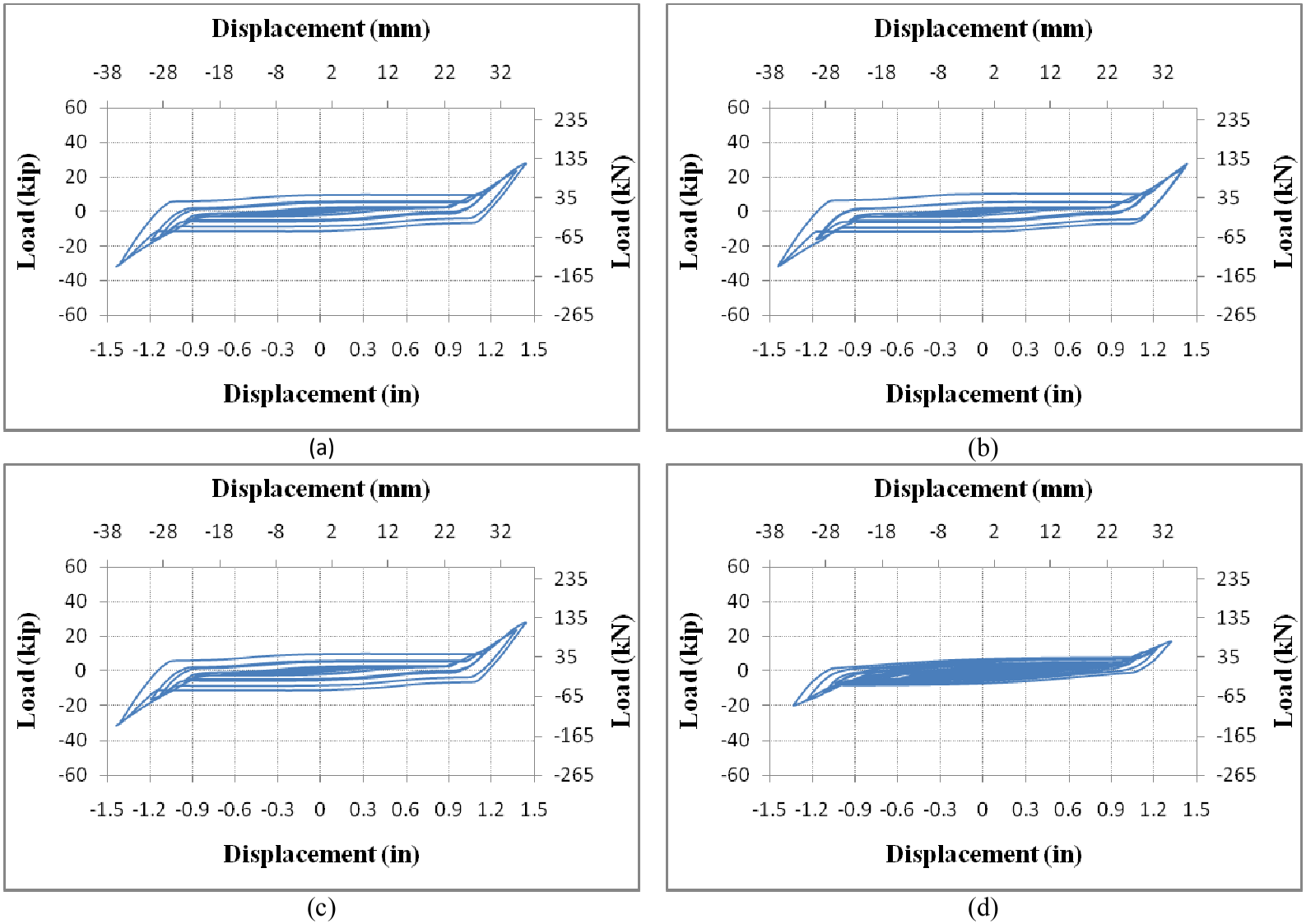

Figure D-9 Load-Displacement Cyclic Plots for: (a) SM-2B-1-1/2-QP-C-SS-DLC-I-3; (b) SM-2B-1-1/2-QP-C-SS-DLC-I-4; (c) SM-2B-1-1/2-QP-C-SS-DLC-I-5; and (d) SM-2B-1-1/2-FP-HX-SS-DLC-I-1

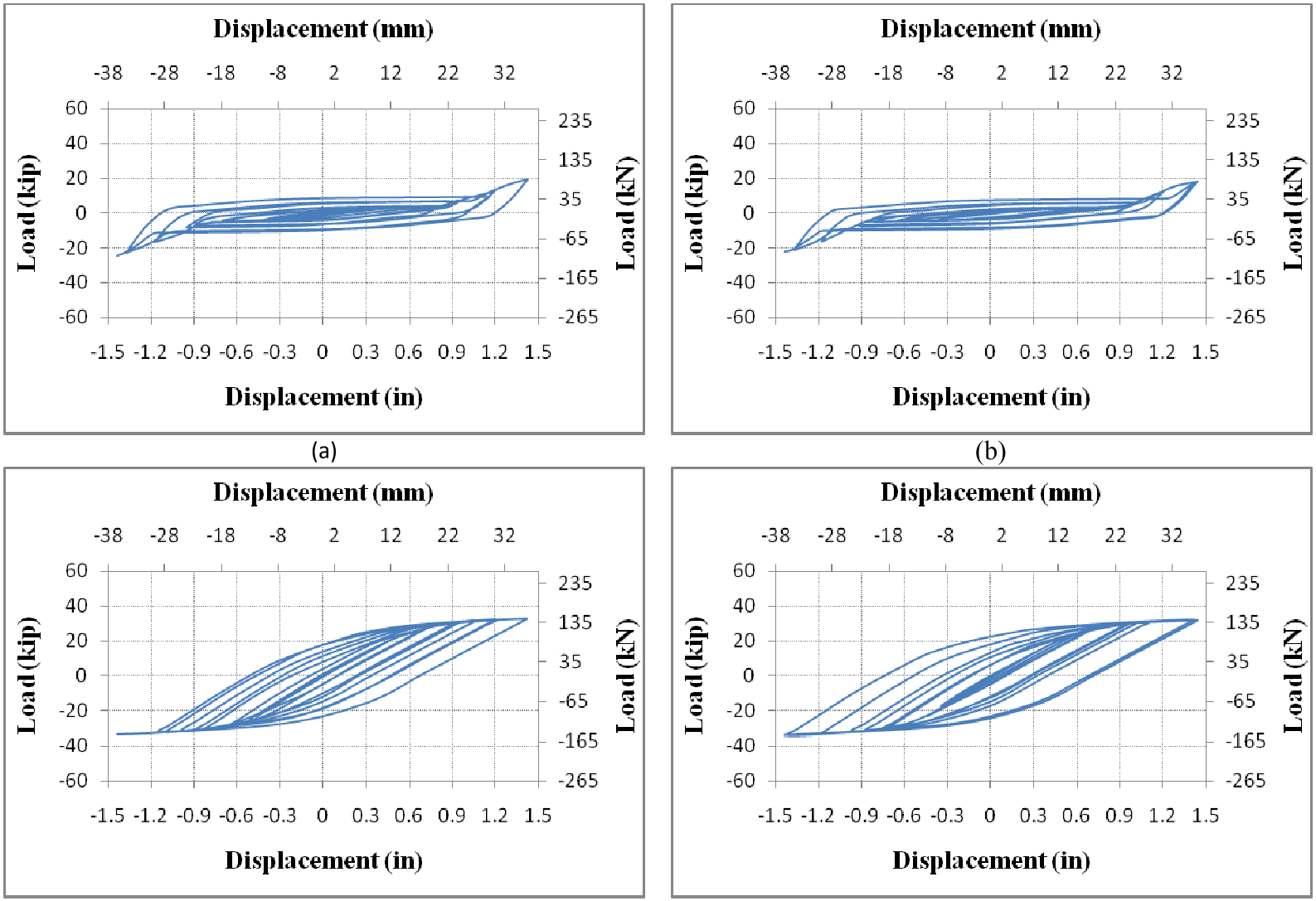

Figure D-10 Load-Displacement Cyclic Plots for: (a) SM-2B-1-1/2-FP-C-NS-DLC-I-1; (b) SM-2B-1-1/2-FP-C-SS-DLC-I-1; (c) SM-2B-1/4-1-FP-C-SS-DLC-I-1; and (d) SM-2B-1/4-1-FP-C-SS-DLC-I-2

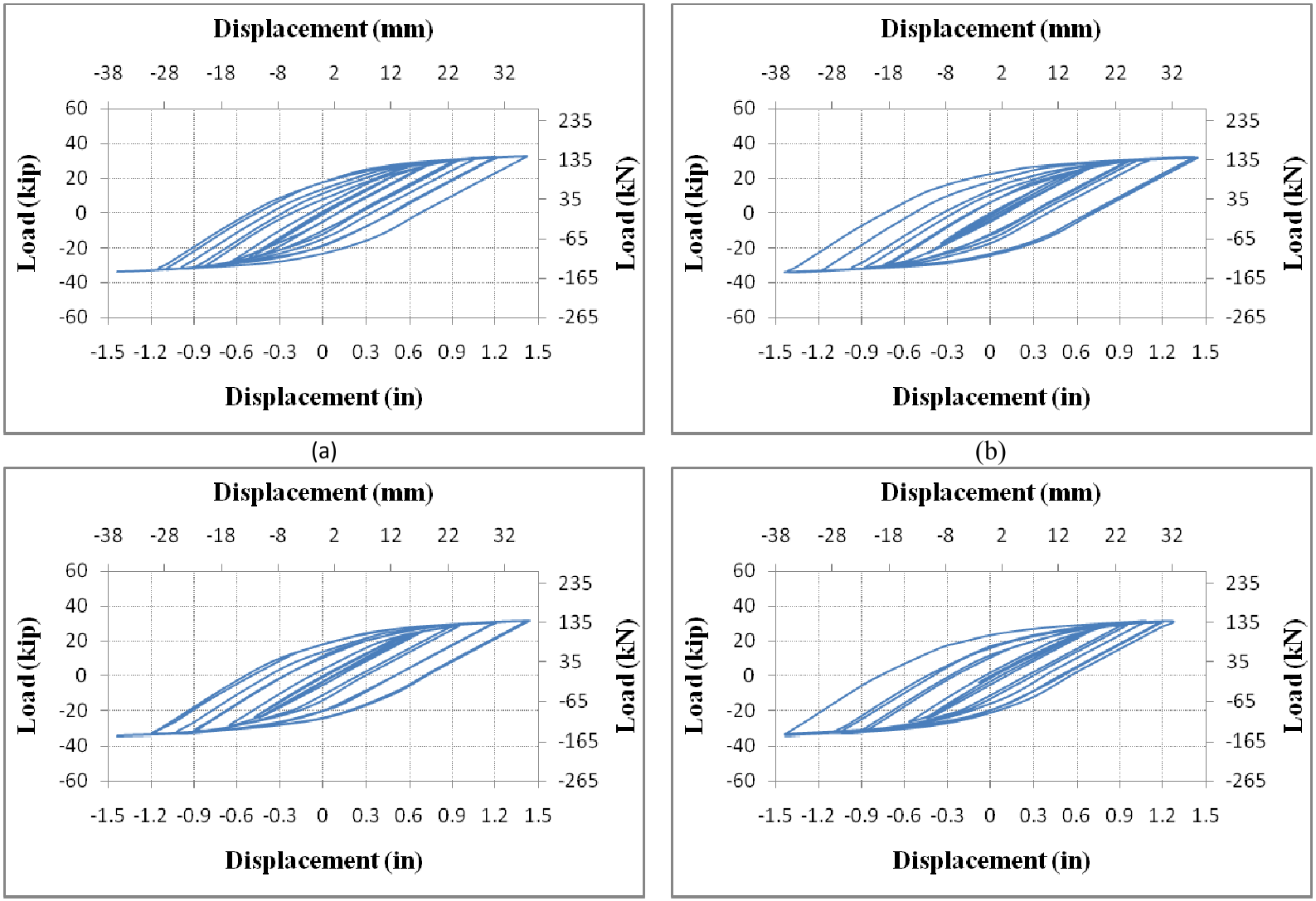

Figure D-11 Load-Displacement Cyclic Plots for: (a) SM-2B-1/4-1-FP-C-SS-DLC-I-3; (b) SM-2B-1/4-1-FP-C-SS-DLC-I-4; (c) SM-2B-1/4-1-FP-C-SS-DLC-I-5; and (d) SM-2B-1/4-1-FP-C-SS-DLC-II-1

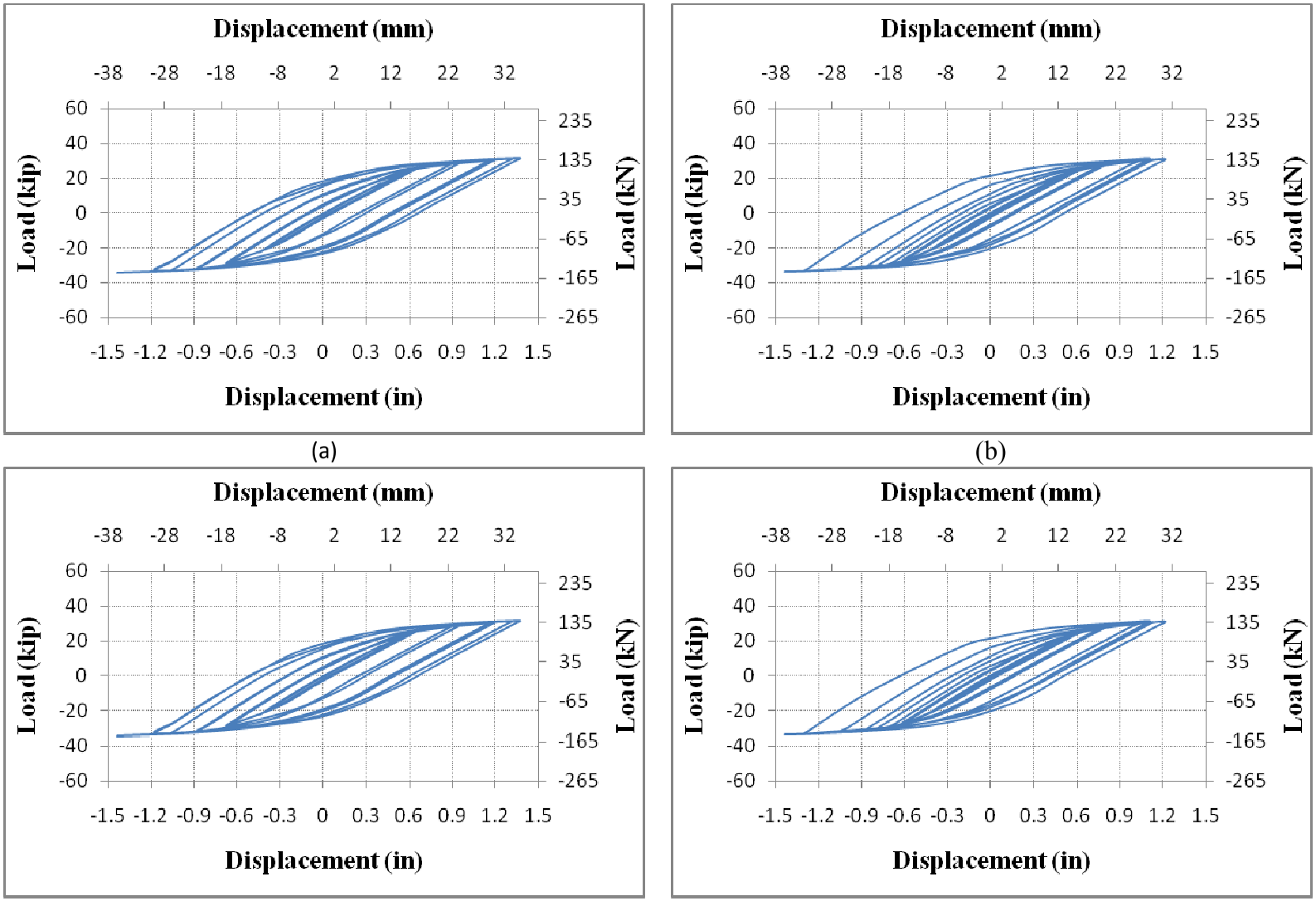

Figure D-12 Load-Displacement Cyclic Plots for: (a) SM-2B-1/4-1-FP-C-SS-DLC-II-2; (b) SM-2B-1/4-1-FP-C-SS-DLC-II-3; (c) SM-2B-1/4-1-FP-C-SS-DLC-II-4; and (d) SM-2B-1/4-1-FP-C-SS-DLC-II-5

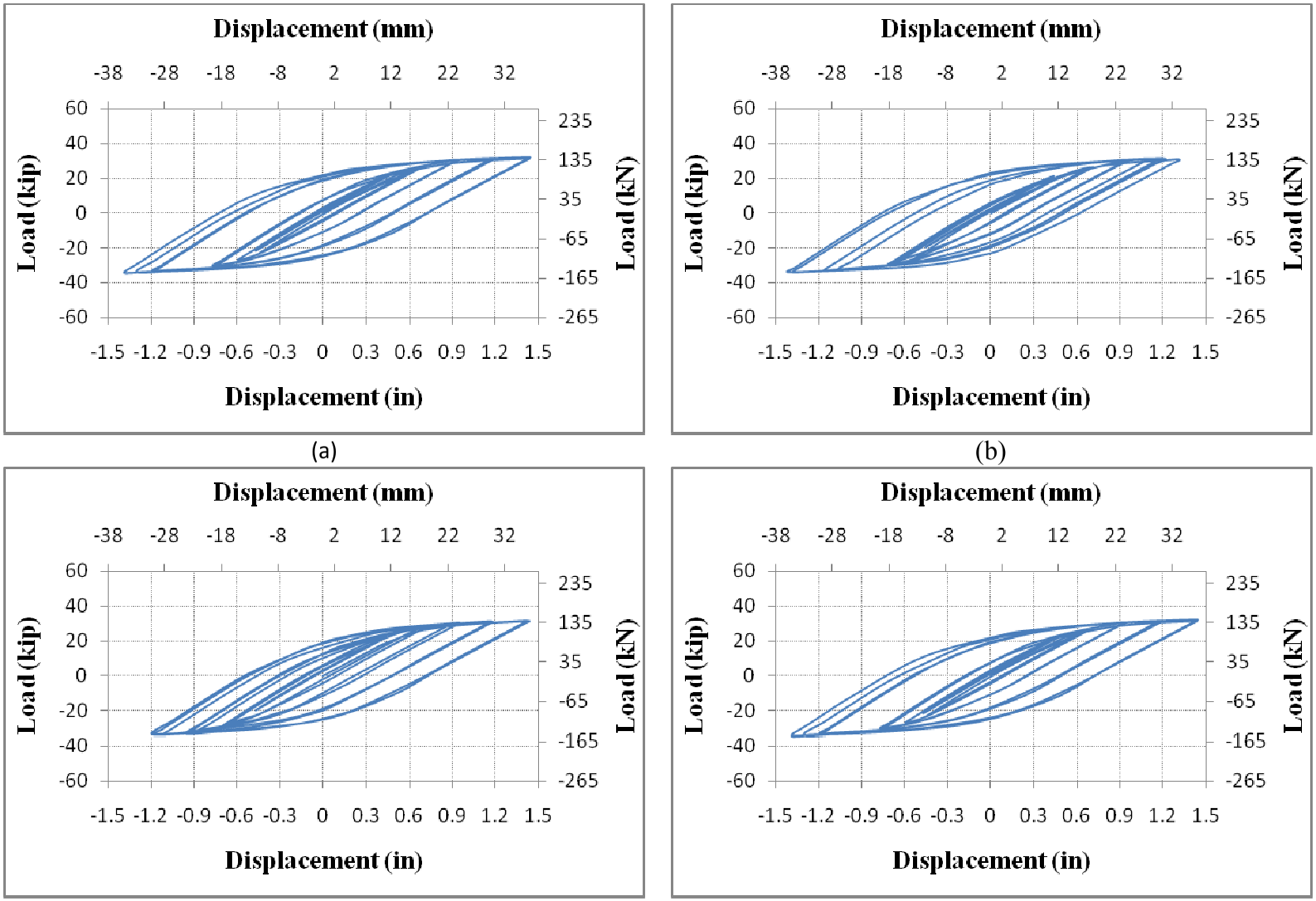

Figure D-13 Load-Displacement Cyclic Plots for: (a) SM-2B-1/4-1-FP-C-SS-DLC-III-1; (b) SM-2B-1/4-1-FP-C-SS-DLC-III-2; (c) SM-2B-1/4-1-FP-C-SS-DLC-III-3; and (d) SM-2B-1/4-1-FP-C-SS-DLC-III-4

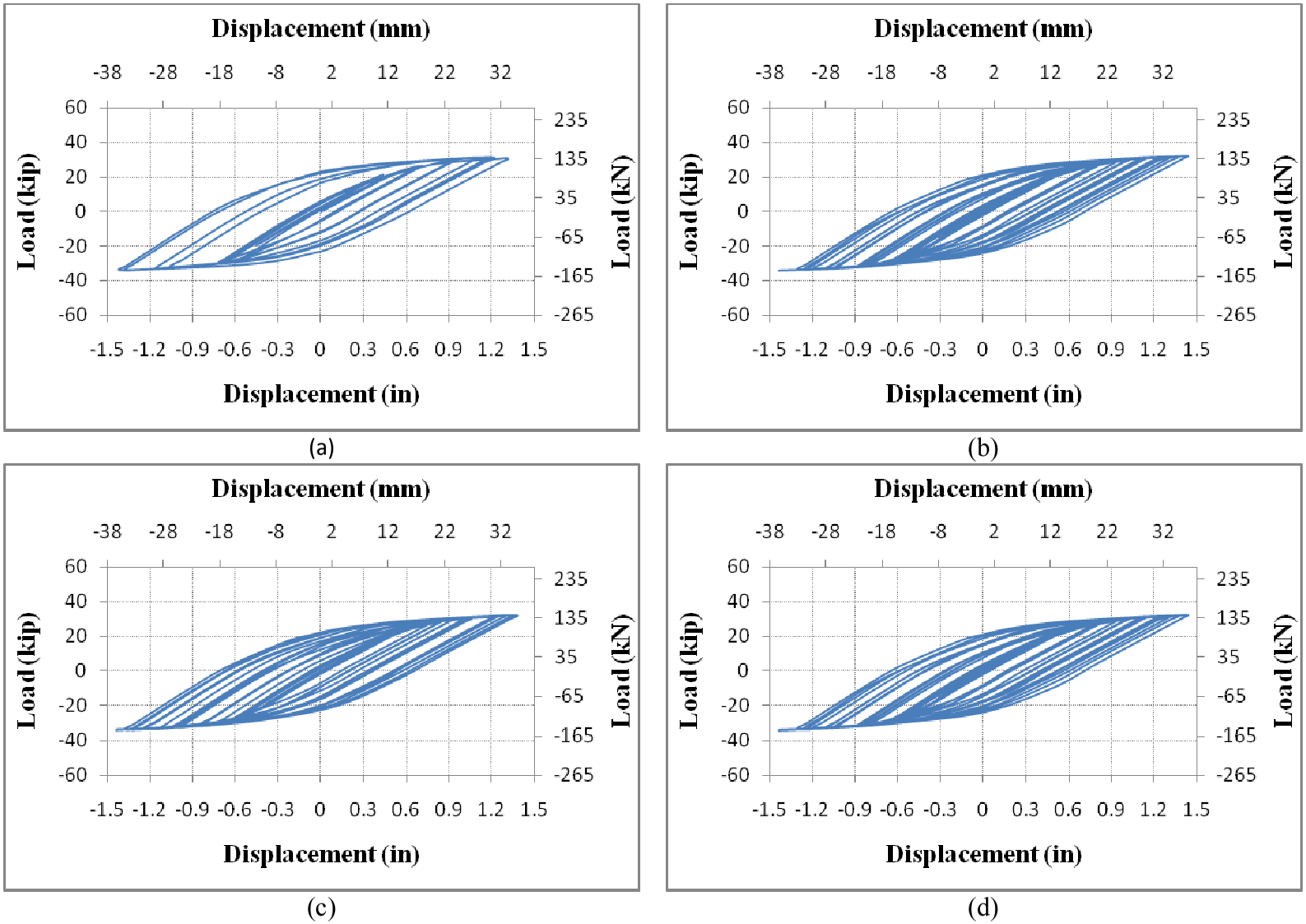

Figure D-14 Load-Displacement Cyclic Plots for: (a) SM-2B-1/4-1-FP-C-SS-DLC-III-5; (b) SM-2B-1/4-1-FP-C-SS-DLC-IV-1; (c) SM-2B-1/4-1-FP-C-SS-DLC-IV-2; and (d) SM-2B-1/4-1-FP-C-SS-DLC-IV-3

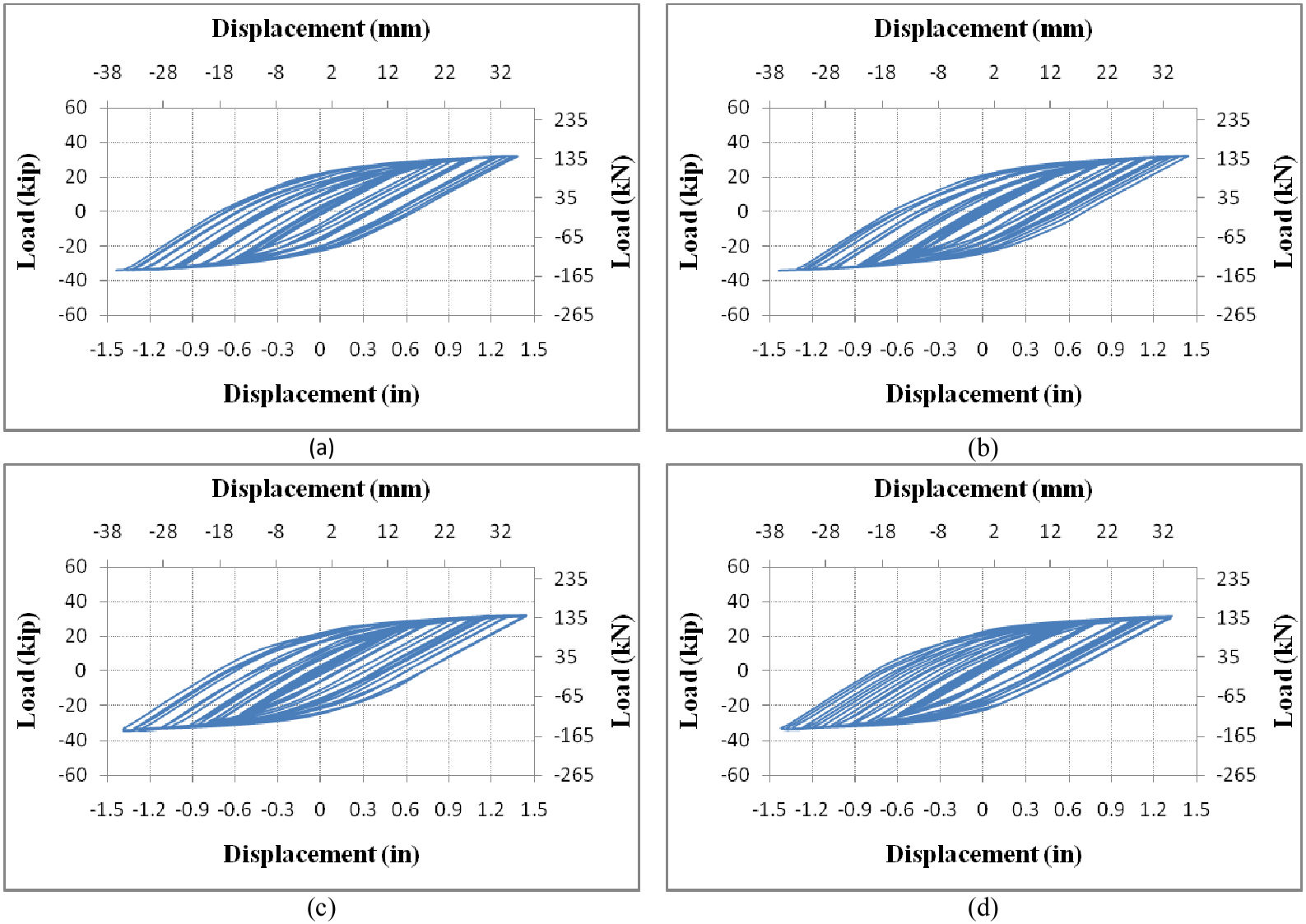

Figure D-15 Load-Displacement Cyclic Plots for: (a) SM-2B-1/4-1-FP-C-SS-DLC-IV-4; (b) SM-2B-1/4-1-FP-C-SS-DLC-IV-5; (c) SM-2B-1/4-1-FP-C-SS-DLC-V-1; and (d) SM-2B-1/4-1-FP-C-SS-DLC-V-2

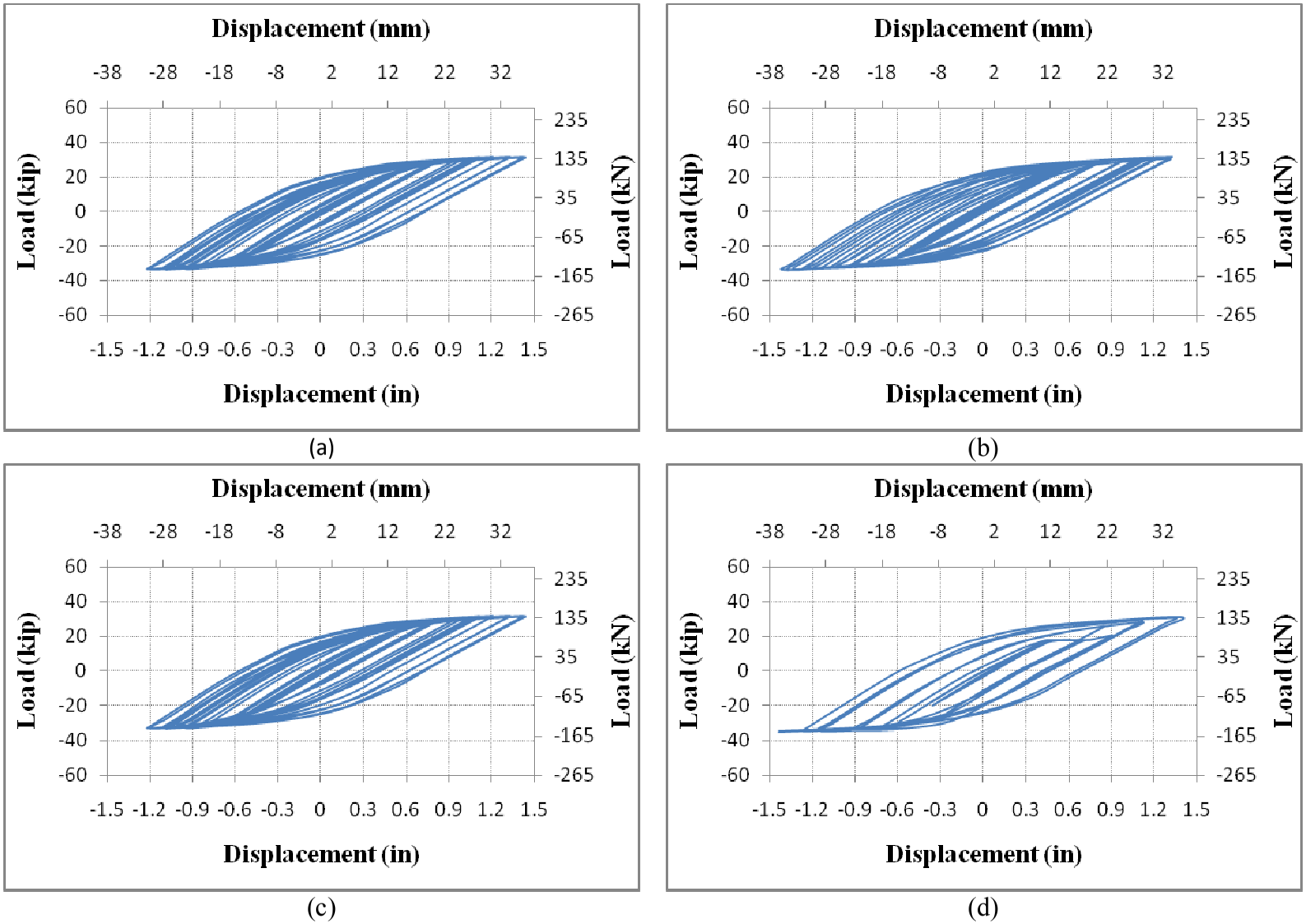

Figure D-16 Load-Displacement Cyclic Plots for: (a) SM-2B-1/4-1-FP-C-SS-DLC-V-3; (b) SM-2B-1/4-1-FP-C-SS-DLC-V-4; (c) SM-2B-1/4-1-FP-C-SS-DLC-V-5; and (d) SM-2B-1/4-1-HP-C-SS-DLC-I-1

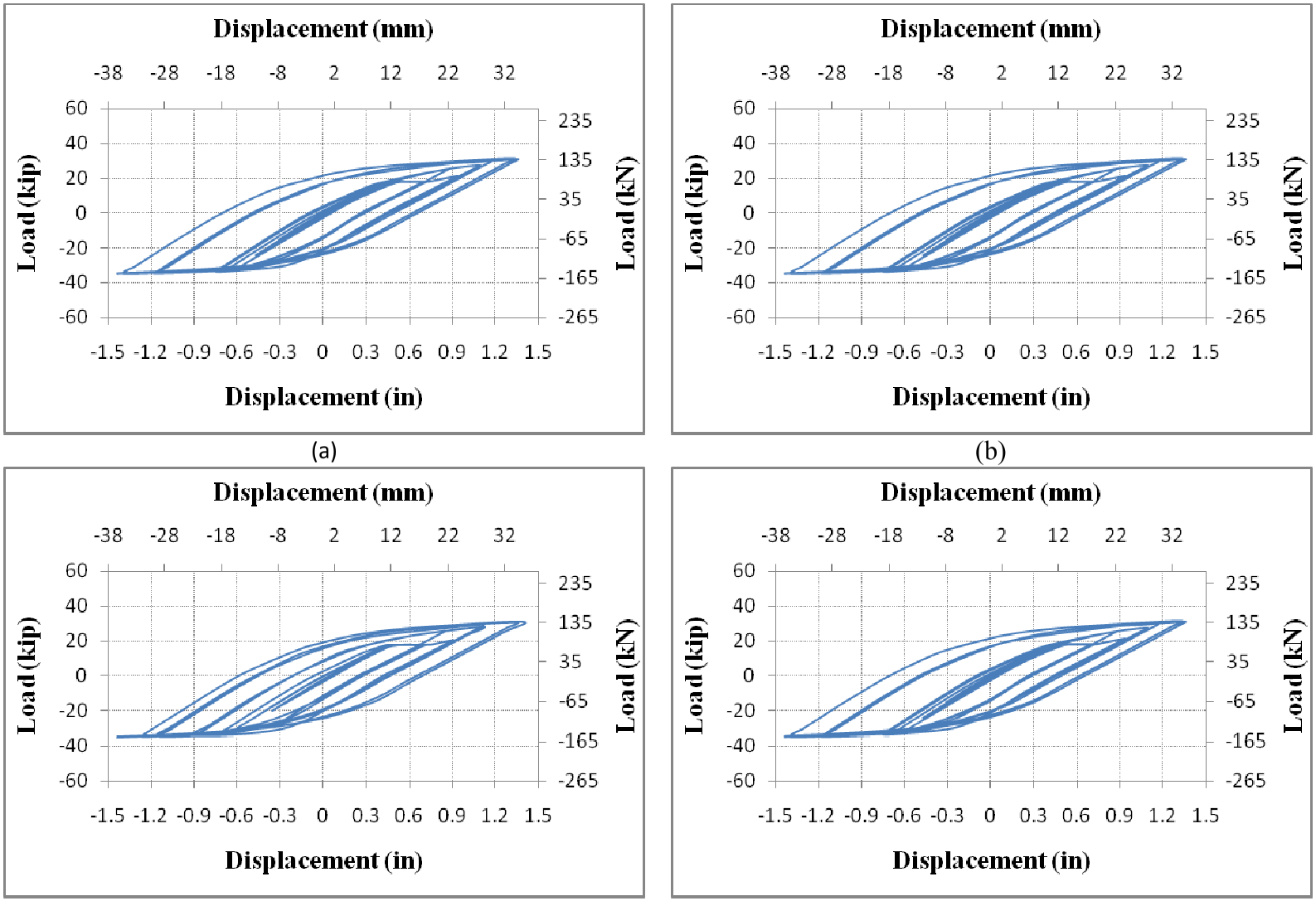

Figure D-17 Load-Displacement Cyclic Plots for: (a) SM-2B-1/4-1-HP-C-SS-DLC-I-2; (b) SM-2B-1/4-1-HP-C-SS-DLC-I-3; (c) SM-2B-1/4-1-HP-C-SS-DLC-I-4; and (d) SM-2B-1/4-1-HP-C-SS-DLC-I-5

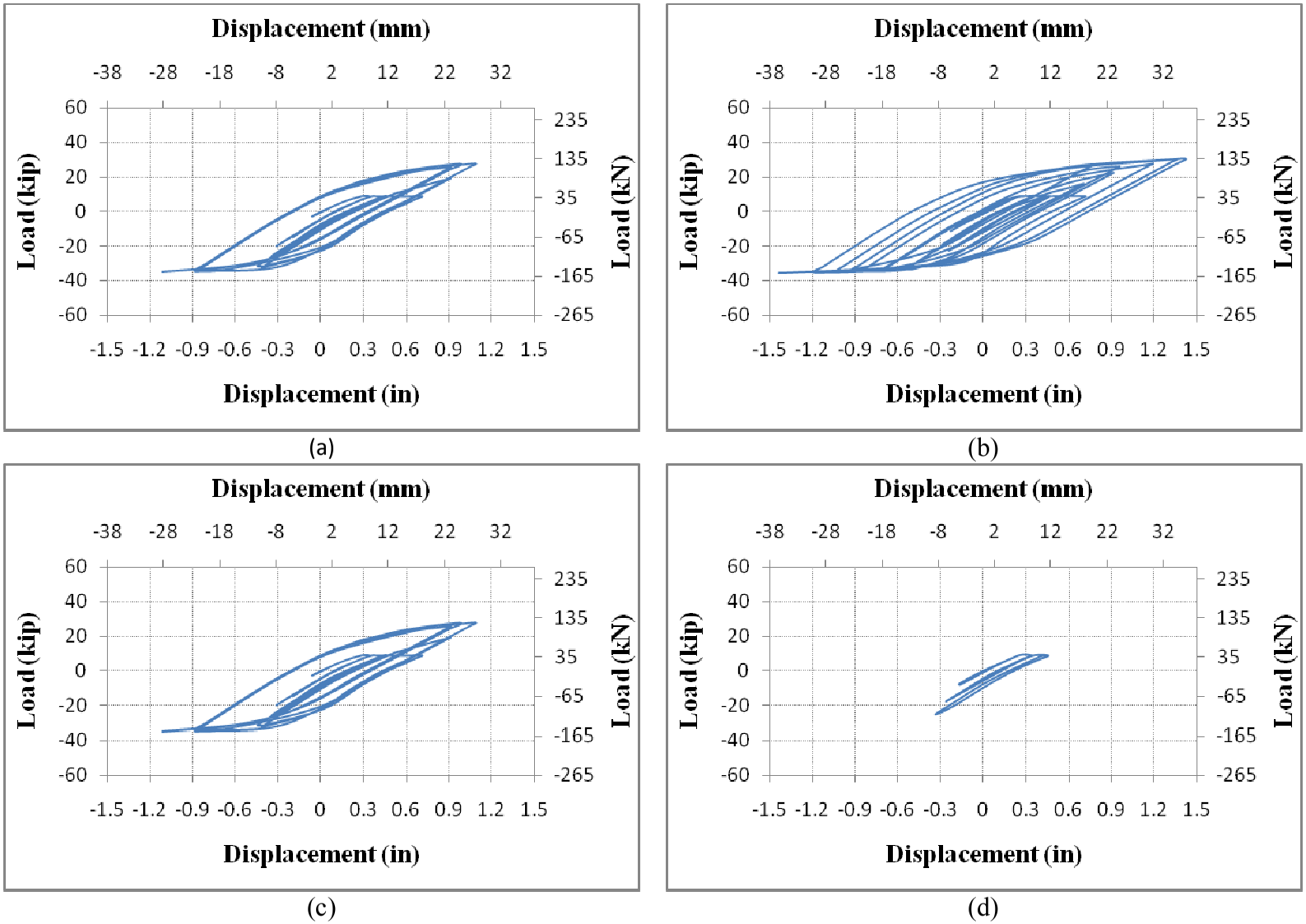

Figure D-18 Load-Displacement Cyclic Plots for: (a) SM-2B-1/4-1-QP-C-SS-DLC-I-1; (b) SM-2B-1/4-1-QP-C-SS-DLC-I-2; (c) SM-2B-1/4-1-QP-C-SS-DLC-I-3; and (d) SM-2B-1/4-1-QP-C-SS-DLC-I-4

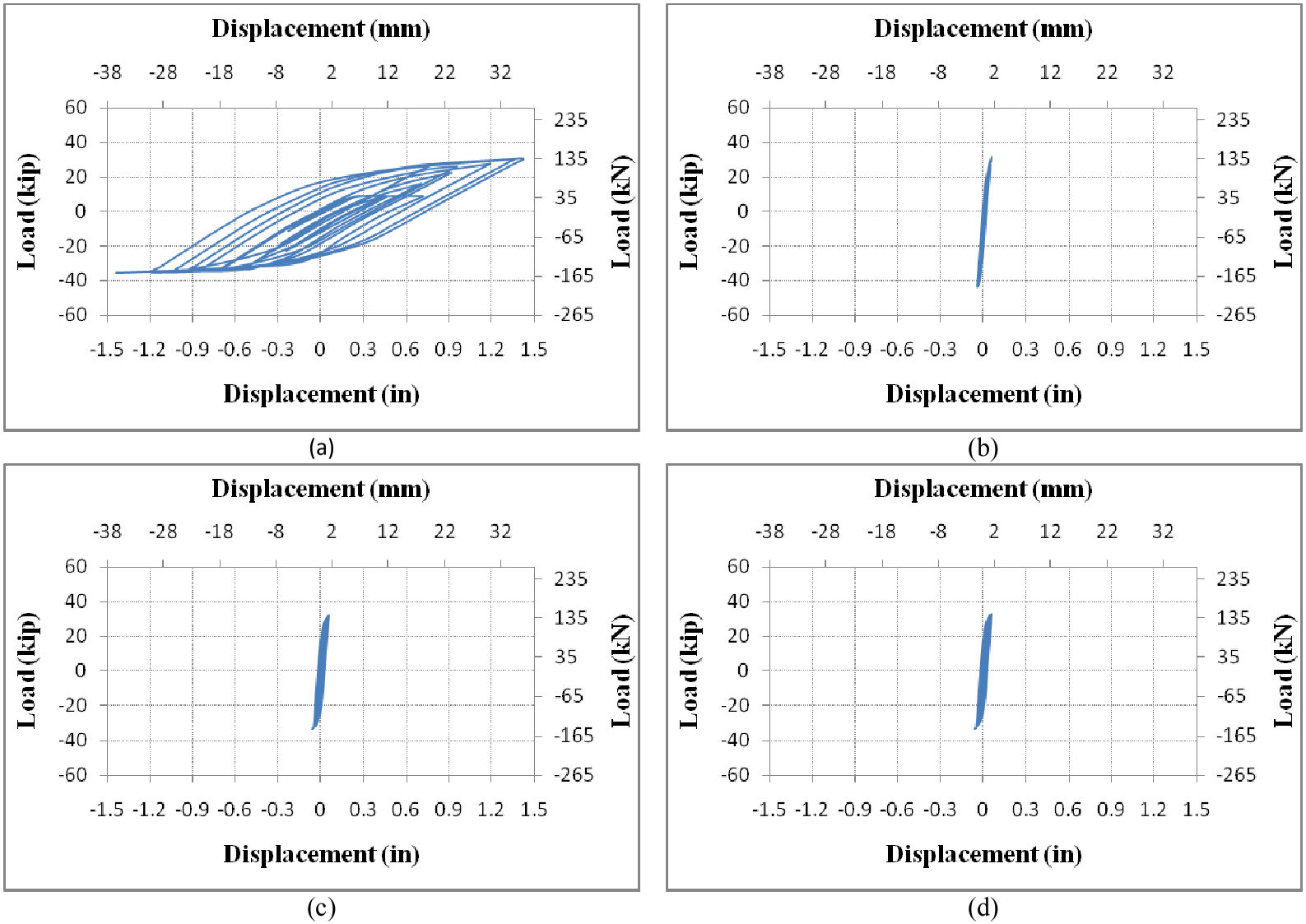

Figure D-19 Load-Displacement Cyclic Plots for: (a) SM-2B-1/4-1-QP-C-SS-DLC-I-5; (b) SM-2B-1/4-1-FP-TH-SS-DLC-I-1; (c) SM-2B-1/4-1-FP-HX-SS-DLC-I-1; and (d) SM-2B-1/4-1-FP-C-SS-DLC-I-1

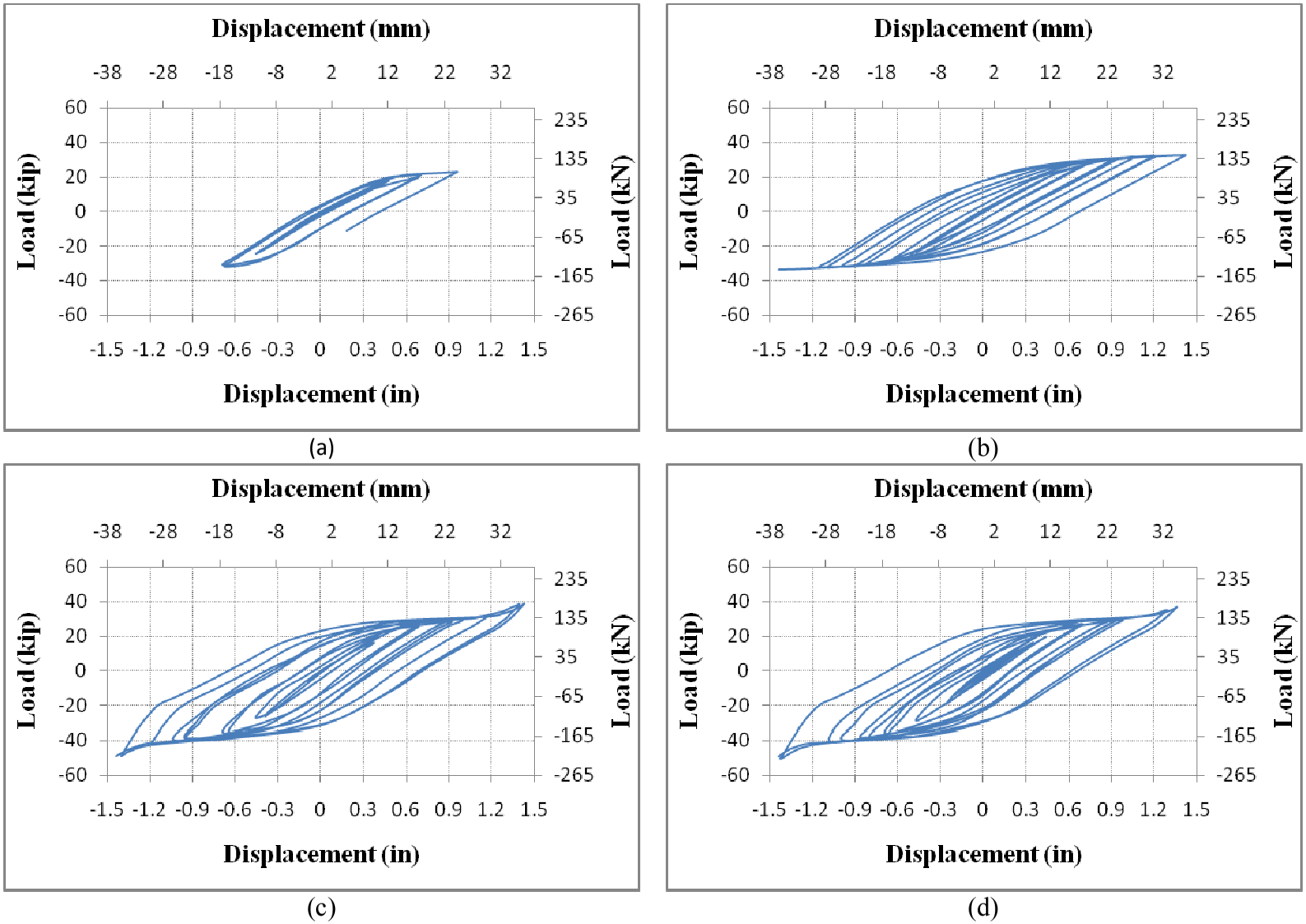

Figure D-20 Load-Displacement Cyclic Plots for: (a) SM-2B-1/4-1-FP-C-NS-DLC-I-1; (b) SM-2B-1/4-1-FP-C-SS-DLC-I-1; (c) SM-2B-1-1-FP-C-SS-DLC-I-1; and (d) SM-2B-1-1-FP-C-SS-DLC-I-2

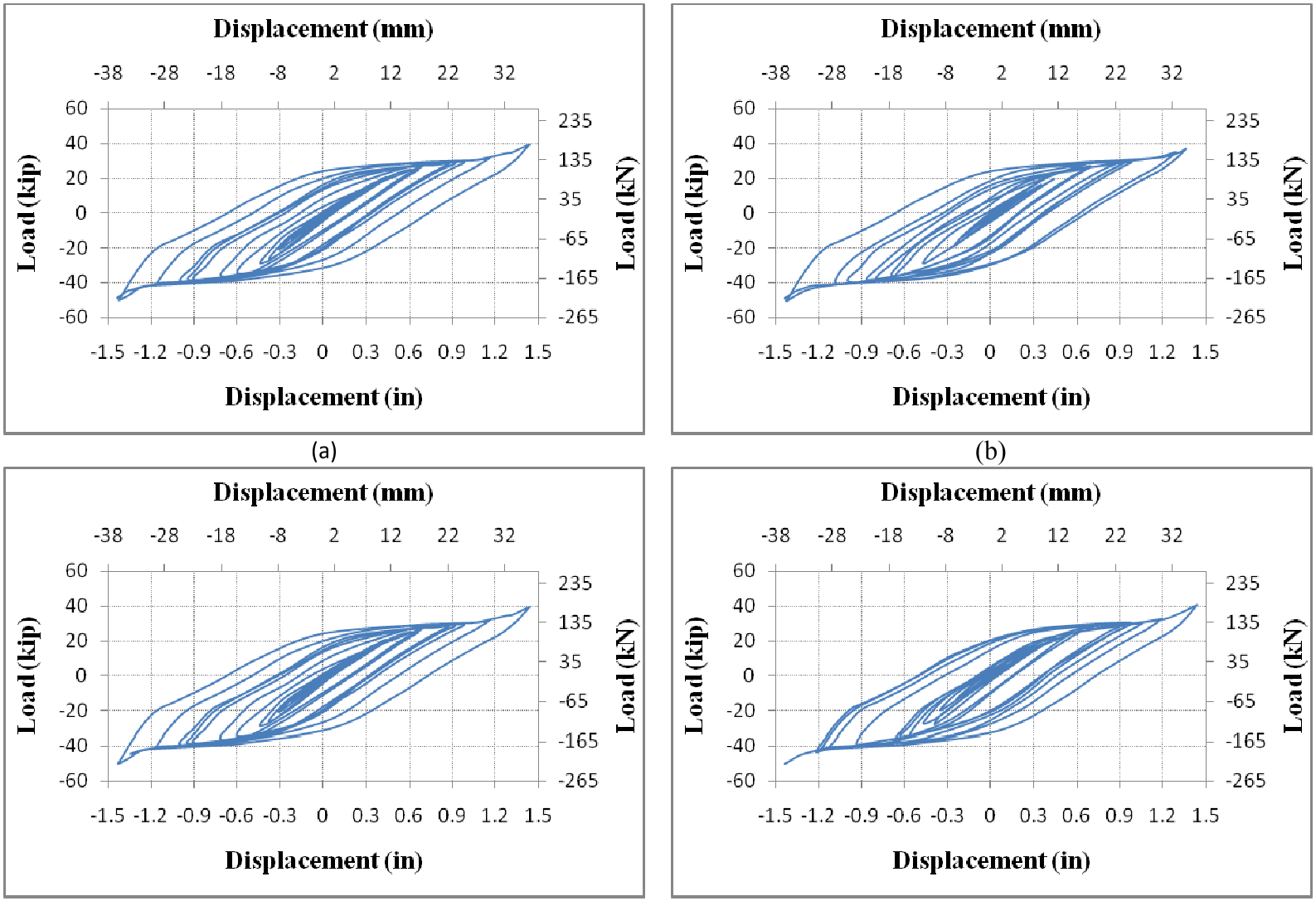

Figure D-21 Load-Displacement Cyclic Plots for: (a) SM-2B-1-1-FP-C-SS-DLC-I-3; (b) SM-2B-1-1-FP-C-SS-DLC-I-4; (c) SM-2B-1-1-FP-C-SS-DLC-I-5; and (d) SM-2B-1-1-FP-C-SS-DLC-II-1

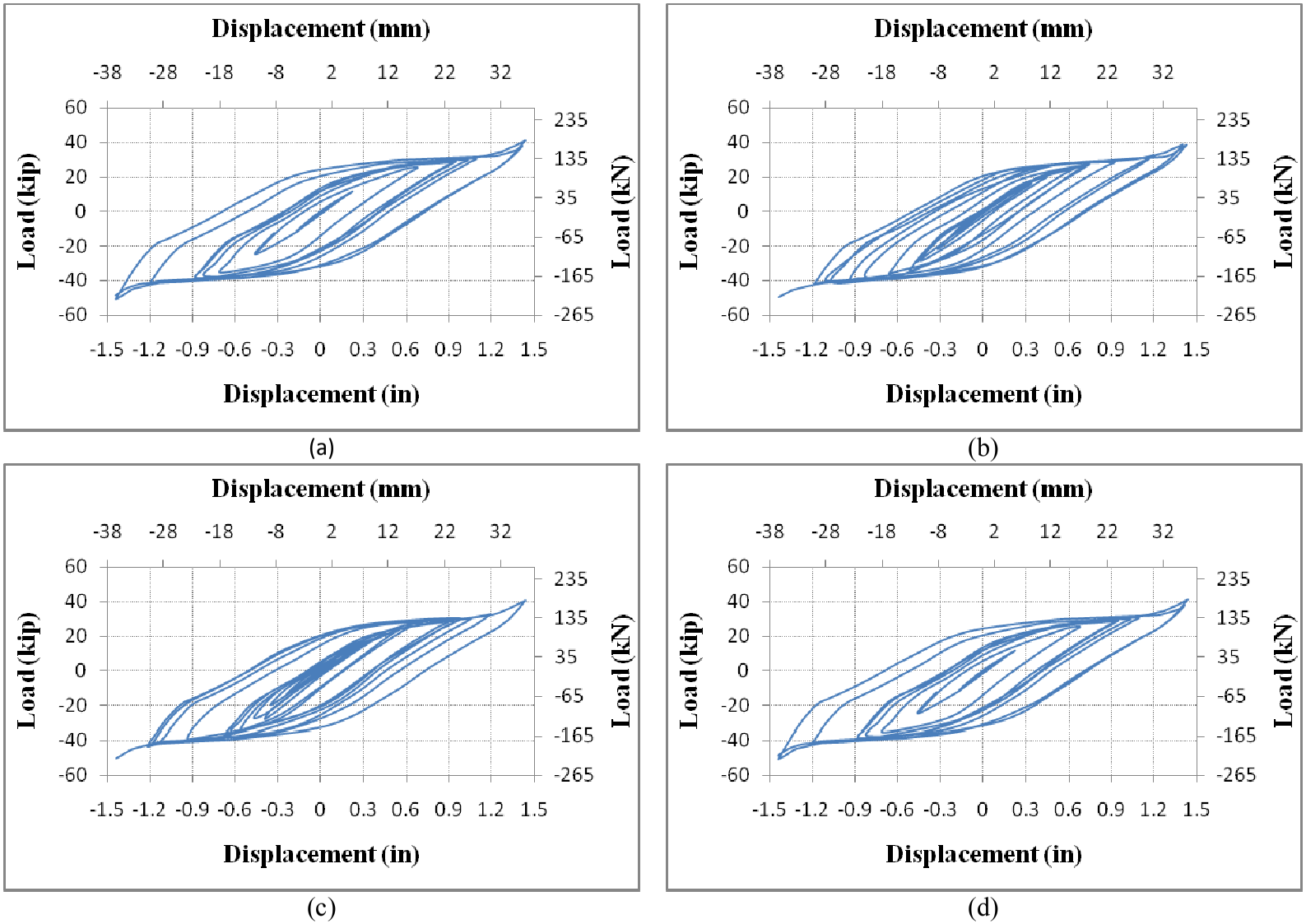

Figure D-22 Load-Displacement Cyclic Plots for: (a) SM-2B-1-1-FP-C-SS-DLC-II-2; (b) SM-2B-1-1-FP-C-SS-DLC-II-3; (c) SM-2B-1-1-FP-C-SS-DLC-II-4; and (d) SM-2B-1-1-FP-C-SS-DLC-II-5

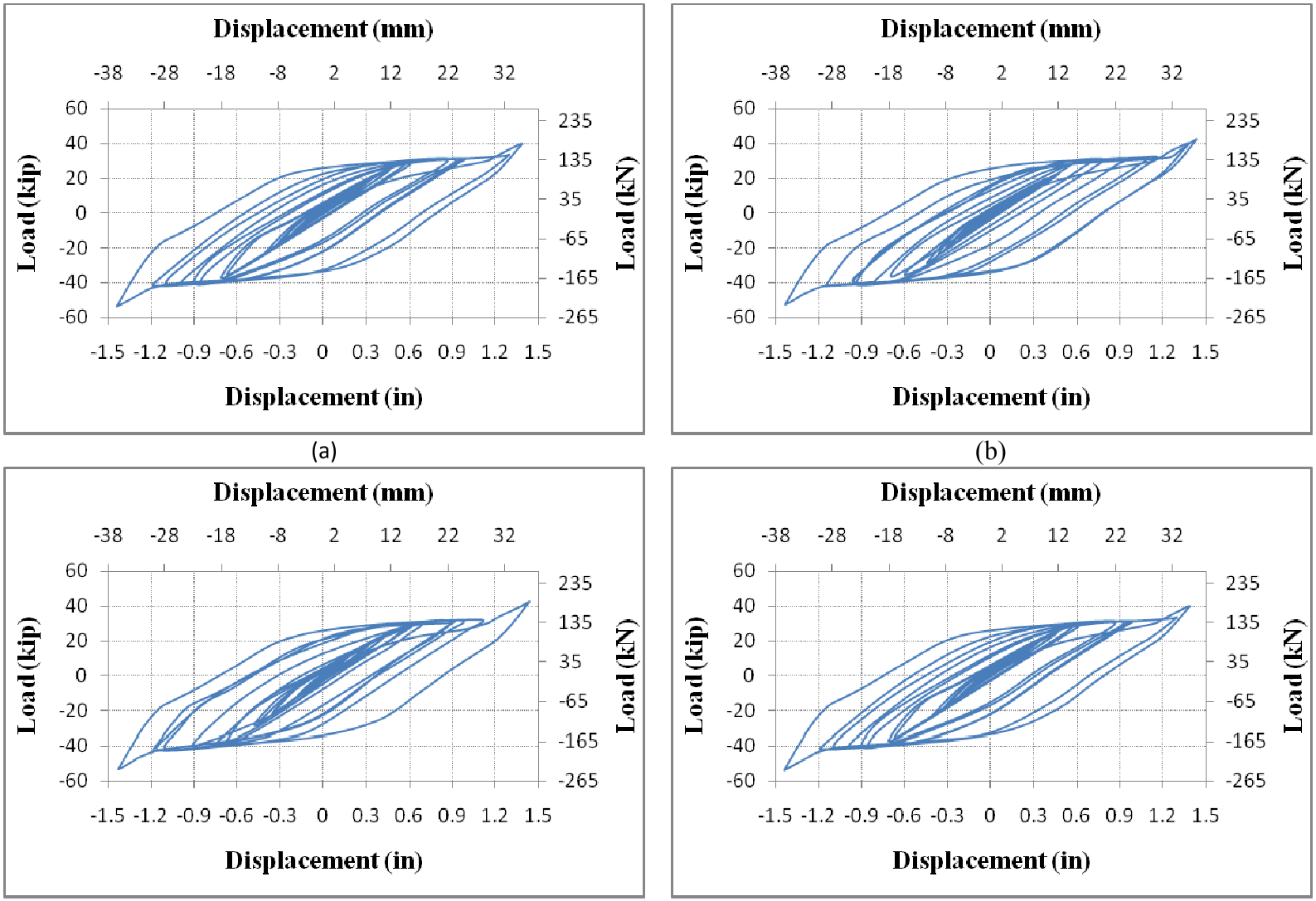

Figure D-23 Load-Displacement Cyclic Plots for: (a) SM-2B-1-1-FP-C-SS-DLC-III-1; (b) SM-2B-1-1-FP-C-SS-DLC-III-2; (c) SM-2B-1-1-FP-C-SS-DLC-III-3; and (d) SM-2B-1-1-FP-C-SS-DLC-III-4

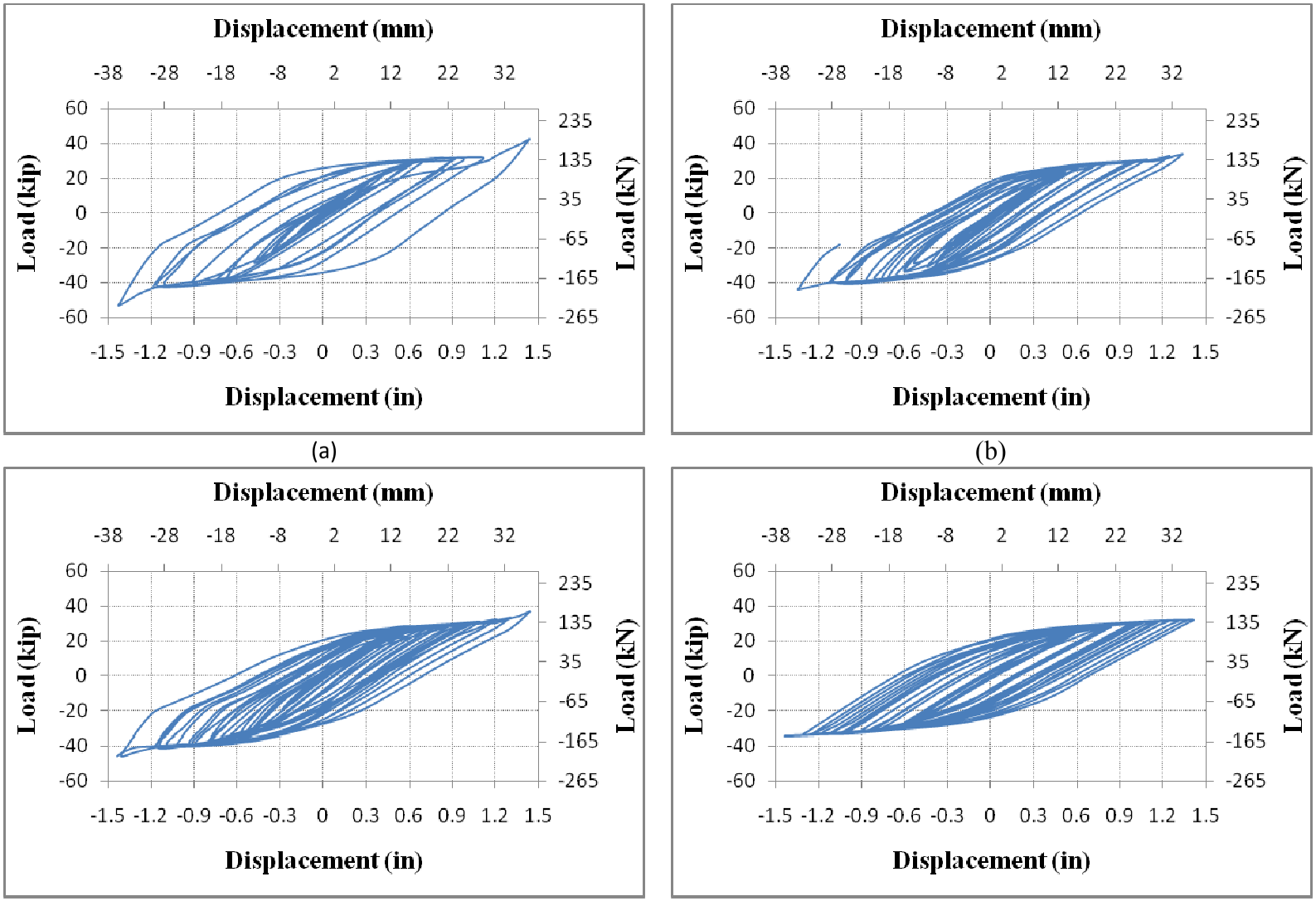

Figure D-24 Load-Displacement Cyclic Plots for: (a) SM-2B-1-1-FP-C-SS-DLC-III-5; (b) SM-2B-1-1-FP-C-SS-DLC-IV-1; (c) SM-2B-1-1-FP-C-SS-DLC-IV-2; and (d) SM-2B-1-1-FP-C-SS-DLC-IV-3

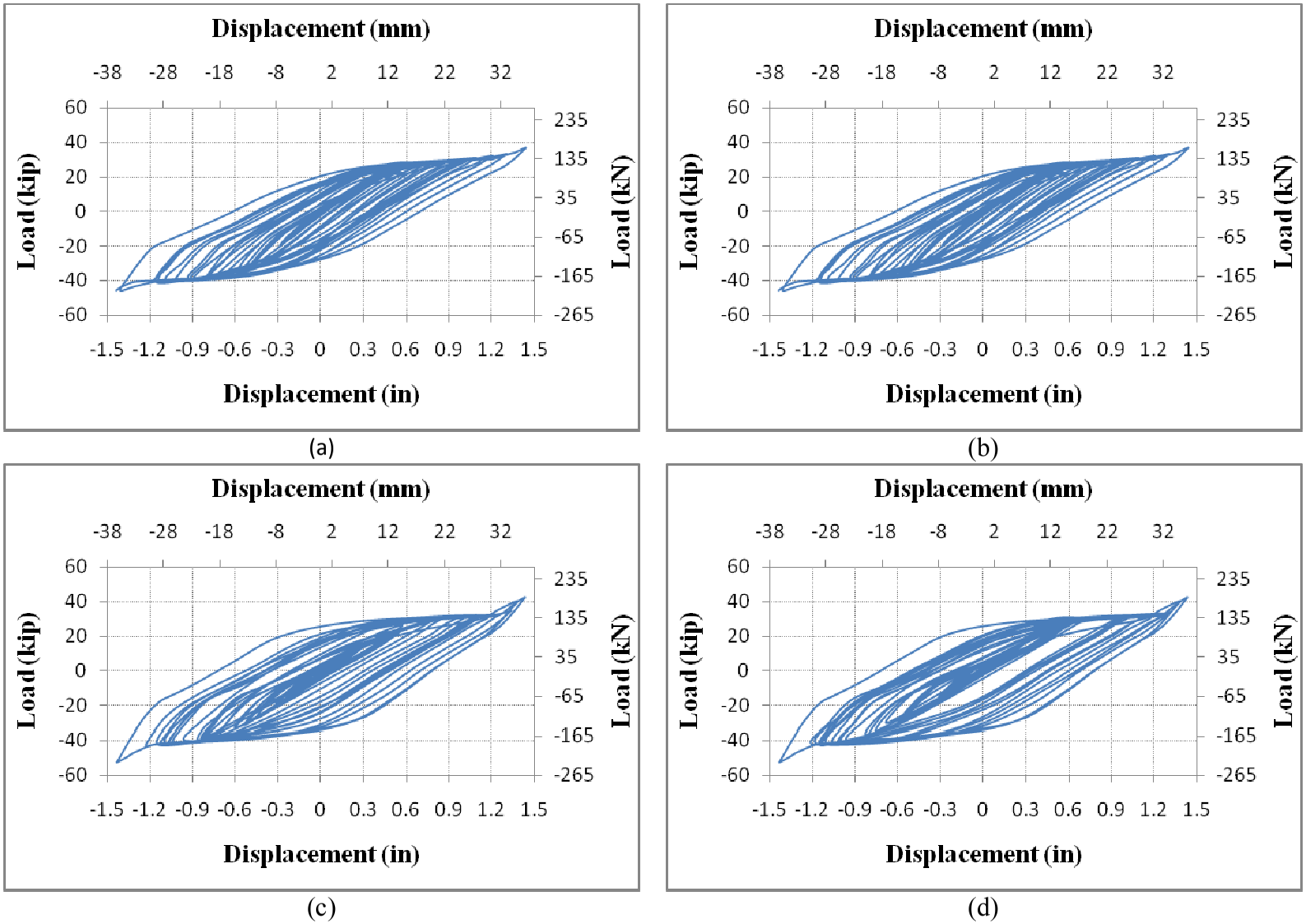

Figure D-25 Load-Displacement Cyclic Plots for: (a) SM-2B-1-1-FP-C-SS-DLC-IV-4; (b) SM-2B-1-1-FP-C-SS-DLC-IV-5 (c) SM-2B-1-1-FP-C-SS-DLC-V-1; and (d) SM-2B-1-1-FP-C-SS-DLC-V-2

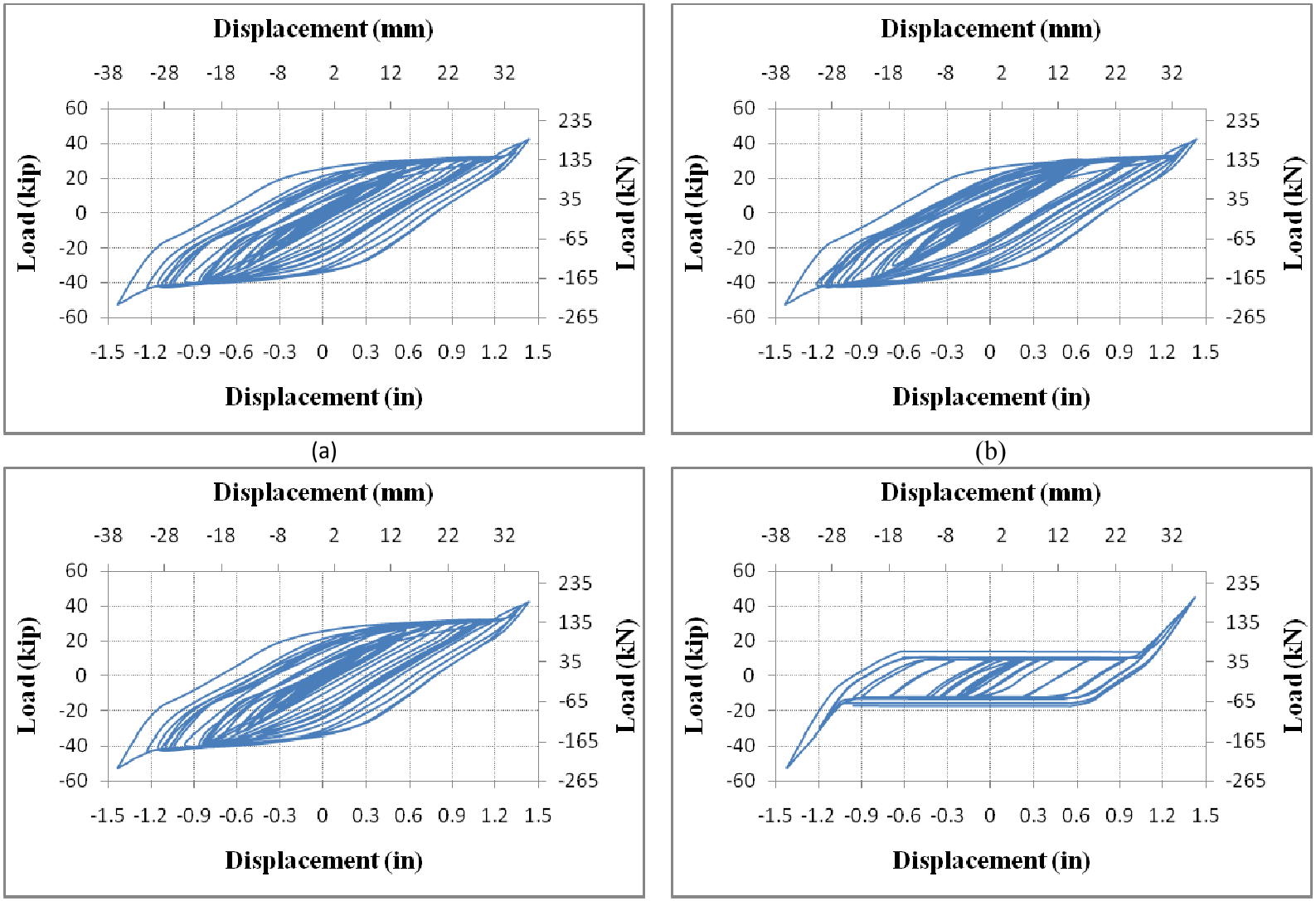

Figure D-26 Load-Displacement Cyclic Plots for: (a) SM-2B-1-1-FP-C-SS-DLC-V-3; (b) SM-2B-1-1-FP-C-SS-DLC-V-4; (c) SM-2B-1-1-FP-C-SS-DLC-V-5; and (d) SM-2B-1-1-HP-C-SS-DLC-I-1

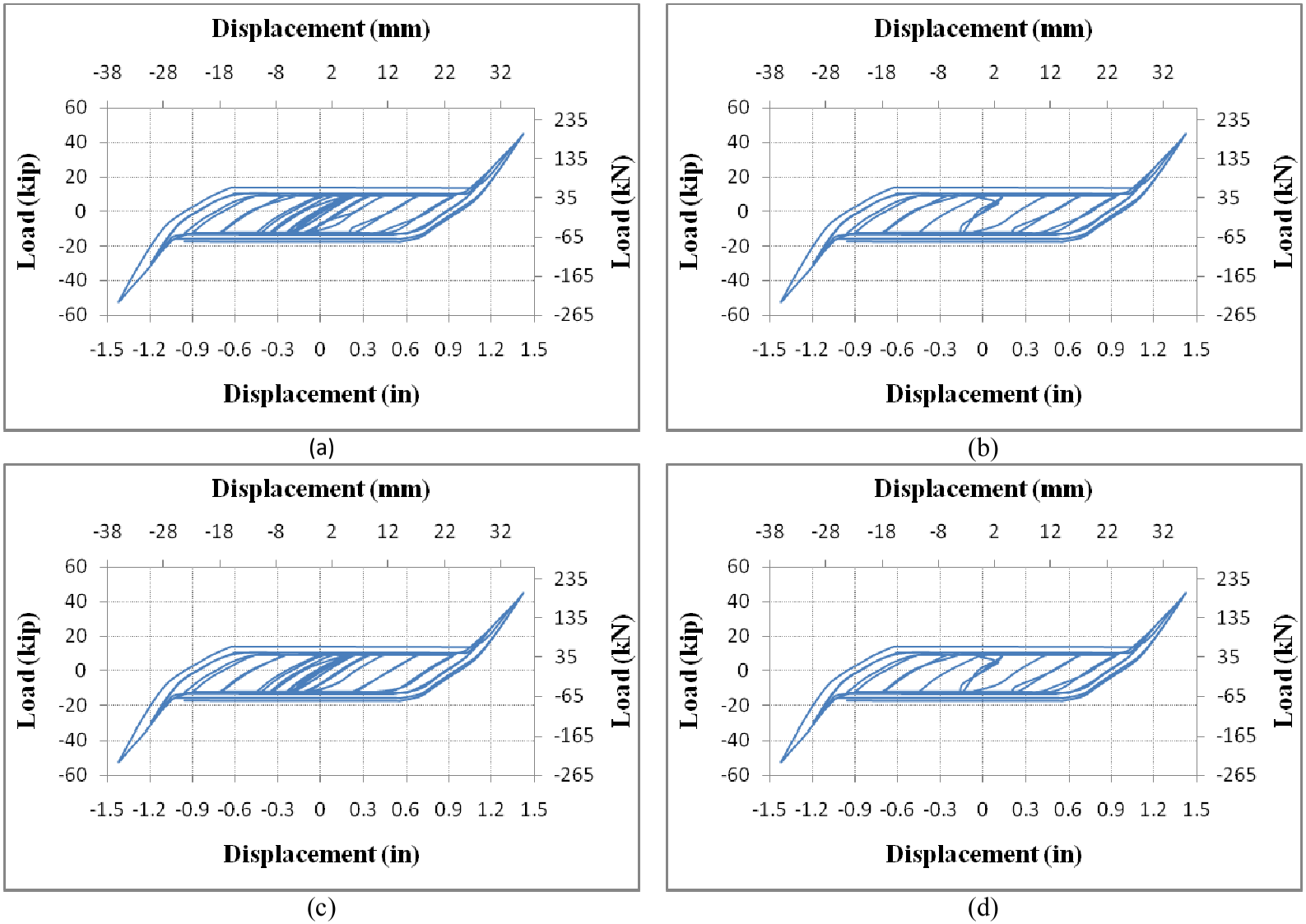

Figure D-27 Load-Displacement Cyclic Plots for: (a) SM-2B-1-1-HP-C-SS-DLC-I-2; (b) SM-2B-1-1-HP-C-SS-DLC-I-3; (c) SM-2B-1-1-HP-C-SS-DLC-I-4; and (d) SM-2B-1-1-HP-C-SS-DLC-I-5

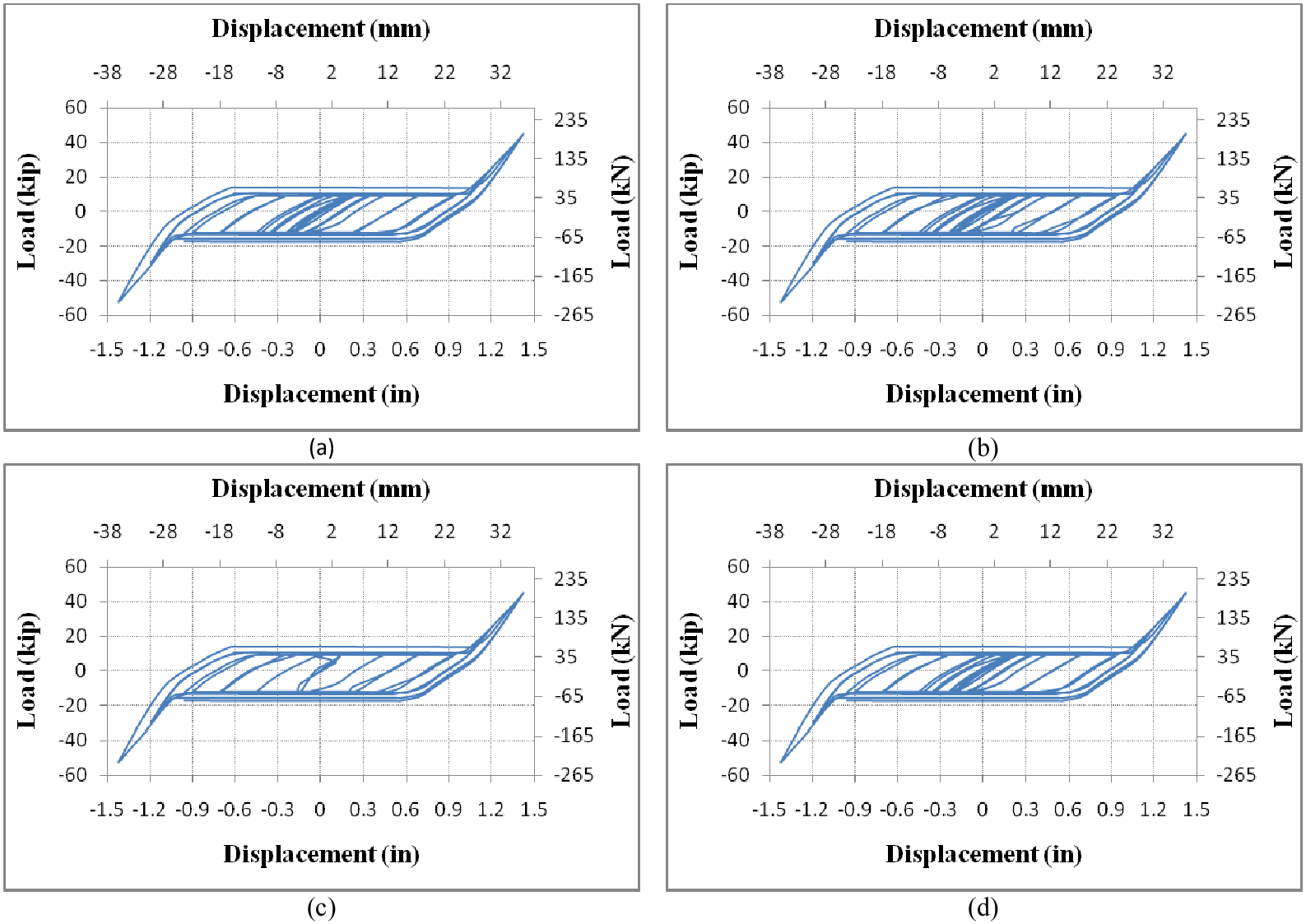

Figure D-28 Load-Displacement Cyclic Plots for: (a) SM-2B-1-1-QP-C-SS-DLC-I-1; (b) SM-2B-1-1-QP-C-SS-DLC-I-2; (c) SM-2B-1-1-QP-C-SS-DLC-I-3; and (d) SM-2B-1-1-QP-C-SS-DLC-I-4

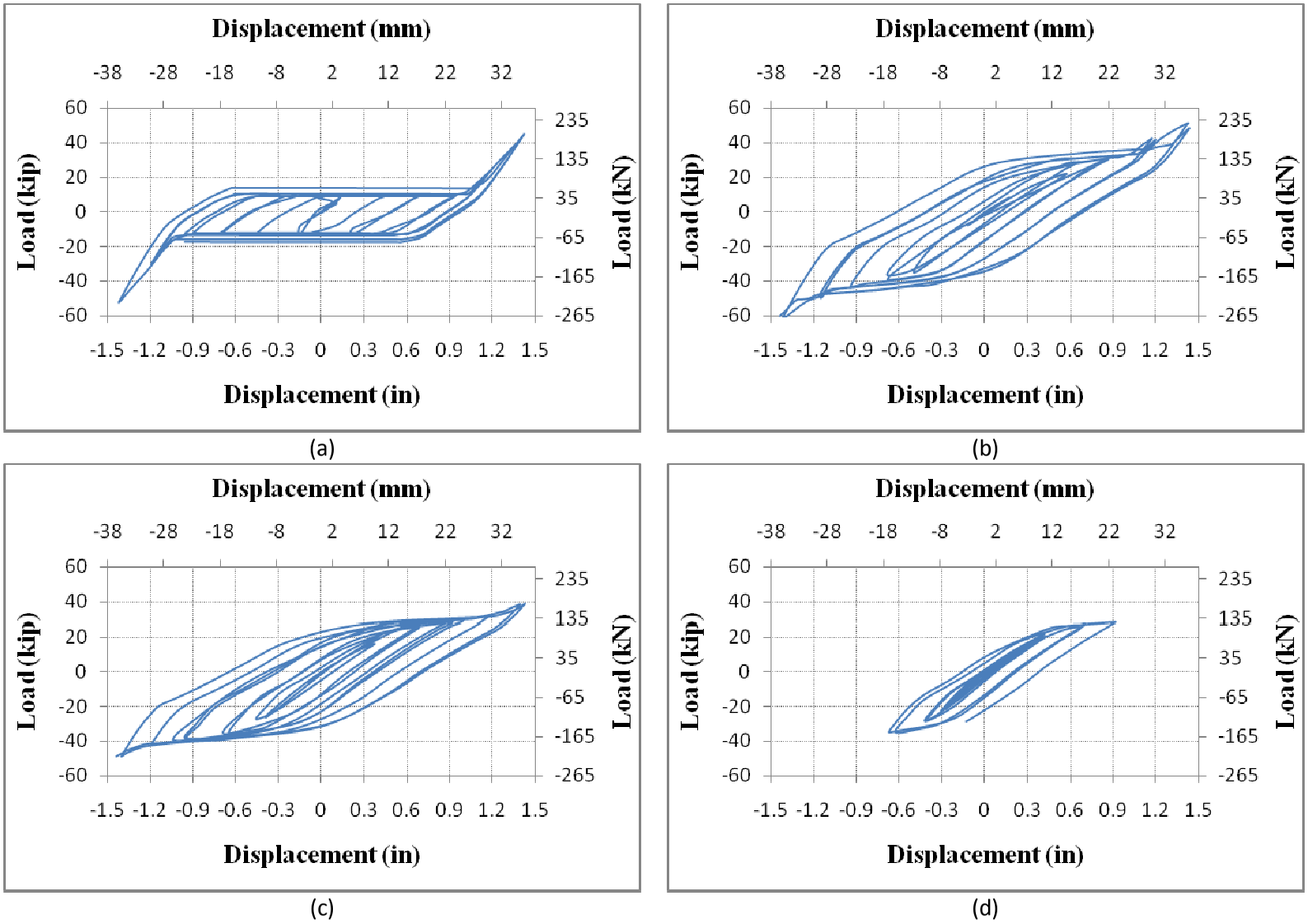

Figure D-29 Load-Displacement Cyclic Plots for: (a) SM-2B-1-1-QP-C-SS-DLC-I-5; (b) SM-2B-1-1-FP-HX-SS-DLC-I-1; (c) SM-2B-1-1-FP-C-SS-DLC-I-1; and (d) SM-2B-1-1-FP-C-NS-DLC-I-1

APPENDIX E

TEE-HANGER MODELS

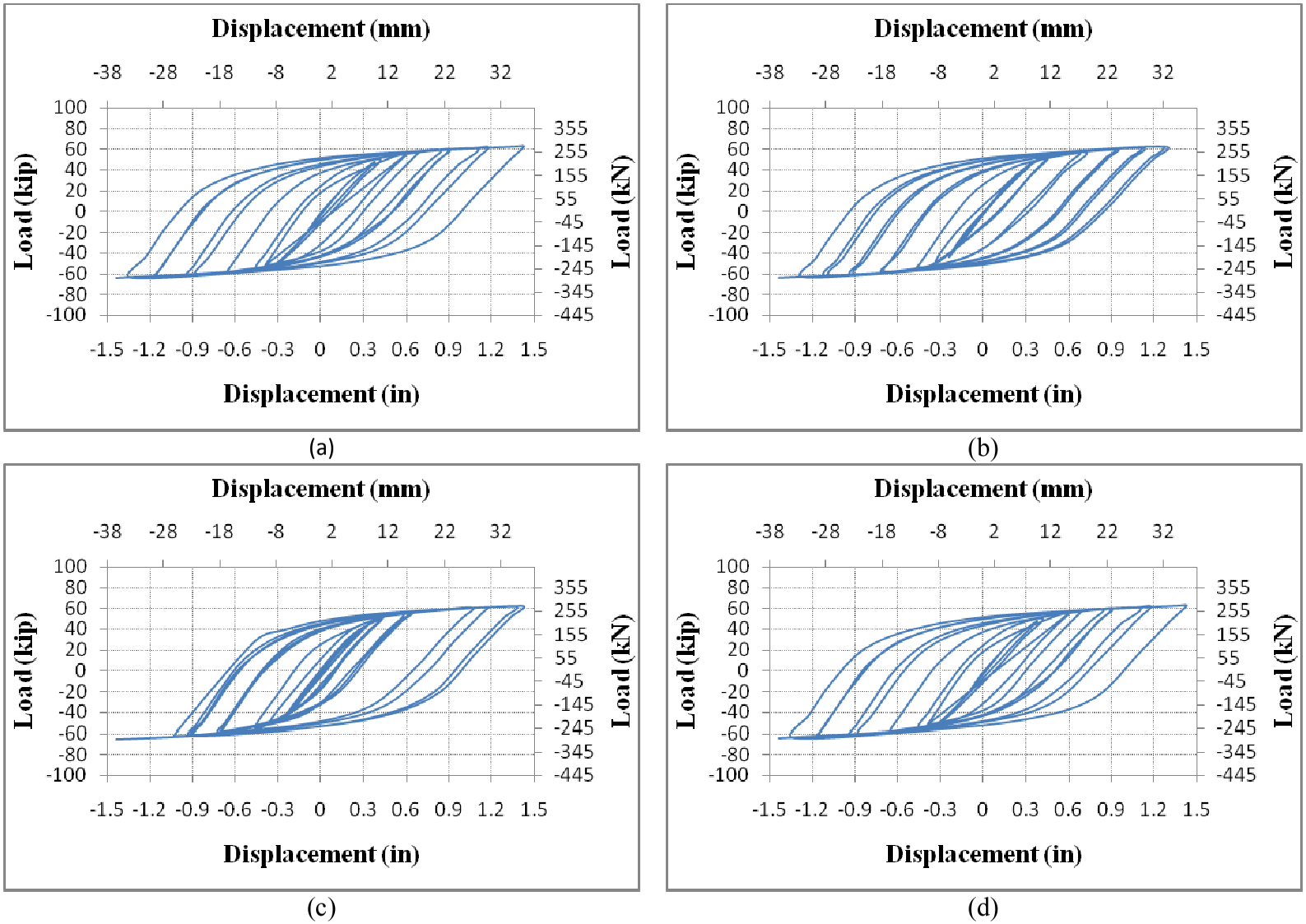

Figure E-1 Load-Displacement Cyclic Plots for: (a) T-1-1-2¾ -FP-SS-C-DLC-I-1; (b) T-1-1-2¾ -FP-SS-C-DLC-I-2; (c) T-1-1-2¾ -FP-SS-C-DLC-I-3; and (d) T-1-1-2¾ -FP-SS-C-DLC-I-4

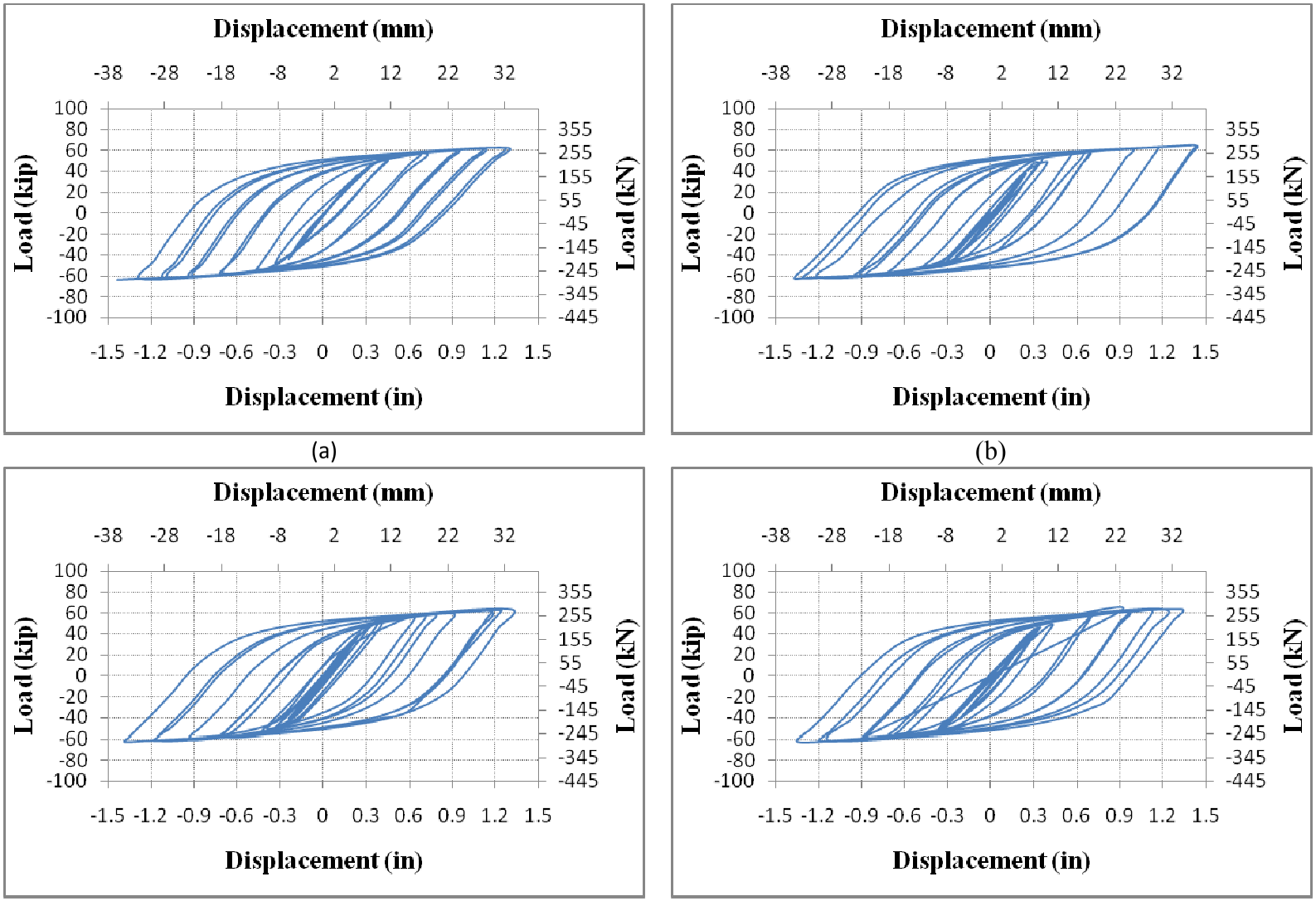

Figure E-2 Load-Displacement Cyclic Plots for: (a) T-1-1-2¾ -FP-SS-C-DLC-I-5; (b) T-1-1-2¾ -FP-SS-C-DLC-II-1; (c) T-1-1-2¾ -FP-SS-C-DLC-II-2; and (d) T-1-1-2¾ -FP-SS-C-DLC-II-3

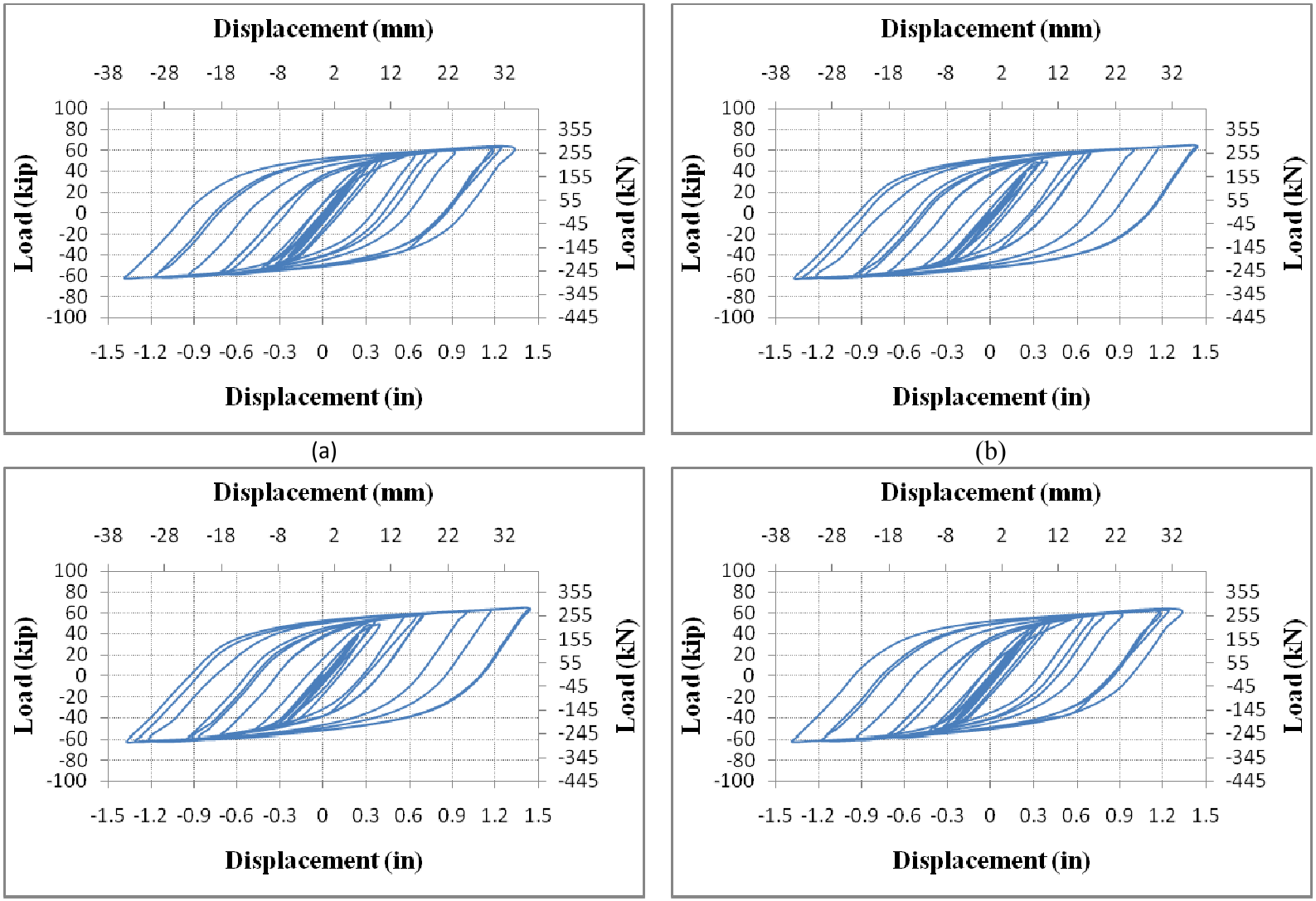

Figure E-3 Load-Displacement Cyclic Plots for: (a) T-1-1-2¾ -FP-SS-C-DLC-II-4; (b) T-1-1-2¾ -FP-SS-C-DLC-II-5; (c) T-1-1-2¾ -FP-SS-C-DLC-III-1; and (d) T-1-1-2¾ -FP-SS-C-DLC-III-2

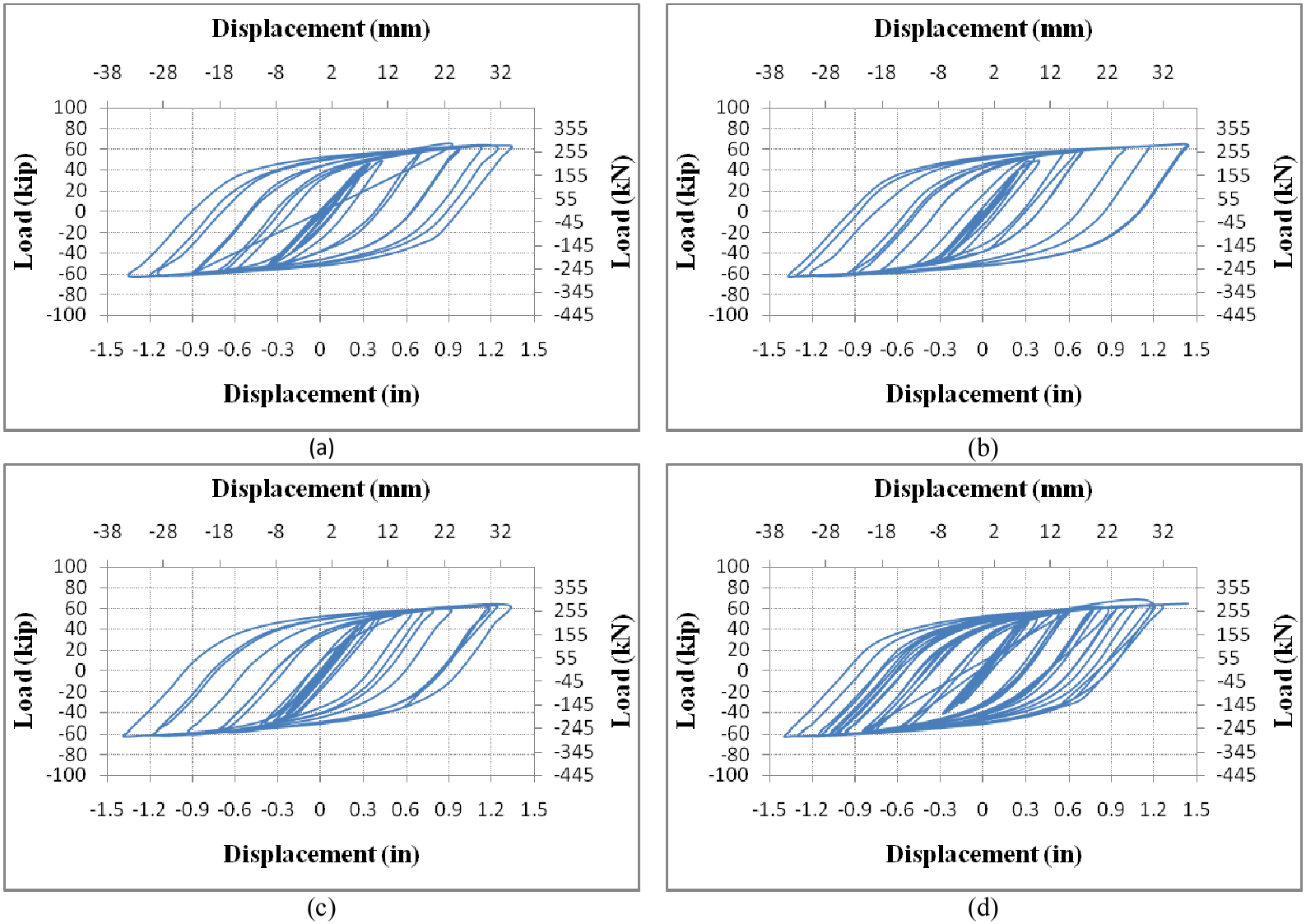

Figure E-4 Load-Displacement Cyclic Plots for: (a) T-1-1-2¾ -FP-SS-C-DLC-III-3; (b) T-1-1-2¾ -FP-SS-C-DLC-III-4; (c) T-1-1-2¾ -FP-SS-C-DLC-III-5; and (d) T-1-1-2¾ -FP-SS-C-DLC-IV-1

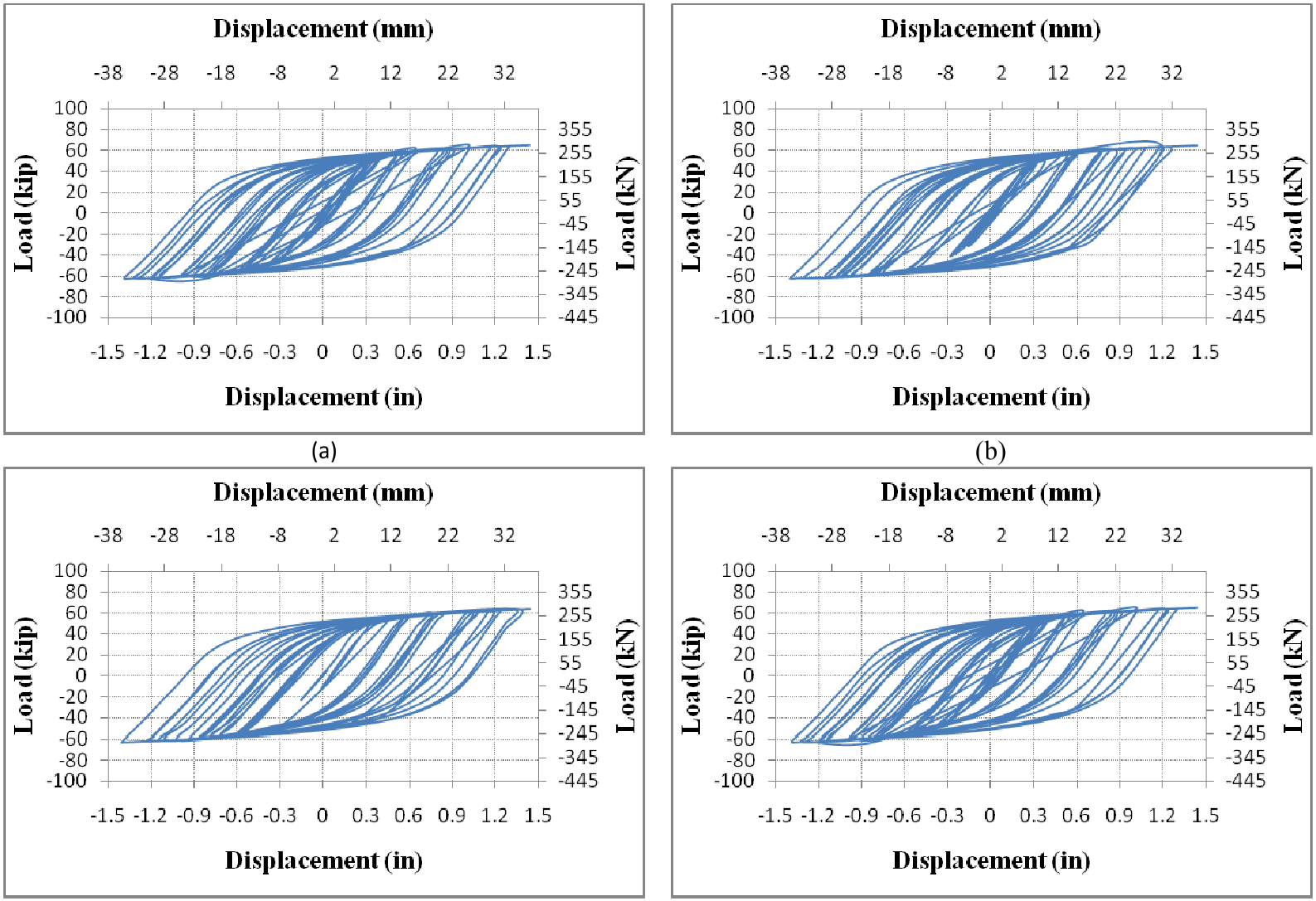

Figure E-5 Load-Displacement Cyclic Plots for: (a) T-1-1-2¾ -FP-SS-C-DLC-IV-2; (b) T-1-1-2¾ -FP-SS-C-DLC-IV-3; (c) T-1-1-2¾ -FP-SS-C-DLC-IV-4; and (d) T-1-1-2¾ -FP-SS-C-DLC-IV-5

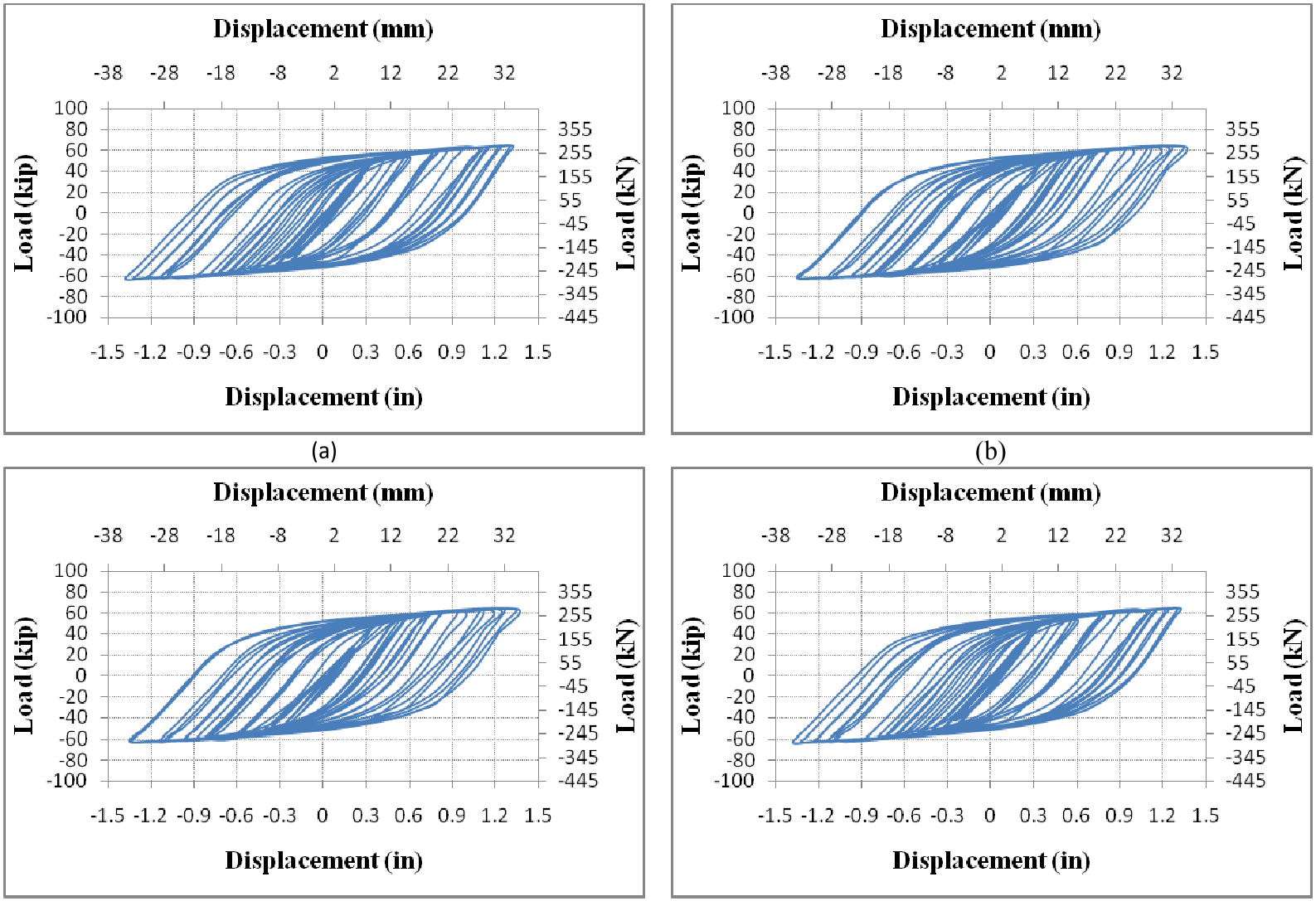

Figure E-6 Load-Displacement Cyclic Plots for: (a) T-1-1-2¾ -FP-SS-C-DLC-V-1; (b) T-1-1-2¾ -FP-SS-C-DLC-V-2; (c) T-1-1-2¾ -FP-SS-C-DLC-V-3; and (d) T-1-1-2¾ -FP-SS-C-DLC-V-4

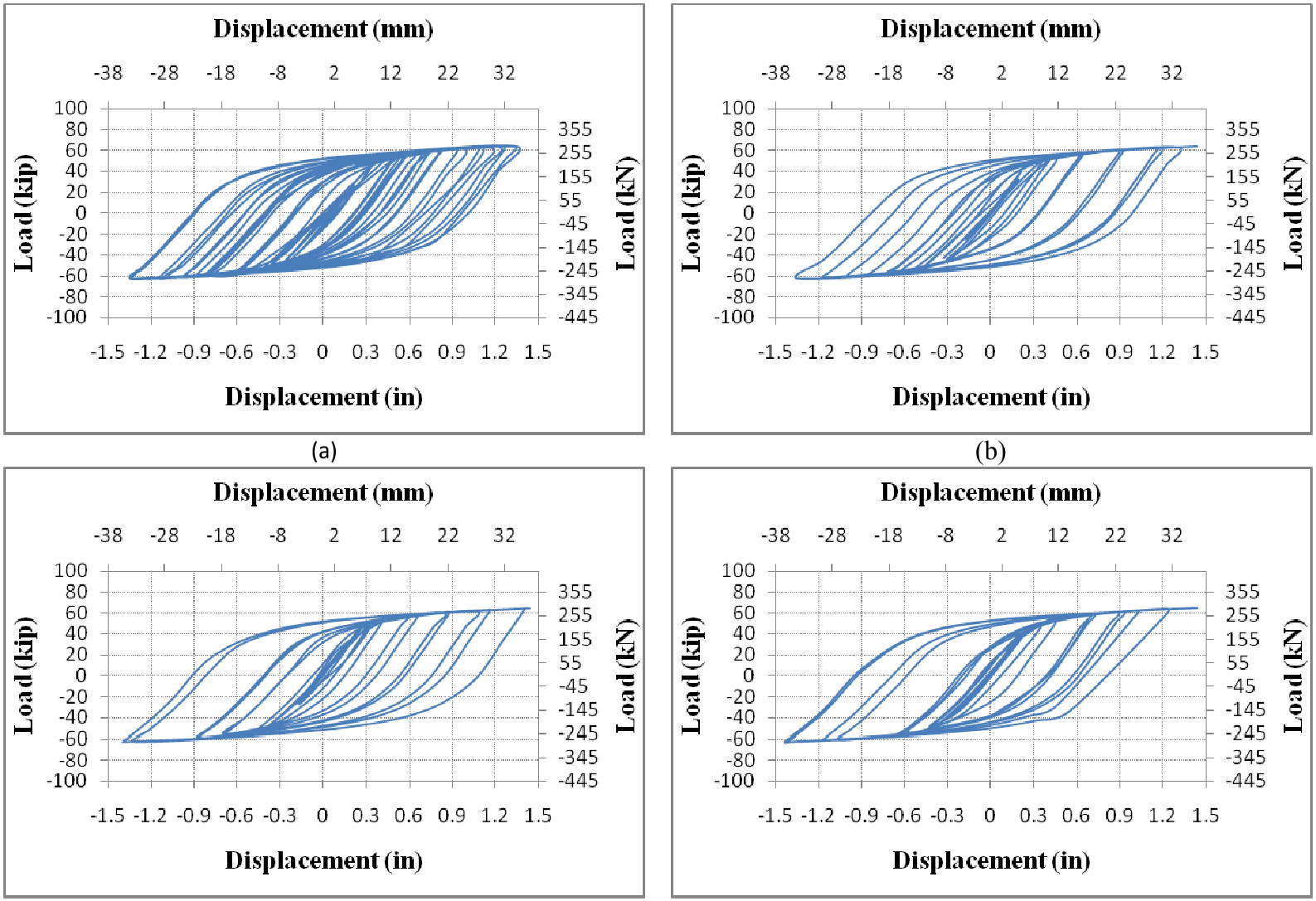

Figure E-7 Load-Displacement Cyclic Plots for: (a) T-1-1-2¾ -FP-SS-C-DLC-V-5; (b) T-1-1-2¾ -HP-SS-C-DLC-I-1; (c) T-1-1-2¾ -HP-SS-C-DLC-I-2; and (d) T-1-1-2¾ -HP-SS-C-DLC-I-3

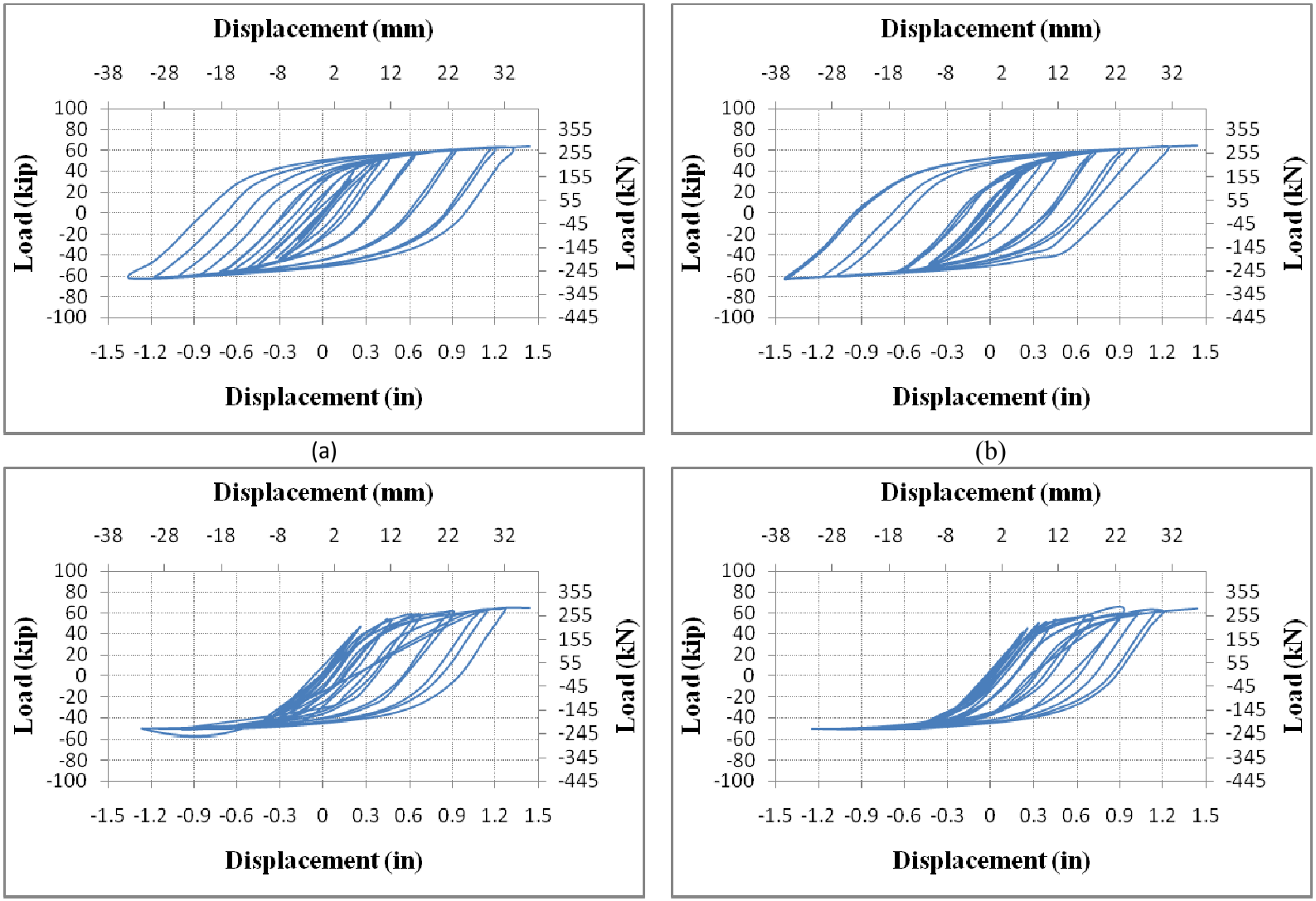

Figure E-8 Load-Displacement Cyclic Plots for: (a) T-1-1-2¾ -HP-SS-C-DLC-I-4; (b) T-1-1-2¾ -HP-SS-C-DLC-I-5; (c) T-1-1-2¾ -QP-SS-C-DLC-I-1; and (d) T-1-1-2¾ -QP-SS-C-DLC-I-2

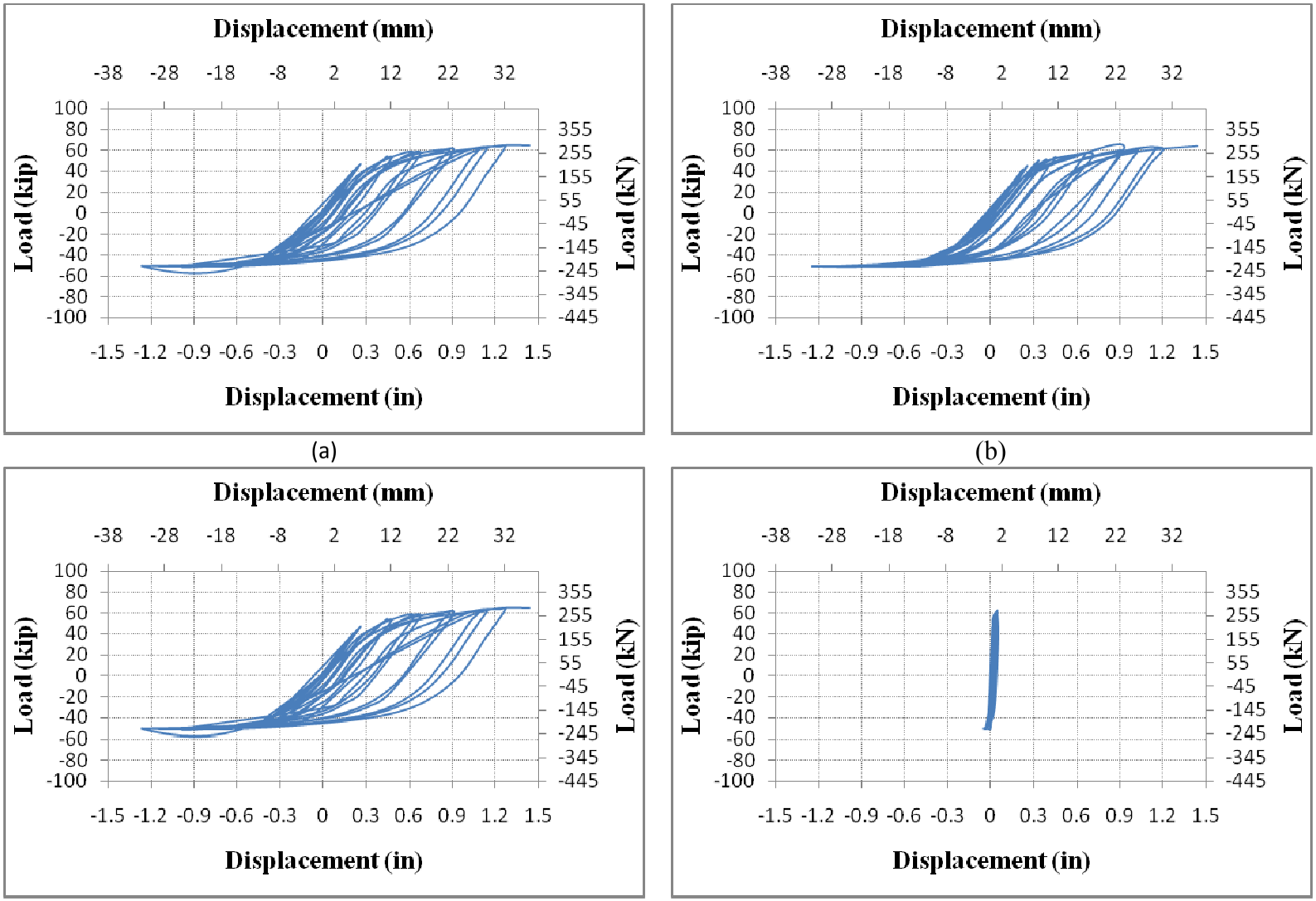

Figure E-9 Load-Displacement Cyclic Plots for: (a) T-1-1-2¾ -QP-SS-C-DLC-I-3; (b) T-1-1-2¾ -QP-SS-C-DLC-I-4; (c) T-1-1-2¾ -QP-SS-C-DLC-I-5; and (d) T-1-1-2¾ -FP-SS-HX-DLC-I-1

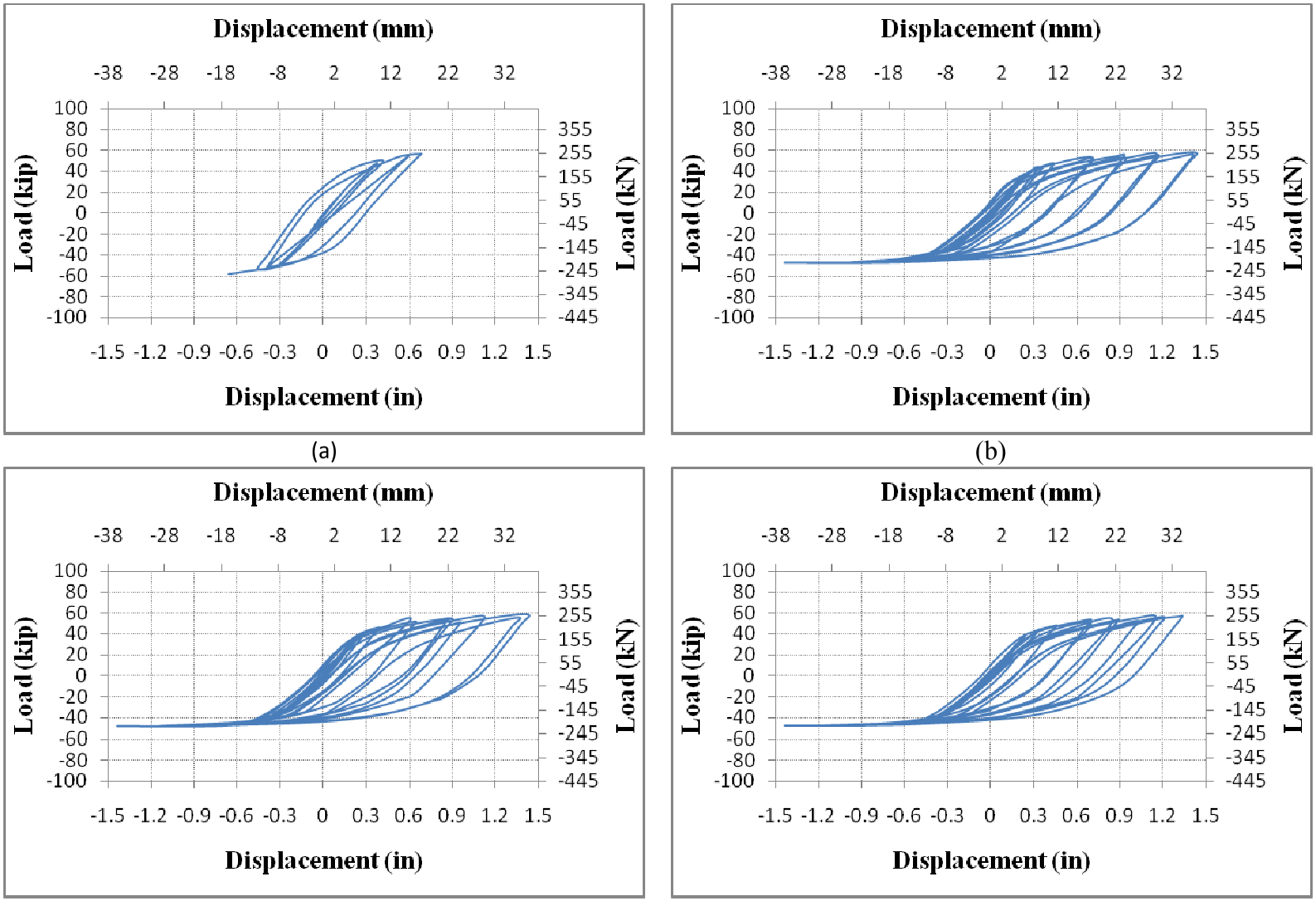

Figure E-10 Load-Displacement Cyclic Plots for: (a) T-1-1-2¾ -FP-NS-C-DLC-I-1; (b) T-1/2-1/2-1-FP-SS-C-DLC-I-1; (c) T-1/2-1/2-1-FP-SS-C-DLC-I-2; and (d) T-1/2-1/2-1-FP-SS-C-DLC-I-3

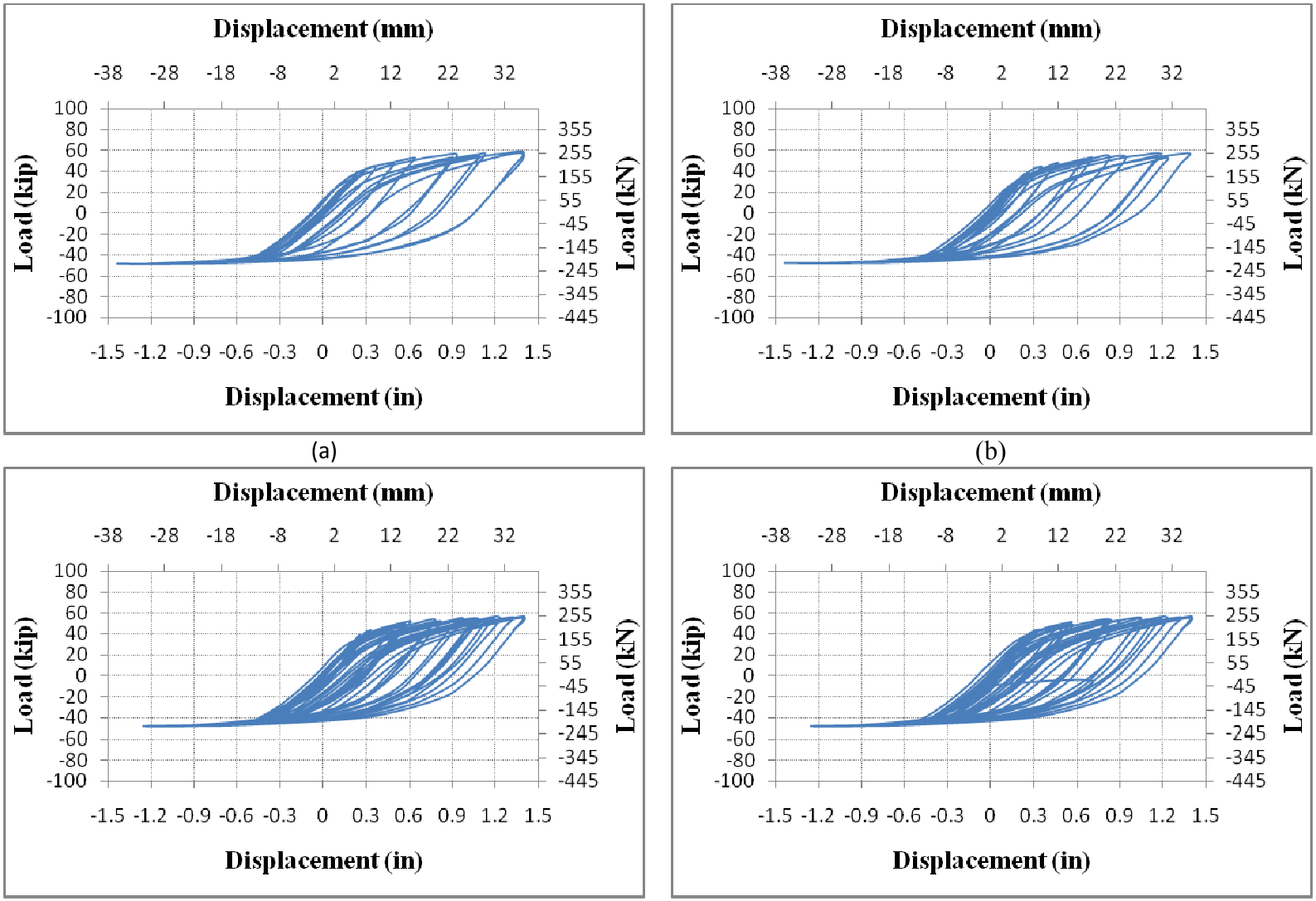

Figure E-11 Load-Displacement Cyclic Plots for: (a) T-1/2-1/2-1-FP-SS-C-DLC-I-4; (b) T-1/2-1/2-1-FP-SS-C-DLC-I-5; (c) T-1/2-1/2-1-FP-SS-C-DLC-II-1; and (d) T-1/2-1/2-1-FP-SS-C-DLC-II-2

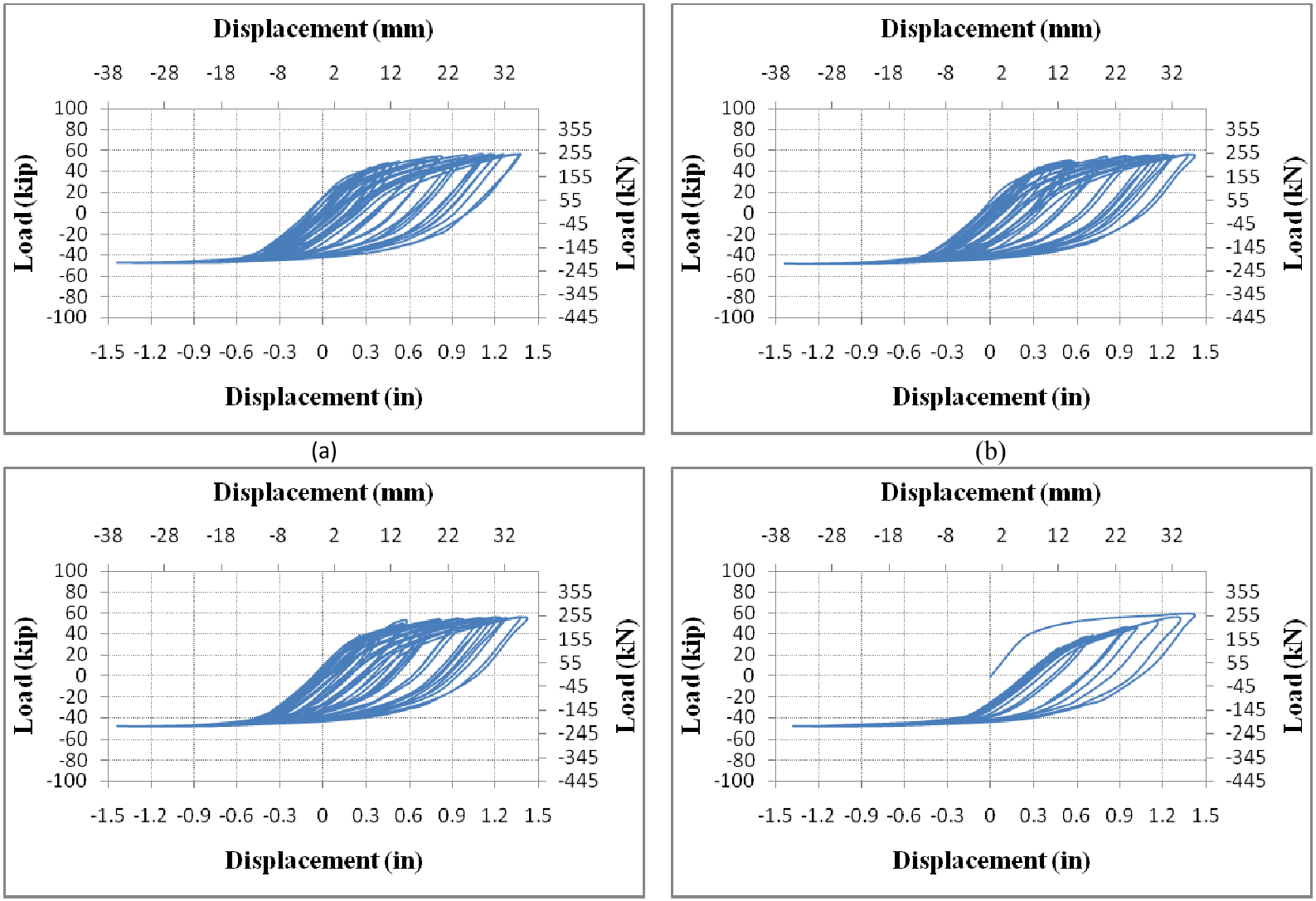

Figure E-12 Load-Displacement Cyclic Plots for: (a) T-1/2-1/2-1-FP-SS-C-DLC-II-3; (b) T-1/2-1/2-1-FP-SS-C-DLC-II-4; (c) T-1/2-1/2-1-FP-SS-C-DLC-II-5; and (d) T-1/2-1/2-1-FP-SS-C-DLC-III-1

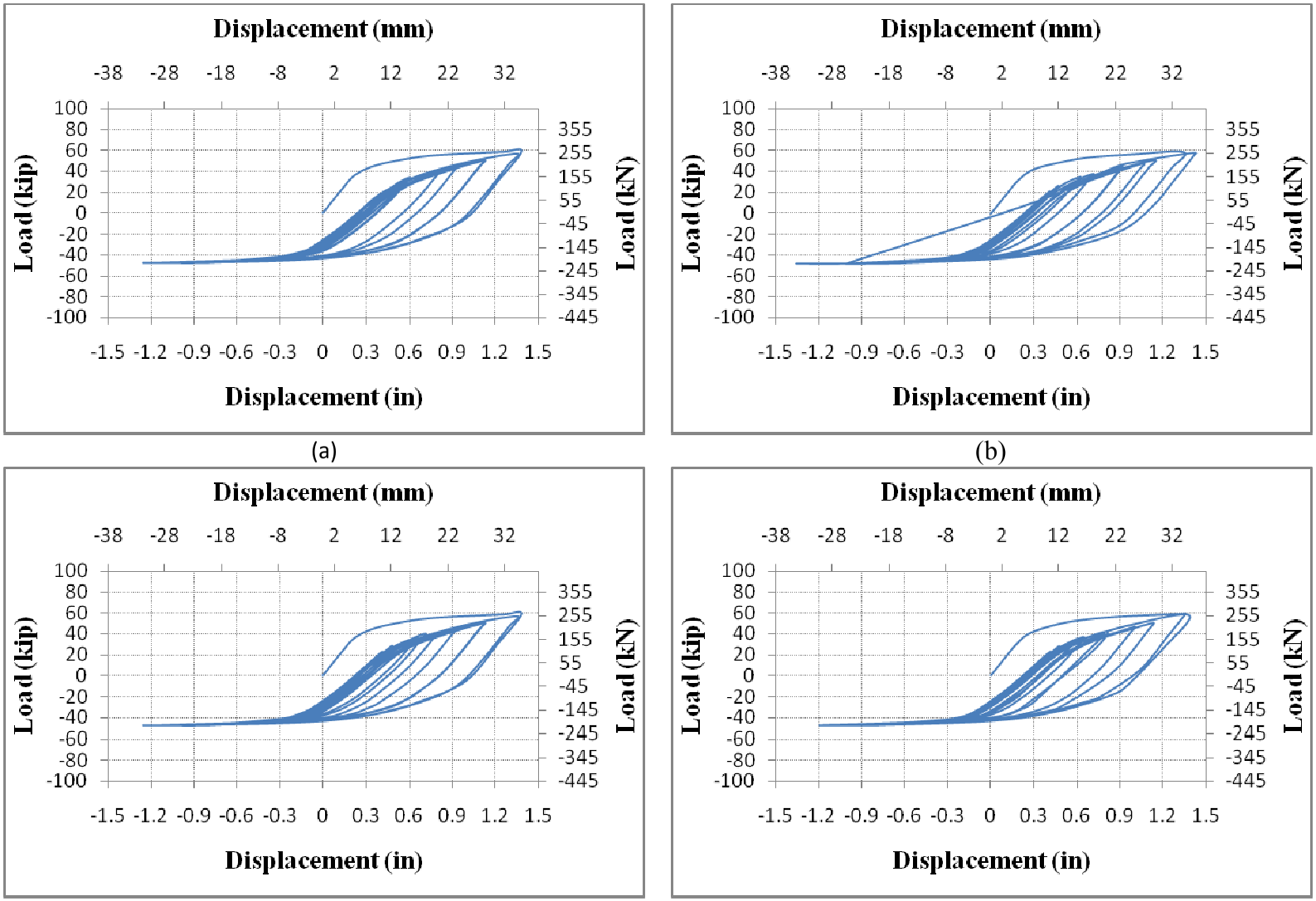

Figure E-13 Load-Displacement Cyclic Plots for: (a) T-1/2-1/2-1-FP-SS-C-DLC-III-2; (b) T-1/2-1/2-1-FP-SS-C-DLC-III-3; (c) T-1/2-1/2-1-FP-SS-C-DLC-III-4; and (d) T-1/2-1/2-1-FP-SS-C-DLC-III-5

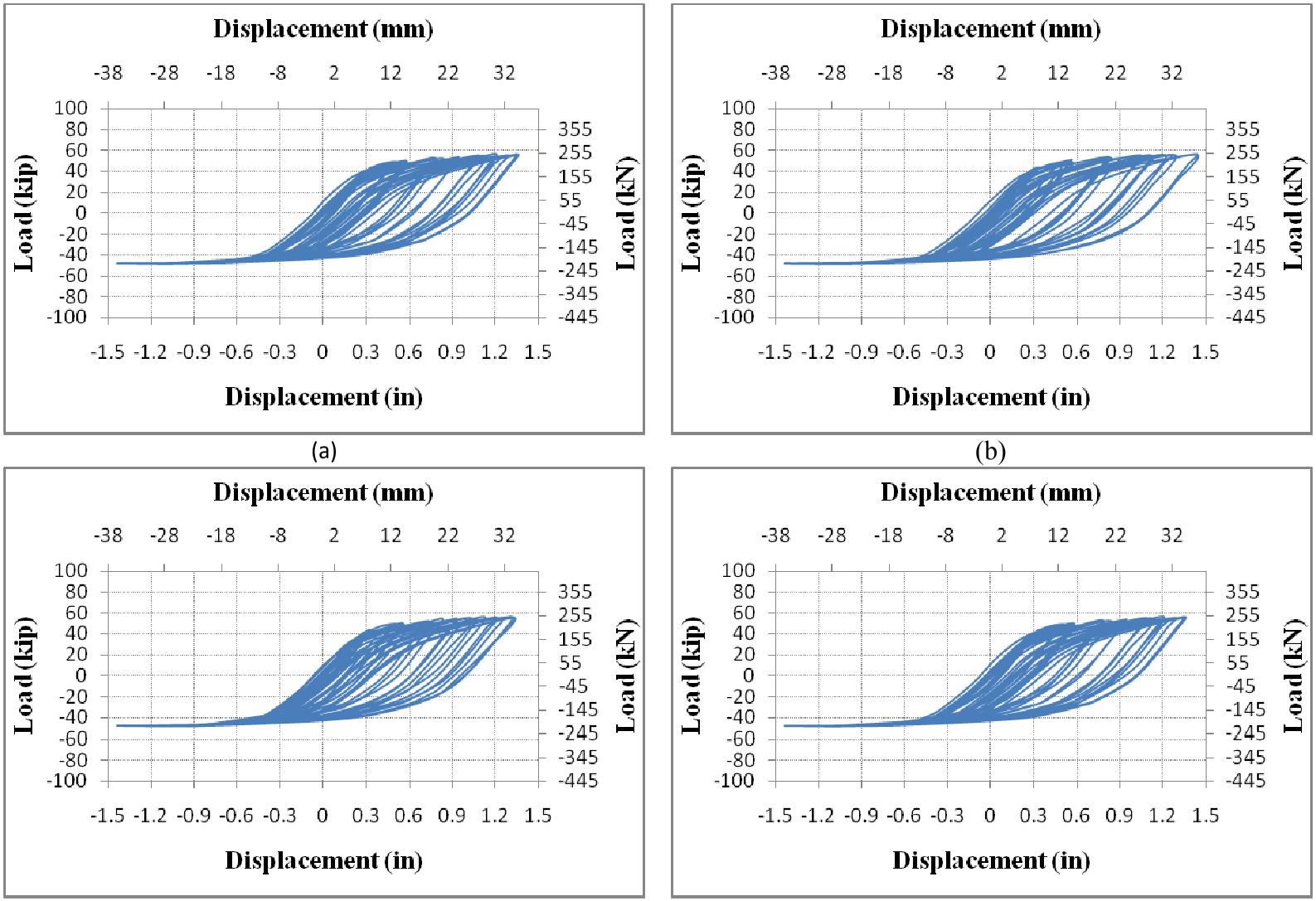

Figure E-14 Load-Displacement Cyclic Plots for: (a) T-1/2-1/2-1-FP-SS-C-DLC-IV-1; (b) T-1/2-1/2-1-FP-SS-C-DLC-IV-2; (c) T-1/2-1/2-1-FP-SS-C-DLC-IV-3; and (d) T-1/2-1/2-1-FP-SS-C-DLC-IV-4

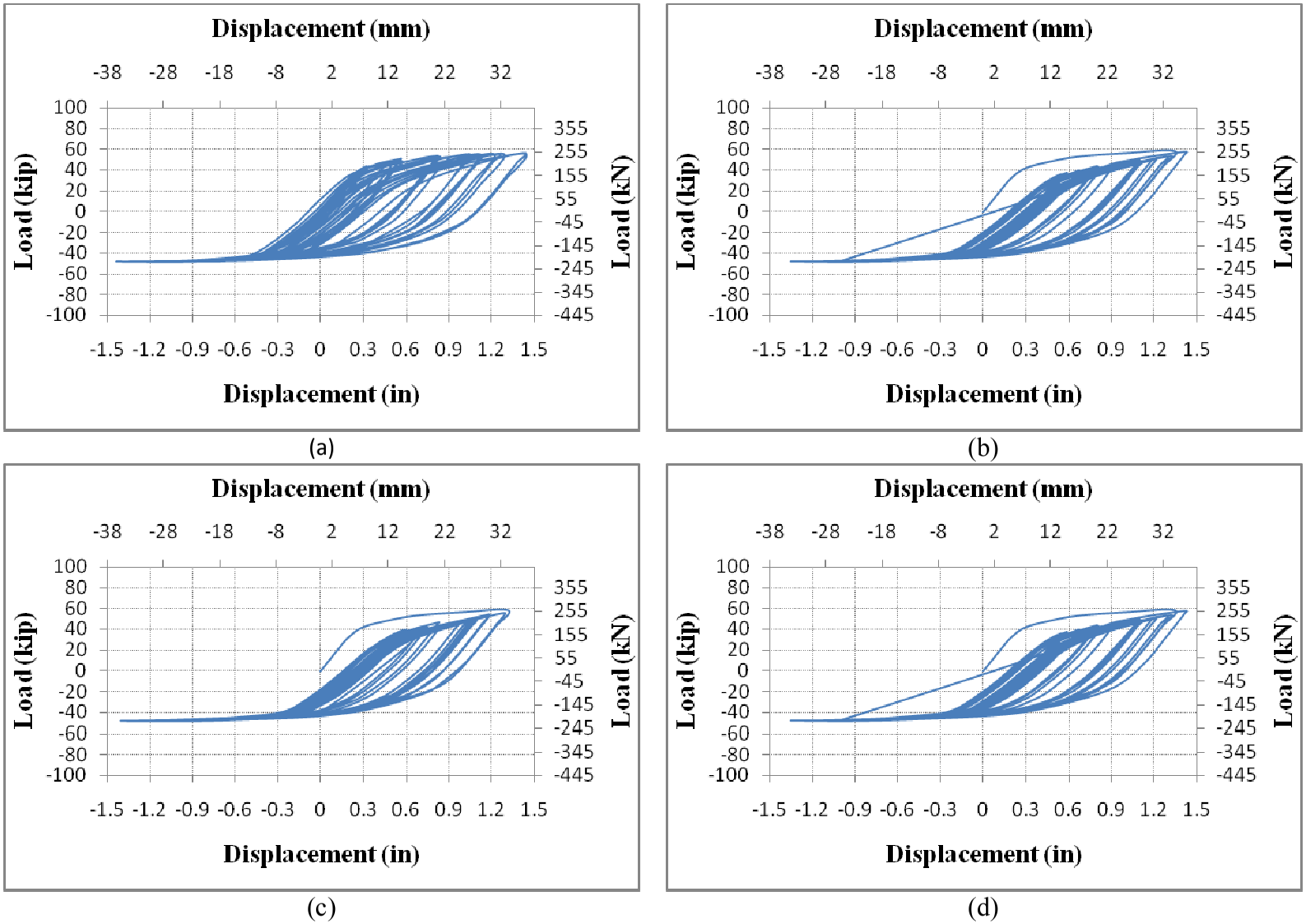

Figure E-15 Load-Displacement Cyclic Plots for: (a) T-1/2-1/2-1-FP-SS-C-DLC-IV-5; (b) T-1/2-1/2-1-FP-SS-C-DLC-V-1; (c) T-1/2-1/2-1-FP-SS-C-DLC-V-2; and (d) T-1/2-1/2-1-FP-SS-C-DLC-V-3

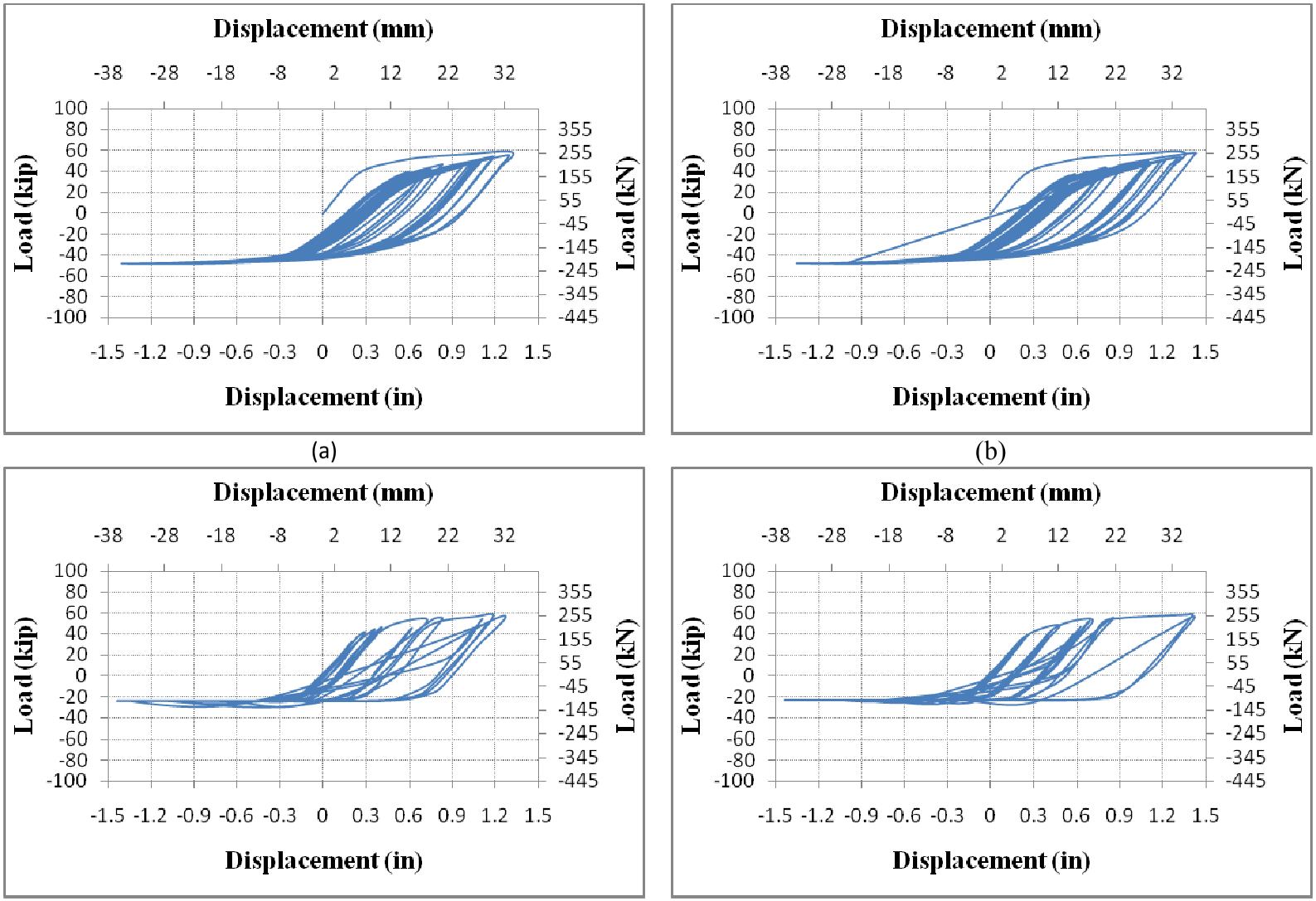

Figure E-16 Load-Displacement Cyclic Plots for: (a) T-1/2-1/2-1-FP-SS-C-DLC-V-4; (b) T-1/2-1/2-1-FP-SS-C-DLC-V-5; (c) T-1/2-1/2-1-HP-SS-C-DLC-I-1; and (d) T-1/2-1/2-1-HP-SS-C-DLC-I-2

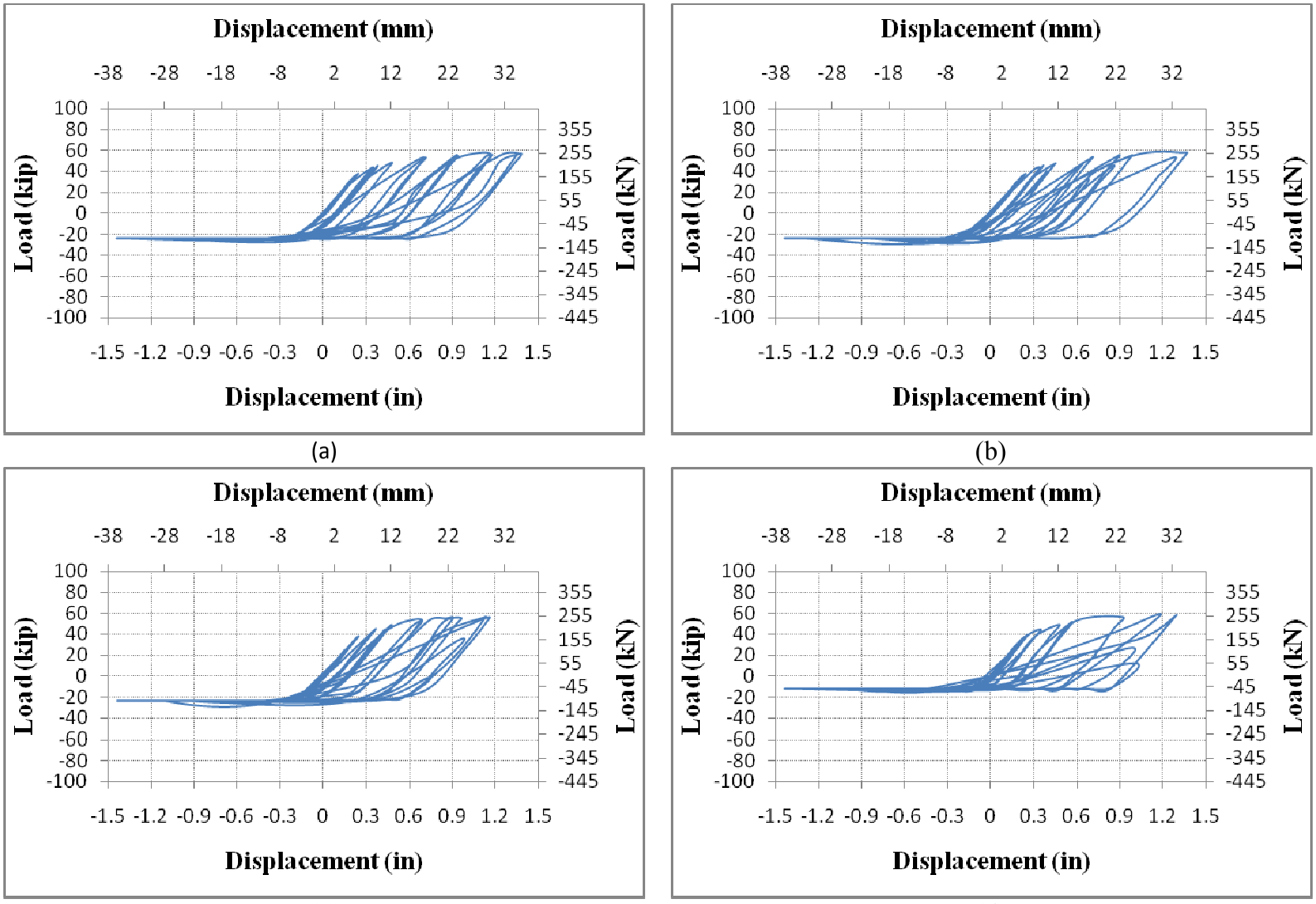

Figure E-17 Load-Displacement Cyclic Plots for: (a) T-1/2-1/2-1-HP-SS-C-DLC-I-3; (b) T-1/2-1/2-1-HP-SS-C-DLC-I-4; (c) T-1/2-1/2-1-HP-SS-C-DLC-I-5; and (d) T-1/2-1/2-1-QP-SS-C-DLC-I-1

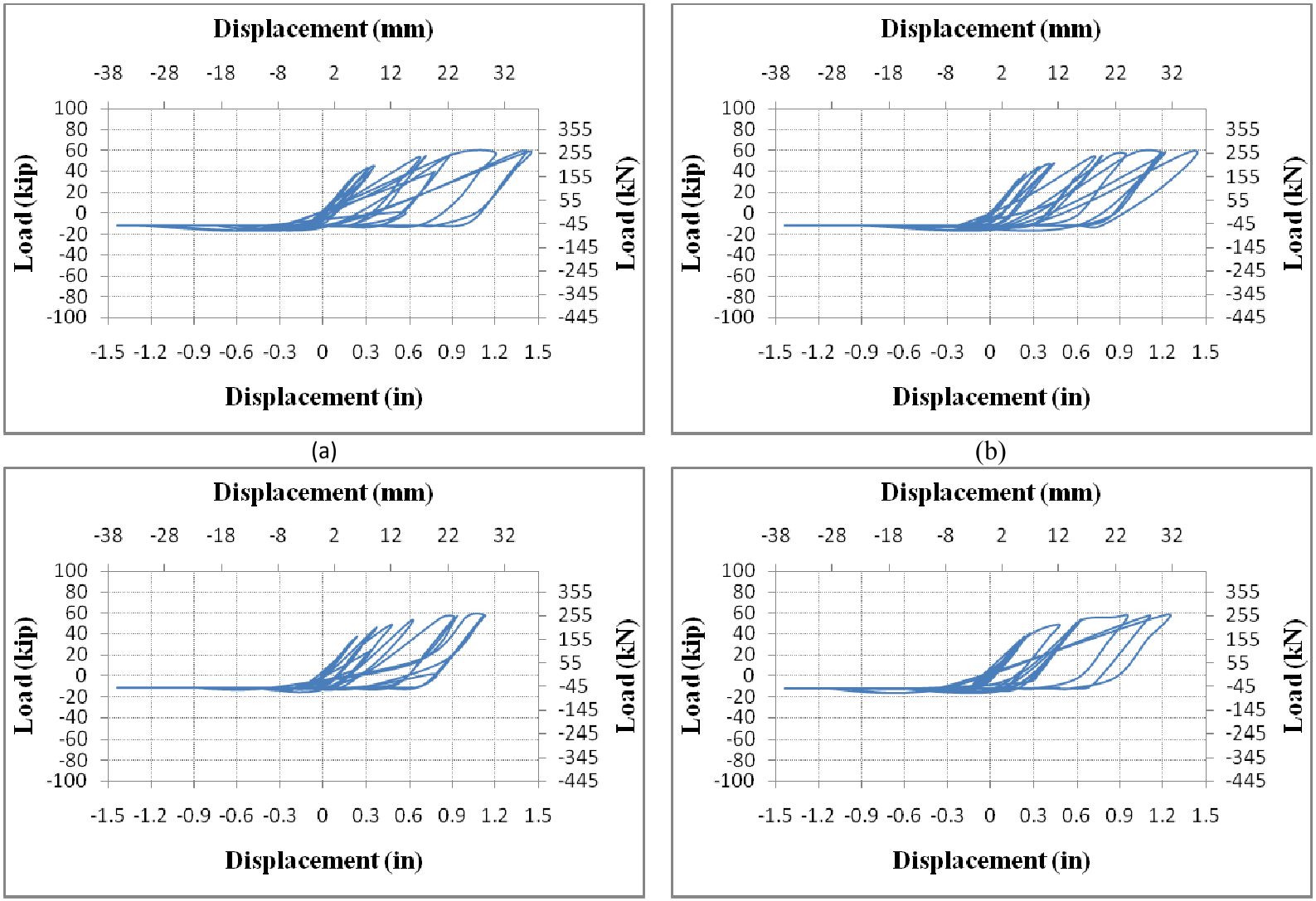

Figure E-18 Load-Displacement Cyclic Plots for: (a) T-1/2-1/2-1-QP-SS-C-DLC-I-2; (b) T-1/2-1/2-1-QP-SS-C-DLC-I-3; (c) T-1/2-1/2-1-QP-SS-C-DLC-I-4; (d) T-1/2-1/2-1-QP-SS-C-DLC-I-5

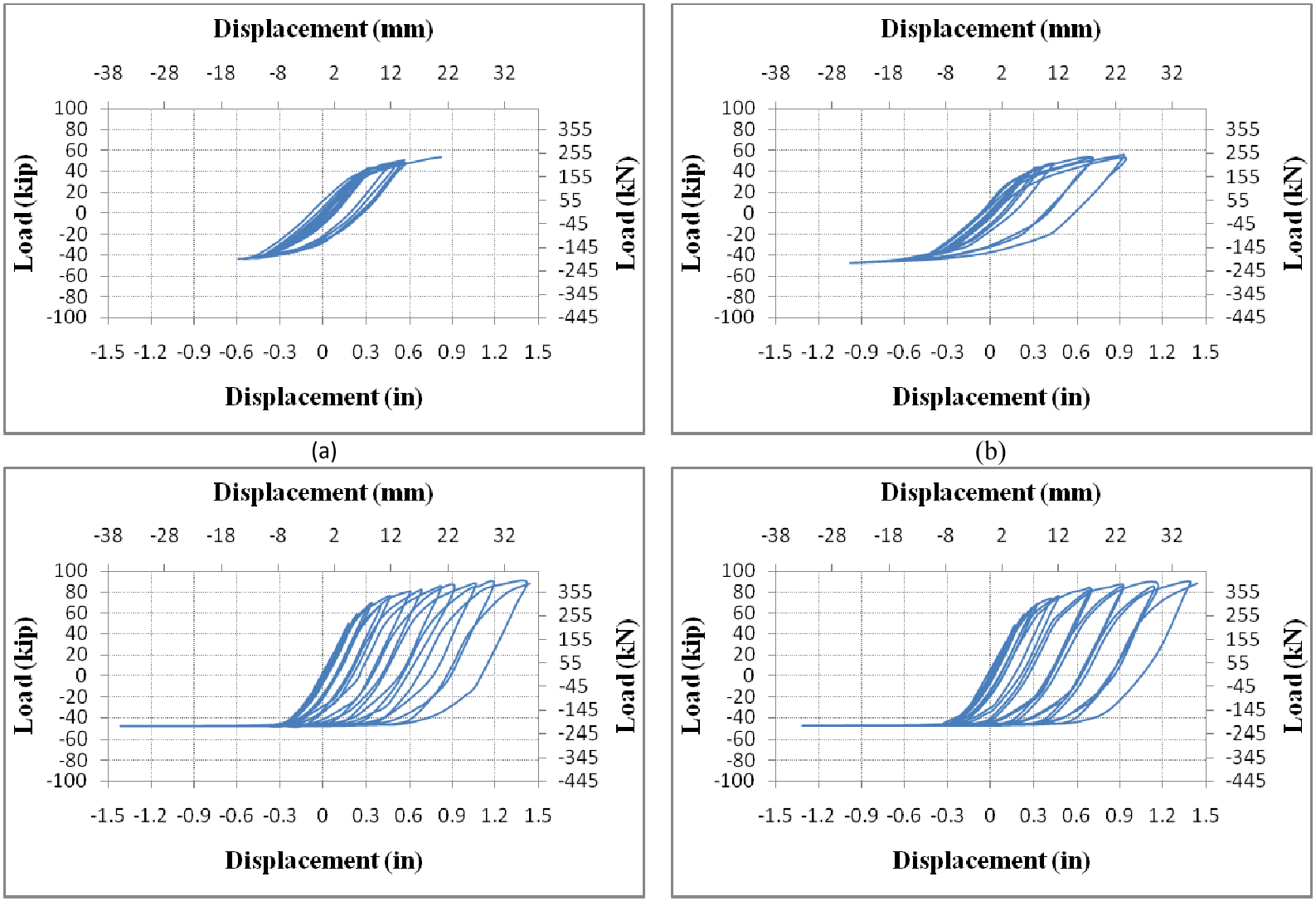

Figure E-19 Load-Displacement Cyclic Plots for: (a) T-1/2-1/2-1-FP-SS-HX-DLC-I-1; (b) T-1/2-1/2-1-FP-NS-C-DLC-I-1; (c) T-1-1/2-1½-FP-SS-C-DLC-I-1; and (d) T-1-1/2-1½-FP-SS-C-DLC-I-2

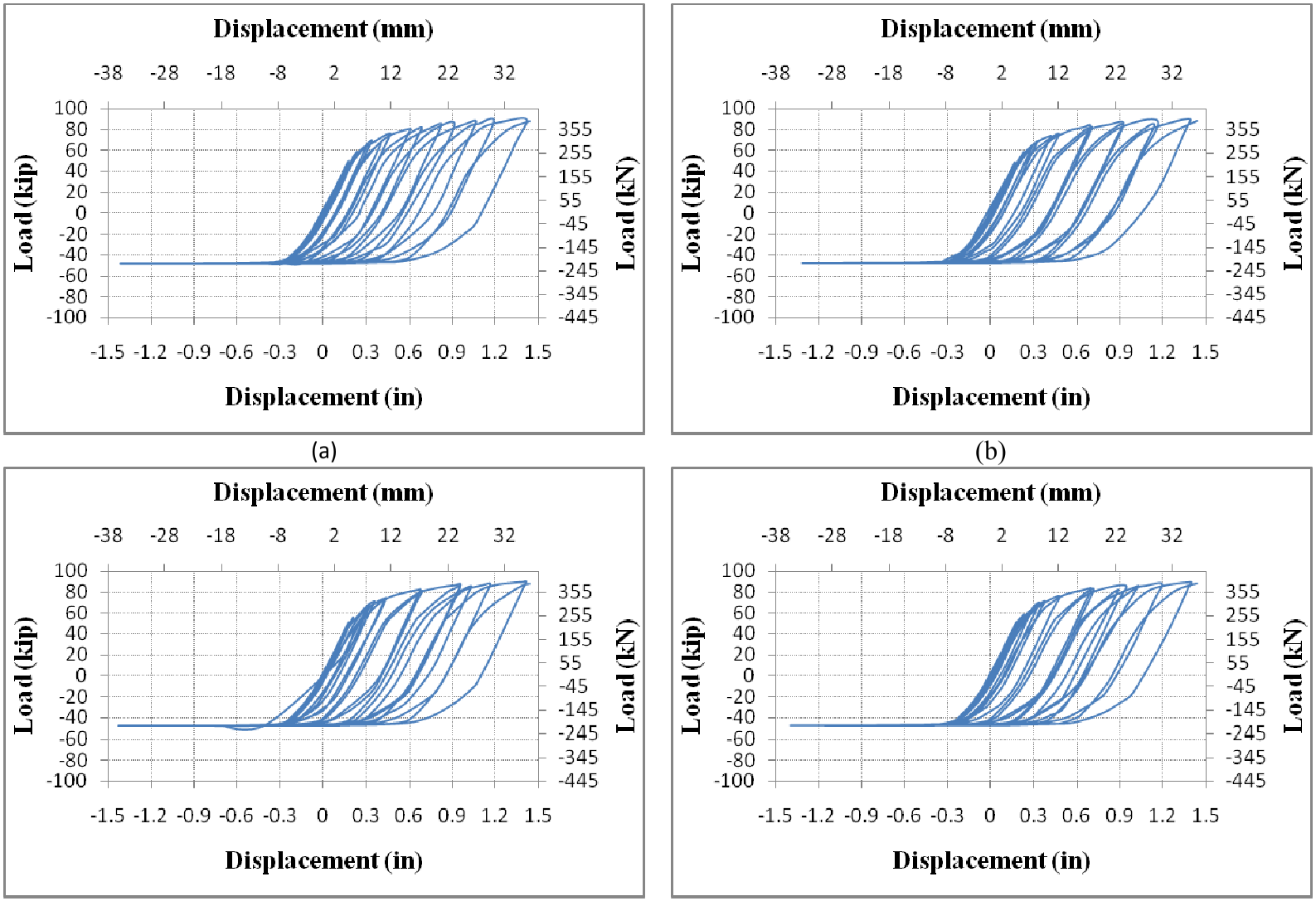

Figure E-20 Load-Displacement Cyclic Plots for: (a) T-1-1/2-1½-FP-SS-C-DLC-I-3; (b) T-1-1/2-1½-FP-SS-C-DLC-I-4; (c) T-1-1/2-1½-FP-SS-C-DLC-I-5; and (d) T-1-1/2-1½-FP-SS-C-DLC-II-1

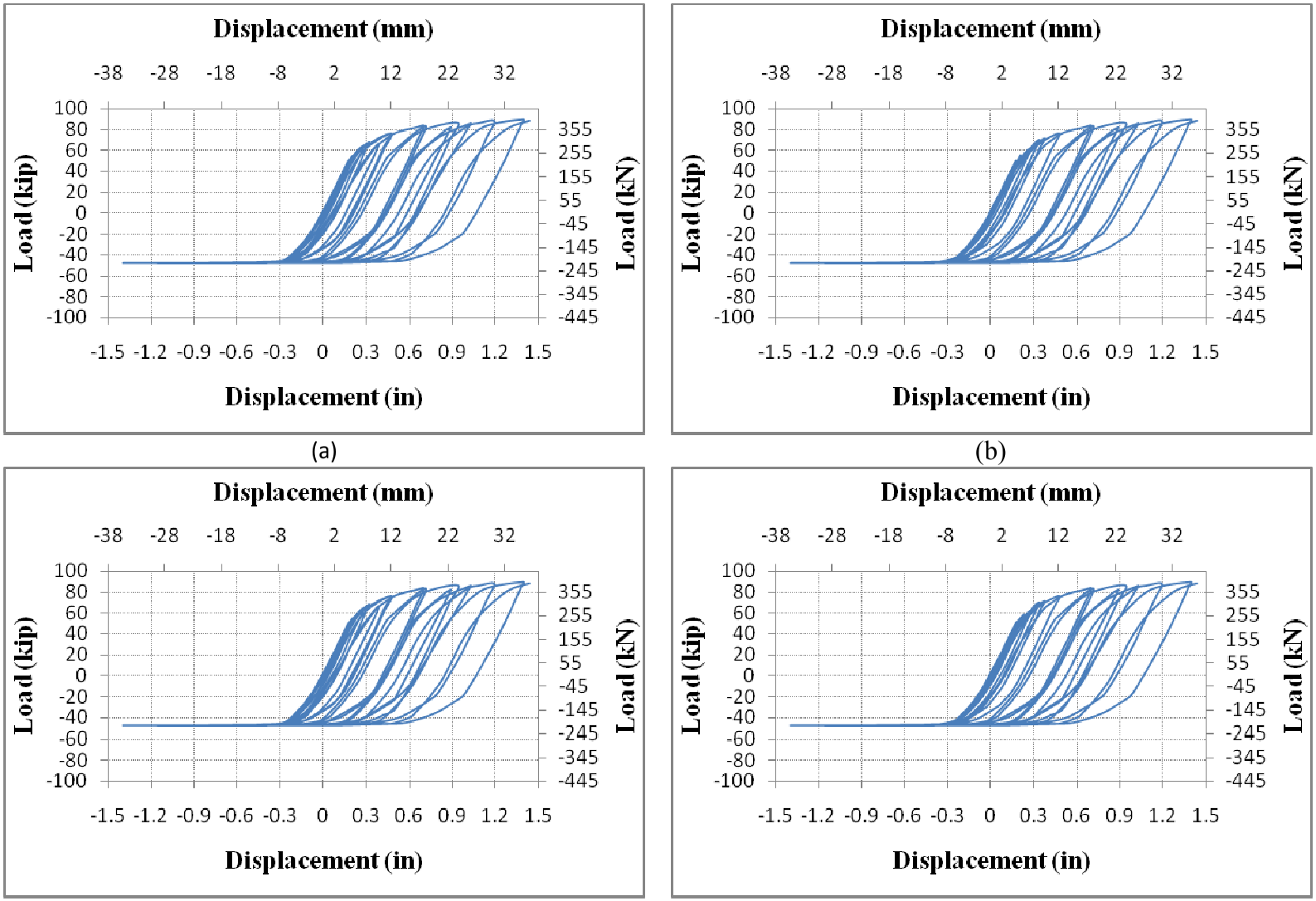

Figure E-21 Load-Displacement Cyclic Plots for: (a) T-1-1/2-1½-FP-SS-C-DLC-II-2; (b) T-1-1/2-1½-FP-SS-C-DLC-II-3; (c) T-1-1/2-1½-FP-SS-C-DLC-II-4; and (d) T-1-1/2-1½-FP-SS-C-DLC-II-5

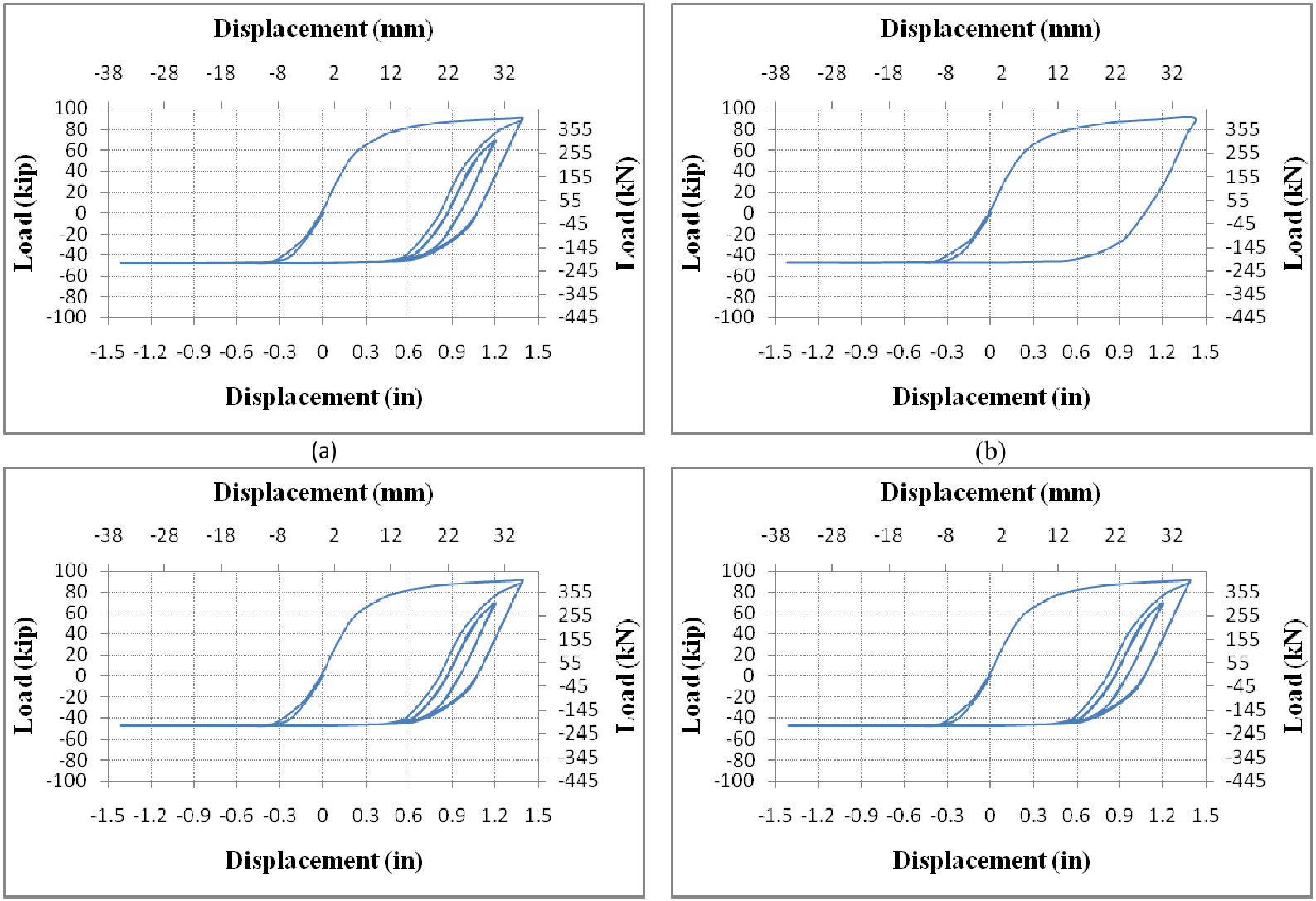

Figure E-22 Load-Displacement Cyclic Plots for: (a) T-1-1/2-1½-FP-SS-C-DLC-III-1; (b) T-1-1/2-1½-FP-SS-C-DLC-III-2; (c) T-1-1/2-1½-FP-SS-C-DLC-III-3; and (d) T-1-1/2-1½-FP-SS-C-DLC-III-4

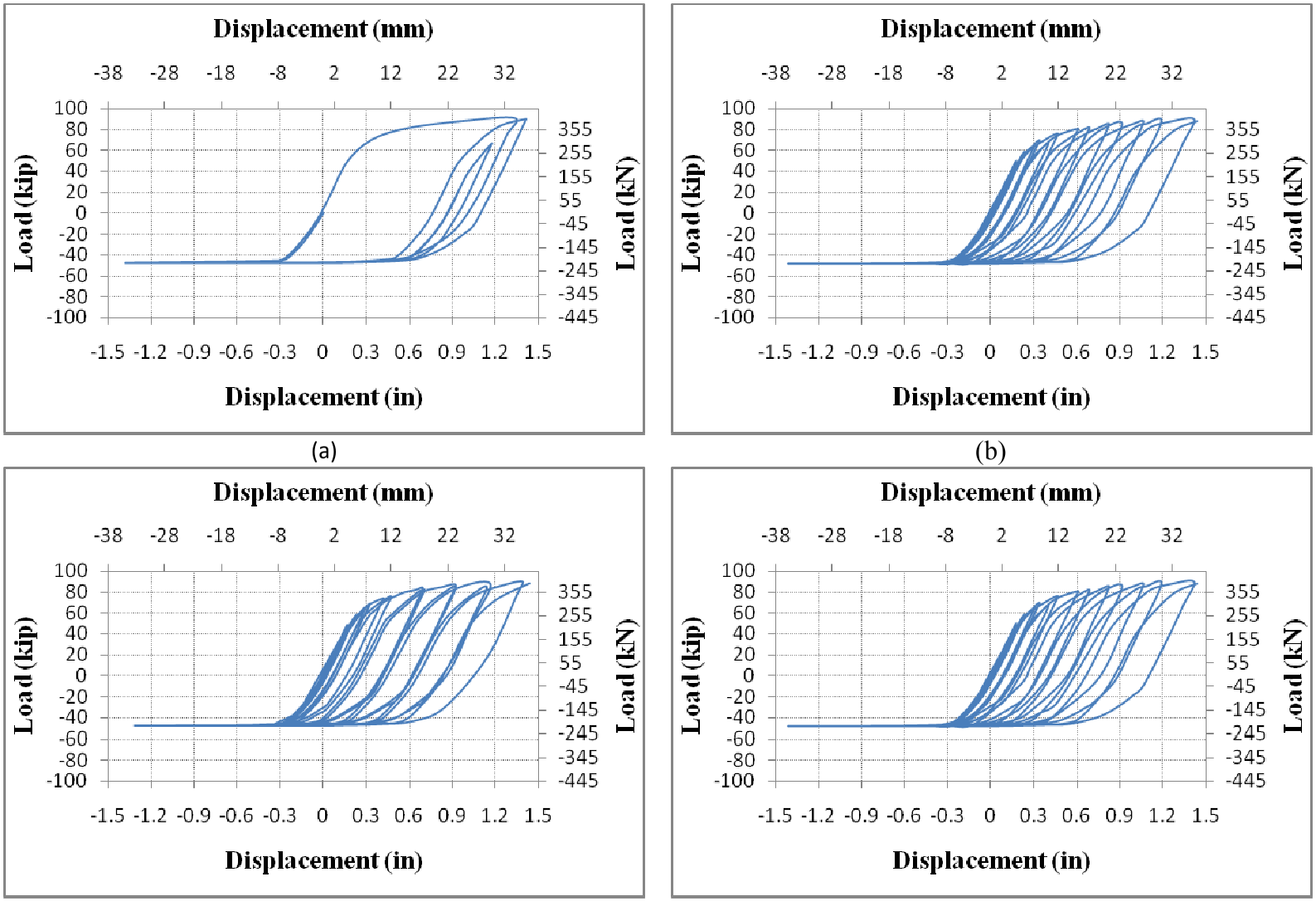

Figure E-23 Load-Displacement Cyclic Plots for: (a) T-1-1/2-1½-FP-SS-C-DLC-III-5; (b) T-1-1/2-1½-FP-SS-C-DLC-IV-1; (c) T-1-1/2-1½-FP-SS-C-DLC-IV-2; and (d) T-1-1/2-1½-FP-SS-C-DLC-IV-3

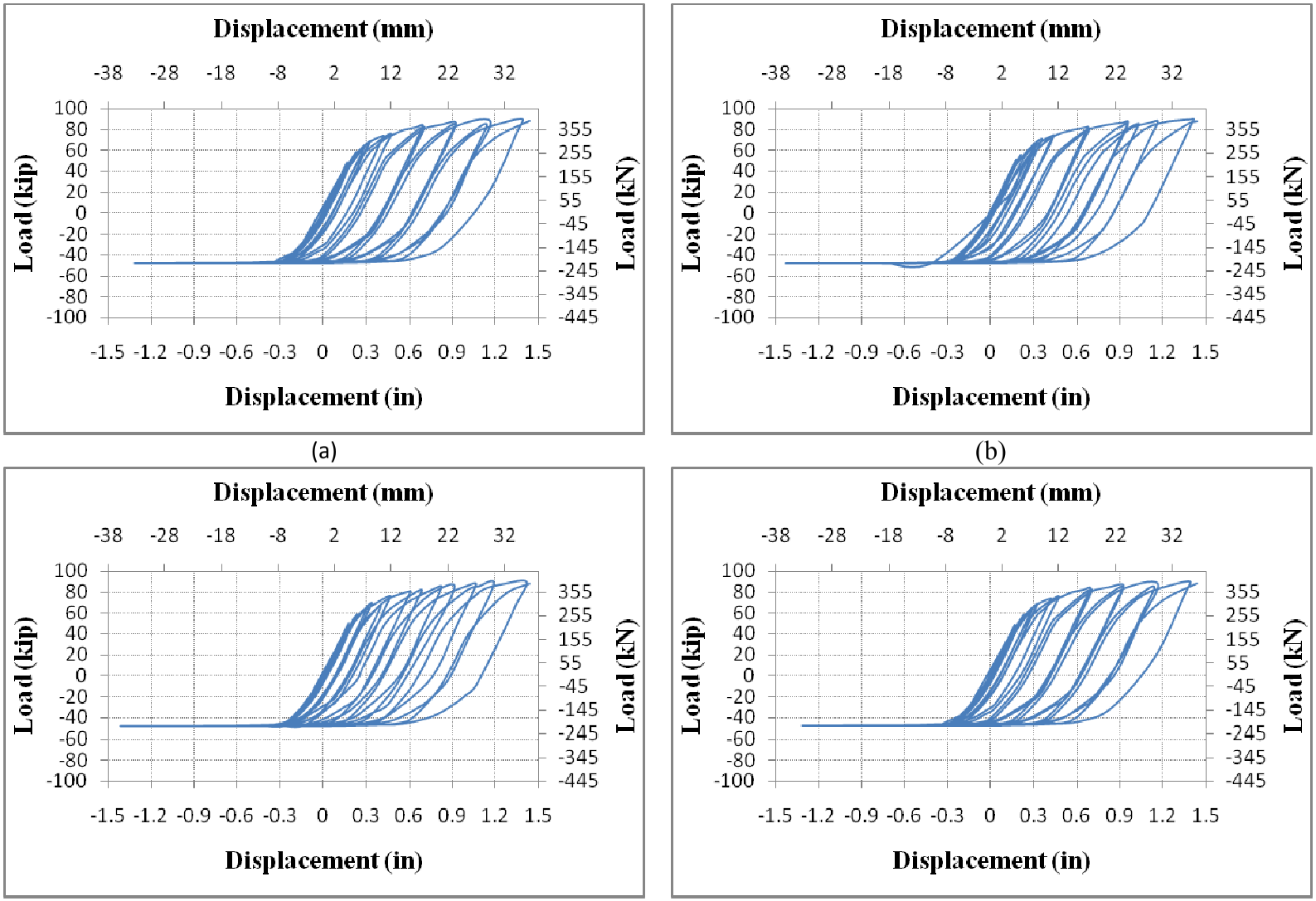

Figure E-24 Load-Displacement Cyclic Plots for: (a) T-1-1/2-1½-FP-SS-C-DLC-IV-4; (b) T-1-1/2-1½-FP-SS-C-DLC-IV-5; (c) T-1-1/2-1½-FP-SS-C-DLC-V-1; and (d) T-1-1/2-1½-FP-SS-C-DLC-V-2

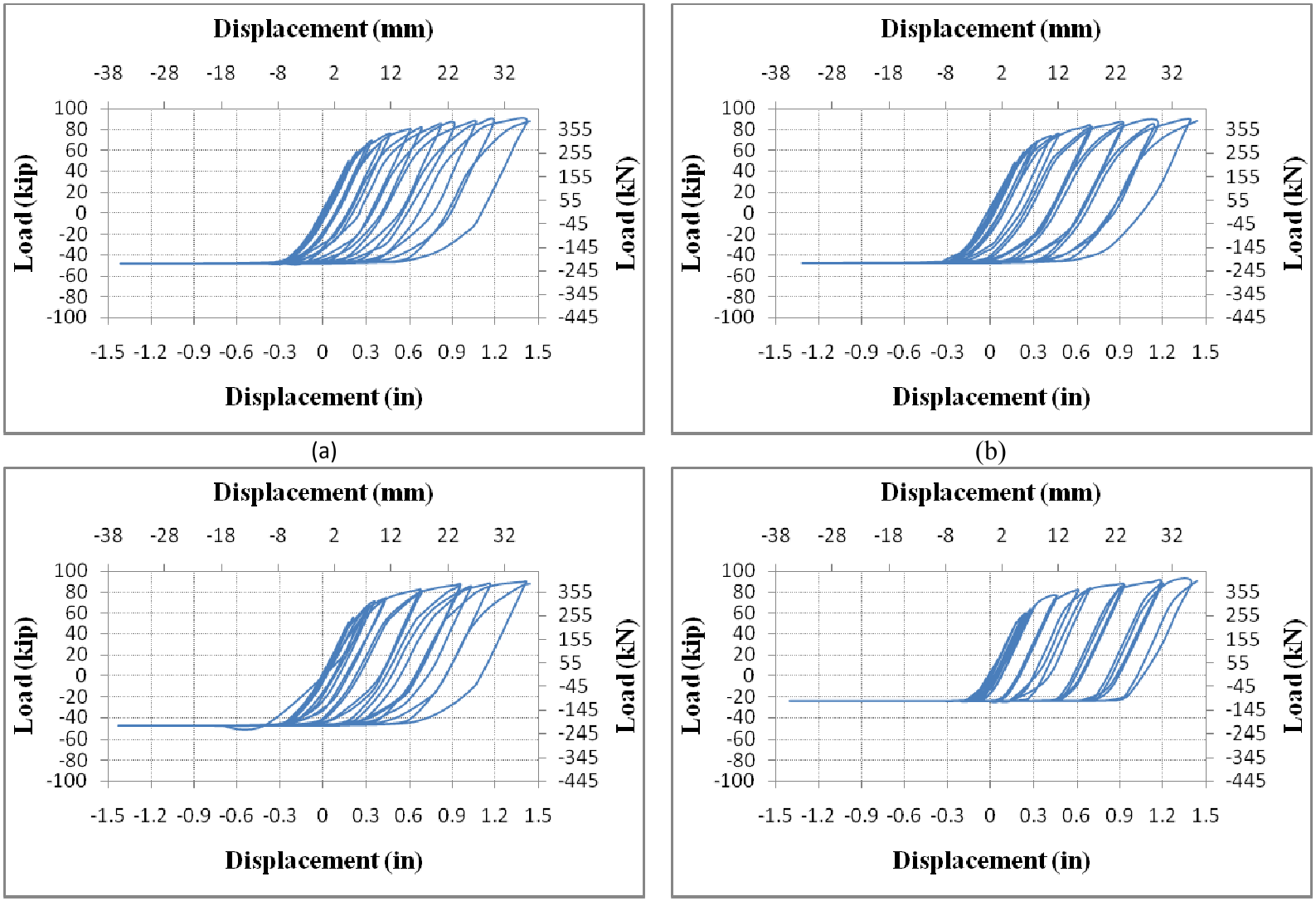

Figure E-25 Load-Displacement Cyclic Plots for: (a) T-1-1/2-1½-FP-SS-C-DLC-V-3; (b) T-1-1/2-1½-FP-SS-C-DLC-V-4; (c) T-1-1/2-1½-FP-SS-C-DLC-V-5; and (d) T-1-1/2-1½-HP-SS-C-DLC-I-1

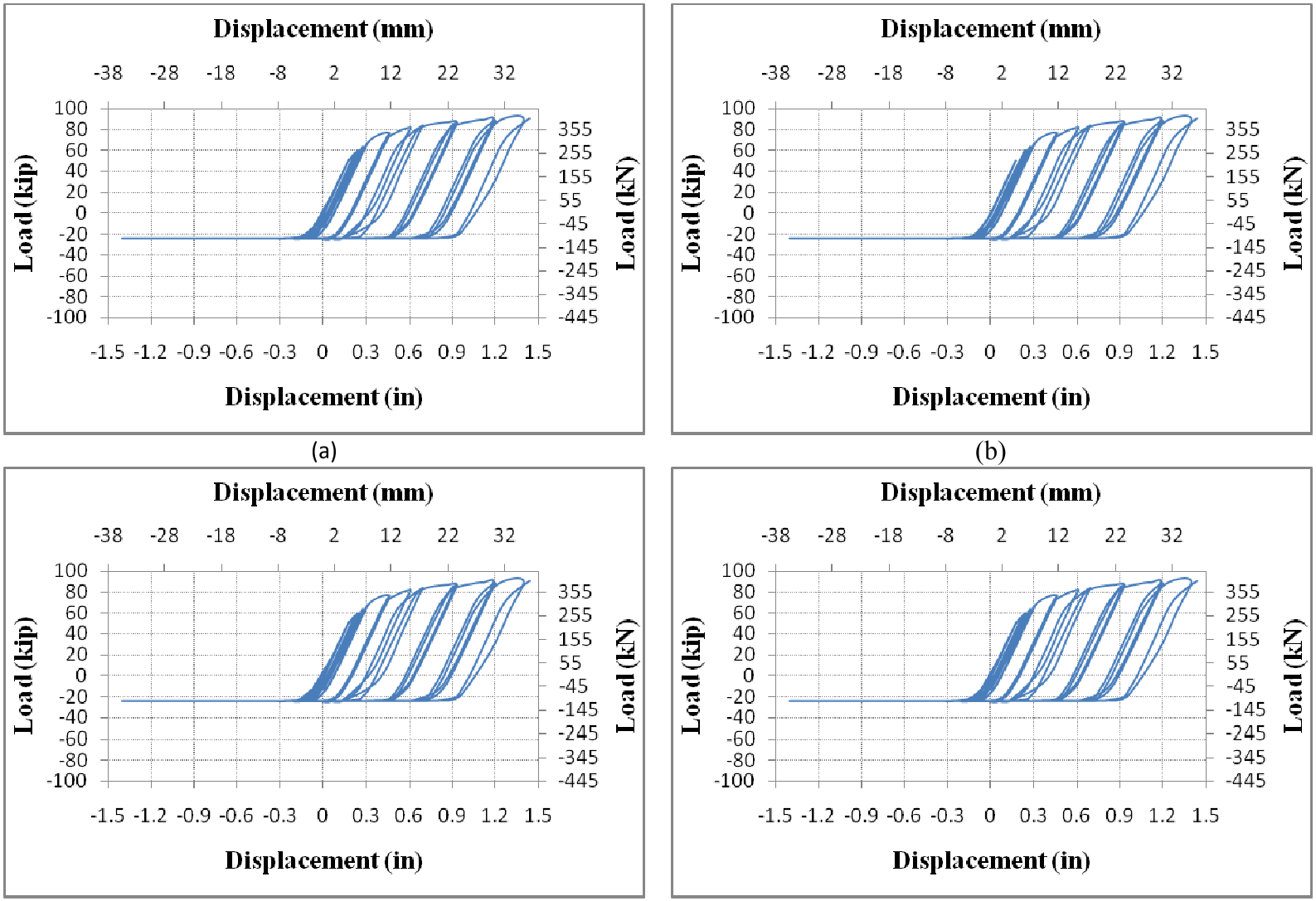

Figure E-26 Load-Displacement Cyclic Plots for: (a) T-1-1/2-1½-HP-SS-C-DLC-I-2; (b) T-1-1/2-1½-HP-SS-C-DLC-I-3; (c) T-1-1/2-1½-HP-SS-C-DLC-I-4; and (d) T-1-1/2-1½-HP-SS-C-DLC-I-5

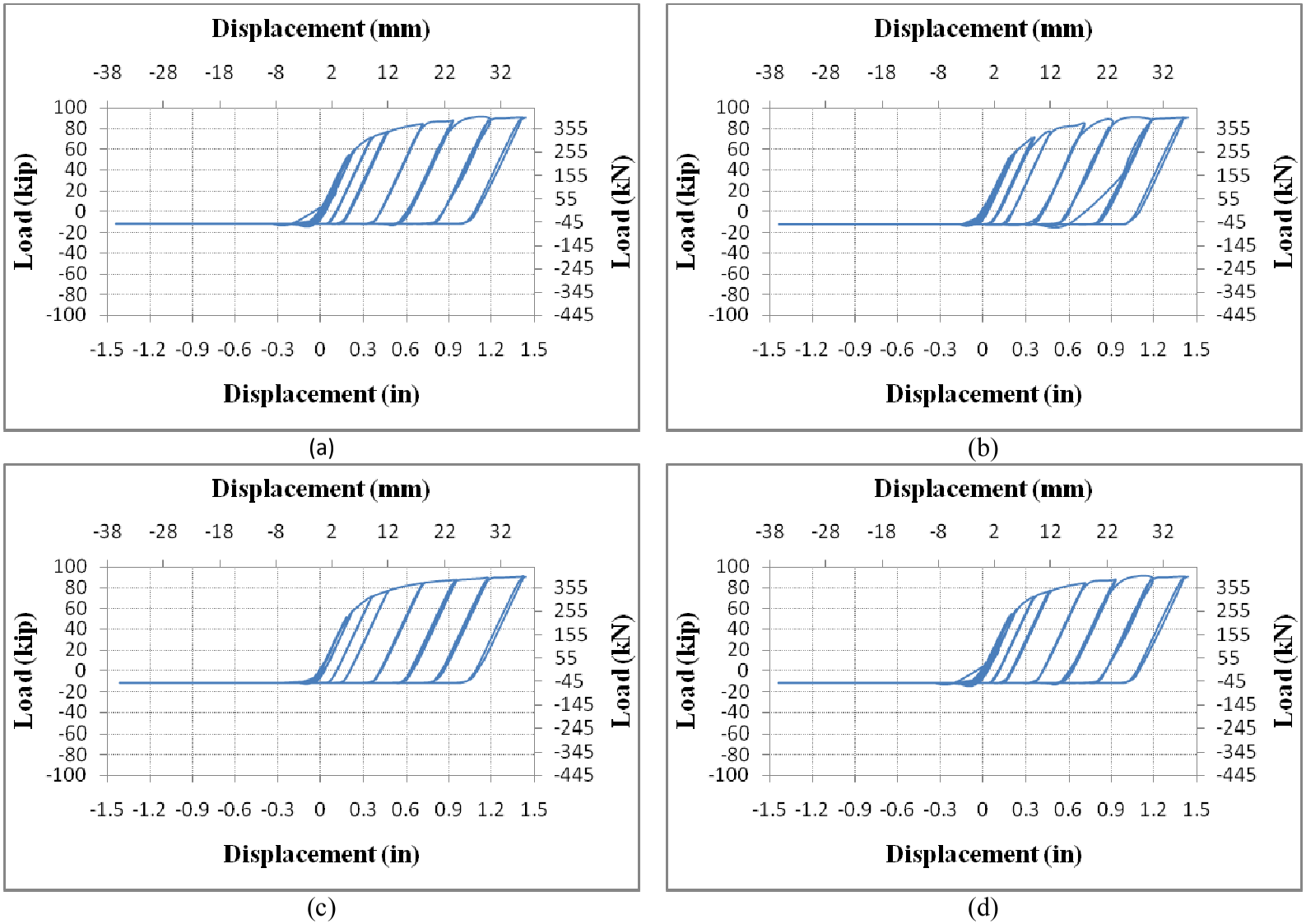

Figure E-27 Load-Displacement Cyclic Plots for: (a) T-1-1/2-1½-QP-SS-C-DLC-I-1; (b) T-1-1/2-1½-QP-SS-C-DLC-I-2; (c) T-1-1/2-1½-QP-SS-C-DLC-I-3; and (d) T-1-1/2-1½-QP-SS-C-DLC-I-4

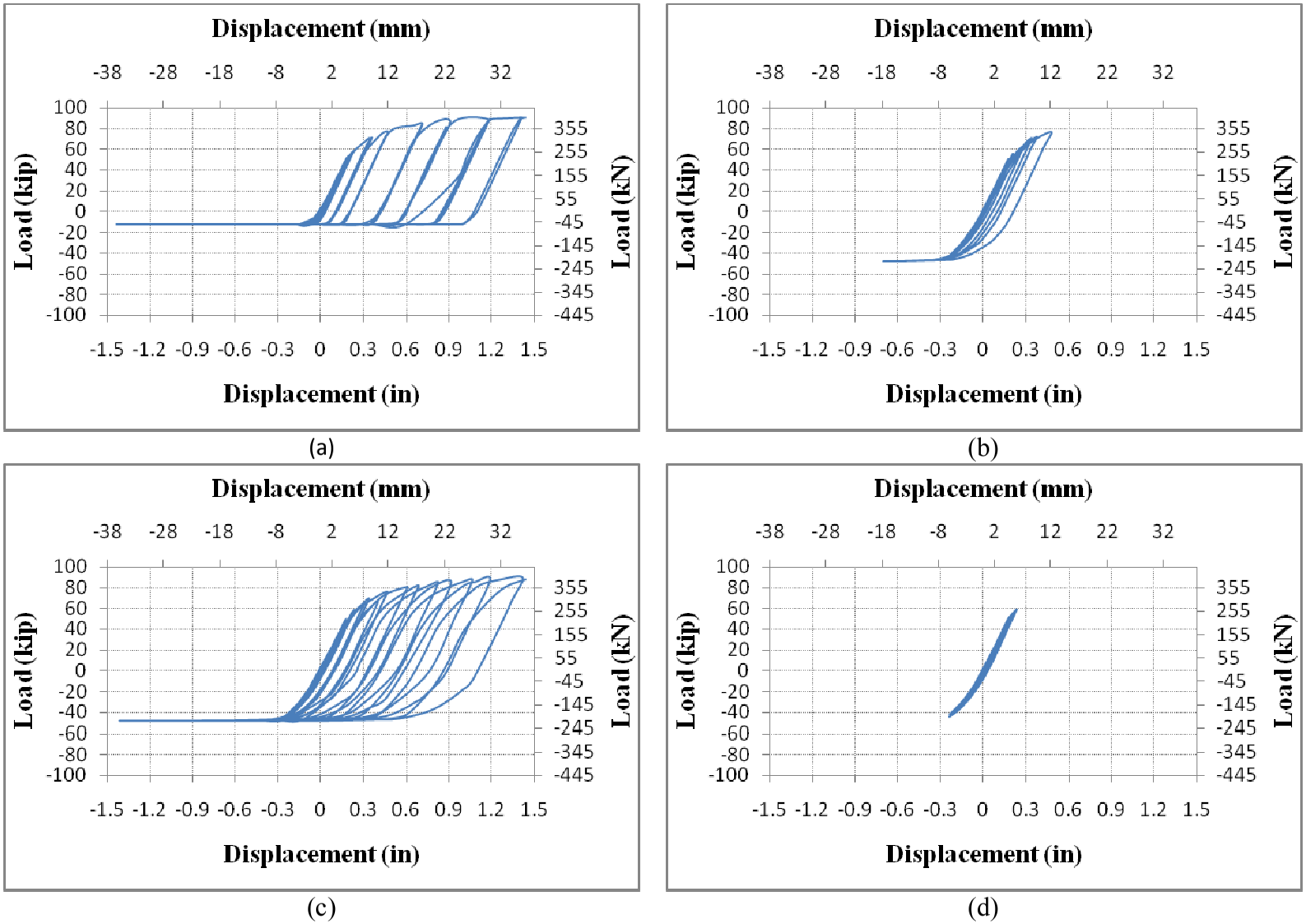

Figure E-28 Load-Displacement Cyclic Plots for: (a) T-1-1/2-1½-QP-SS-C-DLC-I-5; (b) T-1-1/2-1½-FP-SS-HX-DLC-I-1; (c) T-1-1/2-1½-FP-SS-C-DLC-I-1; and (d) T-1-1/2-1½-FP-NS-C-DLC-I-1

APPENDIX F

EXTENDED END-PLATE CONNECTION MODELS

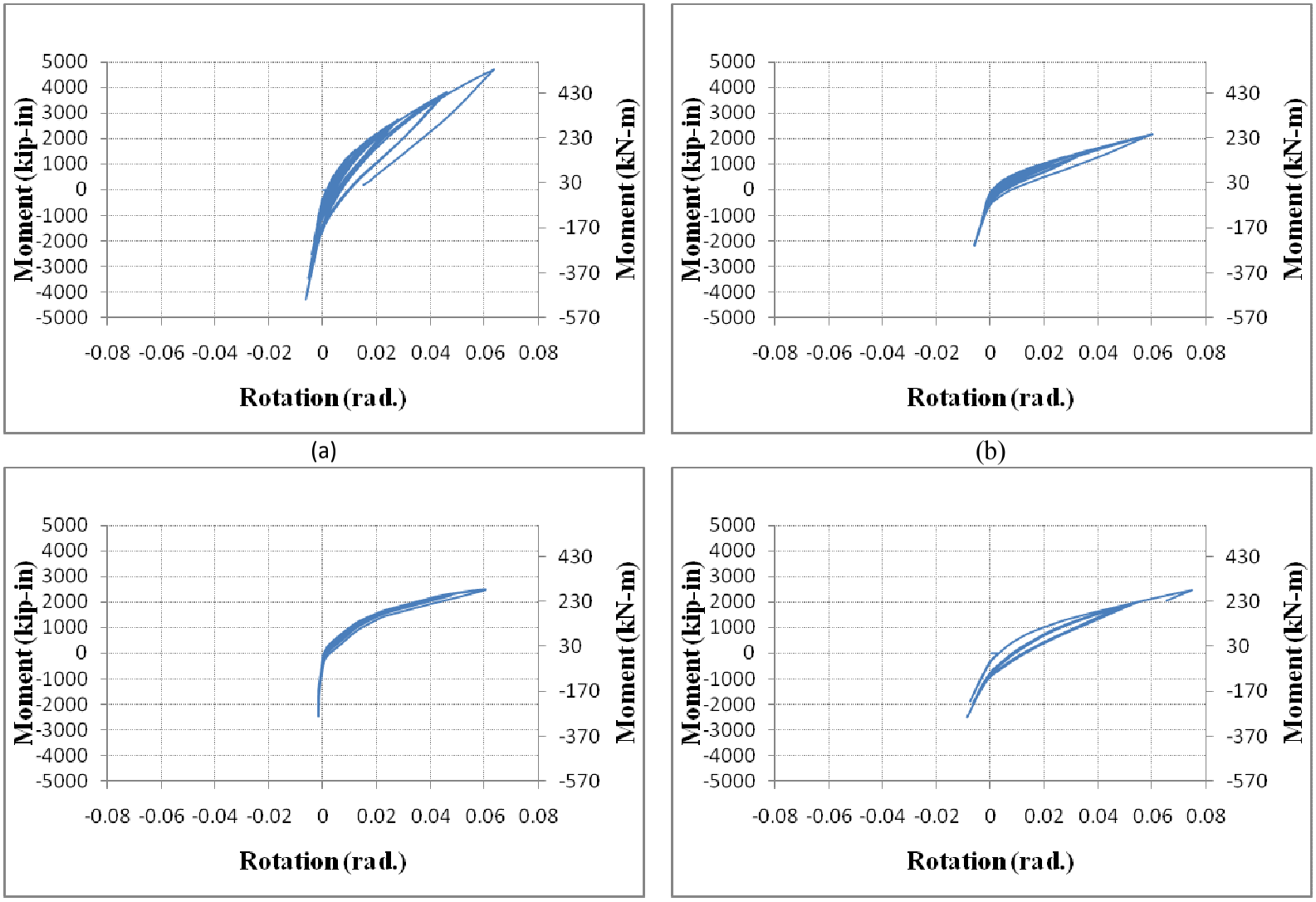

Figure F-1 Load-Displacement Cyclic Plots for: (a) EEP-1/2-1/2-FP-DLC-I-1; (b) EEP-1/2-1/2-HP-DLC-I-1; (c) EEP-1/2-1/2-QP-DLC-I-1; and (d) EEP-1/2-1/2-LLC-I-1

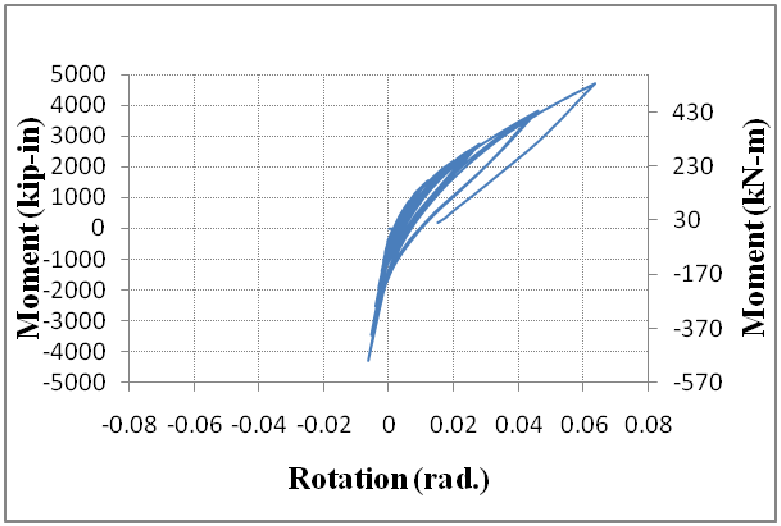

(a)

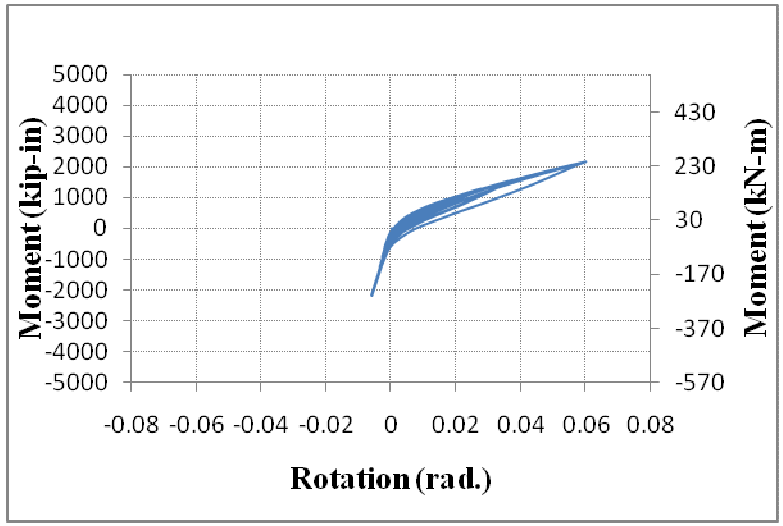

(b)

Figure F-2 Load-Displacement Cyclic Plots for: (a) EEP-1/2-1/2-FP-DLC-I-1; and (b) EEP-1/2-1/2-HP-DLC-I-1

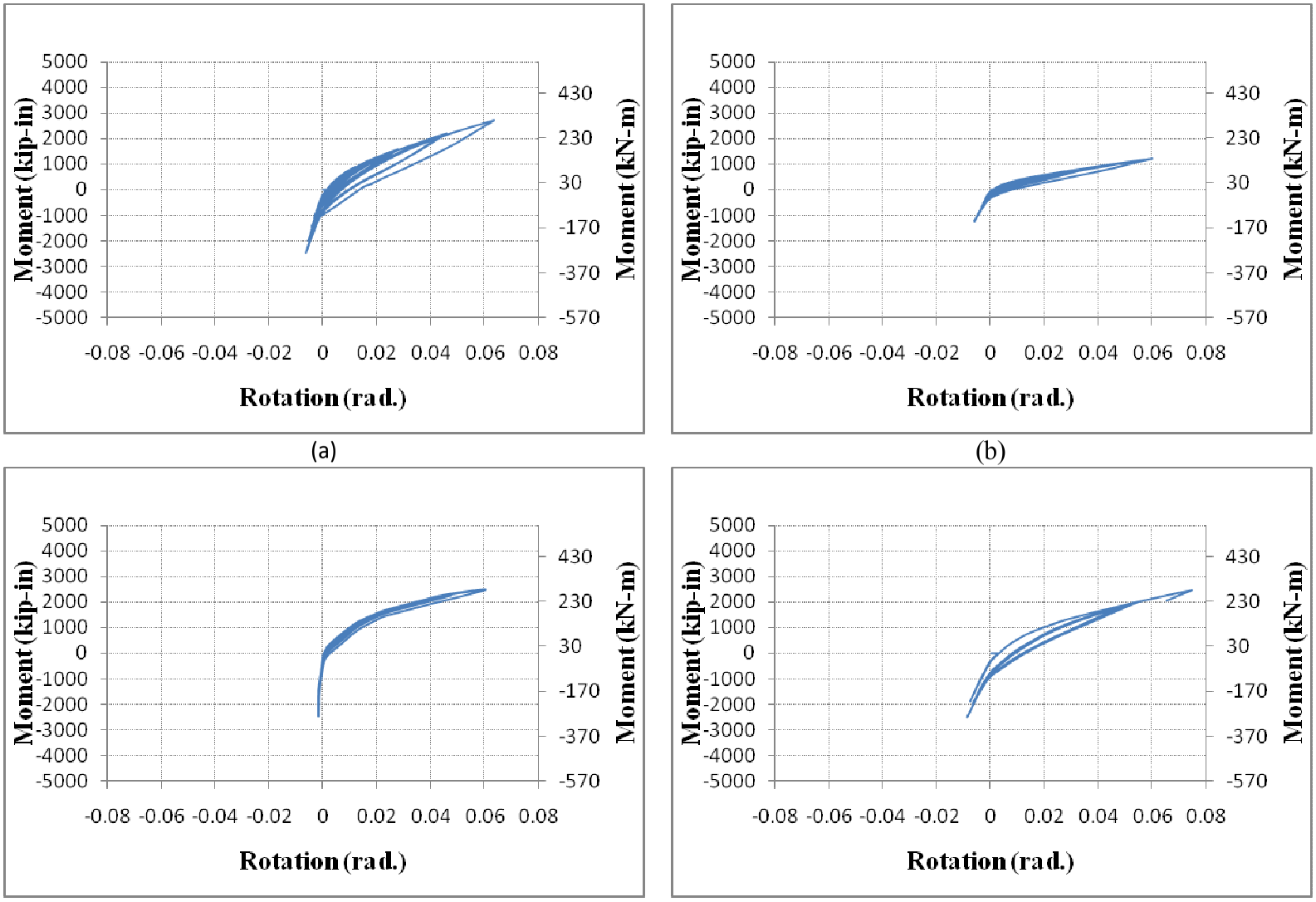

Figure F-3 Load-Displacement Cyclic Plots for: (a) EEP-1/2-1-FP-DLC-I-1; (b) EEP-1/2-1-HP-DLC-I-1; (c) EEP-1/2-1-QP-DLC-I-1; and (d) EEP-1/2-1-LLC-I-1

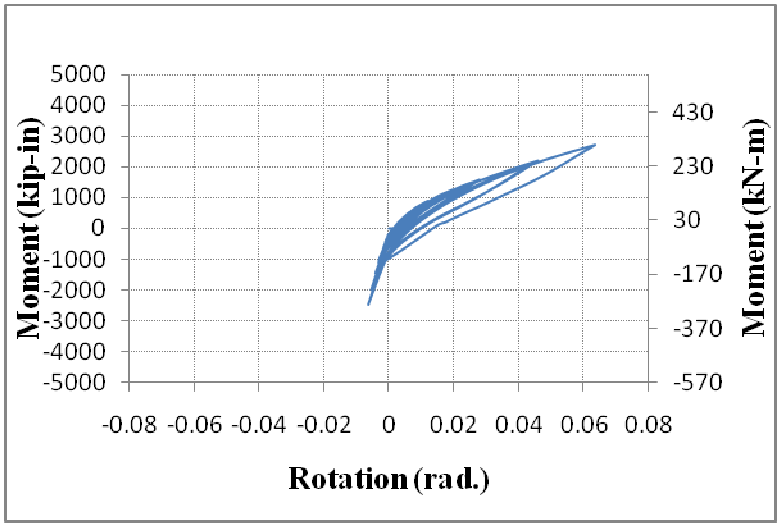

(a)

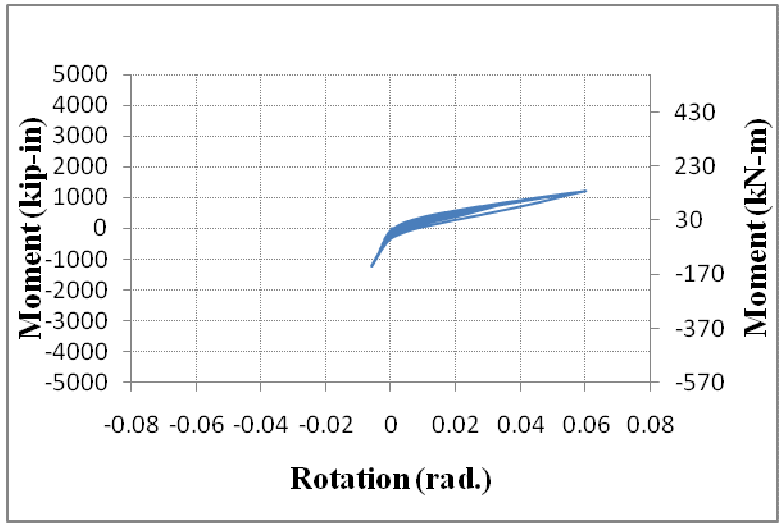

(b)

Figure F-4 Load-Displacement Cyclic Plots for: (a) EEP-1/2-1-FP-DLC-I-1; and (b) EEP-1/2-1-HP-DLC-I-1

APPENDIX G

ENERGY DISSIPATION CHARTS

Figure G-1 Welded shear surface model Case 1

Figure G-2 Welded shear surface model Case 2

Figure G-3 Single bolted shear surface model Case 1

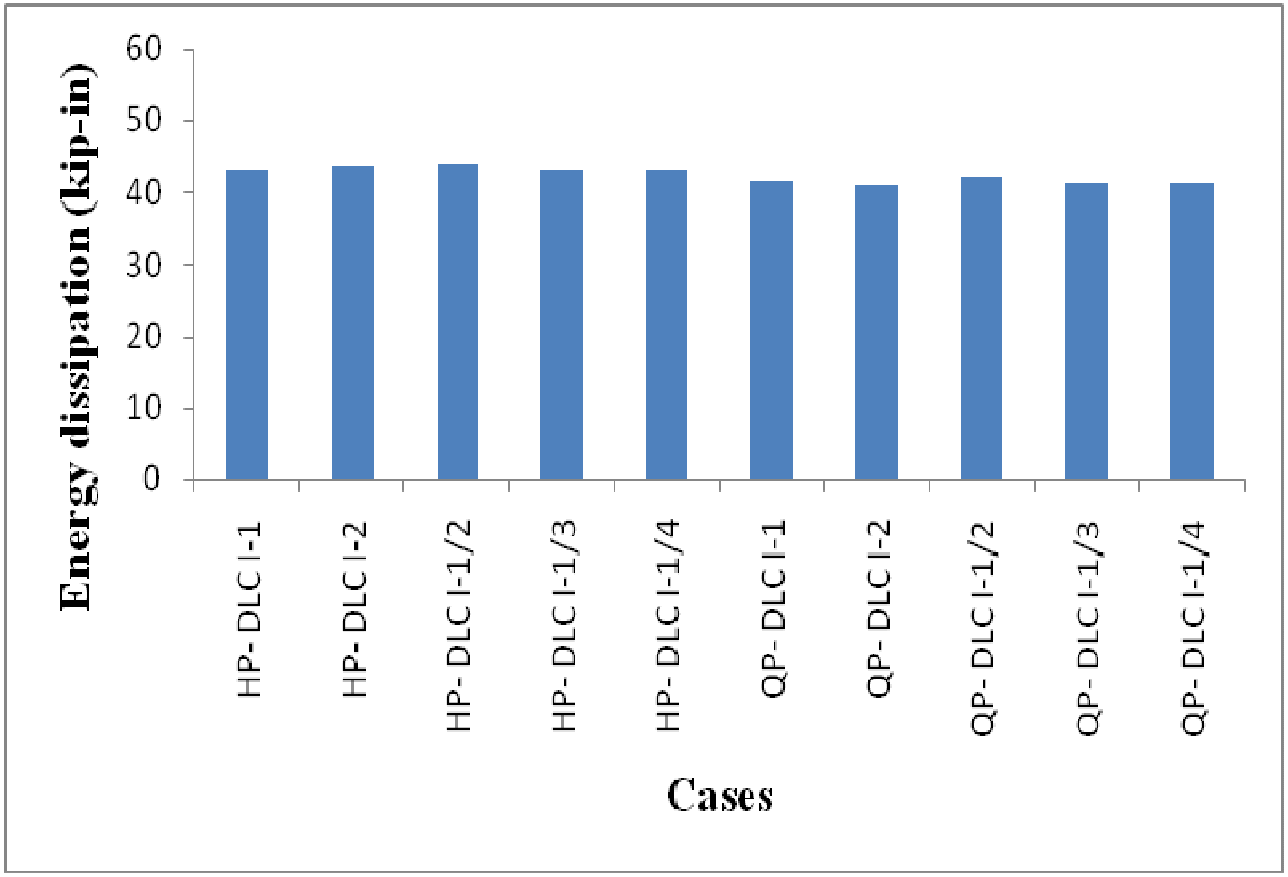

Figure G-4 Single bolted shear surface model half and quarter pretension Case 1

Figure G-5 Single bolted shear surface model Case 2

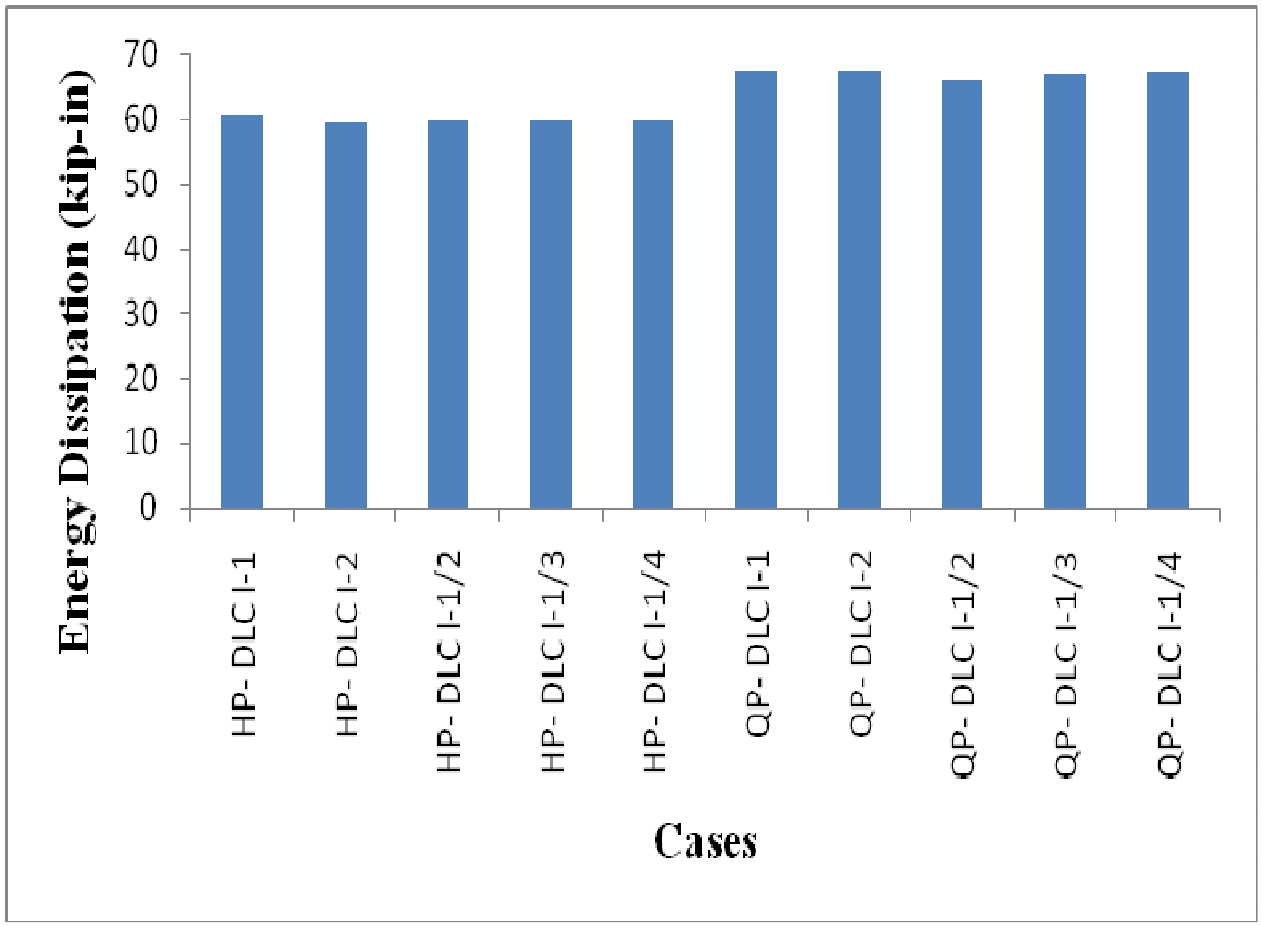

Figure G-6 Single bolted shear surface model half and quarter pretension Case 2

Figure G-7 Single bolted shear surface model Case 3

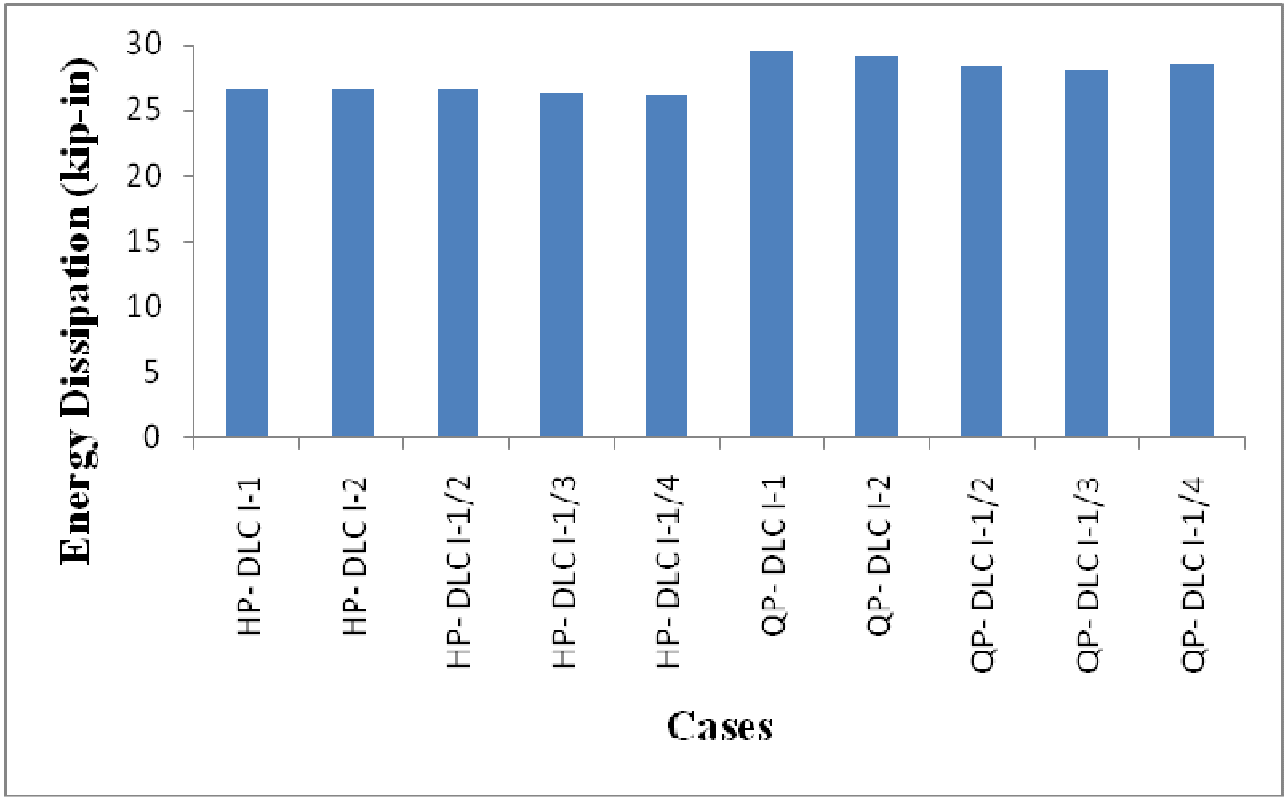

Figure G-8 Single bolted shear surface model half and quarter pretension Case 3

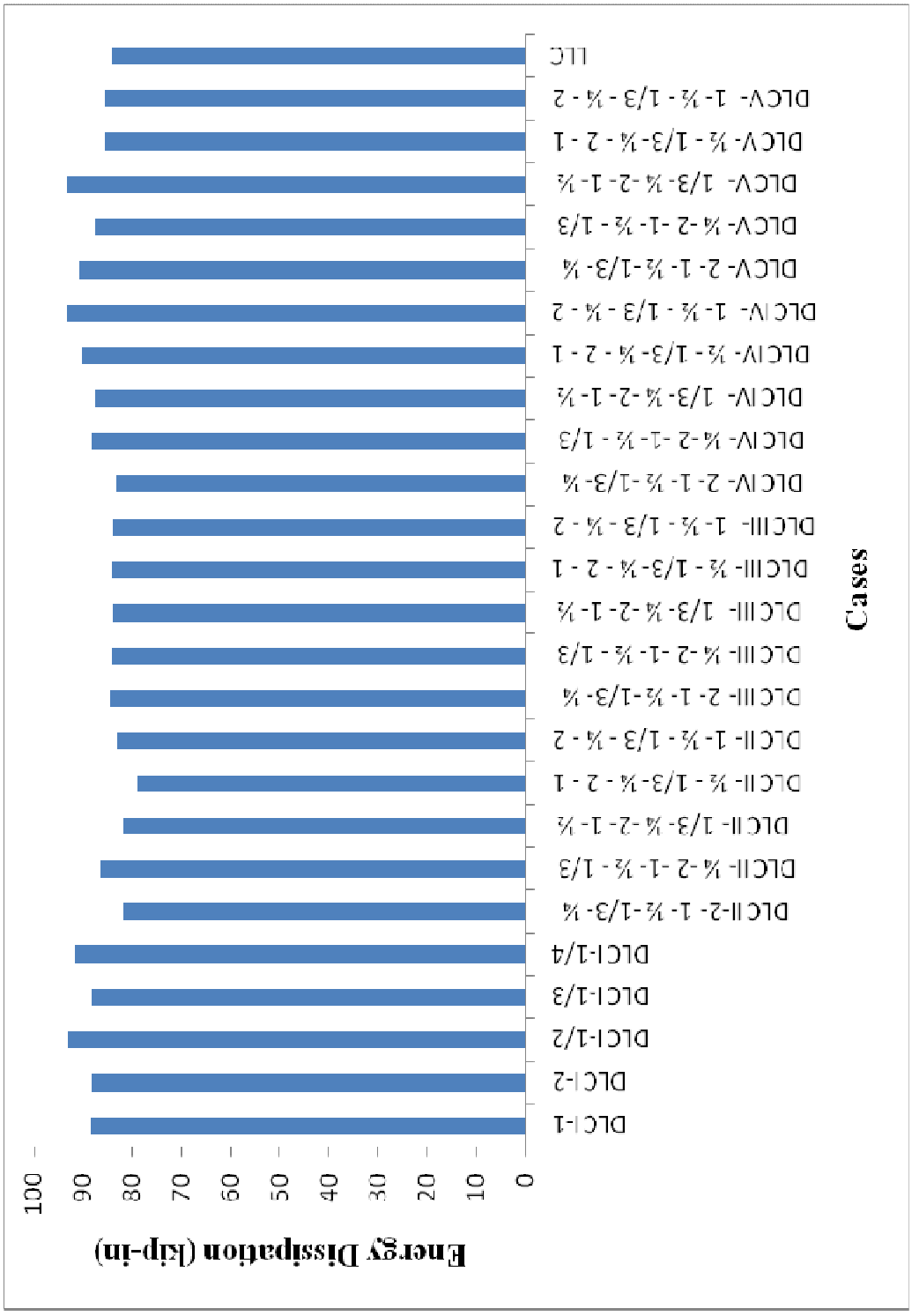

Figure G-9 Double bolted shear surface model Case 1

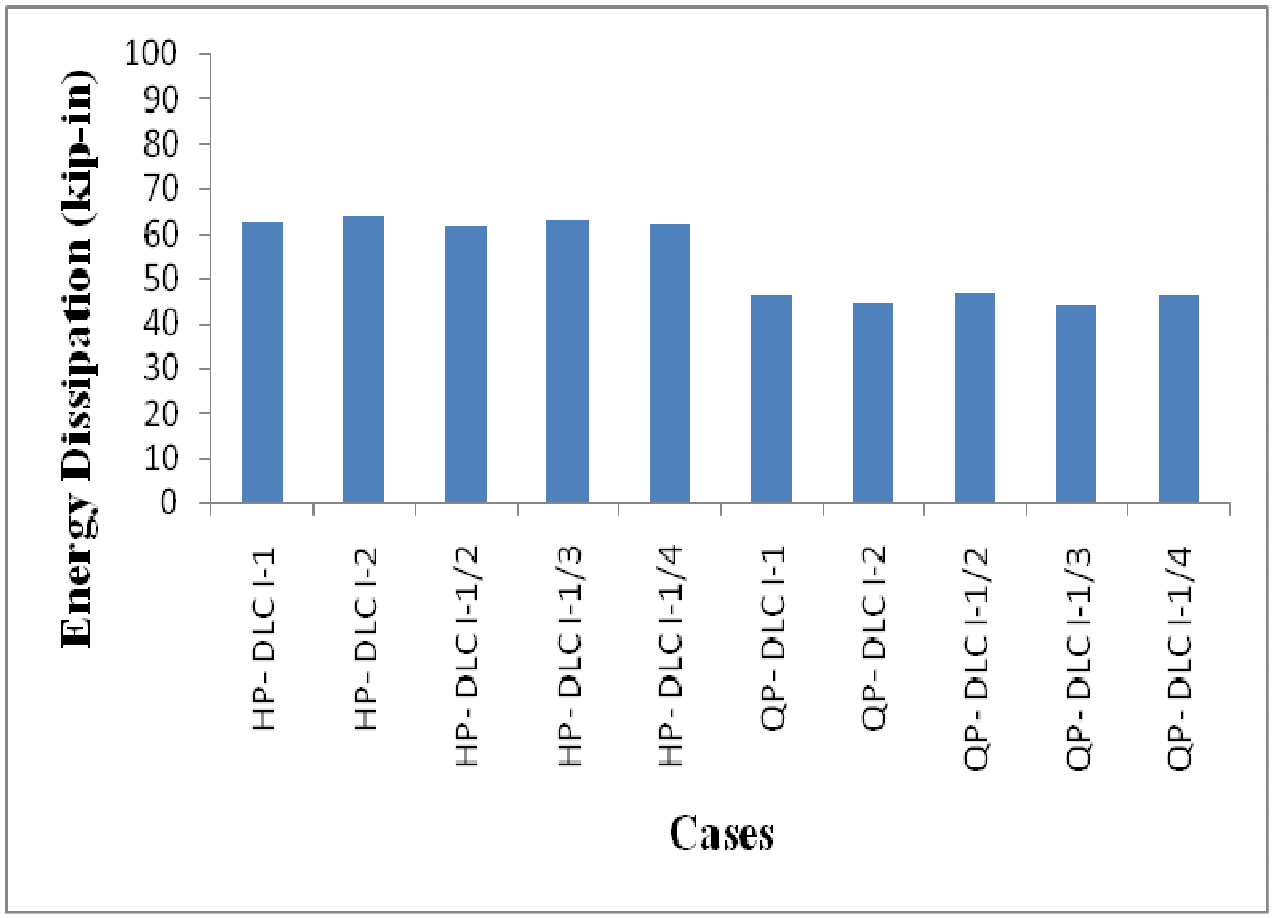

Figure G-10 Double bolted shear surface model half and quarter pretension Case 1

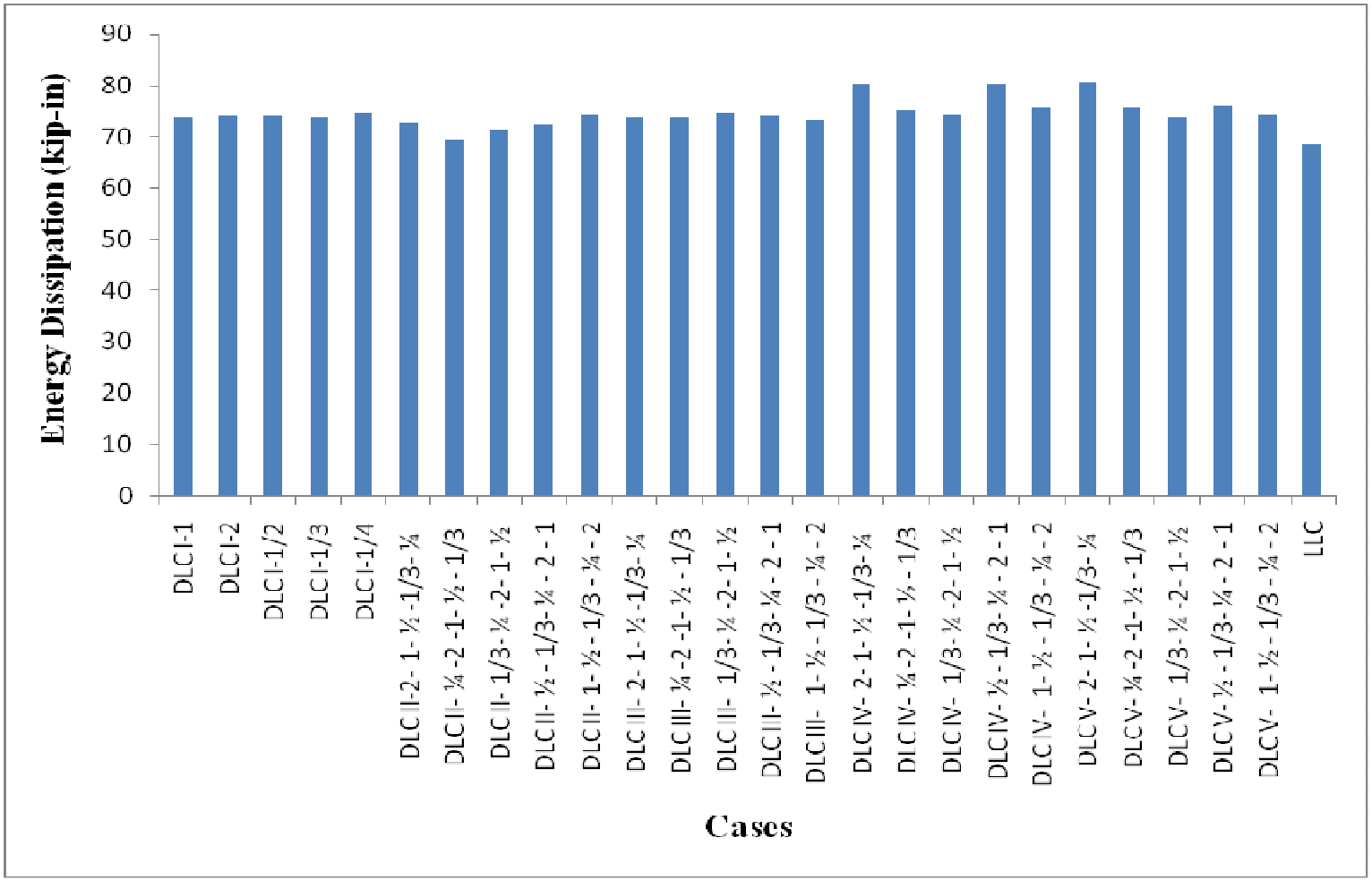

Figure G-11 Double bolted shear surface model Case 2

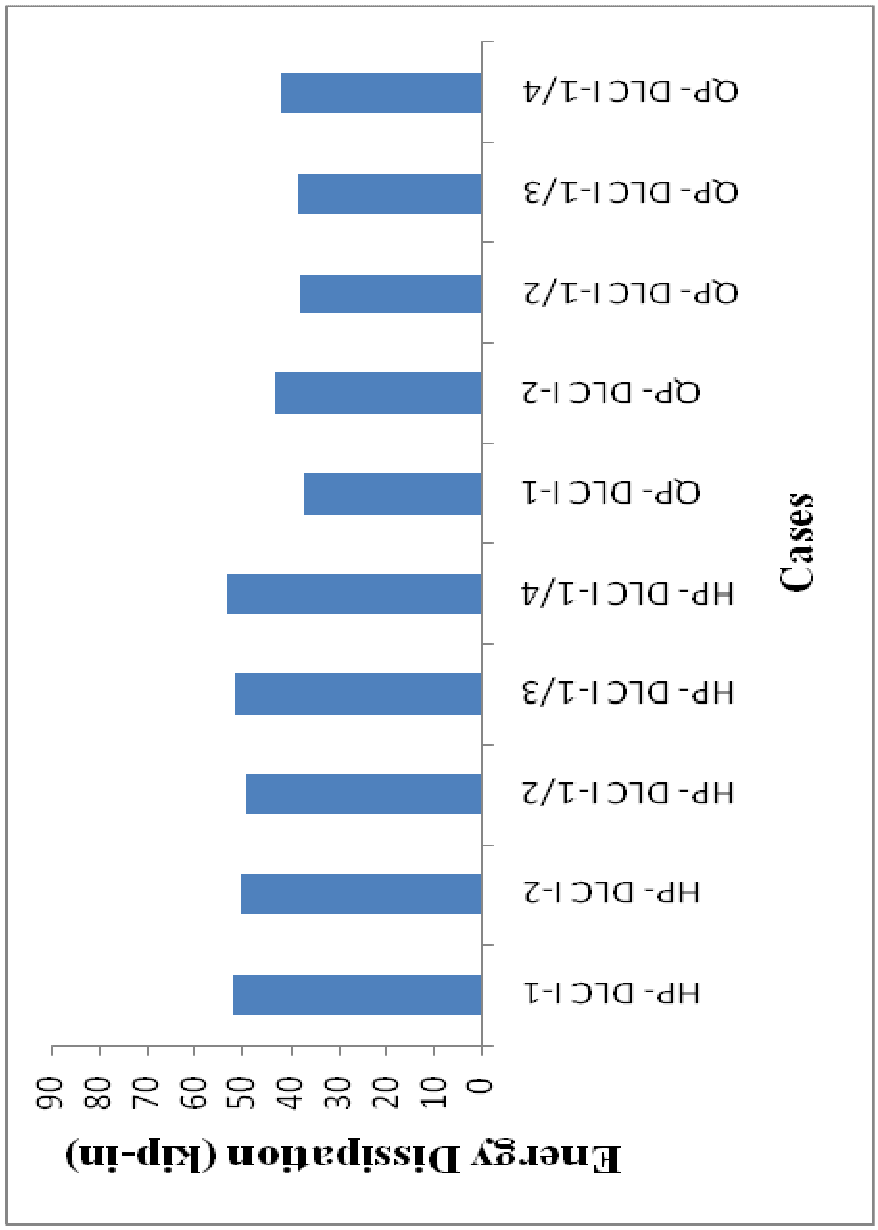

Figure G-12 Double bolted shear surface model half and quarter pretension Case 2

Figure G-13 Double bolted shear surface model Case 3

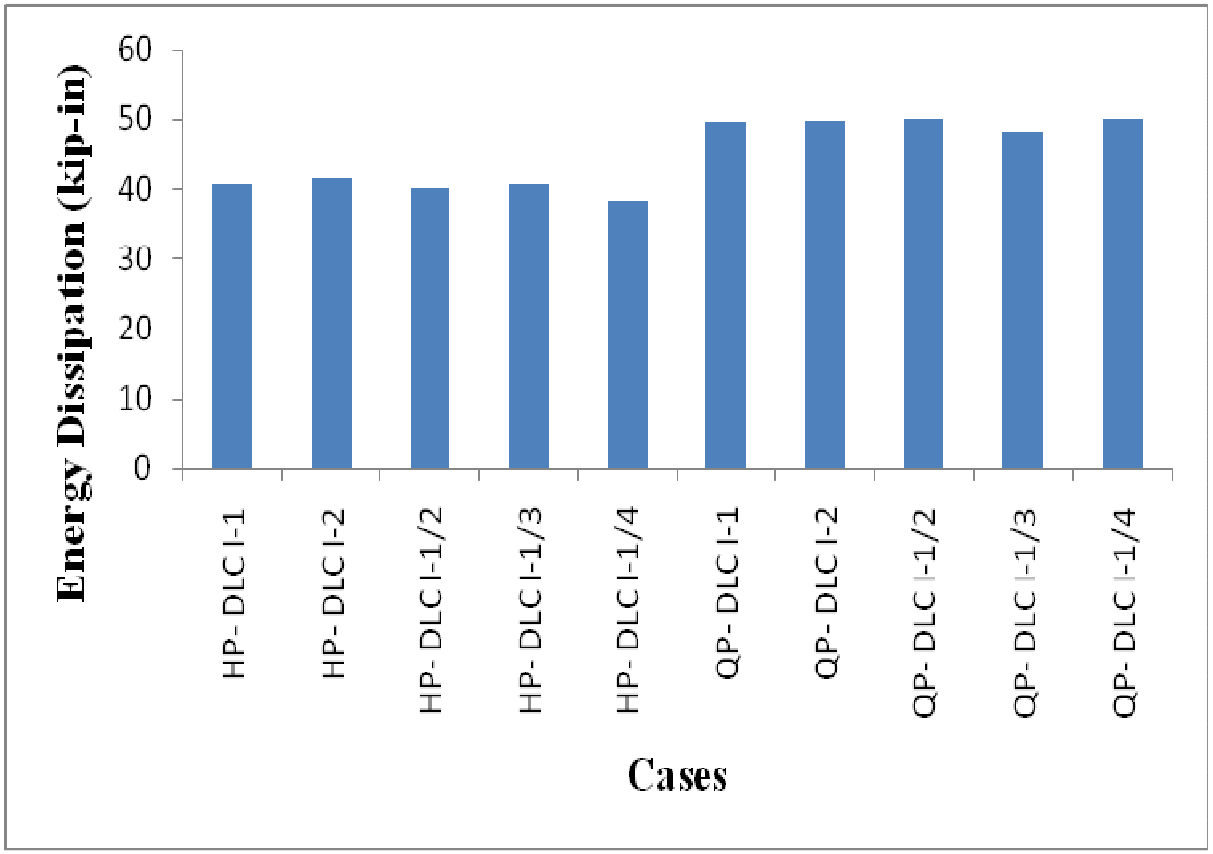

Figure G-14 Double bolted shear surface model half and quarter pretension Case 3

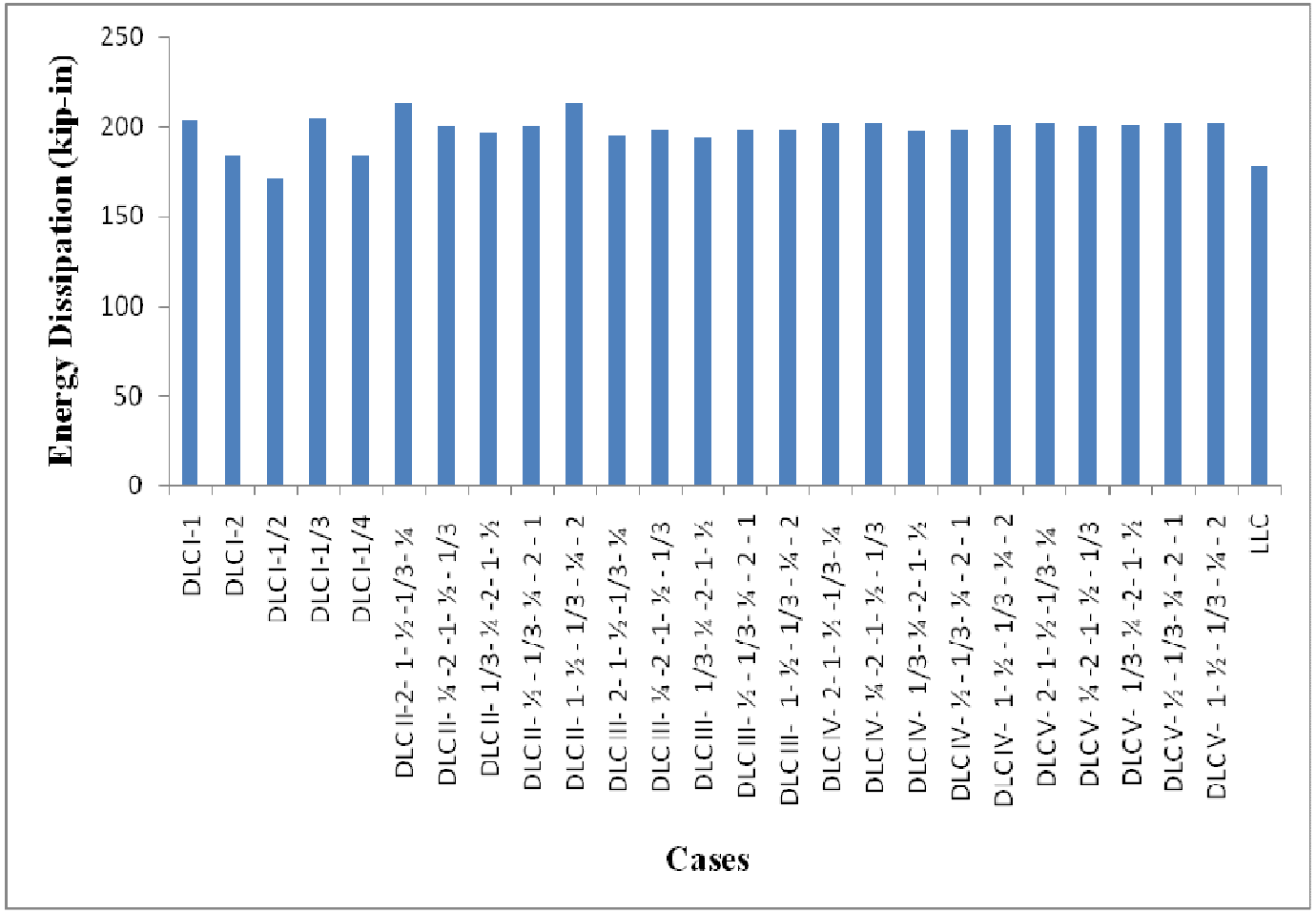

Figure G-15 Tee-hanger model Case 1

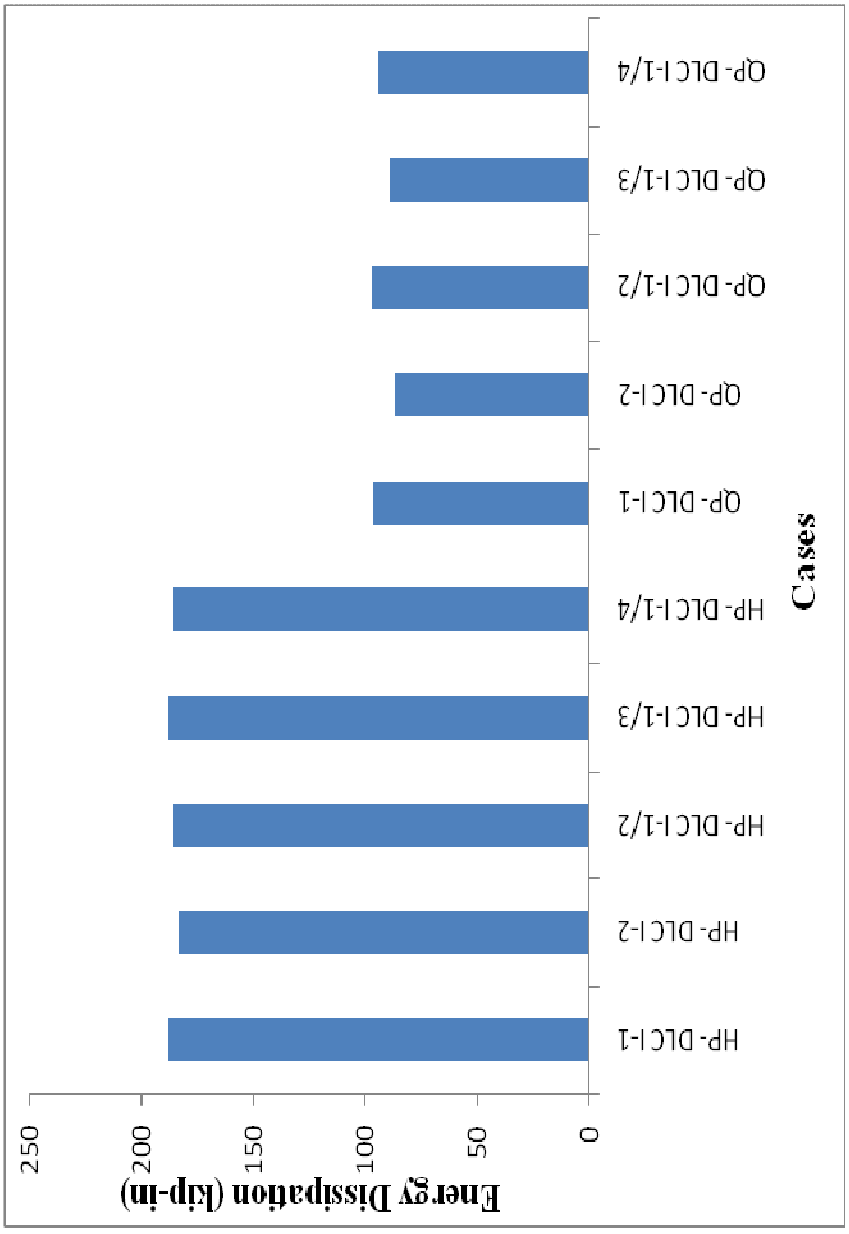

Figure G-16 Tee-hanger model half and quarter pretension Case 1

Figure G-17 Tee – hanger model Case 2

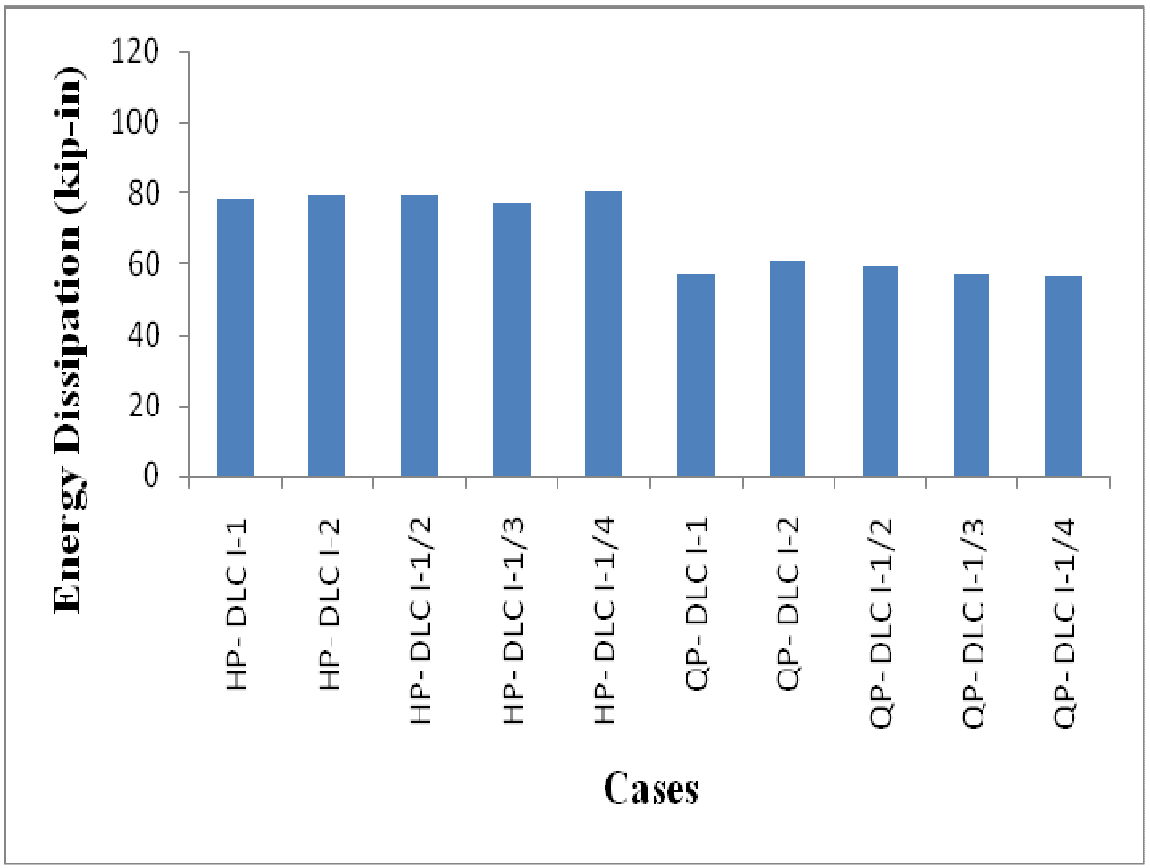

Figure G-18 Tee-hanger model half and quarter pretension Case 2

Figure G-19 Tee - hanger model Case 3

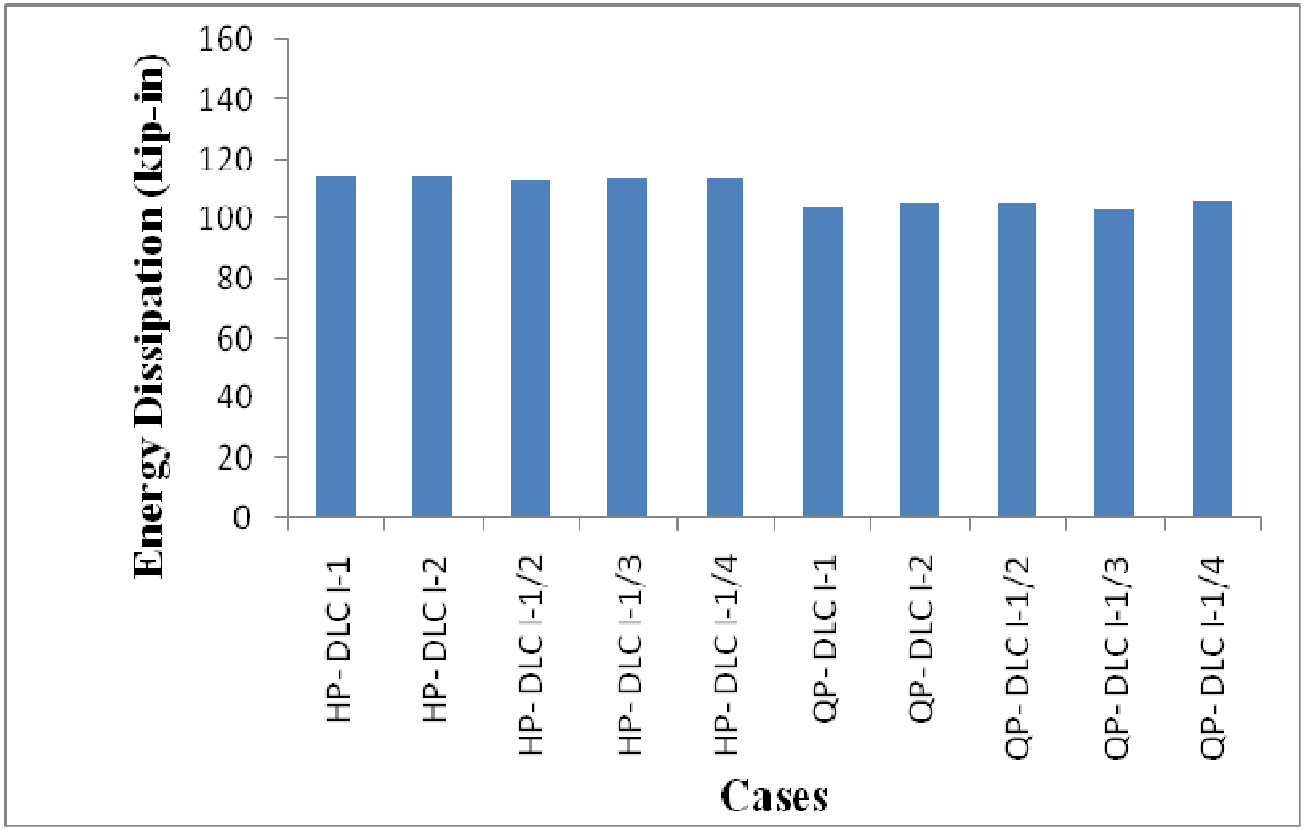

Figure G-20 Tee - hanger model half and quarter pretension Case 3

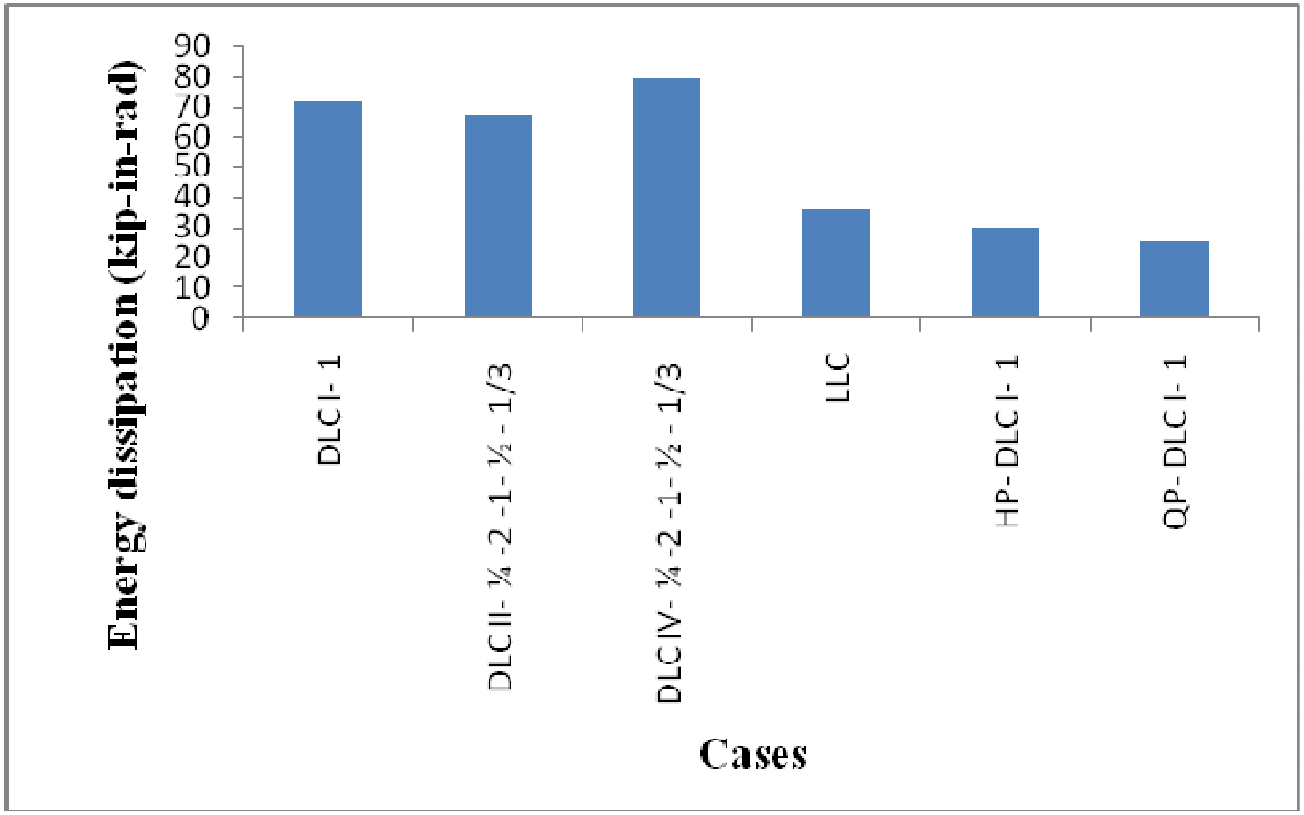

Figure G-21 Extended end-plate connection model Case 1

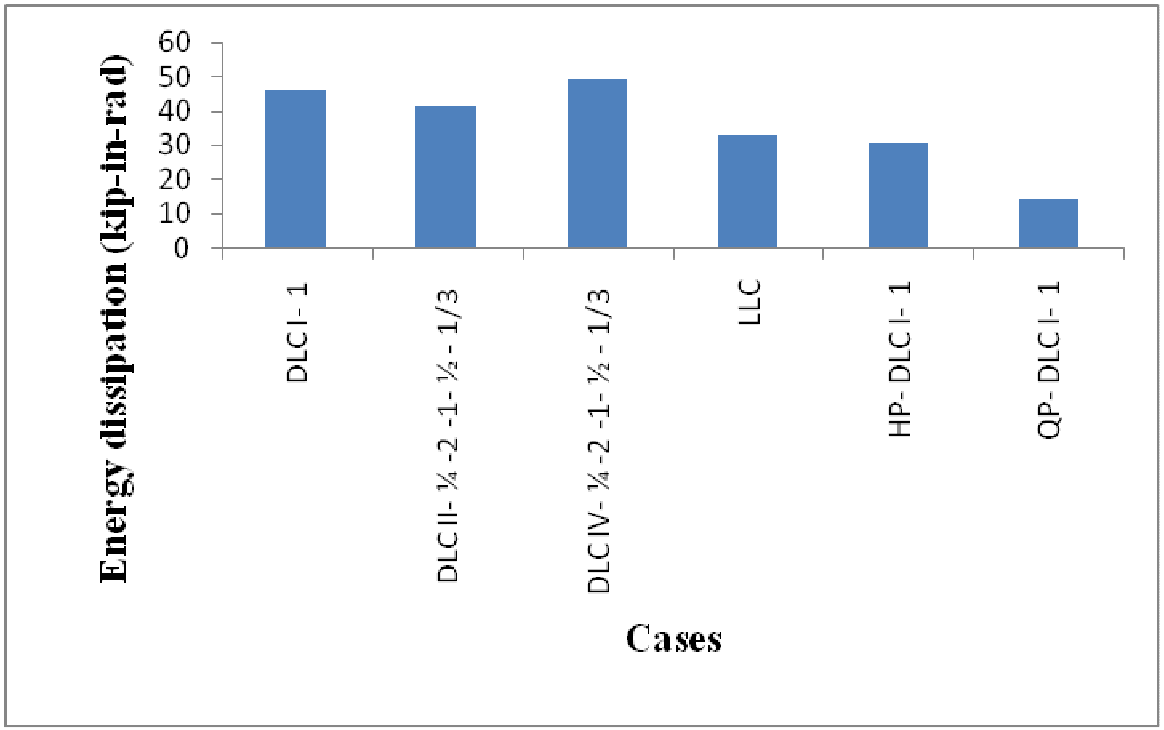

Figure G-22 Extended end-plate connection model Case 2

REFERENCES

ABAQUS/Standard User's Manual version 6.6, Hibbit, Karlson & Sorenson, Pawtucker, RI, 2006

AISC (1999), "Load and resistance factor design specification for structural steel building." *"American Institute of Steel construction"*, Chicago, IL

Anil, Ö. (2008). "Strengthening of RC T-section beams with low strength concrete using CFRP composites subjected to cyclic load." *Construction and Building Materials,* 22(12), 2355-2368.

Bursi, O. S., and Jaspart, J. P. (1998). "Basic issues in the finite element simulation of extended end plate connections." *Computers & Structures,* 69(3), 361-382.

Bursi, O. S., Ferrario, F., and Fontanari, V. (2002). "Non-linear analysis of the low-cycle fracture behaviour of isolated Tee stub connections." *Computers & Structures,* 80(27-30), 2333-2360.

Cabrero, J. M., and Bayo, E. (2007). "The semi-rigid behaviour of three-dimensional steel beam-to-column joints subjected to proportional loading. Part I. Experimental evaluation." *Journal of Constructional Steel Research,* 63(9), 1241-1253.

Deng, C., Bursi, O. S., and Zandonini, R. (2000). "A hysteretic connection element and its applications." *Computers & Structures,* 78(1-3), 93-110.

Feng, Z. -., Hjiaj, M., de Saxcé, G., and Mróz, Z. (2006). "Influence of frictional anisotropy on contacting surfaces during loading/unloading cycles." *International Journal of Non-Linear Mechanics,* 41(8), 936-948.

Girão Coelho, A. M., Bijlaard, F. S. K., and Simões da Silva, L. (2004). "Experimental assessment of the ductility of extended end plate connections." *Engineering Structures,* 26(9), 1185-1206.

Kovács, N., Calado, L., and Dunai, L. (2008). "Experimental and analytical studies on the cyclic behavior of end-plate joints of composite structural elements." *Journal of Constructional Steel Research,* 64(2), 202-213.

Lam, L., Teng, J. G., Cheung, C. H., and Xiao, Y. (2006). "FRP-confined concrete under axial cyclic compression." *Cement and Concrete Composites,* 28(10), 949-958.

Liew, J. Y. R., Teo, T. H., and Shanmugam, N. E. (2004). "Composite joints subject to reversal of loading—Part 1: experimental study." *Journal of Constructional Steel Research,* 60(2), 221-246.

Liew, J. Y. R., Yu, C. H., Ng, Y. H., and Shanmugam, N. E. (1997). "Testing of semi-rigid unbraced frames for calibration of second-order inelastic analysis." *Journal of Constructional Steel Research,* 41(2-3), 159-195.

Lin, X. Z., and Chen, D. L. (2008). "Strain controlled cyclic deformation behavior of an extruded magnesium alloy." *Materials Science and Engineering: A,* 496(1-2), 106-113.

Mace, B. R., and Manconi, E. (2008). "Modelling wave propagation in two-dimensional structures using finite element analysis." *Journal of Sound and Vibration,* 318(4-5), 884-902.

Maggi, Y. I., Gonçalves, R. M., Leon, R. T., and Ribeiro, L. F. L. (2005). "Parametric analysis of steel bolted end plate connections using finite element modeling." *Journal of Constructional Steel Research,* 61(5), 689-708.

Massingham, M., and Irving, P. E. (2006). "The effect of variable amplitude loading on stress distribution within a cylindrical contact subjected to fretting fatigue." *Tribology International,* 39(10), 1084-1091.

Mo, D., Guo-Qiu, H., Zheng-Fei, H., Zheng-Yu, Z., Cheng-Shu, C., and Wei-Hua, Z. (2008). "Crack initiation and propagation of cast A356 aluminum alloy under multi-axial cyclic loadings." *International Journal of Fatigue,* 30(10-11), 1843-1850.

Mohamadi-shooreh, M. R., and Mofid, M. (2008). "Parametric analyses on the initial stiffness of flush end-plate splice connections using FEM." *Journal of Constructional Steel Research,* 64(10), 1129-1141.

Mourad, S., Ghobarah, A., and Korol, R. M. (1995). "Dynamic response of hollow section frames with bolted moment connections." *Engineering Structures,* 17(10), 737-748.

Pirondi, A., Bonora, N., Steglich, D., Brocks, W., and Hellmann, D. (2006). "Simulation of failure under cyclic plastic loading by damage models." *International Journal of Plasticity,* 22(11), 2146-2170.

Sánchez-Santana, U., Rubio-González, C., Mesmacque, G., Amrouche, A., and Decoopman, X. (2008). "Effect of fatigue damage induced by cyclic plasticity on the dynamic tensile behavior of materials." *International Journal of Fatigue,* 30(10-11), 1708-1719.

Shao, Y., Zhu, Z., and Mirmiran, A. (2006). "Cyclic modeling of FRP-confined concrete with improved ductility." *Cement and Concrete Composites,* 28(10), 959-968.

Shi, G., Shi, Y., and Wang, Y. (2007). "Behaviour of end-plate moment connections under earthquake loading." *Engineering Structures,* 29(5), 703-716.

Verderame, G. M., Fabbrocino, G., and Manfredi, G. (2008). "Seismic response of r.c. columns with smooth reinforcement. Part I: Monotonic tests." *Engineering Structures,* 30(9), 2277-2288.

Wang, W., Wu, S., and Dai, H. (2006). "Fatigue behavior and life prediction of carbon fiber reinforced concrete under cyclic flexural loading." *Materials Science and Engineering: A,* 434(1-2), 347-351.

Yorgun, C., and Bayramoglu, G. (2001). "Cyclic tests for welded-plate sections with end-plate connections." *Journal of Constructional Steel Research,* 57(12), 1309-1320.

BIOGRAPHICAL INFORMATION

Sanjog Chandrakant Sabnis was born on July 8, 1982 in Mumbai, India, the son of Alka Sabnis and Chandrakant Sabnis. He completed his high school education at D.S. High school, Mumbai in 1998. Then he enrolled to Datta Meghe College of Engineering, Mumbai, India and earned his B.E (Bachelor of Engineering) in Civil Engineering, in June 2006. He also worked as an executive engineer at H & R Johnson India (Ltd.) Mumbai India for 6 months as a full time and 6 months as an intern.

Sanjog Sabnis has started his M.S. (Master of Science) program in department of Civil & Environmental Engineering at the University of Texas at Arlington, Arlington, Texas, in August 2006 and earned M.S. degree in Civil & Environmental Engineering in December 2008. During his master degree he was appointed a graduate research assistant of Dr. Abolmaali. His thesis was on effect of displacement control loading on general connecting surface using finite element analysis. .